2015

UTILISING PROBABILISTIC TECHNIQUES IN THE ASSESSMENT OF EXTREME COASTAL FLOODING FREQUENCY- MAGNITUDE RELATIONSHIPS USING A CASE STUDY FROM SOUTH-WEST ENGLAND

Whitworth, Michael Robert Zordan

UTILISING PROBABILISTIC TECHNIQUES IN THE ASSESSMENT OF EXTREME COASTAL FLOODING FREQUENCY- MAGNITUDE RELATIONSHIPS USING A CASE STUDY FROM SOUTH-WEST ENGLAND

By

MICHAEL ROBERT ZORDAN WHITWORTH

A thesis submitted to the University of Plymouth in part fulfilment for the degree of

DOCTOR OF PHILOSOPHY

School of Geography, Earth and Environmental Science

July 2014

Copyright Statement

In memory of my Dad

Malcolm Zordan Whitworth

Michael Robert Zordan Whitworth

Utilising probabilistic techniques in the assessment of extreme coastal flooding frequency-magnitude relationships using a case study from south-west England

Abstract

Recent events such as the New Orleans floods and the Japanese tsunami of 2011 have highlighted the uncertainty in the quantification of the magnitude of natural hazards. The research undertaken here has focussed on the uncertainty in evaluating storm surge magnitudes based on a range of statistical techniques including the Generalised Extreme Value distribution, Joint Probability and Monte Carlo simulations. To support the evaluation of storm surge frequency magnitude relationships a unique hard copy observed sea level data set, recording hourly observations, was acquired and digitised for Devonport, Plymouth, creating a 40 year data set. In conjunction with Devonport data, Newlyn (1915-2012) tide gauge records were analysed, creating a data set of 2 million data points. The different statistical techniques analysed led to an uncertainty range of 0.4 m for a 1 in 250 year storm surge event, and 0.7 m for a 1 in 1000 storm surge event. This compares to a 0.5 m uncertainty range between the low and high prediction for sea level rise by 2100. The Geographical Information system modelling of the uncertainty indicated that for a 1 in 1000 year event the level uncertainty (0.7 m) led to an increase of 100% of buildings and 50% of total land affect. Within the study area of south-west England there are several critical structures including a nuclear licensed site. Incorporating the uncertainty in storm surge and wave height predictions indicated that the site would be potentially affected today with the combination of a 1 in 1000 year storm surge event coincident with a 1 in 1000 wave. In addition to the evaluation of frequency magnitude relations this study has identified several trends in the data set. Over the data period sea level rise is modelled as an exponential growth ($0.0001 mm/yr^2$), indicating the modelled sea level rise of 1.9 mm/yr and 2.2 mm/yr for Newlyn and Devonport, will potentially increase over the next century by a minimum of 0.2 m by 2100.The increase in storm frequency identified as part of this analysis has been equated to the rise in sea level, rather than an increase in the severity of storms, with decadal variations in the observed frequency, potentially linked to the North Atlantic Oscillation. The identification as part of this study of a significant uncertainty in the evaluation of storm surge frequency magnitude relationships has global significance in the evaluation of natural hazards. Guidance on the evaluation of external hazards currently does not adequately consider the effect of uncertainty; an uncertainty of 0.7 m identified within this study could potentially affect in the region of 500 million people worldwide living close to the coast.

Table of Contents

Table of Figures

Table of Tables

Acknowledgements

Firstly I would like to thank my supervisors, Jim, Geoff and Iain; especially Jim who has offered support and encouragement throughout my PhD and career. A special thanks goes to Sarah for her continued support, encouragement and occasional nags. Thank you for the final proof read. Thank you to Dr Jon Hill of Imperial University for modelling the Lisbon tsunami. I would like to thank and acknowledge the various data sources including the Channel Coast Observatory, Edina, the Hydrographic Office and the Met office. Finally, thanks to all the Plymouth University members of staff and PhD students for their wisdom, knowing you are not suffering alone and the philosophical debates in the JSV.

Author's Declaration

At no time during the registration for the Degree of Doctor of Philosophy has the author been registered for any other University award without prior agreement of the Graduate Committee.

The study was self-financed in collaboration with the School of Geography, Earth and Environmental Sciences.

Publications:

Babcock. 2008. NED-REP-1783. Flood hazard to Devonport Dockyard from storm surges and wind induced waves. Internal Document.

N.B. Independent Technical Assessment Certificate attached in Appendix A

Presentation and Conferences Attended:

Naval Nuclear Safety Board (2008)-Flood Hazard to Devonport Dockyard form storm surges and wind induced waves

Babcock Management Safety Committee (2008)- Flood Hazard to Devonport Dockyard form storm surges and wind induced waves

EGU2011-4561- The use of probabilistic techniques in the evaluation of storm surge hazard and risk-Poster Presentation

EGU2011-4571- Sea level rise and storminess for the south-west of England-Poster Presentation (Combined with above)

External Contacts:

Dr. Jon Hill Imperial College London

Babcock Marine

Word Count of main body of thesis:

51,000

Name: Michael R. Z. Whitworth Signature:

Date:

Reports that say there's -- that something hasn't happened are always interesting to me, because as we know, there are known knowns; there are things that we know that we know. We also know there are known unknowns; that is to say we know there are some things we do not know. But there are also unknown unknowns, the ones we don't know we don't know

Donald Rumsfeld. 2002

The unknown known; that which we intentionally refuse to acknowledge that we know

Slavoj Žižek. 2002

Chapter 1 Introduction

1.1 Project Overview

When evaluating coastal inundation scenarios there are two fundamental questions for coastal planners; firstly; what are the present day scenarios of storm surges and waves; secondly; how will this change in the future with projected sea-level rise (Figure 1.1).

Significant research has been undertaken on the uncertainties of sea-level rise on the coastal environment with research pointing to an increased flooding risk for many low lying coastal regions due to an overall rise in sea-level over the next century (Nicholls et al., 1999; Houghton et al., 2001). Global assessments of the uncertainties indicate a range of sea-level rise between 0.18 m and 0.59 m by 2100 (IPCC, 2007), leading to an increase in the number of people affected annually to range from 7 to 29 million (Nicholls, 2004). A U.K. assessment indicated an uncertainty range between 0.12 m and 0.76 m by 2100 (UKCP, 2009), leading to a range of 4.5-6.9 million people affected (Hall et al., 2005).

International guidance on the evaluation of natural hazards including storm surges is given for nuclear sites in International Atomic Energy Association guidance, recommending the evaluation of frequency magnitude relationships using the Generalised Extreme Value methodology (IAEA, 2003; IAEA, 2011). However, U.S. guidance on the evaluation of extreme wind speeds, recommends the evaluation of frequency-magnitude relationships based on the Weibull distribution (Cheng and Yeung, 2002). The utilisation of only one statistical technique might not consider the full range of uncertainties or possible scenarios (Punya et al., 2012; Rahmen et al., 2012), yet there are several statistical techniques that allow the evaluation of frequency-magnitude relationships (Coles, 2001). However, these techniques all have deficiencies in how the available data sets are utilised, the required data length and the ability to evaluate the frequency magnitude relationship, leading to further uncertainties in the evaluation of frequency magnitude relationships (Pugh and Vassie, 1980; Cheng and Yeung, 2002).

Recent events such as the New Orleans flood and the Japanese tsunami of 2011, have highlighted the uncertainties in the quantification of uncertainties of natural hazards in the coastal environment. Therefore, the principal aim of this research is

to quantify the uncertainty in the evaluation of frequency magnitude relationship and evaluate the potential impact of these uncertainties on the coastal environment. To undertake this evaluation of the uncertainties storm surges have been chosen due to the availability of long term tide gauge data sets. The south-west of England, between Newlyn and Plymouth (Figure 1.3) has been chosen as the study area as, unusually, this area has an excellent historical record of tidal data. Historical sea-level data sets exist for Newlyn, with digitally recorded data for every hour almost continuously from 1915 to the present day are available. This record is the longest within the United Kingdom (National Tidal and Sea-level Facility, 2007) and one of the longest continuous in the world, only Brest in France has a longer record which dates back to 1807 (Permanent Service for Mean Sea Level, 2014). The Newlyn data set will allow a comprehensive assessment of the uncertainties of frequency-magnitude predictions. In addition to the Newlyn data set, the study area also has a second, shorter data set from Devonport in Plymouth with 20 years of hourly digital data, and 20 years worth of hard copy hourly data, spanning the years 1962-2012 (10 years of missing data). Several authors (for example Tawn and Vassie, 1989) highlight the deficiencies of several different statistical techniques at evaluate frequency magnitude relationship. The relatively close proximity of Devonport to Newlyn (100 km) will allow a comparison of the predictions of frequency magnitude relationships made for each site based on different length data sets providing an understanding of the uncertainties in prediction methodology due to data length. Further data sets that exist for the study area include weather data from Mt Batten (Plymouth) for the period 1962-2008 in digital form of daily average pressure, wind speed and wind direction, and limited wave data (7 years) from Polperro (Cornwall) recorded in digital form every 30 minutes. In addition to the data sets, south-west England has a range of infrastructure including a nuclear facility. Within a Geographical Information System (GIS) the uncertainties can be modelled, and overlain on to the regional infrastructure data to provide a measure of the affect of the uncertainty. Furthermore, the U.K. has undertaken research in to the uncertainties of sea-level rise (UKCP, 2009) and the impacts of sea-level rise (DEFRA, 2006). Modelling these uncertainties within a GIS will allow a detailed comparison of the uncertainties of storm surge predictions with sea-level rise uncertainties and the associated impacts on the coastal environment.

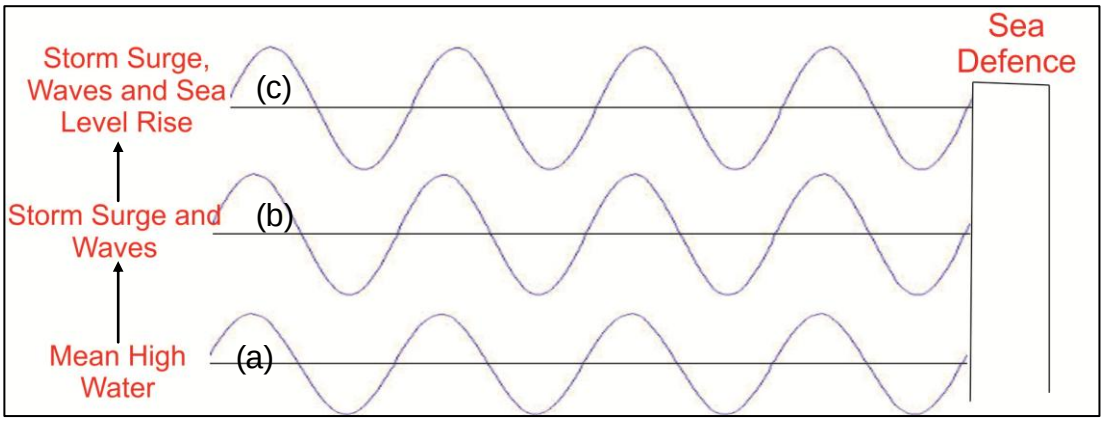

Figure 1.1 Illustration of the change in mean high water (a) with (b) storm surges and (c) storm surges and sea-level rise with waves superimposed.

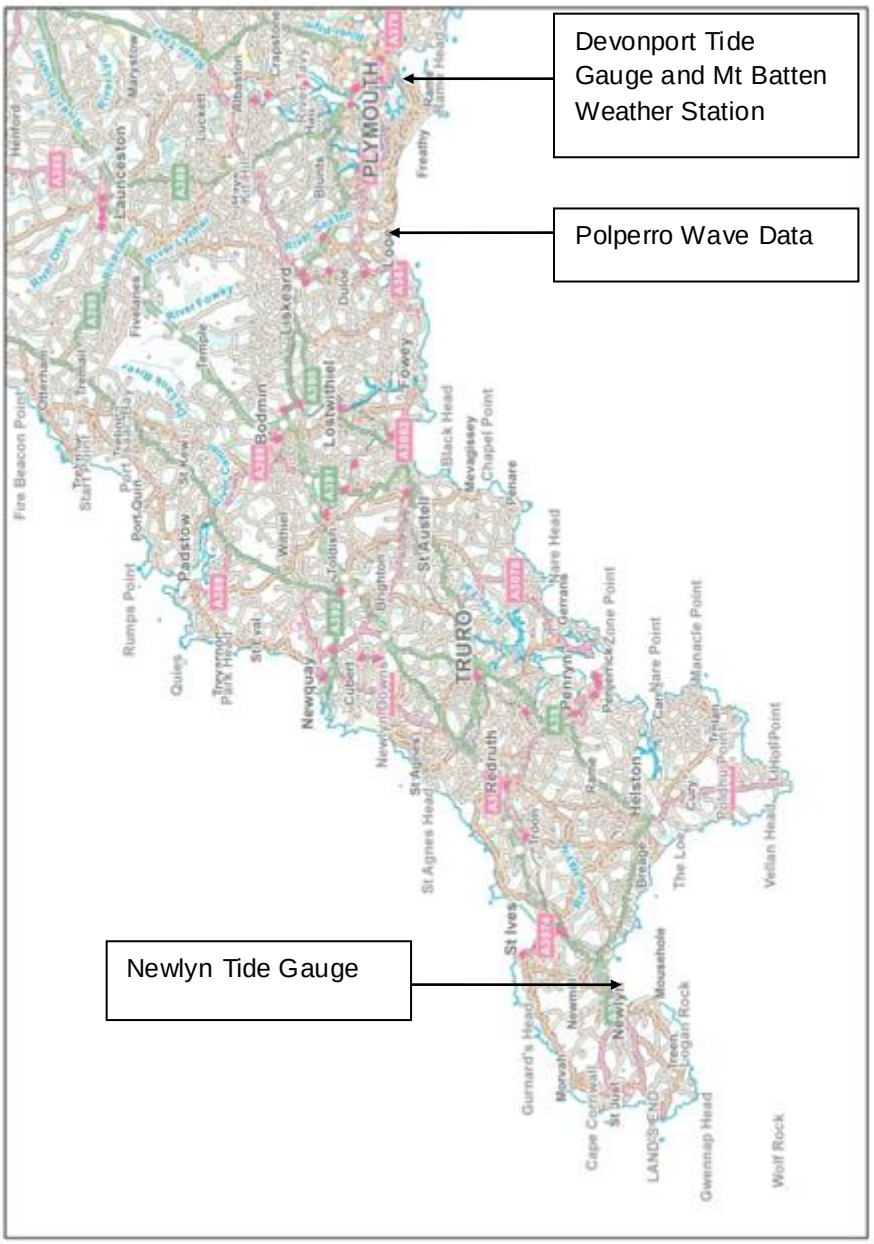

Figure 1.2 Location of study area between Plymouth and Newlyn.

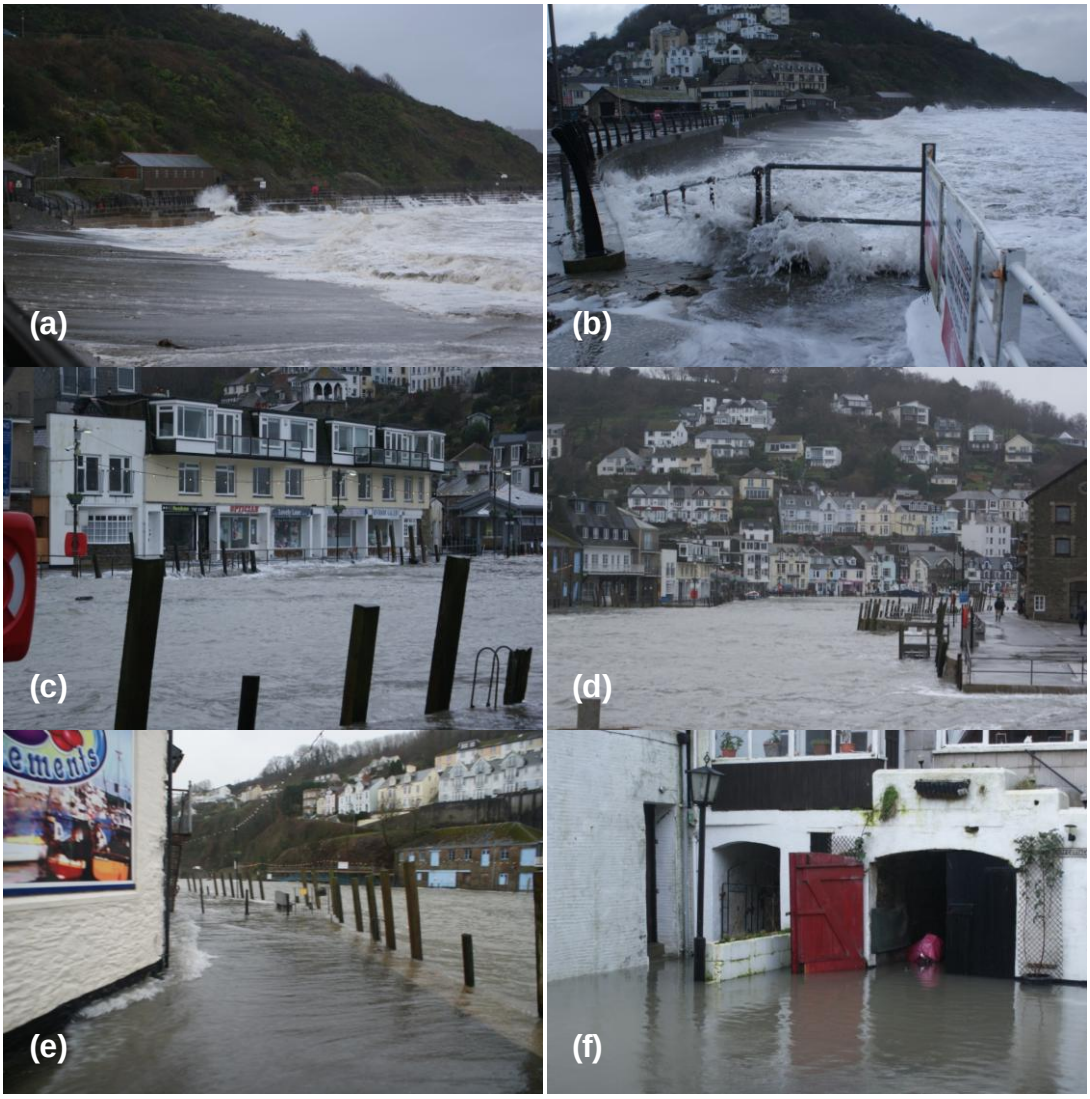

Figure 1.3 Photo montage of storm surge conditions at Looe, Cornwall on the 5th February 2014 during a high tide at 0925 (Photos by author).

1.1.1 Study Area and Source Screening

The study area is defined by the extent of the available Light Detection and Ranging (LiDAR), elevation data. The data covers a stretch of South-West England coastline between Plymouth (Devonport), Devon and Penzance (Newlyn), Cornwall. The LiDAR data covers the steep coastline, interspersed with flooded quaternary river valleys that form the present day estuaries of the Tamar, Plym, Fal and Fowey. Beyond the study area, Cornwall and the area adjacent to Plymouth is dominated by a high stand formed by granitic intrusions that comprise Bodmin Moor, Lands End and Dartmoor. Drainage lines typically flow either north or south to the study area, with some drainage lines forming moderately steep and incised valley systems. These drainage lines typically flow in to the estuary systems of the study area. Beyond the sea cliffs the sea bed of the coast of the study area drops of rapidly to a depth of -50 m, within ~ 5-10 km. The bathymetry change typically runs parallel to the coast. Beyond the -50 m contour the sea bed flattens forming the intercontinental shelf, with a rate of change of depth of approximately 1m/km.

The location of the tide gauges at Devonport and Newlyn are given in Figures 1.4a and 1.4b, respectively. The Devonport tide gauge is located in an enclosed basin within the Tamar Estuary. The tide gauge is located within a part of the study area where the gauge could potentially record not only the storm surge and astronomical tide, but also contain a fluvial component from the river Tamar. However, the estuary adjacent to the tide gauge is approximately 9 km^2, with water depths in excess of 9 m. Therefore, the contribution of fluvial waters to the observed levels at the tide gauge are considered to be small and will be dominated by the astronomical tide (>6 m) and storm surge component. As such the contribution from fluvial sources is excluded from the analysis of the Devonport tide gauge. In comparison to Devonport, Newlyn can be considered to contain only a combination of astronomical tidal and storm surge component as the tide gauge is located on a pier that extends into the open sea, with water depths of approximately 10 m.

Within the study area there are 4 potential sources of flooding:

1. Fluvial.
2. Urban Flooding caused by rainfall run off.
3. Coastal Flooding caused by storm surges and waves.
4. Tsunami.

From a review of historical archives no instances of fluvial flooding have occurred within the study area. However, flash flooding could occur within the moderately steep drainage lines, illustrated in the flooding of Boscastle on the North Cornwall coast in 2004. No incidence of significant urban flooding, caused by rainfall run off was identified in an archival search. As discussed in Section 2.4.4 and Section 2.6 over 30 incidents of coastal flooding has occurred within the study area, with on occurrence of one tsunami, with 3 other possible events. These historical records and observations indicate that coastal flooding and tsunami dominate the flood hazard to the study area. In addition to the historical occurrence of flood events, the population of the south west of England is concentrated within coastal communities, with the main centres located on the estuaries of the Plym, Tamar, Fal and the beach fronts of Par, Penzance and Newlyn.

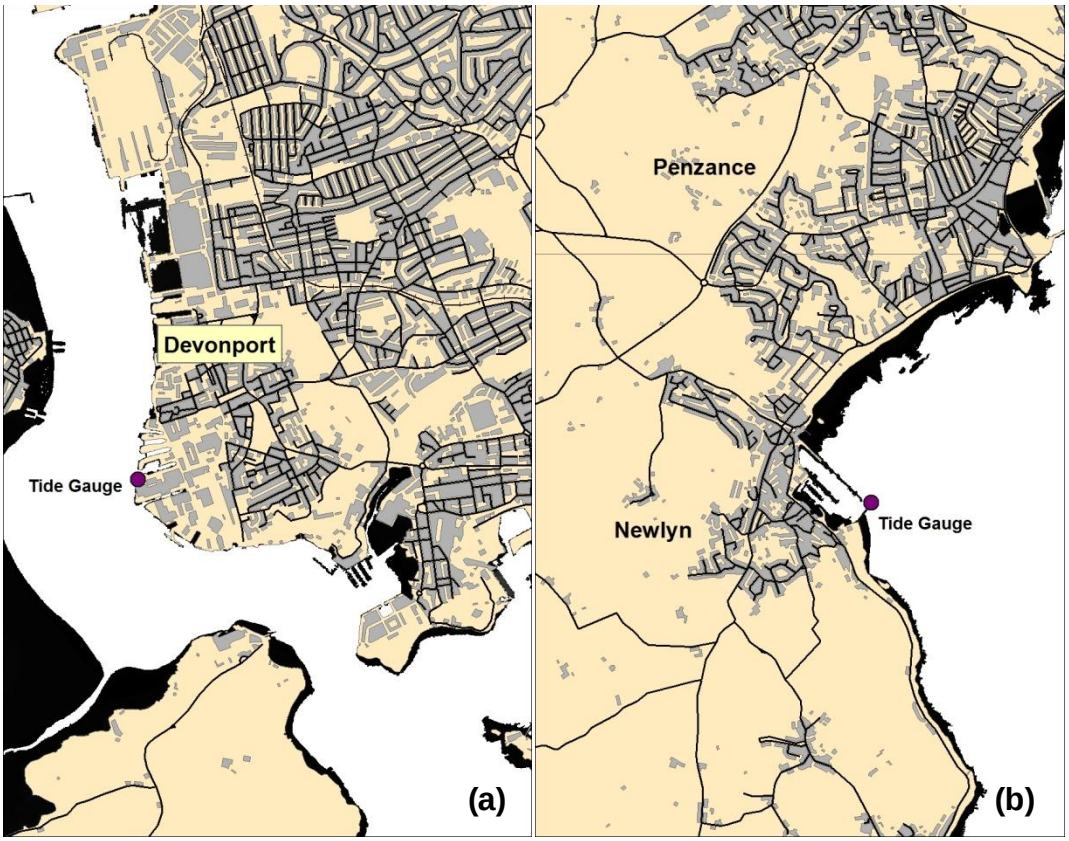

Figure 1.4 Location of tide gauges (a) Devonport and (b) Newlyn.

1.2 Project Objectives

The following Section details the overall aim of the research, with details of the individual objectives required to achieve this aim.

1.2.1 Overall Research Aim and Objectives Summary

The overall aim of this research is:

Using a case study approach, evaluate the utilisation of probabilistic techniques in the assessment of extreme coastal flooding frequency-magnitude relationships. Allowing the identification of the dominant uncertainty in coastal processes, the frequency-magnitude predictions or sea-level rise predictions.

The main project objectives are:

1. To digitise data for the period 1962-1987 for Devonport, increasing the data length to 40 years. This will allow a comparison with Newlyn and an evaluation of the uncertainties in frequency magnitude relationships. In addition the increased data set will provide greater confidence in the modelled sea-level trend for the study area.
2. To critically evaluate storm surge and wave height frequency-magnitude relationships and the level of uncertainty using the following probabilistic modelling techniques:
    a. Extreme Value Analysis.
    b. Monte Carlo Simulations.
3. Using a Geographical Information System to produce visual representations of inundation levels due to storm surge, including an evaluation of the sensitivity of south-west England to inundation as a result of the uncertainty in frequency magnitude predictions and sea-level rise predictions.
4. To provide guidance on how uncertainty might be incorporated within planning and design decisions.

1.2.2 Extending the Devonport Record

Many of the regions at risk from storm surges within the U.K. have insufficient historical data available for analysis (Bernier et al., 2007). In addition there is significant uncertainty in the predictions for storm surge magnitudes (Haigh et al., 2006) and sea-level rise scenarios (UKCP, 2009). Typically, for analysis of storm surge magnitudes with a high degree of confidence using the Generalised Extreme Value methodology as recommended by IAEA (2003), requires in the order of 40 years worth of data (Coles, 2001). However, a number of statistical techniques are available to allow predictions of storm surge magnitude based on limited data (Coles, 2001). Therefore, an understanding of the uncertainties associated with frequency magnitude predictions and the selection of the most appropriate method of analysis is of critical importance to planners and designers responsible for protecting coastal areas (Coles and Tawn, 1990).

The Newlyn record between 1915-2012 (Section 1.1), comprising over 100,000 data points has been used in several previous studies to evaluate storm surge magnitudes (Dixon & Tawn, 1994) and sea-level trends (Woodworth et al., 1999). Plymouth (Devonport) has a sea-level data set digitally recorded every hour from 1990 to the present day. However, this record suffers from data gaps and shifts in recorded datums and has provided difficulties for analysis of storm surges and evaluation of sea-level trends. For example, Woodworth et al., (1999) using the data set from 1987-1998, noted that problems exist with the tide gauge record from Devonport and in their discussion on the analysis of sea-level trend they point to potential datum shifts giving large confidence interval bands compared with that available for Newlyn. As part of this study data was acquired for Devonport from the United Kingdom Hydrographic Office. These data were in hard copy form with observed sea-level measurements recorded every hour from 1962 to 1987. This data effectively increases the Devonport data set by 20 years, or 50%, equating to approximately 50,000 data points. Therefore a core component of this study was the digitisation of this data to produce a homogeneous 40 year data set spanning 1962 to 2012 (allowing for 10 years of missing data). The utilisation of this recently acquired and digitised data for Devonport will allow a greater degree of confidence in modelling the sea-level trend for Plymouth and the evaluation of frequency magnitude relationships, the uncertainties in predictions and a detailed comparison with the Newlyn data set. Section 5.2 and Section 5.3 reviews the Devonport and Newlyn data sets (Section 5.2) and the observed trends within each data set (Section 5.3), identifying if the updated 40 year data set for Devonport provides

more comparable trends to Newlyn, removing the potential difficulties in analysis identified by Woodworth et al., (1999).

1.2.3 Evaluation of Storm Surge, Tsunamis and Wave Magnitude

The Newlyn and extended Devonport data sets, provide a basis to evaluate storm surge magnitudes. However, there are a variety of techniques that can be utilised in the evaluation of storm surge magnitudes. This project aims to evaluate the most commonly used statistical techniques and evaluate their applicability to the available data sets and the level of uncertainty within the statistical techniques. In addition a fundamental problem that this project aims to address is how different techniques can be applied to locations with short data sets (<10 years) and how the level of uncertainty compares to the longer data sets. This has significant global importance as typically many sites have less than 10 years worth of data.

Storm surge is only one characteristic of coastal inundation, further components that can lead to significantly increased flood levels and add to the overall level of uncertainty, include wave height and sea-level rise (Reeves et al., 2012). Figure 1.3 shows the complex nature of storm surge events at a given location, as it is the combination of tide, storm surge and waves. Figure 1.3 gives photos from a storm surge at Looe (Cornwall) on the 4th February 2012 during high tide. Looe is a interesting case study as the town is affected by flooding from the beach front as also the adjacent estuary. Figure 1.3(a) and (b) shows the conditions on the beach front, where waves were observed to be in the order of 2 m. Figure 1.3 (c) and (d) show the conditions within the estuary, with the mean observed water level was approximately 0.25 m below the quay wall. Inundation did not occur via the beach but occurred due the superposition of 0.3-0.5 m high waves on to the observed water level within the estuary as shown in Figure 1.3 (e). The overall combination of tide, storm surge and waves can lead to significant impacts on local communities (Figure 1.3 (f)). To evaluate the uncertainty associated with the affect of wave height on inundation levels, statistical analysis of historical data for both wave height (Polperro) and wind speed (Mt Batten), are undertaken to model the uncertainty and explore the contribution to overall inundation levels.

A further aim of the project is to compare the hazard posed by storm surges with the hazard posed by tsunamis to south-west England. Historically the stretch of

coastline between Newlyn and Devonport has been affected by tsunamis on several occasions, most notably as a result of the 1755 Lisbon earthquake (Borlase, 1761-1762; Devonport Management Ltd, 2003; DEFRA, 2005). Unlike tidal records, were the data is near continuous for the length of the record, tsunamis records are separated by long time periods without any further occurrence. An analysis of the tsunamis hazard by DEFRA (2005), identified the largest event to be approximately 1 m for south west England. However, historical accounts of the 1755 and 1761 tsunamis (Borlase, 1755-1756; Borlase, 1761-1762; Huxham, 1755) indicate a magnitude of between 1 m to 2 m at certain points along the south-west coastline. In addition to the historical accounts, a tsunami signal within the Newlyn tide gauge record has previous been identified (Dawson et al., 2000). Therefore, to supplement the historical records, a tsunamis model of the 1755 Lisbon Earthquake will be developed to evaluate the sensitivity of the south-west coastline to tsunami inundation.

Although weather systems can be considered chaotic (e.g. Ref), how a weather system generates a storm surge i.e. wind set up and barometric affect (pressure) is well understood. Furthermore, storm surge warnings within the U.K. are made up to 7 days in advance (Environment Agency, 2010). This is in contrast to a tsunami, were although the method of tsunami generation is known, the prediction of an earthquake that might generate a tsunami is poorly understood. Section 2.6 shows that similar magnitude earthquakes from the same source zone have generated a tsunami, where others have not. Despite this difference attempt have been made to utilise the historical record to understand the different magnitudes of a tsunami (e.g. Papadopsalous, 2003) or storm surges (e.g. Haige et al., 2010) and the frequency with which they might occur. This is termed within this study as a frequency magnitude relationship. The typical methodology to evaluate this relationship is to use statistical techniques such as Extreme Value Analysis (power law, Generalised Extreme Value) or Monte Carlo analysis. The significant difference between a tsunami and storm surge and therefore the applicability of a specific technique is that for a tsunami the record is often limited and spatially disparate, where as the analysis of storm surges, within this study utilises a homogenous data set of over 100 years of tide gauge records.

1.2.4 Visual Representation and Evaluation of Inundation Scenarios

A simple numerical representation of an inundation level is often difficult to visualise in a three dimensional environment and potentially has little meaning to the end user. To allow an effective comparison and the evaluation of the potential consequences of different inundation scenarios, including the affect of statistical uncertainty, requires the visualisation of the data and a form of measurement of the consequences of each scenario. For example to evaluate the cost-benefit of a possible flood mitigation scheme requires a comparison of the cost of implementing the scheme against the cost of a potential flood if the mitigation scheme was not in place. To evaluate the impact of different inundation scenarios and the statistical uncertainty, a large scale Geographical Information Systems (GIS) model will be developed incorporating Light Detection and Ranging (LIDAR) Elevation data and infrastructure data. The main output will be a measure for each scenario the area of building and land affected.

1.2.5 Evaluation of South-west England to Sea-level Rise

To provide a detailed comparison of the impact of the different inundation levels and the statistical uncertainties with the uncertainties within different sea-level rise predictions, the sea-level rise calculate within this study and those of UKCP (2009) will be modelled within the same GIS system as the inundation levels. For each sea-level rise scenario the total area of land and buildings will be calculated, allowing a comparison of the sea-level rise and the statistical uncertainty of inundation level predictions. This will enable the dominant uncertainty in coastal processes to be identified; namely frequency magnitude prediction uncertainty or sea-level rise uncertainty.

1.2.6 Hazard Analysis Methodology and Applicability to Decision Makers

Wamsler (2014) identified that in the field of hazard and risk analysis there lacks “toolkits” that can be utilized by decision makers in the evaluation of hazard and risk. A final aim of this project is to provide a toolkit that will provide detailed methodology to analyse a specific hazard, evaluate the uncertainty and model

within a GIS. An approach will be identified that will allow the incorporation of uncertainty in to planning and design.

1.2 Outline of Project

To evaluate the uncertainty within statistical analysis, an important component is to understand the data set, and the different components that produce the observations. Chapter 2 outlines the components that make up observed inundations levels, separating out the components of observed sea levels recorded via tide gauges in to the individual components of astronomical tides, storm surges and mean sea level and identifies how tsunamis and waves contribute to inundation levels. Chapter 2 discusses each component and the literature. Chapter 3 reviews the relevant techniques of statistical analysis and visual representation, demonstrating what information can be derived from the observed sea-level data sets and how this information can be illustrated. Using the observed sea-level data sets and the techniques identified in Chapter 3, Chapter 4 outlines the methodology to evaluate sea-level rise, storm surge magnitudes, wave magnitudes and how this can be visualised within a GIS. The results are split in to two separate chapters. Chapter 5 focuses on the result of the statistical data analysis. Chapter 6 develops a range of inundation scenarios incorporating storm surges, waves and sea-level rise, including a comparison with tsunami inundation levels and evaluates them within a Geographical Information System (GIS), allowing the identification of the dominant uncertainty on inundation levels. The discussion within Chapter 7 aims to focus firstly on the different techniques used to evaluate storm surge magnitudes, their applicability to use within south-west England and how these techniques might be applied to sites with a limited data set. To validate the outputs from Chapters 5 and 6, a comparison is made between the predictions made within this study and the south-west storm surges of January and February 2014. The focus then shifts to the sensitivity of south-west England to the different predictions of storm surges and sea-level scenarios, based on the output from the GIS analysis. Chapter 8 concludes the study by summarising the finding, discussing how the results and approaches used within this study can be utilised for planners, designers and decision makes in the evaluation of uncertainty for a variety of natural hazard phenomena, e.g. rivers and landslides.

Chapter 2 Observed Water Levels at Tide Gauges

2.1 Introduction

Tide gauge data play a key role in understanding coastal processes and have been used to evaluate several factors including sea-level rise (Gehrels & Woodworth, 2013) and storm surge predictions (Haigh et al., 2010). To analyse the potential affect of uncertainty in frequency magnitude prediction on the south-west England under different sea-level rise scenarios, and to provide an insight into the wealth of information that can be derived from tide gauge data, requires a detailed understanding of the observed water levels at a given point in time.

The observed tide at any given time can be represented as the combination of two components (Figure 2.1), a gravitational tidal component and a meteorological component, with the mean sea level being an average over time of the observed sea level.

The following formula provides a simple representation of the water levels observed at a given location (Pugh, 1987):

$$X(t) = Z_o(t) + T(t) + S(t) \quad (2.1)$$

Where $X(t)$ = observed level.

$Z_o(t)$ = mean sea level.

$T(t)$ = tidal component (gravitational).

$S(t)$ = meteorological surge component.

Chapter 2 outlines the component of observed water levels recorded at tide gauge locations highlighted in equation 2.1 and illustrated in Figure 2.1. Section 2.2 discusses the individual components of astronomical tide and provides introduction to the theory of tides and the prediction of tides at a given location. Mean sea level and the changes in mean sea level over time are evaluated in Section 2.3, with Section 2.4 explaining the theory of storm surges; the history of storm surges within the U.K. and the south-west of England, and previous evaluations of the uncertainty within frequency magnitude predictions. Additional phenomena that contribute to inundation levels including wave height and wind set up (Section 2.5), and tsunami

(Section 2.6) are also highlighted. Accompanying each component, literature relating to previous analysis, predictions and uncertainty is examined to provide background context to the purpose of understating the components of the observed levels at tide gauge stations.

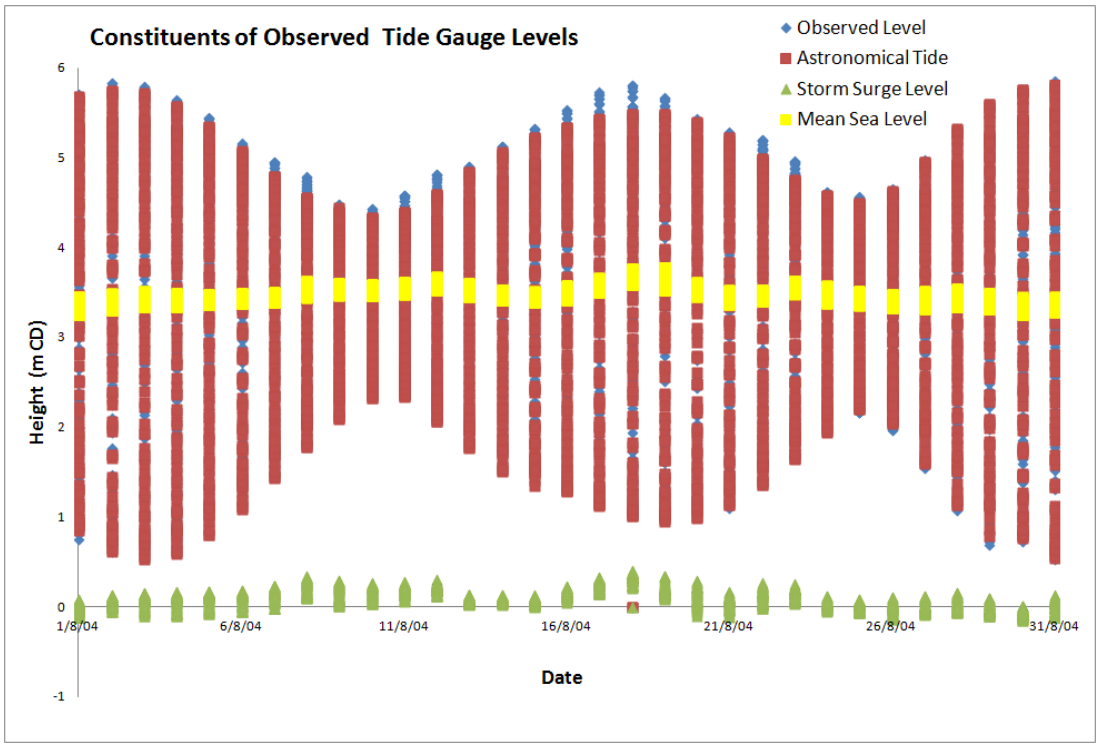

Figure 2.1 A graphical representation of the constituents of observed water levels at tide gauges, showing the raw observed data, the astronomical tidal component and the extracted storm surge and mean sea-level components.

2.2 Astronomical Tide

The theory of tides is based on Newton's theory of gravitation and the equations of fluid motion developed by Euler (Reeve et al., 2012). A summary of the theory of tides is given below, for more detailed information refer to Reeve et al., (2012) and Boon (2011).

If initially only the forces acting on the Earth-Moon system are considered and it is assumed that both the Earth and the body of water covering the Earth is frictionless, then the body of water would be free to deform in response to the forces acting upon it (Boon, 2011). Due to the gravitational forces of the Moon the water body would deform and reach an equilibrium state, simplistically illustrated as two bulges (Figure 2.2a). At the same time, the Earth's gravity acts offsetting the deformation until an equilibrium is reached, resulting in a prolate spheroid for the water body with the axis aligned with the Earth-Moon centre line. The Earth is free to rotate through the water body, so a person stood at a point on the Earth's surface would observe as the Earth rotates, two high and two low tides, known as a semi-diurnal tide. However, the Moon is inclined with respect to the Earth, known as the Lunar Declination. This declination leads to the bulge being inclined along the Earth-Moon axis (Figure 2.2b). This declination leads to one high tide being greater than another (diurnal inequality) and in the extreme case this can give rise at certain locations to only one high tide (diurnal tide). A further cycle occurs over a period of 27.55 days, as the Moon moves from being closest to the Earth, where the forces are stronger producing a greater than normal tidal range (Perigrean tides), to where the Moon is furthest from the Earth, producing a smaller tidal range (Apogean Tides).

In addition to the Moon, the Sun's gravitational forces affect the range of astronomical tides. By the principle of superposition of forces, when the lunar and solar forces are in line they act along the same axis extending the prolate spheroid (Reeve et al., 2012). This gives rise to a greater tidal range and these are known as spring tides. When the lunar and solar forces are at right angles, the tidal range will be smaller, producing neap tides. The location of the Moon and Sun relative to the Earth to produce spring and neap tides is illustrated in Figure 2.2c and 2.2d, respectively.

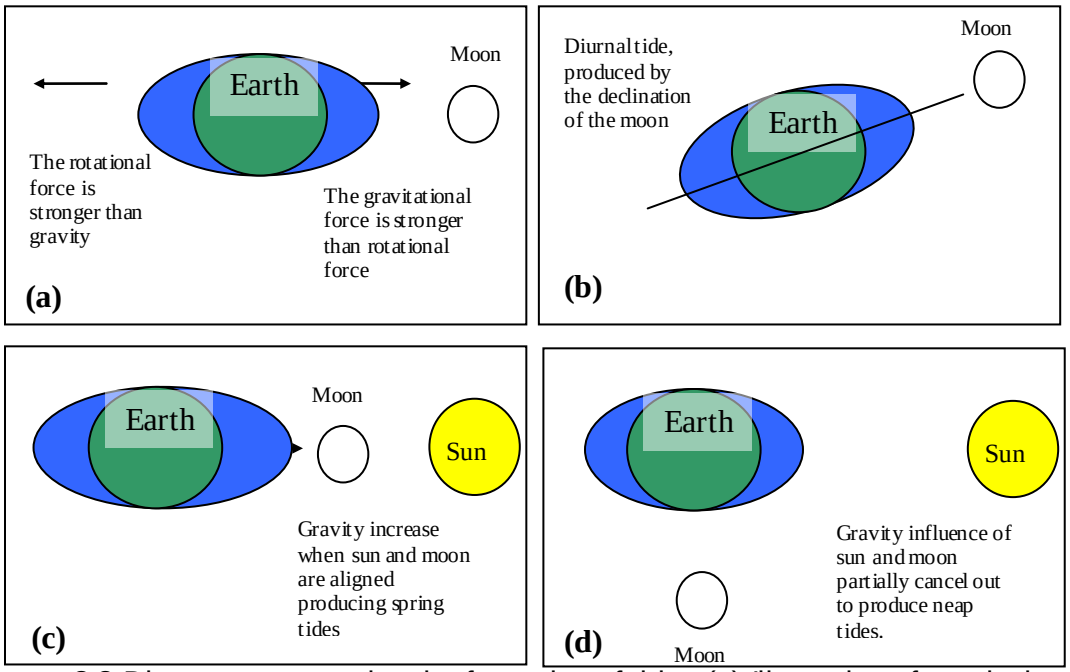

Figure 2.2 Diagram representing the formation of tides (a) Illustration of gravitation and rotation forces due to the moon (b) the affect of the moons declination to produce diurnal inequality. The alignment of the sun and moon to produce (c) spring tides and (d) neap tides.

Considering tidal components to be only comprise the gravitational forces of the Sun and Moon, and that these forces are constant is over simplistic. The predicted tide can also be affected by the declination of the Sun and Moon, plus the orbits of the Sun and Moon are elliptical and therefore the distance from the Earth and thus the forces vary. Each of these components is called a tidal constituent and for some locations there are over 60 in a given year (Kamphuis, 2006). Typically to model all the constituents requires an analysis of 18.6 years worth of data (Kamphuis, 2006). To allow a tidal prediction requires an analysis of each of the constituents and can be represented by the harmonic summation:

$$N_T(t) = \sum_{i=1}^{I} a_i \cos(\omega_i t + \alpha_i) \qquad (2.2)$$

Where: $N_T(t)$ is the tidal water level at time t,

α_i and a_i are amplitudes and phase angles of the tidal constituents.

ω_i are the angular frequencies (Kamphuis, 2006).

For the purpose of this study a tidal prediction software package POLTIPS (POL, 2007), which undertakes a harmonic summation of the tidal constituents for the sites of interest, has been used to generate the predicted astronomical tides. Summary tidal predictions for Devonport and Newlyn are given within Table 2.1.

	Devonport (mCD)	**Newlyn (mCD)**
Highest astronomical tide	6.05m	6.13m
Mean high water springs	5.53m	5.54m
Mean high water neaps	4.43m	4.34m
Mean low water neaps	2.23m	2.01m
Mean low water springs	0.80m	0.80m
Lowest astronomical tide	0.14m	0.18m
Conversion factor CD to ODN	-3.22m	-3.05m

Table 2.1. Summary predictions of the tides at Devonport and Newlyn (NTSLF, 2013).

2.3 Mean Sea Level

Mean sea level is the average observed sea level at a given location over a given period of time. Where coastal engineers were previously concerned primarily with storm surge and wave heights for the design of coastal structures, now due to the observed change in sea level the design needs to take into account potential future changes in mean sea level (Reeve et al., 2012).

The change in mean sea level is controlled by two components:

Eustatic Sea-level rise due to global temperature change: this is composed of the following constituents: thermal ocean expansion; melting of glaciers and ice caps in Greenland, and Antarctic ice sheets. All but the latter in most models increase mean sea level.

Isostatic The re-adjustment of a land mass caused by the unloading of the land from the last ice age. In areas formerly glaciated such as Canada, land is rising at a rate that can exceed 10 mm/y, adjacent areas to the ice sheet are subsiding at rates as high as 2-5 mm/yr (Houston and Dean, 2012). The presence of ice sheets over northern U.K has caused the land to rise relative to the sea in North England and Scotland and the land to fall relative to the sea in South and South-West England (Woodworth, 2006).

2.3.1 Eustatic Sea-Level Change

The Late Holocene provides a base line for the observations of recent sea-level change over the last 200 years. An analysis of the sea-level change from salt marsh records from both the northern and southern hemisphere spanning the last 2000 years indicates that sea-level change has been fairly constant with an average increase of 0.1 to 0.2 mm/yr. Meyssignac and Cazenave (2012) evaluated palaeo-climate data and estimated that sea levels rose between 0.05 m and 0.07 m per century over the last 2000 years. However, there is significant variability in the timing of when rates of sea-level rise started to increase above the background rates of the Late Holocene. Jeverjava et al., (2008) in a review of sea-level records of the last 300 years identified an acceleration in sea level within the records of 0.01 mm/yr^2, which appeared to have started at the end of the 18th Century. By contrast, Woodworth et al., (2009) identified evidence for acceleration that commenced around 1920-1930, with a decrease in the rate centred around the

1960's. The date when the sea-level change increased above the background of the late Holocene is confirmed by Gehrels & Woodworth, (2013) found by combining paleo sea-level records and tide gauge records that sea level began to rise between 1905 and 1945.

The background rate of the Late Holocene is significantly lower than the rate observed from tide gauges over the last 200 years. Church and White (2006), in a review of global tide gauge records for the period 1950-2000, combined with Altimetry data for 1992-2000 found an average sea-level change of 1.8 mm/yr +/- 0.3 mm/yr. Holgate (2007) identified a trend from 1904 to 2003 of 1.74 mm/yr. However, analysing a subset of the data Holgate (2007) identified variable rates of sea-level rise, with rates between -1.49 mm/yr centred on 1964 and +5.31 mm/yr centred around 1980.

Drawing the evidence together there appears to be a consensus that the rate of sea-level change over the last century is between 1.7 mm/yr (Church and White, 2011) and 1.8 mm/yr (Meyssignac and Cazenave, 2012). This would give a sea-level rise for the period 1900-2010 of between 0.17 and 0.21 m.

In the various analyses of sea-level records, there have been attempts to identify accelerations within the data set. Depending on the choice of data set, length of data set and the method of analysis varying results have been documented (IPCC, 2007). Based on a 60 year period of oscillation that takes in to account the main components of variability an acceleration component has been identified within the sea-level records. The acceleration varies between: 0.000 mm/yr^2 (Ray and Douglas, 2011) and 0.013 mm/yr^2 in the Jevrejeva et al., (2008) analysis. The results of Jevejava et al., (2008) are comparable to the rate identified in Church and White (2011) of 0.012 mm/yr^2 .

Based on an analysis of satellite altimetry data for the period 1992-2010 there appears to be an increase in the rate of sea-level rise over this time period. Meyssignac and Cazenave (2012) identified a rate of 3.2 mm/yr +/- 0.5 mm. This rate is comparable to the rate of Church and White (2011) for the same period and Jeverjava et al., (2008) for the period 1992-2002. Both Church and White (2011) and Jeverjava et al., (2008) conclude that there is good agreement when comparing to the tide gauge data for the same period with Church and White (2011) identifying a rate of 2.8 mm/yr +/- 0.8 mm/yr. IPCC (2007) caution that this rate, being based

on altimeter readings alone, does not necessarily reflect a recent acceleration in sea-level rise

Rates of sea-level change for the U.K have been assessed by several authors (e.g. Holgate, 2007), with the most comprehensive study having been undertaken by Woodworth et al., (1999, 2009). Woodworth et al., (2009) in an update of the tide gauge data analysis undertaken in 1999, analysed sea-level trends for the U.K from tide gauge data and found sea-level rates of between -0.68 mm/yr and 2.73 mm/yr. Excluding isostatic rates Woodworth et al., (2009) identified an average rate for the U.K of 1.4 mm/yr +/- 0.2 mm/yr. Within the three longest records Woodworth et al., (2009) calculated an acceleration component of between 0.0062 mm/yr^2 and 0.0096 mm/yr^2. In an analysis of sea-level change for tide gauge sites around the English Channel Haigh et al., (2009) found comparable rates of between 0.8 mm/yr and 2.3 mm/yr. In their study Haigh et al., (2009) identified that higher rates of sea-level rise within the more recent records are comparable with the rates identified within subsets of the complete data set, supporting the assessment of the IPCC (2007), that the higher levels in the analysis of interferometry data is not necessarily indicative of an acceleration.

2.3.2 South-West England Rates

Woodworth, (1987) calculated mean sea-level rise for Newlyn at 1.72 mm/yr for the period 1919-1982, for Devonport the value was 0.8 mm/yr for the period 1962-1982. Subsequent work by Woodworth et al., (1999) observed trends at Newlyn for the period 1991-1996 giving an average of 1.68 mm/yr +/- 0.12 mm/yr. For Devonport a value of 1.24 mm/yr +/- 0.85 mm/yr was calculated for the same period. Woodworth et al., (2009) identified rates of 1.71 mm/yr and 2.65 mm/yr for Newlyn (1915-2008) and Devonport (1962-2008) respectively. These rates are comparable to the rates identified by Haigh et al., (2009).

2.3.3 Future Eustatic Sea-level Change

Based on four world scenarios, known as SRES A1, A2, B1 and B2 sea-level rise was calculate based on a projected temperature rise for each scenario (IPCC, 2007). IPCC (2007) calculated sea-level rise by 2100 ranged between 0.18 m and 0.59 m. Within the report it cautions that the value of 0.59 m should not be considered as the upper bound as it does not include unknown or poorly understood

factors including changes in ice flow dynamics, which could contribute between 0.1 m and 0.2 m by 2100.

A United Kingdom specific assessment was undertaken as part of U.K. Climate Program in 2009 (UKCP 2009, 2009a). Based on low, medium and high scenarios a range of sea-level rise between 0.11 m and 0.78 m was produced, with a mid-range estimate of between 0.30 m and 0.46 m. To combat the uncertainty with the upper bound projection, the UKCP (2009) developed an upper bound scenario known as H++. This scenario was developed to undertake an assessment of vulnerability to an extreme sea-level rise. The scenario produced a range of sea-level rise of between 0.93 m and 1.8 m. This scenario is considered highly unlikely although no specific probability was applied.

The H++ of UKCP (2009) scenario is considered by Nicholls et al., (2011) who concluded that due to uncertainty in the climate models including the response of the large ice sheets of Greenland and Antarctica that large increases in the 21st Century cannot be ruled out. Nicholls et al., (2011) estimated for a temperature rise of 4 degrees (within the global range of temperatures modelled in the SRES scenarios) that global sea level could rise between 0.5 m and 2 m by 2100.

2.3.4 Isostatic Adjustment

To provide an estimate of late Holocene land level changes Shennan and Horton (2002) undertook an analysis of over 1200 radio-carbon dated Holocene samples thought to have formed at approximately mean sea level, for 52 locations throughout Great Britain. The analysis identified a maximum level of uplift rate for central western Scotland of 1.6 mm/yr with a maximum subsidence rate in south-west England of approximately 1.2 mm/yr.

Shennan et al., (2012) update these rates based on a revised Glacial Isostatic Adjustment model (Bradley et al., 2011). Based on this model the maximum uplift rates for central and western Scotland was reduced from 1.6 mm/yr to 1.2 mm/yr with the maximum rates of subsidence for south west England reduced from 1.2 mm/yr to 1.1 mm/yr.

In an alternative approach Teferele et al., (2006) looked at Continuous GPS (CGPS) and Absolute Gravity (AG) data from a data set of over 40 stations throughout the

U.K .over the time period of 1995 to 2005. For the south-west of England they found isostatic adjustment rates of between 0.0+/-0.5 mm/yr based on CGPS and -0.5+/-0.9 mm/yr for the AG data. Teferele et al., (2006) compared the rates obtained from CGPS and AG with the rates for Newlyn calculated by subtracting the global sea-level rise average from the observed sea-level rise trend at Newlyn and identified that theoretically subsidence rates at Newlyn should be of the order of 0.2 mm/yr. Teferele et al., (2009) revisited the data set, incorporating a correction factor based on a comparison between the velocities of the CGPS and the AG data. This gave a corrected value of subsidence for Newlyn between 0.4 and 0.5 mm/yr. A nearby station of Camborne, Cornwall gave a value between 0.7 and 2.1 mm/yr.

The United Kingdom Climate Change Programme (UKCP, 2009) considers isostatic adjustment in their guidance on relative sea-level rise for the U.K. UKCP (2009) adopted the findings of Bradley et al., (2009), who modelled the vertical movements based on a Glacial Isostatic model and compared the data with the CGPS data of Teferele et al., (2009). Based on UKCP (2009) vertical land movement for the study area ranges between -1.2 mm/yr and 1.0 mm/yr.

2.3.5 The North Atlantic Oscillation (NAO)

A significant component of the variability observed within the tide gauge records of the United Kingdom and the subsequent analysis can be related to the North Atlantic Oscillation. The North Atlantic Oscillation (NAO) refers to the redistribution of atmospheric mass between the Arctic and the subtropical Atlantic and is a leading pattern of weather and climate variability over the Northern Hemisphere (Hurrell et al., 2001; Hurrell and Deser, 2010). The change in atmospheric mass can produce significant changes in surface air temperature, winds, storminess and precipitation over the Atlantic and adjacent areas. Figure 2.3 shows the possible effects of a positive and negative NAO, with Figure 2.4 showing the normalised pressure index between Lisbon, Portugal and Rekyavik, Iceland which the NAO is measured against.

A positive NAO index is associated with a northward shift in Atlantic storm activity with increased storm activity from southern Greenland, Iceland and into northern Europe (Hurrell and Deser, 2010). The recent upward trend of the NAO represents a significant fraction of the temperature increase observed during the time period. This leads to issues in calculating trends including wave height, storm surge

intensity and sea-level rise while taking in to account the variability linked to the NAO (Hurrell and Deser, 2010; Woodworth et al., 2007). Analysis of pressure changes within the U.K. and Iceland indicates that the records show trends towards larger magnitude events in recent decades, with a particular increase in southern regions of the U.K (Alexander and Tett, 2005). The greatest increase in storm events has occurred since 1950, with the changes in severe winter storms (Nov-Feb) showing a strong correlation with changes in the North Atlantic Oscillation. The dependence of storm surges magnitudes and the NAO is confirmed by Woodworth et al., (2007) who found that storm surges show an increase with an increase in the magnitude of a positive NAO. In addition to storm surges, the recent upward trend towards more positive NAO winters has been associated with increased wave heights over the north Atlantic (Hurrell and Deser, 2010).

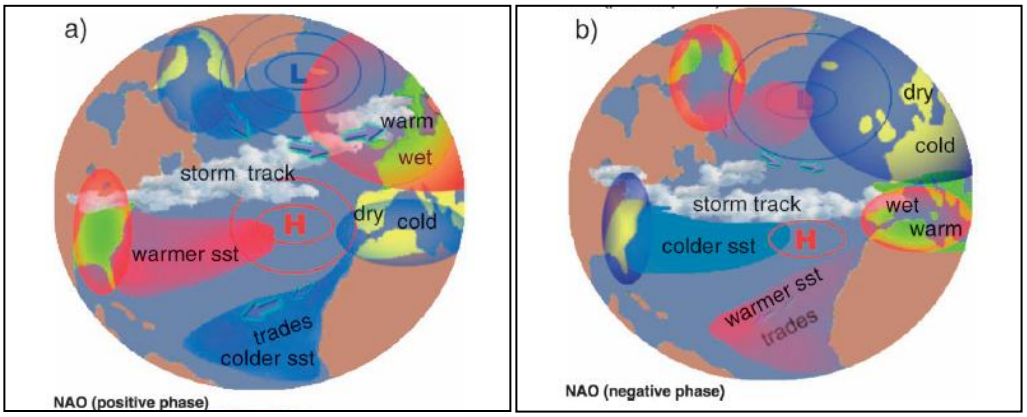

Figure.2.3. General structure of the positive and the negative phases of the North Atlantic Oscillation, showing centers of high and low pressure together with significant anomalies in atmospheric and oceanic conditions (Bojario and Gimero, 2003).

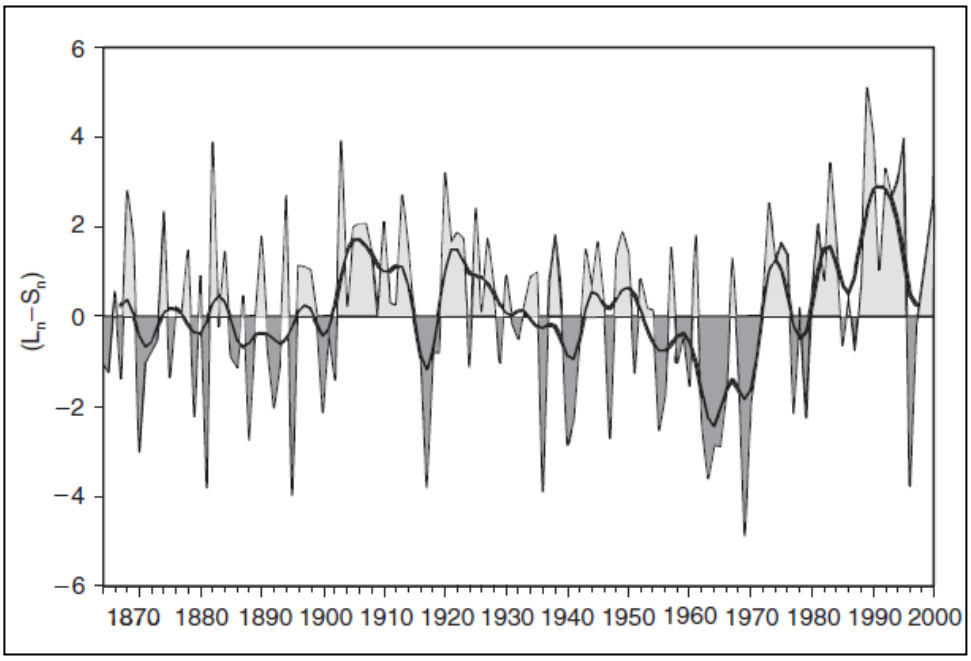

Figure 2.4 Winter (December–March) index of the NAO based on the difference of normalized sea-level pressure between Lisbon, Portugal, and Stykkisholmur/Reykjavik, Iceland from 1864 to 2000. The heavy solid line represents the index smoothed to remove fluctuations with periods >4 years (Hurrell, 2001).

2.4 Storm Surge

2.4.1 Introduction

In England and Wales alone it is estimated that 1.8 million residential properties, 140,000 commercial properties, 1.4 million hectares of agricultural land are at risk from flooding, equating to approximately 4-5 million people and a total capital value of £222 billion are currently at risk of flooding (DEFRA, 2006). Furthermore, DEFRA (2006) estimate that within the south-west of England £9 billion worth of assets are at risk, with average annual damages in the order of £51 million, with the influence of climate change this could increase to £60 million annually by 2075. Over £500 million is spent each year on flood defence in the UK, and the total annual cost of flooding has been estimated at over £1 billion (Purvis et al., 2007).

The following Sections define what a storm surge is and provide details to the main causes that contribute to storm surge levels. To place storm surges in to context, examples of storm surges around the U.K, with specific reference to the study area are outlined including the effect on coastal communities.

2.4.2 Storm Surge Definition

Figure 2.1 shows graphically the components of an observed sea level, broken down in to the astronomical, sea-level rise and storm surge component. To define a storm surge, Formula 2.1 can be rearranged:

$$S(t) = X(t) - Z_o(t) - T(t). \qquad (2.3)$$

This formula shows that a storm surge is the difference between the observed water level and predicted tide component (Pugh, 1987). Law (1998) defined a storm surge as a change in sea level resulting from meteorological conditions rather than astronomical tides.

A storm surge can be separated into two main causes that contribute to a change in sea level, atmospheric pressure and wind set up, also known as wind surge. There are other contributions that cannot easily be quantified, including bathymetry and the shape of the coastline, and therefore are excluded from consideration. How wind set up and atmospheric pressure changes contribute to the overall level observed at tidal gauges are described below.

2.4.2.1 Responses to Atmospheric Pressure

When the surface of water is loaded with a force, the level of the water will decrease proportionally to the size of the force. Changes in atmospheric pressure produce changes in the forces acting vertically on the sea surface. The conversion between changes in atmospheric pressure and changes in sea level is given by Pugh (1987):

$$\Delta\varsigma = -0.993\Delta P_a \qquad (2.4)$$

where $\Delta\varsigma$ = change in sea level (cm).

ΔP_a = change in atmospheric pressure.

This means that a decrease in 1 millibar of pressure will produce an increase in sea level of 1 cm. This relationship is called the inverted barometer effect or static sea-level response.

Typical values for the year range between 980-1030 mb, taking standard pressure of 1013mb gives a range of sea-level changes of +0.33 m to -0.17 m. The 1953 storm surge had a minimum pressure of 970 mb (43 mb below average) contributed 0.43 m to the overall storm surge (Environment Agency, 2012).

2.4.2.1 Wind Set Up

Wind set up is the result of frictional forces of wind acting over a body of water and is given by the formula Pugh (1987):

$$\frac{\Delta\xi}{\Delta x} = \frac{Cd * pa * W^2}{g * p * D} \qquad (2.5)$$

Where $\frac{\Delta\xi}{\Delta x}$ = wind set up.

C_d =drag coefficient given by 10^3 C_d =0.63 +0.066W (Pugh, 1987).

P_a = air density.

P = density of water.

W = wind speed.

D = water depth.

From equation 2.5 it is apparent that the controlling factors are wind speed and water depth; the greater the wind speed the greater the wind set up; the shallower the water body, the greater the wind set up.

2.4.3 United Kingdom Historical Storm Surges

Lamb (1991) catalogued storms within the North Sea and surrounding coasts, identifying 166 storms over the last 5000 years. The affects of these storms ranged from the flood of 120BC which potentially caused the migrations of the Celtic population from North West Germany to the "All Saints Flood" of 1570 where the entire coast of the Netherlands was flooded between Flanders and Groningen, and up to the northwest of Germany. A more detailed record for the U.K. was produced by Zong and Tooley (2003), who identified over 500 storm surge events around the British Isles for the period 1792 to 1990.

The most significant coastal flood event to have affected the U.K., and described as the worst peace time disaster (Pollard, 1978), occurred on the 31st January 1953, resulting in over 300 deaths in Britain and over 2000 in Holland (Steers, 1953). It was estimated that approximately 15 billion m^3 of water was forced in to the north sea (Rossiter, 1954), with an estimated wind set up in the region of 2 m (Pugh, 1987). The total surge height ranged between 0.9 m and 2.5 m, however, as the peak surge did not combine with a high astronomical tide the inundation levels were not as high as they could have been (Pugh, 1987).

2.4.4 South-West England Storm Surges

Table 2.2 is a combined record of storm surges that have affected the south-west of England based on the records of Zong and Tooley (2003) and Lamb (1991), supplemented by a search of local newspaper archives as part of the research undertaken for this thesis. Over the period 1703-2014 these records identified 30 storm surges that have affected south-west England. It should be noted that half the recorded events post date 1945.

An indication of the affect of storm surges on the study area is given by the 27th October 2004 storm surge. This event was claimed to be the one of the "worst storm surges the region had experienced for nearly 25 years (Western Morning News,

2004), and was probably the most severe since 1991. The maximum observed levels at Newlyn and Devonport were 6.42 mCD and 6.35 mCD, respectively. This represented a storm surge of approximately 0.8 m at Newlyn and 0.7 m at Devonport. Flooding occurred all across south-west England, including Newlyn, Penzance, Torquay, Dawlish and as far as Lyme Regis (Western Morning News, 2004; Evening Herald, 2004). One of the worst affected areas was Looe in Cornwall, where over 30 properties including commercial establishments were flooded. Transport infrastructure was also severely affected with coastal roads closed, the main Plymouth to Exeter train line closed at Dawlish and the ferries between Plymouth and Roscoff in France suspended (Western Morning News, 2004; Evening Herald, 2004). The significant affect of a relatively frequent storm surge, possibly between 1 in 25 to 1 in 50 year event, raises the question of what might be the affect if a larger storm surge, coupled with an increase in sea-level rise occurred in the south-west of England.

The recent storms of January and February 2014 are discussed in Chapter 7 and used as a method to validate the findings of the study.

2.4.5 Storm Surge Predictions for South-West England

Several storm surge predictions have been made for south-west England. The Environment Agency (2012) give guidance for Newlyn and Devonport based on the Spatially Revised Joint Probability methodology of Dixon and Tawn (1997). For a 1 in 200 year storm surge event a value of 3.66 mODN and 3.69 mODN was adopted for Newlyn and Devonport, respectively. For a 1 in 1000 year event a level of 3.85 mODN and 3.96 mODN is given. Devonport Royal Dockyard Ltd undertook two separate studies that predicted for a 1 in 10,000 year event a level of 3.97 mODN (DML, 1997) and 4.20 m (DML,1999). The later value is based on the predictions and methodology of Dixon and Tawn (1997). Whitworth et al., (2005), using a Gumbell Type 1 distribution, calculated a value of 3.97 m ODN for Devonport.

Date	Location	Source
Dec 6th/7th 1703	Cornwall and Devon. Destroyed Eddystone Lighthouse	Lamb, 1991
Oct 11th 1811	Exmouth, Budleigh Salterton	Zong and Tooley, 2003
Dec 25th 1821	Plymouth, Cawsand	Zong and Tooley, 2003
Nov 22nd 1824	Sidmouth, Plymouth	Zong and Tooley, 2003 Evening Herald Anon, published by The Religious Tract Society, London, 1824
Oct 20th 1846	Devon and Cornwall	Lamb, 1991
Oct 25th 1859	Devon and Cornwall	Lamb, 1991
Jan 10th 1866	Torbay	South Devon Times
Jan 24th 1868	Cornwall	Lamb, 1991
Jan 5th 1867	Portland, Weymouth, Penzance	Zong and Tooley, 2003
Oct 19th 1875	Dawlish	Zong and Tooley, 2003
Feb 3rd 1904	Weymouth, Portland, Penzance	Zong and Tooley, 2003
1917	Hallsands	Zong and Tooley, 2003
Dec 21st 1945	Dawlish, Teignmouth	Zong and Tooley, 2003
Jan 29th 1947	Looe, Saltash, Brixham	Zong and Tooley, 2003 Western Morning News
Jan 29th 1948	Looe, Saltash, Brixham	
Dec 10th 1957	Saltash, Devon	Zong and Tooley, 2003
Oct 8th 1960	Exmouth, Torquay	Zong and Tooley, 2003
Feb 10th 1974	Dawlish	Zong and Tooley, 2003
Sept14th 1976	Polperro	Zong and Tooley, 2003
Oct 14th 1976	Torquay	Zong and Tooley, 2003
Jan 4th 1978	Torcross	Zong and Tooley, 2003
Dec 1981	Devon and Cornwall	Western Morning News/Evening Herald
20th Dec 1989	Sidmouth, Dawlish, Kingsbridge, Dartmouth, Plymouth	Zong and Tooley, 2003 Western Morning News
25th Jan 1990	Localised Areas of Devon and Cornwall	Western Morning News
Sept 12th 1993	Torquay, Brixham	Western Morning News
Oct 29th 1996	Devon and Cornwall	Western Morning News
Oct 28th 2004	Penzance, Looe, Devonport, Torbay	Evening Herald
Jan 18th 2007	Devon and Cornwall	Evening Herald
Jun 27th 2011	Cornwall- Seiche/Tsumani	Evening Herald/Daily Mail
Jan/Feb 2014	Devon and Cornwall	Plymouth Herald, BBC

Table 2.2 Historical Records of Storm surges for Devon and Cornwall.

2.5. Wave Height

Waves can cause significant damage to structures (BBC, 2014) and lead to increase in flood levels and overtopping at coastal locations (Reeve et al., 2012). There are two components related to waves that are of interest to this study, firstly the wave amplitude and secondly wave set up.

Waves are generated by the wind acting over the surface of the oceans, as waves approach the shoreline their height and wavelength are altered by the process of refraction and shoaling before breaking on the shore where the waves generate wave set up, raising the mean water level (Reeve et al., 2012). This process is illustrated in Figure 2.4. For a 5 m wave the wave set up can be of the order of 1.3 m. For detailed wave theory see Reeve et al., (2012) and Kamphuis (2010).

The issue of wave heights at a given location is further complicated by the role of climate change and sea-level rise. An analysis of global trends of wind speed and wave height based on 23 years worth of altimeter readings, identified a global trend of increased wind speeds, and to a lesser extends wave height. However, the greatest rate of increase in wave height was observed at the extremes when compared to the mean (Young et al., 2011). The global trend of increased wave heights is also predicted to occur around the U.K with a small increase in average wave height predicted for south-west England, with an estimated increase of 1m in the annual maximum (UKCP, 2009). With an increase in mean sea level, the point at which a wave breaks increases and migrates towards the shoreline meaning that greater forces will act on coastal defence. The wave energy and thus the forces could potential increase by 2% for a 3.5 mm/yr rise; 4% for a 7 mm/yr rise and 12% for a 19 mm/yr rise by 2090 (Chini et al., 2010; Chini and Stansby, 2012).

A network of wave buoys record wave height at a variety of locations throughout the UK (BODC, 2014, CCO, 2014). This data can be used to predict wave heights at specific locations. As wave height is the key input in to wave set up the data set can also be used to calculate the increase in mean water level and the affect on inundation levels for the study area. How the wave data set can be used to evaluate wave height magnitudes for a variety of return period is given in Section 3.1.

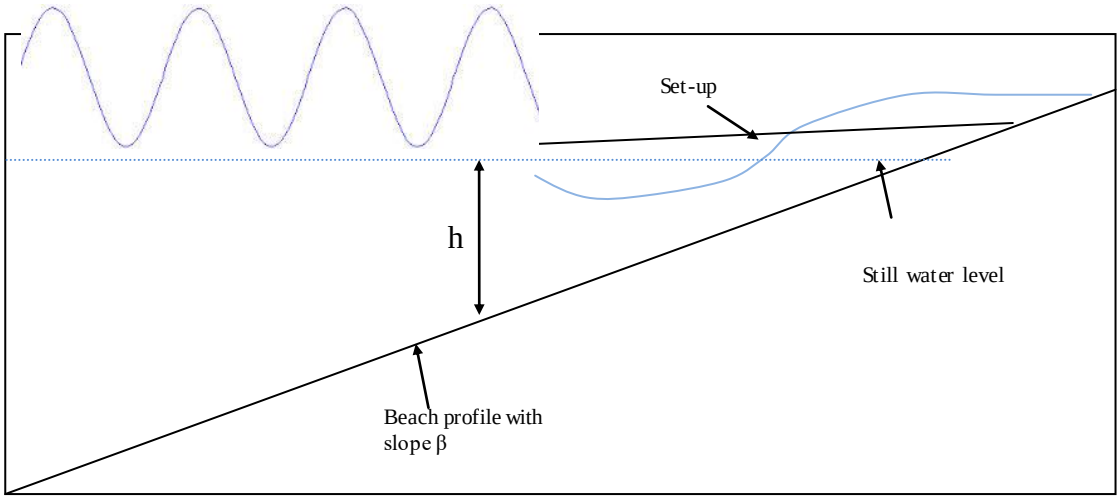

Figure 2.5 Schematic of waves and wave set up at a coastal location.

2.6 A Special Flood Case-Tsunami

2.6.1 Introduction

A tsunami is a Japanese word that describes a 'harbour wave'. The term is used to describe a wave or series of waves that travel across the ocean with exceptionally long wavelengths (in the order of several hundred kilometres) (Dawson and Lockett, 2004). At the coast the inundation level caused by the tsunamis is a function of not only the wave energy but also the topography and bathymetry of the coastline (Dawson and Stewart, 2007). In the open ocean a tsunami wave travels at high velocities of the order of 700 km/hr, the tsunami has a very large wavelength (order of hundreds of kms), with an amplitude in the order of 1m. The wave speed is a function of water depth, so as the water depth decreases so does the velocity of the wave (Reeve et al., 2012; Kamphuis 2006). As the waves approach a shallow coast line the speed of the wave decreases and as a function of conservation of energy the height increases (known as shoaling in fluid dynamics). Due to the complexities of the coastline and the shoaling of the tsunami as it approaches shallow water the waves can reach significant heights leading to extensive inundation.

The main cause of a tsunami is due to a sudden sea floor disturbance caused by an earthquake, displacing the column of water above. Table 2.3 details the main causes of tsunamis generation.

(a) Offshore Earthquake associated with vertical displacement of the sea bed.
(b) Underwater Landslide.
(c) Onshore earthquake that causes (a) and/or (b).
(d) Asteroid impact.
(e) Landslide above sea/water level that descend rapidly into the sea/water i.e. a landslide descending into a dam.
(f) Volcanic eruption and/or volcanic crater collapse into the sea.

Table 2.3 Methods of Tsunamis Generation, adapted from Dawson and Lockett, (2004).

Tsunamis pose a different problem altogether when considering coastal flooding scenarios. A storm surge may be predictable up to seven days in advance, and

typically occurs in winter months, therefore coastal communities including the relevant authorities can anticipate the areas likely to be affected. In comparison a tsunami can occur at any time of year and due to the speed of a tsunami, the travel time from source to the coast can be extremely short. The estimated travel time from the source of the Lisbon earthquake and subsequent tsunami to south-west England was estimated to be 5 hours (Dawson et al., 2000), for the Portuguese coast it would have been significantly less.

The importance of tsunamis to coastal flooding in the U.K. is highlighted by the U.K. government response to the Indonesian Boxing Day Tsunamis (DEFRA, 2005). The U.K government through the Department for the Environment, Food and Rural Affairs (DEFRA) commissioned a study to evaluate the risk poised to the U.K by a tsunami event. The findings and conclusions are discussed below, including a comparison to an earlier study commissioned by Devon Management Ltd (DML, 2002). Prior to this, a case study on the Lisbon Earthquake and subsequent tsunami is presented as this forms the basis for many of the findings from the reports discussed.

The DEFRA (2005) report identified two possible source locations for tsunami generation for Cornwall and South Devon;

1. Tectonic plate boundary west of Gibraltar.
2. Volcanic flank collapse of La Palma in the Canary Islands.

DEFRA (2005) established that the most likely source for a tsunami would be the plate boundary west of Gibraltar. Movement on this boundary caused the Lisbon Earthquake of 1755, which represents the most significant event to have affected the south west of England over the past 500 years.

Other earthquakes along the plate boundary include:

- 11th November 1858 7.2 Ms: no tsunami reported.
- 25th November 1941 8.2 Ms: tsunami observed at Newlyn, maximum amplitude of 0.2 m.
- 28th February 1969 7.3 Ms: record lost from Newlyn.
- 26th February 1975 7.9 Ms: tsunami observed at Newlyn, Maximum amplitude of 0.06 m.

- Potentially large earthquakes in 1531 and 1344, however, no evidence that a tsunami reached Cornwall.
- Geological evidence of high magnitude tsunami circa 216-218 BC, and indication it was of a similar magnitude to the 1755 event (DEFRA, 2005).

2.5.2 Lisbon Earthquake 1755

On the 1st November 1755 at 9.20am an earthquake of approximate magnitude 8.5 (Sousa et al., 1992) occurred off the Portuguese coast. The earthquake had an epicentre along the Azores-Gibraltar Plate boundary, which forms part of the boundary between the Eurasian and African plate boundaries (Sousa et al., 1992; Dawson et al., 2000).

The majority of the destruction linked to the earthquake was caused by the tsunami generated. In Lisbon the tsunami was estimated to be between 5 and 13 m high and led to the loss of over 60 000 people. Large parts of coastal Morocco were also flooded. The tsunami also led to the loss of over 1000 lives along the Spanish coast. The affects of the tsunami reached as far as Barbados in the Caribbean. Eye witness accounts detailed in DML (2002) show that the tsunami reached Cornwall and Devon approximately 5 hours after the Earthquake, 2pm at Penzance (Borlase, 1755-1756, p373-385), and 4pm at Plymouth (Huxham, 1755-1756, p 371-373). Several tsunami waves were observed over a period of half an hour at Plymouth, (Huxham, 1755-1756, p 371-373). At Penzance over 4 fluxes were observed, with the full fury lasting for two hours, although the whole "commotion ceased about low water 5 and a half hours after" (Borlase, 1755-1756, p 373-385).

It is estimated that the first wave, although not the largest coincided with high tide (DML, 2002, Dawson et al., 2000). This is confirmed by Borlase, (1755-1756, p 373-385) who stated "a little after 2pm….about half our after ebb the sea was observed to advance suddenly from the eastward…". The run up height at its maximum is estimated to have been for Cornwall approximately 2 m. Borlase, (1755-1756, p 373-385) details reports of no run up at Mounts Bay, at Penzance it was observed to be 2-3 ft (~1m), and at Newlyn 5 ft (1.5 m). It should be noted that the distance between the three locations is 5 km. The level observed at Plymouth was between

1-2 ft (0.6 m) elevation. Huxham, (1755 to 1756, p 371-373) gave the following account at Plymouth:

"….At once quite dry in the mud though the minute or 2 before in 4 to 5 feet of water, in less than eight minutes the tide returned with the utmost rapidity and floated the boats so that they had near 6ft of water." (Huxham, 1755-1756, p 371-373)

A further earthquake in the vicinity of the 1755 earthquake occurred on the 31st March 1761, (Salvador, 1761-1762, p 135-140). The earthquake occurred at 12 o'clock and "lasted a full 5 minutes…about an hour and a half afterwards the sea began to ebb and flow about eight feet perpendicular" (Salvador, 1761-1762, p 135-140). A tsunami was observed at The Isles of Scilly, Mounts Bay, Penzance and Newlyn, at about 5pm, (Borlase, 1761-1762, p 418-433). Estimated levels were 5 ft (1.5 m) at the Scilly Isles and 6 ft (~2 m) at Penzanze and Newlyn (Borlase 1761-1762, p 418-433). DEFRA (2005) do not discuss this event, although it had previously been identified by Dawson et al., (2000).

Borlase, (1761-1762a, p 507-515) also noted "remarkable agitation of the sea" on the 28th July 1761, observing the sea flowing and retreating several times. The first agitation was observed to be about 6 ft. Interestingly Borlase, (1761-1762a, p 507-515) observed that "by the papers, the like agitations were felt in the harbours of Falmouth, Fawy (Fowey) and Plymouth". However, the trigger mechanism for this earthquake has not been identified. It is unlikely that it was an Earthquake along the plate boundary west of Gibraltar as accounts would be available similar to those of the 1st November 1755 and 31st March 1761 events. This suggests that these were triggered by another mechanism or a different plate boundary.

DEFRA, (2005) concluded that the maximum amplitude of tsunamis to affect the south-west coast would be between 0.8 m and 1 m, corresponding to the value given by DML (2002). This is lower than observations made by Borlase (1755-1756) and Huxham (1755-1756) of up to 5 ft or 1.5 m. Furthermore the approach of DEFRA (2005) of assuming a uniform level for the whole of the south-west coast is over- simplistic. Borlase (1755-1756) highlights how slight changes in the location can affect the observed levels (a difference of 5ft between locations 3 miles apart). This is further emphasised by DML (2002) which modelled the 1755 tsunami for Plymouth Sound, including the Tamar and Plym estuaries. Their findings showed

that for the Tamar the amplitude was approximately halved (1m to 0.5m), with the Plym showing amplification by about a third.

Although there is a limited historical record for the occurrence of tsunamis to have affected the south west of England, from the review above it is clear that there is the potential for the south west of England to be affected. A component of this study will be to compare the magnitude and frequency to storm surges and waves and how this might affect coastal inundation along the south west of England.

2.7 Discussion

Tide gauge records provide important information, and are a key data set in evaluating frequency magnitude relationships, mean sea-level changes and the degree of uncertainty. The tide gauge data records the observed sea-level at a given point in time and is comprised of three components:

1. Astronomical tide created by the gravitation forces of the sun and moon, which can be determined by a harmonic analysis of the different tidal constituents.
2. Mean sea level comprising two components:
    a) Isostatic adjustment due to the loading applied from previous glacial periods. For south-west England the predictions give a range of uncertainty of between 0 mm/yr to -1.0 mm/yr (- indicates subsidence).
    b) Eustatic due to the thermal expansion of the oceans and the melting of glaciers and ice caps. Current day sea-level rise is estimated to be approximately 1.4 mm/yr, with an acceleration component between 0 mm/yr^2 and 0.001 mm/yr^2. Future predictions of mean sea-level change point to a increase in mean sea level between 0.12 m and 0.78 m by 2100.
3. Storm surges predominantly caused by changes in atmospheric pressure and wind set up causing a rise (positive storm surge) or fall (negative storm surge) in the observed sea levels. Predictions for south-west England for a 1 in 10,000 year event indicate a range between 4.2 m ODN and 3.9 m ODN indicating an uncertainty range of 0.3 m.

In addition to the component of observed sea levels, inundation levels can be affected by wave height and wave set up and tsunami. Future uncertainty relating to the effect of climate change on wave energy indicates a range between 2% and 12% increase in wave energy by 2100 depending upon the scenario. Historical tsunami accounts from the 1755 Lisbon earthquake indicate the south-west could be affected by between a tsunami of height between 0.6 m (Plymouth) and 2 m (Newlyn). Present day assessments and modeling indicate a range between 0.8 m and 1.0 m, with a possible increase in amplitude by up to a third due to the shape of the coastline (i.e. Plym Estuary).

3.0 Introduction

Chapter 2 outlined the main constituents of tide gauge data and provided details of the information that can be obtained from the Devonport and Newlyn data sets. Chapter 3 provides background justification in the form of a literature review for both the statistical techniques used to predict storm surge and wave height magnitudes and the modelling techniques used to illustrate the affect the statistical predictions have on the coast of south west England.

3.1 Statistical Techniques

Typically statistical techniques utilise a data set in three ways:

1. A technique that utilises either the annual maximum, i.e. Generalised Extreme Value (GEV) Distribution, or a series of independent observations from a year, i.e. r-largest.
2. A technique that utilises data above a certain threshold, therefore does not limit the number of observations per year, i.e. Generalised Pareto Ditribution (GPD) also known as the Peak Over Threshold (POT).
3. A technique that utilises the complete data set, i.e. the Joint Probability method of a Monte Carlo analysis.

This research focuses on four main techniques ranging from use of only the annual maximum (GEV), to utilising up to 10 annual observations (r-largest) to utilising the full data set (Joint Probability and Monte Carlo analysis).

3.1.1 Extreme Value Analysis

Extreme Value analysis is a statistical technique that based on having an understanding of the probability of a series of observed data can allow extrapolation to evaluate the unseen highs and lows (extremes) of the data. The techniques are based on the assumption that a random variable X is said to be continuous, if it can take on an infinite number of possible values associated with intervals of real numbers and if there is a function f(x) called the probability density function such that (Schaeffer and McClare, 1995):

$f(x) \geq 0 \; for \; all \; x$

$$\int_{-\infty}^{\infty} f(x)dx = 1$$

$$P(a \leq X \geq b = \int_{a}^{b} f(x)dx$$

The probability density function (pdf) describes the probability of a specific outcome occurring. The probability of a specific outcome being less than or equal to x is given by the integral of f(x) and is known as the cumulative distribution function (cdf) (Schaeffer and McClare, 1995).

A commonly used distribution, because it is able to represent a large amount of real world data sets is the Normal Distribution. The Normal Distribution is represented by:

$$f(x) = \frac{1}{\sigma\sqrt{2\pi}} e^{\frac{-(x-u)^2}{2\sigma^2}} \qquad (3.1)$$

Where:

$\sigma = Standard \; deviation.$

$u = Mean.$

The standard deviation and the mean of the normal distribution are known as the shape parameters and can be used to evaluate the probability of occurrence of a give value of x.

Figure 3.1 illustrated the pdf and cdf for the types of extreme value distributions that comprise the GEV distribution.

3.1.2 Extreme Value Techniques

Typically there are 3 types of Extreme Value distributions that the different techniques attempt to fit the data to. These are collectively known as the Generalised Extreme Value Distributions which has the general form shown below (Coles, 2001):

$$f(x) = \exp\{-[1+\xi(\frac{x-\mu}{\sigma})]^{-\frac{1}{\xi}}\} \qquad (3.2)$$

The three parameters of the distribution are:

- A location parameter (μ).
- A scale parameter (σ).
- A shape parameter (ξ).

As $\xi \rightarrow 0$, the Type 1 (Gumbel) distribution is obtained; as $\xi > o$, the GEV is known as the Type 2 (Frechet) distribution and; as $\xi < 0$ the GEV is known as the Type 3 (Weibull) distribution.

The Weibull distribution has a finite value which means it decays to a point where the maximum value cannot be exceeded. The Gumbel distribution has no upper bound meaning therefore it can take on infinite high values. The Frechet distribution has no upper bound but due to the shape of the distribution can lead to high values with greater probability than would be obtained with the Gumbel distribution. Examples of the three distributions and their return level plots are shown in Figure 3.1.

One of the main drawbacks of the Generalised Extreme Value distribution is that it uses only the annual maximums and therefore it wastes a significant amount of relevant data (Reeve et al., 2012). To combat this limitation the r-largest approach was developed by Smith (1986). In an extension to the Generalised Extreme Value Distribution taking the r largest values for each year, the Generalised Extreme Value Distribution then takes the form:

$$f(z) = \exp[-\{1+\xi(\frac{x^{(r)}-\mu}{\sigma})\}^{-\frac{1}{\xi}}]\prod_{k=1}^{r}\frac{1}{\sigma}\{1+\xi(\frac{x^{(k)}-\mu}{\sigma})\}^{-\frac{1}{\xi}-1} \qquad 3.3$$

The three parameters (μ,σ,ξ) correspond to the parameters of the GEV model (Butler et al., 2006). For each year the selected r values must be selected from independent storm events.

An alternative methodology that incorporates values above a specific threshold is known as the Generalised Pareto Model or Distribution. Pickards (1971, 1975) is attributed with developing the arguments that lead to the Generalized Pareto Model for the Peak Over Threshold approach. In this approach a threshold is determined and the data above that threshold fitted to the Generalised Pareto distribution (GPD):

$$H(z) = 1 - \{1 + \frac{\xi(z-u)}{\tilde{\sigma}}\}^{-\frac{1}{\xi}} \quad (3.4)$$

Where x – u > 0 and $\tilde{\sigma} = \sigma + \xi(u - \mu)$. As in the Generalised Extreme Value the Generalised Pareto Distribution has three parameters; a location parameter (μ), a scale parameter (σ) and a shape parameter (ξ). In the case of sea-level extremes the GPD gives the probability of exceeding a high value given that it already exceeds a high threshold. When applying the GPD method the choice of threshold is crucial. With too high a value too much data could be discarded, leading to high variance of the estimate (Gilleland and Katz, 2006). Too low a choice can lead to bias because the theory of the GPD is based on requiring a high threshold.

The final Extreme Value Analysis technique that is utilised in this study is the Joint Probability method. To utilise the complete hourly records for observed sea level to predict return periods for extreme events Tawn and Vassie (1980) developed the Joint Probability method by considering the surge and astronomical tidal probability functions separately. The method separates out the tide and surge elements and calculates the probability of each specific tide and surge height and then recombines them in the form of a matrix.

For a detailed description and derivation of the Generalised Extreme Value Distribution, the r-largest distribution and Generalised Pareto Distribution reference should be made to Coles (2001), and for the Joint Probability approach see Tawn and Vassie (1980). The remaining sections of this Chapter outlines how these techniques have been applied within a variety of subjects to evaluate extreme values including wind, waves and storm surges.

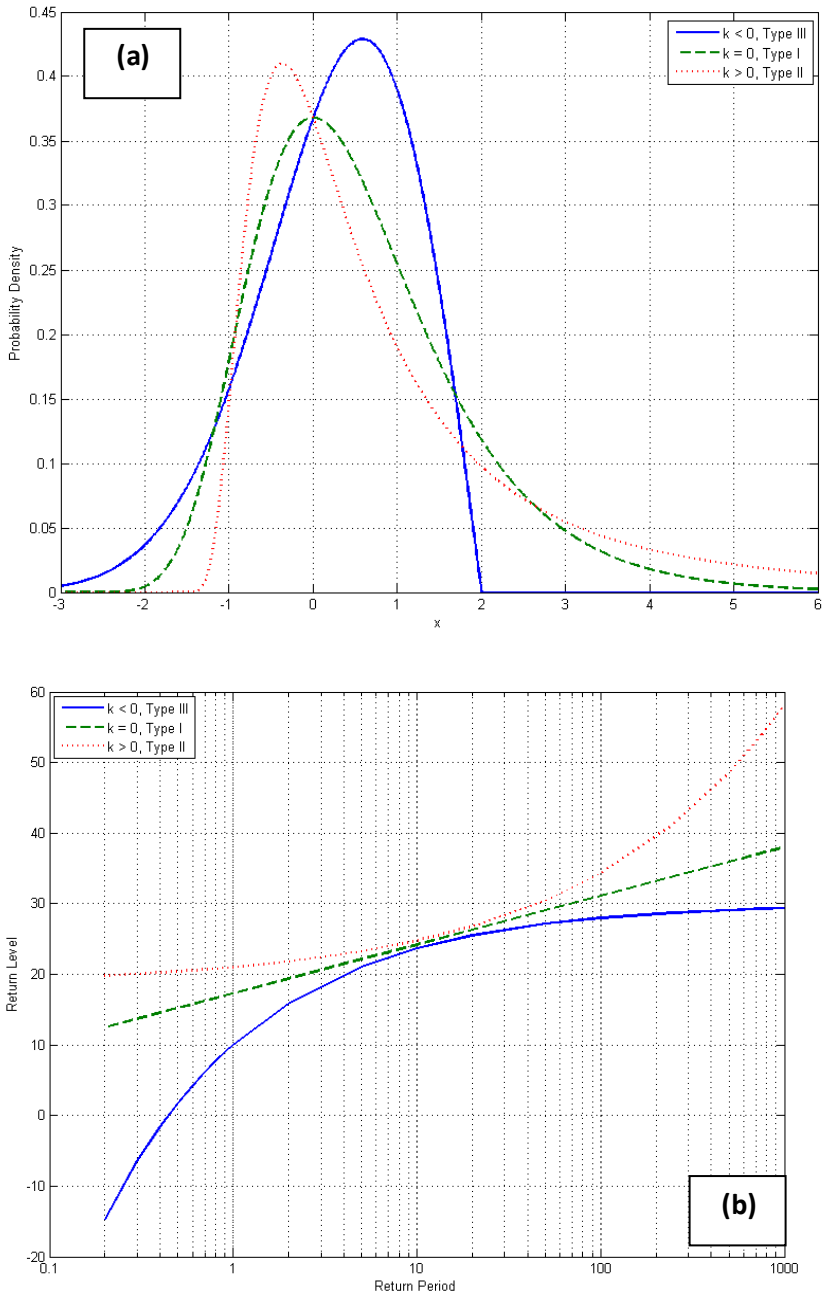

Figure 3.1 Generalised Extreme Value Distribution (a) Probability Density Function plot, (b) Cumulative Distribution Function in the form of a return period plot.

3.2 Methods in Practice

The prediction of sea conditions plays a crucial role in the design of coastal defences and offshore structures. A variety of extreme value analysis techniques have been used to evaluate wave height, wind speed and storm surges. The following sections illustrate how these extreme value analysis methods have been used within the natural hazards environment. The section specifically focuses on how different approaches have been used to evaluate frequency magnitude relationships of wind, waves, and storm surges floods. These topics relate to the main subject matter of this research and those discussed within Chapter 2.

3.2.1 Wind and Waves

Current U.S. guidance on design wind speeds guidance recommends using the Weibull distribution to evaluate extreme winds and 3 second gusts. Cheng and Yeung (2002) investigated the distribution of wind speed using the Generalised Extreme Value (GEV) distribution to evaluate whether the distribution fits Type 1 (Gumbel), Type 2 (Frechet) or Type 3 (Weibull). The analysis was based on hourly wind data from 143 stations in the U.S. with continuous record lengths ranging between 15 years and 38 years. The GEV analysis indicated that the Type 3 Weibull distribution was the best representation of the data set. However, Cheng and Yeung (2002) found that a based on goodness of fit statistics analysis, that the Type 1 (Gumbel) revealed higher accuracy for wind speeds (Figure 3.2). Cheng and Yeung (2002) only assessed return periods up to 1 in 50 years, concluding that the Type 1 distribution is likely to overestimate higher return period events, but fail to highlight that the Type 3 methodology is likely to significantly underestimate these events. The findings of Cheng and Yeung (2002) are confirmed by the studies of Xiao et al., (2006), who investigated the probability distributions of wind speeds in Hong Kong. Using 45 years worth of data of Xiao et al., (2006) found that both the Weibull and Gumbel provide good fits to the data set with the Gumbel providing the upper bound.

The GEV methodology allows an evaluation of return periods by fitting the data to Type 1 to Type 3 distributions without a prior knowledge of the distribution type. Harris (2005), in a review of both the GEV method and the Generalised Pareto Distribution (GPD) showed systematic errors. Based on an analysis of 40 years of wind data from the U.K. Harris (2005) found that the GEV method tended to eliminate the Type 1 distribution despite it providing the best fit for the data. Harris, (2005) justifies caution when using the GEV and recommends significance tests and

visual checks to ensure the best distribution is selected. Harris (2005) also found that the GPD was extremely sensitive to the choice of threshold. The same problem relating to the selection of a threshold was identified a by An and Padney (2005), who showed using 25 years of data, from 6 different locations within the U.S. that the threshold chosen could vary the prediction for a 1 in 50 year even by as much as 20 mph and for a 1 in 500 year by as much as 30 mph. Harris (2005) and An and Pandey (2005) both conclude that the fluctuation in the GPD is linked to the fact that the methodology does not necessarily ensure the values chosen above a certain threshold are independent. An and Pandey (2005) adapted the GPD by ensuring the values above a threshold chosen were independent, calling it the method of independent storms. This approach provided stable results for both the 1 in 50 year and 1 in 500 year return periods despite the choice of threshold and was found to correspond closely with the predictions made by the Gumbel and Weibull methods.

Several probabilistic techniques have been used in an attempt to identify the distribution that best describes extreme waves. Soares and Scotto (2004) used the r- largest methodology to predict significant wave height using 24 years of 3 hourly North Sea data. Soares and Scotto (2004) found that the methodology provided a good fit of the data from visual inspection and probability plots (Figure 3.3), however, no comparison was made to other techniques and a critical evaluation carried out. Both the r-largest and the GEV analysis using the annual maximum gave the same mean value for all return period, however, the r-largest had significantly smaller confidence intervals. The study of Soares and Scotto (2004) differs from an earlier study by Soares and Scotto (2001), where they studied different distributions of the same data set from 1980 to 1988 and found that the Weibull providing the best fit of the data. The use of a Weibull distribution to best describe significant wave height was identified by Repko et al., (2004). Repko et al., (2004) looked at 4 different distributions in a study of 2 sites in the U.S with 20 years worth of continuous data. Repko et al., (2004) found that the Weibull best represents the data and reflects the fact that an upper limit is likely to exist.

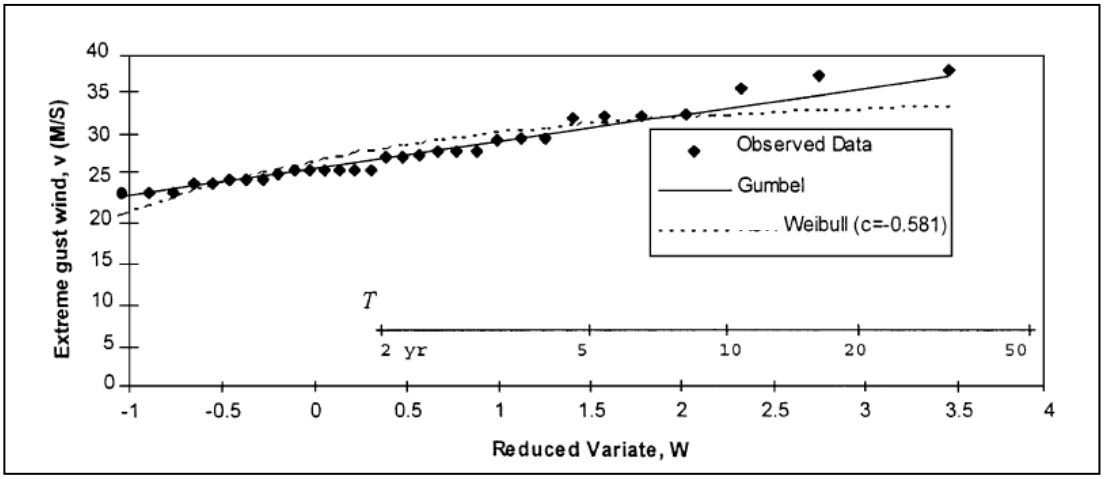

Figure 3.2. Comparison of Gumbel and Weibull analysis (Cheng and Yeung, 2002).

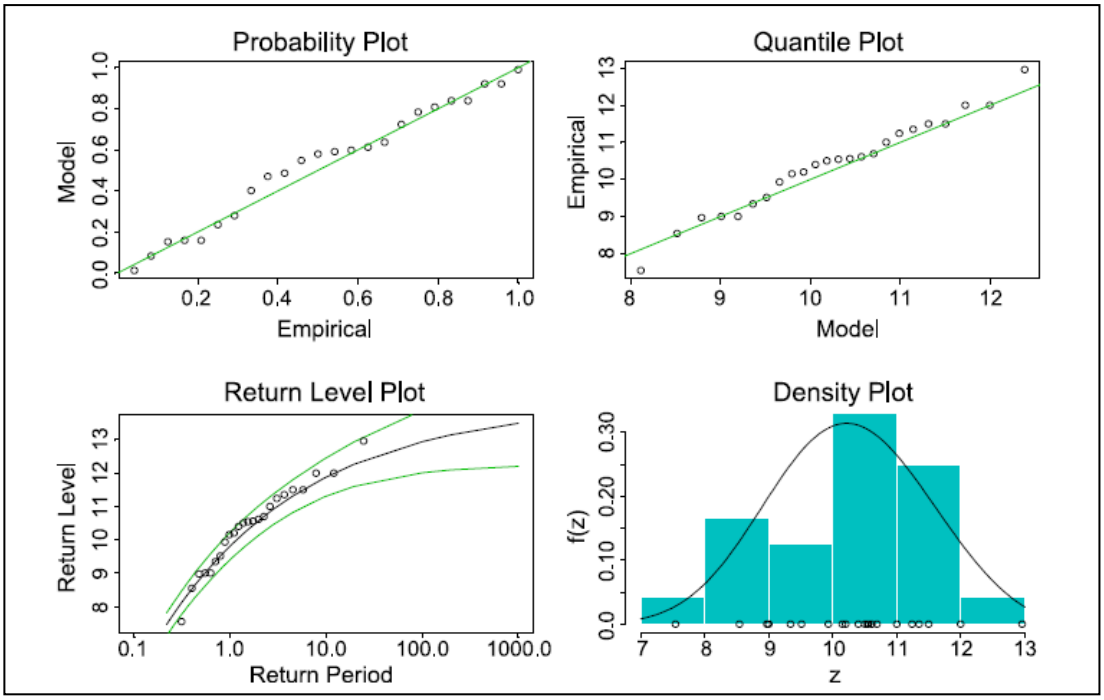

Figure 3.3. Diagnostic plots of the r-largest distribution fit to northern North Sea (Soares and Scotto, 2004).

3.2.2 Storm Surges

The evaluation of storm surge extremes is of critical importance to engineers and planners when evaluating the areas likely to be inundated from coastal flood events. Typical probabilistic techniques employ methodology that utilise the annual maximum peak height from a data set. Watton (2000) assessed a variety of techniques for storm surges using a long (1935-1996) data set for New Jersey, USA. Watton (2000) evaluated over a dozen different distributions utilising the annual maximum and tested the goodness of fit to the data set by visual inspection of the probability plots. Watton (2000) found that most probability density functions provided a good fit for the data, however, many underestimated the largest extremes. No comparison of techniques that utilise more data than just the annual maximum was assessed by Watton (2000).

Although throughout the world large (N>25) data sets exist of sea level observations, many of the areas at risk from coastal inundation and therefore of interest have limited data sets (Coles and Tawn, 1990). For areas that have a data set of 10 to 25 years it has been demonstrated that the r largest approach can be applied (Tawn and Vassie, 1989). Dupuis (1997) demonstrated the robustness of the r largest approach on data sets from Venice for the period 1931-1981. Dupuis (1997) compared the annual maximum approach which utilised the whole data set, to the r largest which utilised a subset of the data and demonstrated that the r largest method could provide an adequate prediction of the return periods when compared to the annual maximum.

For data sets of less than 10 years the methodologies that use the annual maximum and the r largest are likely to be unreliable when predicting extremes (Pugh and Vassie, 1980). Pugh and Vassie (1980) developed the Joint Probability method that separates out the storm surge and tidal components and evaluates the probability functions for each one. This method utilises significantly more of the data as all recorded daily-hourly values are included. Pugh and Vassie (1980) compare the Joint Probability method to the more traditional techniques and found that the method compare favourably. However, in Tawn and Vassie (1989) they identify two deficiencies; firstly the joint probability method will not allow probabilities of sea levels greater than the observed combination of the highest astronomical tide and surge. Secondly only a sample of surges were used in the original methodology and that the sample rate can significantly affect the distribution. Tawn and Vassie (1989) proposed a revised joint probability to take account of these deficiencies. When compared to the joint probability method (13 years data set) and the Gumbel

distribution of the 5 largest annual events for a 30 year period, Tawn and Vassie, (1989) found that the revised Joint Probability provided a much better correlation to the Gumbel distribution and provided a better fit to the data. Furthermore the revised joint probability provided similar confidence intervals and showed greater stability when different data lengths were analysed.

Tsimplis and Blackman (1997) looked at evaluating extreme sea levels for the 18 ports around the Aegean and Ionian seas using the Gumbel, r largest, Gumbel Joint Probability, Generalised Extreme Value, r largest and the Generalised Extreme Value joint probability. Tsimplis and Blackman, (1997) showed that there was little difference in the predictions of extreme sea levels when comparing the predictions of the various distributions. From statistical analysis it was shown that the Generalised Extreme Value distribution provided the best fit to the data. This is in contrasts to the findings from Onofrio et al., (1999) who using a similar methodology found that the probability density function of the storm surge was best represented by the Gumbel distribution. This was compared to annual maximum methods for longer data sets with the predictions and goodness of fit being comparable.

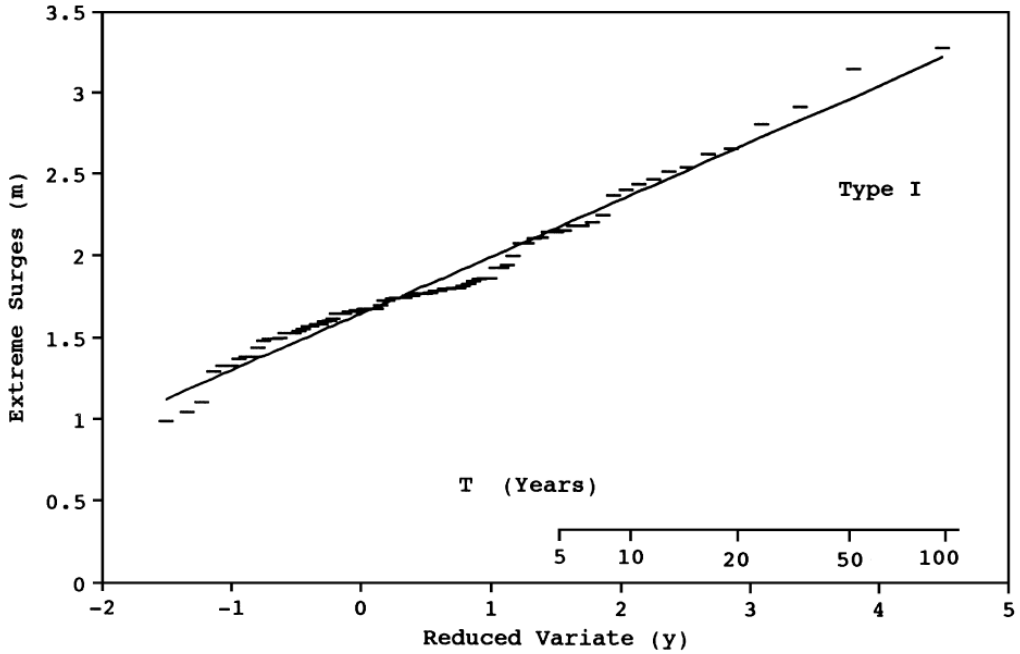

Figure 3.4. Extreme surges at Buenos Aires (1905-1993) fitted by the GEV distribution (Type 1 or Gumbel) (Onofrio et al., 1999).

3.2.3 Monte Carlo Simulations

A Monte Carlo simulation fits a specific Probability Density Function (PDF) to the data, based on a comparison between the modelled and real data. A Monte Carlo analysis has the ability to compare up to 40 different PDFs to the data (Palisade, 2014). Similar to the GEV the PDF output from a Monte Carlo analysis will be a series of shape parameters that describe the PDF.

To illustrate the process two data sets, positive storm surge values and astronomical tidal level, have been simulated in Figures 3.5 and 3.6 respectively. The blue histogram data represents the original data with the solid line representing the fitted PDF. Due to the problems inherent in data (i.e. insufficient amount of data or missing data), fitting a distribution not only models any missing data but also allows the extrapolation of the unknown or uncertain extremes of the data.

A Monte Carlo simulation then randomly combines the two PDFs to produce an ouput which is a function of the two PDFs. In the example the combining of the storm surge and tidal levels in Figures 3.5 and 3.6 gives the output as illustrated in Figure 3.7. The different inundation levels are expressed as a probability, which in turn can also be described using a PDF. From the relationship between inundation level and probability a return level plot can be created and extrapolated to the required return period.

Monte Carlo simulations have a range of applications within the natural sciences, and the following review focuses on the application of Monte Carlo simulations within the coastal and fluvial environment.

To undertake a probabilistic assessment and evaluate the uncertainty, Rahmen et al., (2002) evaluated the PDF of 3 catchments affecting a river basin to evaluate flood frequencies. Using up to 20 years worth of data Rahman et al., (2002) ran a Monte Carlo analysis to calculate extreme events. Rahman et al., (2002) found that the Monte Carlo simulations successfully allowed for the skewed nature of the data and provided a better fit of the data when compared to the deterministic approaches. With the data set Rahman et al., (2002) found that it was realistic to predict to 1 in 100 year event, although the authors acknowledged that better use of the Monte Carlo technique could yield more realistic estimates beyond 1 in 100 year events. Pinya et al., (2009) used a similar approach as part of a statistical assessment of the risk of inland flooding. Pinya et al., (2009) undertook Monte Carlo simulations of a range of inputs (peak flow, volume and duration), for the Vidua river in Denmark based on 45 years worth of data. Pinya et al., (2009) found

that the Monte Carlo simulations showed significant variation within the higher order probabilities (>50 years), however, it modelled the lower probabilities well. Pinya et al., (2009) found that over 6000 iterations were needed to adequately determine the 1 in 1000 year event. Both Rahman et al., (2002) and Pinya et al., (2009), argued that the current techniques adopted, i.e. deterministic approaches, do not account for the probabilistic and uncertain nature of flood events. Aronica et al., (2012) agrees with this principle as they argue that uncertainty is rarely considered and therefore most risk assessments are deterministic and do not take in to account uncertainty in a meaningful way.

Several authors, for example Niedoroda et al., (2010) argue, that Monte Carlo simulations are generally inefficient at considering extremes or that Monte Carlo simulations require a great number of storms to assure accuracy. Niedoroda et al., (2010) fitted several PDFs to storm surge data in the evaluation of the hazard to coastal Mississippi; they chose to use a Joint Probability approach rather than Monte Carlo simulations. No comparisons were made in the output of the results to allow a comparison with the output of Monte Carlo simulation to justify the selection of the Joint Probability method and provide evidence that the Monte Carlo methodology was not appropriate to the data set.

In an assessment of the structural performance of breakwaters under attack from tsunami, Erigin and Balas (2006) undertook a reliability Monte Carlo simulation. Erigin and Balas (2006) utilised 30,000 Monte Carlo simulations to evaluate the tsunami occurrence probability against structural performance, with a comparison to storm surge and earthquake structural performance (without tsunami). Erigin and Balas, (2006) found that the chance of failure within a 100 year time frame increased from 3.3 % to 4.1 %.

In a comprehensive assessment of submarine landslide tsunami hazard, Grilli et al., (2009) undertook a Monte Carlo analysis based on series PDFs relating to submarine landslide occurrence (i.e. depth of failure, slope angle) with the aim to incorporate unseen or uncertain data. This approach was instead of specifying a series of discrete values for the submarine landslide parameters and undertaking a deterministic analysis, Grilli et al., (2009) then undertook a Monte Carlo simulation to calculate the amplitude of tsunamis and tsunami wave run up distance for a variety of probabilities based on the input PDFs. A comparison with 2-D modelling and historical records found a good correlation with both the input parameters and the final output.

In a series of papers on coastal landslide activity and coastal cliff recession, Lee et al., (2001), (2002) and Hall et al., (2002) undertook a series of probabilistic analysis to simulate coastal recession as methods utilising historical records did not reflect potential uncertainty and variability. The output distributions were used to model a series of coastal recession steps in to the future and calculate the probability of a variety of recession rates. One conclusion is that seldom is there enough historic data to conclusively identify the preferred distributions. This is illustrated when comparing the observed rates of coastal recession with the predicted rates at certain locations (Lee et al., 2002).

Islam and Peterson (2008) and Grinten et al., (2013) used Monte Carlo simulations to evaluate the sensitivity of the data on wind characteristics and the affect on storm surges. Islam and Peterson (2008) identified that there was limited historical information, and when it is difficult to use just historical records there is a requirement to indirectly obtain wind speed statistics. Using 30 years worth of data, Islam and Peterson (2008) undertook a random Monte Carlo simulation (1000 iterations) of the parameters (including wind speed) of the shallow water wave equation that govern the evaluation of storm surges for tropical cyclones. From this output and based on the bathymetry at the site a Monte Carlo simulation combines the parameters to produce a series of 1000 storm surges. Although the wind speed output from the Monte Carlo simulation was converted to return period, no attempt was made to convert the storm surge output to a return period. The storm surge output from the Monte Carlo simulation was compared to previous studies, it was found that the maximum surge identified from the Monte Carlo compared well to previous studies. In an attempt to identify the errors within storm surge modelling, Grinten et al., (2013) used Monte Carlo simulations to evaluate the affect of gustiness on surge height. The analysis simulated the extremes of wind speeds and calculated the overall affect on storm surge amplitude. It was found that gustiness alone did not explain the overall errors within the storm surge modelling.

In a rare comparison between Monte Carlo simulations and Extreme Value Analysis, de Moel et al., (2012) undertook a Monte Carlo simulation of storm surges by separating out the sea level record in to its individual components (tide, surge and mean sea level) and then randomly recombining them using Monte Carlo simulation to produce a series of return periods. A comparison with the Generalised Extreme Value (GEV) and Generalised Pareto Distribution (GPD) found that using Monte Carlo simulations to produce annual maxima provided good results. de Moel et al., (2012) concluded that Monte Carlo methodology can produce comparable to the GEV and GPD results with relatively short data sets (<15 years) and therefore

the Monte Carlo methodology performs better than the GEV or GPD which typically required a data set length >15 years (de Moel et al.,2012).

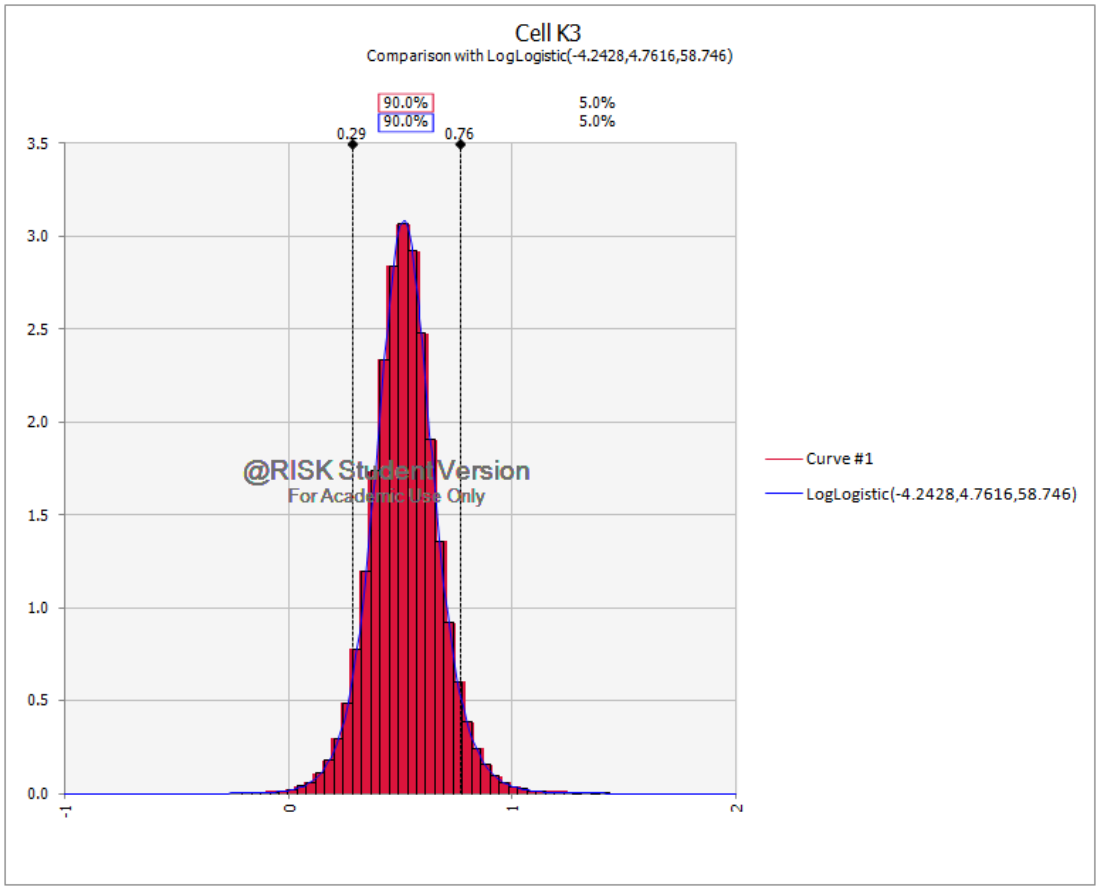

Figure 3.5 Monte Carlo analysis comparison graph between observed storm surge data (red histogram) and modelled PDF (blue line).

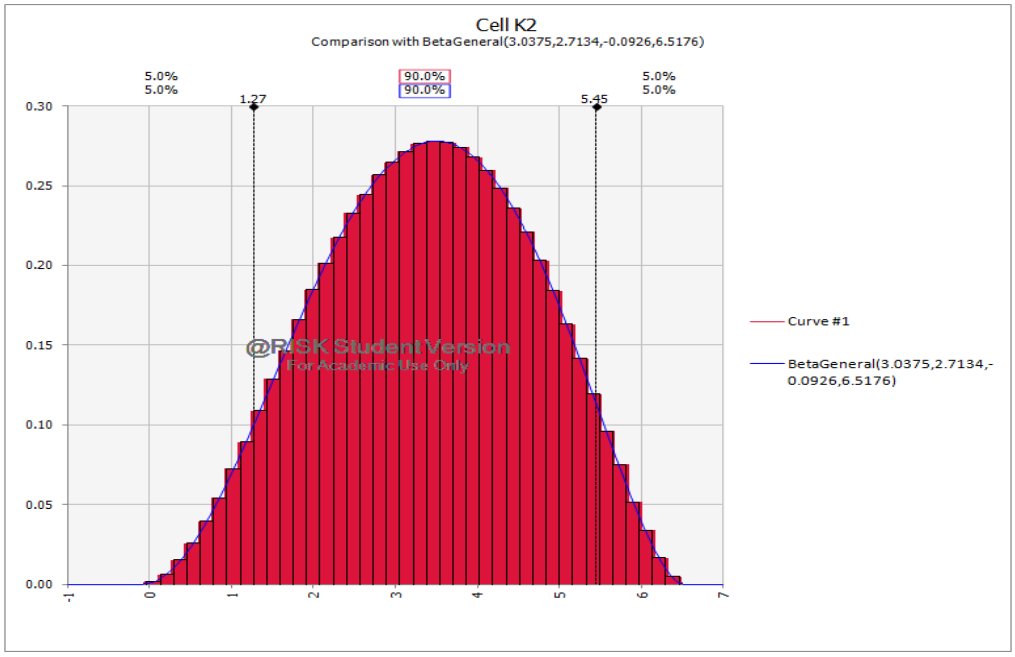

Figure 3.6 Monte Carlo analysis comparison graph between observed astronomical tidal levels (red histogram) and modelled PDF (blue line).

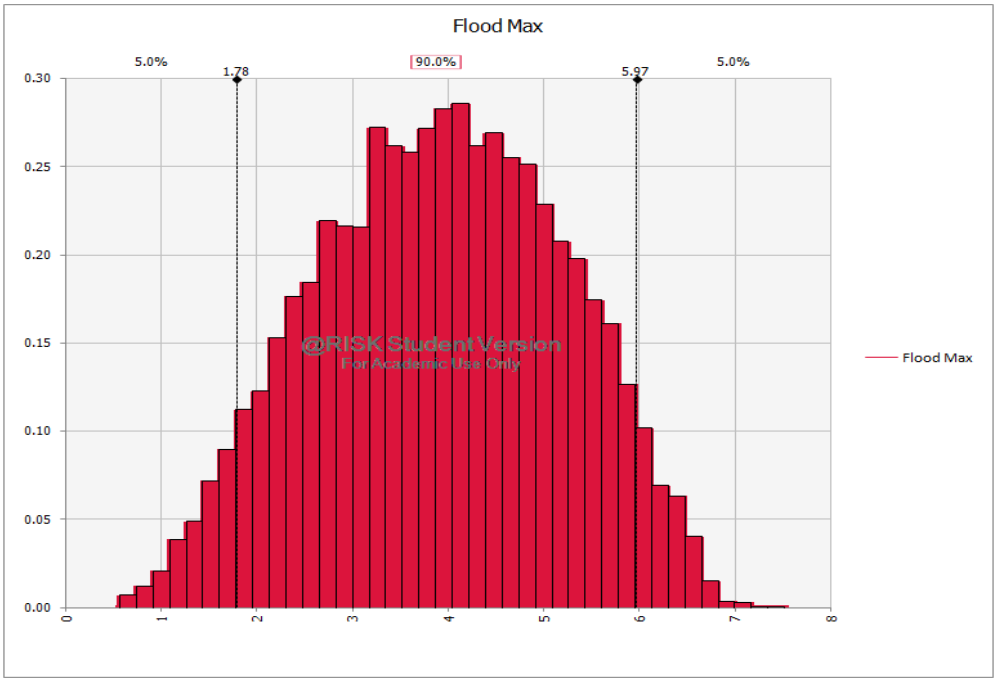

Figure 3.7. Monte Carlo simulation output based on the inputs of storm surge (Figure 3.5) and astronomical tidal levels (Figure 3.6). The output is the probability of a given inundation level.

3.2.4 Tsunami

From a review of the published literature the assessment of tsunami frequency magnitude relationships is often based on the seismic hazard relationship of Guttenberg and Richter which states that:

$$\boldsymbol{LogN_k = a_k - b(T1)}$$

Where N_k is the cumulative number of tsunamis of intensity equal to or larger that T1 observed in a time interval of k. A_k and $_b$ are shape parameters (Papadopsalous, 2003).

Papadopsalous (2003) used this technique to evaluate the frequency magnitude relationship of earthquake induced tsunamis in the Corinth Gulf, Greece. The assessment was based on a record of over 40 tsunamis spanning a period from 1400 to present 2003. A review of the probability plots of the empirical data versus the model prediction indicates a good fit with an r^2 value >0.9. Kim and Choi (2013) utilised the same approach to undertake a Probabilistic Safety Assessment for Nuclear Power Plants in Korea based on historical data and tide gauge records. The power law of Guttenberg and Richter gave an r^2 value of 0.79, this compares to an exponential function of the data gave an r^2 value of 0.97. As limited data often exists for tsunami events, attempts have been made to evaluate potential source zones that could generate an earthquake large enough to trigger a tsunami. Geist and Parsons (2009), rather than evaluate the probability of a tsunami evaluated the potential of two zones that could produce a large enough earthquake to create a tsunami and affect the U.S Atlantic Coast. As Papadopsalous (2003), Geist and Parsons (2009) utilise the Guttenberg and Richter relationship for evaluating earthquake magnitude, concludion that a magnitude Mw>8.0 would generate a tsunami with large enough run up, therefore, directly relating the earthquake frequency with tsunami frequency. No evaluation of the relationship between earthquake magnitude and tsunami magnitude was undertaken. In an assessment of tsunami hazard in Central American Pacific, Brizuela et al., (2014) identified that the historical record of 106 (1539-present) tsunamis was not adequate to undertake a statistical analysis. Brizuela et al., (2014) utilised a comprehensive record of earthquake (1931) to undertake a statistical analysis. The earthquake analysis was then converted to tsunami frequency magnitude relationships, by computing a reduction factor. However, no comparison is made between this reduced frequency magnitude relationship and the historical record. Kulikov et al., (2005) found that for tsunami risk for the coast of Peru and North Chile that they could not apply the Guttenberg Richter power law relationship due to limited data, despite having a

record of over 300 potential tsunamigenic earthquakes with a magnitude greater than 6. Instead of the Guttenberg Richter relationship, Kulikov et al., (2005) utilised a Gumbel analysis. A review of the return period plots shows good agreement between the empirical data and the model. However, an analysis of earthquake magnitude against tsunami magnitude found a weak correlation with an r^2 value of 0.48. An alternative approach to undertaking a statistical analysis was assessed by Horbitz et al., (2012). Despite having a significant database of tsunami occurrence within the Caribbean, utilised the record to evaluate the worst case scenario, establishing the maximum likely occurrence rather than establish the frequency magnitude relationship.

3.2.5 Discussion

The previous section has outlined how different statistical techniques have been used to evaluate the magnitude-frequency relationships of wind, waves and storm surges. The following provides a discussion on the main limitations of the different methods.

Using the annual maximum as part of the Generalized Extreme Value (GEV) analysis potentially excludes data, i.e. the 40 annual maximum may not be the largest 40 events. However using the 40 annual maximum, assuming they are not the 40 largest, would produce a steeper gradient graph and provide higher values when extrapolated to larger return periods. This method would provide a conservative approach if the return period of interest is greater than the record. If the return frequency of interest was relatively low e.g. 1 in 20 year and smaller than the record, using the annual maximum rather than the largest values would produce an underestimate.

The r-largest method, where the user selects a set number of values from each year suffers from similar problems to the GEV in that whichever values of r are chosen there is the potential that values will be excluded from other years. Choosing the r largest over the whole data set will remove this error, however the method is sensitive to the value of r chosen and different r values will alter the prediction. It is also essential that each r value chosen is independent.

The threshold method suffers from similar problems as the r largest and is dependent on the choice of threshold. The method depends on a large threshold value but too much data can be discarded so the method is a compromise between having a higher enough threshold so that the method is still valid but low enough that sufficient data are incorporated. The method is also dependent upon the user

as several parameters are required to be estimated via visual inspection. Although there are methods to aid this, these methods themselves produce different estimations.

The Joint Probability Approach also has several shortcomings these are outlined below:

1. The probability of all events will always add up to 1. Meaning that all events have been accounted for as you cannot have a total probability greater than 1. Therefore it is not valid to extrapolate to events outside of this data set.
2. The largest event will always be the largest tide (highest astronomical tide if a greater than 18.6 year record) with the largest recorded storm surge event. This therefore does not take in to account an uncertain or unseen data as all possible scenarios have assumed to have occurred.

Monte Carlo analysis has been found to be effective in evaluating frequency magnitude relationships, and it has been identified to be more effective than several other statistical techniques including the GEV and GPD. However, typically the approach has not optimized the Monte Carlo simulation and the number of iterations and has not been utilised to evaluate beyond a 1 in 100 year event.

A principle aim of this research is to review the applicability of the main statistical analysis techniques (GEV, r-largest, Joint Probability and Monte Carlo) to the prediction of wind, wave and storms surge magnitude frequency relations and the impact the different approach have on the overall level of uncertainty when modelling inundation.

In a similar manner to the assessment of storm surge frequency magnitude relationships, the assessment of tsunamis is based primarily on the Guttenberg Richter power law relationship, a form of extreme value analysis. The relationship for tsunami is similar in form to those of storm surges in that it is primarily a Log law between magnitude and frequency, adjusted with a series of shape parameters. The assessment of tsunamis differs from storm surges due to the quality and nature of the records available. Whilst storm surges are primarily based on a homogenous, continuous data set from tide gauges, tsunami assessments are based on a spatial disparate record. As such a tsunami assessment is often based on firstly an assessment of the frequency magnitude relationship of the source (i.e. earthquakes) and a relationship between earthquake and tsunami magnitude inferred. From a review of the literature the Guttenberg Richter relationship has not been applied to

storm surges, the relationship could potentially apply to a disparate site with limited tide gauge data, but a significant archival record of large storm surges.

A note of caution should be made with regards the analysis of extreme values from a series of historical records or observations. The records for either a storm surge or tsunami are incomplete due to only recording data for a relatively short period of time, and therefore, there is the potential for events to have existed or occurred that could exceed the maximum observed value and fail to be predicted using the methodology outlined in this chapter. These outliers have been termed in the literature as “Dragon Kings” (Suveges and Dawson, 2012). Although the phenomenon has not been observed within the literature for storm surges, it has been observed in fluvial floods. Suveges and Dawson 2012, in an analysis of the catastrophic floods in Venuzuela in 1999, found that traditional techniques could not account for either the magnitude or cluster of the fluvial events. It is worth noting that the data record for the assessment was relatively short, from 1965 to 2000 and despite the mean value from a GPD analysis failing to predict the 1999 event, the 95% confidence interval approximated the value. Despite the lack of literature of a similar event for storm surges, the potential of an outlier to occur needs to be considered.

3.3 Visual Representation

3.3.1 Geographical Information Systems

A Geographical Information System (GIS) constitutes an integrated tool box for spatial data, input, storage, management, manipulation, analysis, modelling, output and displaying (ESRI, 2013; Delaney, 1999; DeMers, 2000). Importantly a GIS allows the user to view, understand, question, interpret, and visualize data in many ways that reveal relationships, patterns, and trends in the form of maps, globes, reports, and charts (ESRI, 2013).

Within a GIS spatial data representing human and natural phenomena from the real world is typically stored in three ways: firstly as spatial data i.e. the coordinates of a specific feature; secondly attribute data which stores a description or descriptions of a feature i.e. the population, age distribution, and finally topology data which describes the spatial relationships of data. Data is typically stored in two ways, either vector data or raster data. Vector data comes in the form of either a polygon which might represent a city boundary, a line which might represent a stream or road network and point data which might represent a specific building or a borehole location. Figure 3.8 shows the different forms of vector data Raster data divides the world in to grids and cells with typically each cell assigned a value to describe it's attributes for example the elevation of a specific cell.

Different data sets can be incorporated in to a database within GIS and relationships can be identified between the different data sets. Figure 3.9 shows the four data types utilised within this study to develop a GIS data base for south west England. Using an input of a specific flood level, for example a flood level with a return period of 1 in 100 years can be simulated within a geographical information system and using the information contained within the database can extract the number of people, land and infrastructure affected. The inundation level can be represented as a polygon or line within GIS with the output data either represented graphically or numerically.

The use of a Geographical Information System to manage and understand complex natural hazards in spatial and temporal contexts is now an essential part of real world phenomena, the output can provide essential information for decision makers (Tarolli and Cavalli, 2013).

Geographical Information Systems (GIS) have been used extensively throughout the world to undertake flood hazard and risk mapping. Brown (2006) argues that a GIS can be an effective framework to integrate and analyse disparate environmental. Brown (2006) modelled future landscape change along the coastline of North Norfolk using a geographical information system. Using a grid based raster, containing a Digital Elevation Model (DEM), land cover map and future sea level rise scenarios as the main layers, evaluated the change in coast line under different management policies. Thumerer et al., (2000) undertook a similar assessment on the east coast of England to evaluate the risk on the coastal environment from future climate change.

Satellite data has often been used to define the flood extent following a flooding event, however, the coverage of the data can be patchy and often taken several days after a flood event (Brivio et al., 2002). Brivio et al., (2002) used a DEM within a GIS to infill the flood extent identified from an interpretation of satellite imagery of the November 1994 flood in Piemonte, Italy (Figure 3.10). The output of the satellite imagery interpretation of the flood extent is illustrated in Figure 3.8. The method of interpolating the flood event from satellite imagery within a geographical information system was also utilised by Islam and Sado, (2000). Islam and Sado, (2000) developed two flood hazard maps based on flood depth and flood frequency. These maps were then combined using a risk matrix and land characteristics within a Geographical Information System to develop risk maps for Bangladesh.

Satellite imagery within GIS has been used to undertake land classification and to evaluate coastal erosion when other information does not exist. Saxena et al., (2013) developed a GIS model to evaluate the hazard and risk to remote parts of the Indian coastline. Saxena et al., (2013) developed the flood hazard map based on a composite of erosion mapping and flood frequency predictions overlain on to elevation data. Using satellite imagery Saxena et al., (2013) developed land characteristics within the GIS model to evaluate the socio-economic impacts of the flood and coastal erosion event over a 100 year timescale. Tram et al., (2008) undertook the same approach, but due to limited coverage of satellite imagery and the remoteness of the locations utilised local knowledge of historical flood events to supplement the satellite information. Using satellite imagery and local knowledge, Tram et al., (2008) developed a flood hazard and risk map with GIS for a Thua Thien Hue Province in Vietnam.

Since 2007 European Union member states as part of a European Directive, have been required to “handle the negative impacts of flood events” (European Union,

2007). Member states were required to evaluate and produce flood hazard maps for low probability (extreme events), medium probability (>100 years) and where applicable high probability events that potentially have significant impact (Muller, 2013). In a review of the European Directive and the approaches undertaken Muller, (2013), identified that typically hazard and risk maps contained the flood extents, inhabitation and socio-economic activity. Muller (2013) identified that despite the directive there was still significantly different approaches undertaken to evaluate hazard and risk, both in the way of evaluating the probability of occurrence as well as the methodology adopted to evaluate hazard and risk.

Geographical Information Systems have been an integral part of evaluating flood hazard and risk within the United Kingdom. An example is that of Hall et al., (2005), who developed a comprehensive GIS database to undertake a broad scale assessment of current and future flood risk in England and Wales. The database contained several layers including elevation data, water courses, coastal defences, buildings and land use. Hall et al., (2005) defined risk as the product of the probability of flooding and the consequential damage summed over all possible flood events. Using predicted sea level rise scenarios and defined flood limits evaluated the risk related to a series of land management policies, Hall et al., (2005) identified that socio-economic changes when incorporated in to the models played an important role in the level of risk for each scenario (Figure 3.11).

Geographical Information Systems have also been used to evaluate the hazard, vulnerability and risk to coastal environments from tsunamis. Papathoma and Dominey-Howes (2003) undertook a tsunamis vulnerability assessment by delineating three hazard zones between 0 and 5 m based on historical tsunamis information. This approach was also utilised by Park et al., (2013), but in evaluating tsunami levels from simulated models rather than historical information. Typically the tsumami assessments, as in the examples of Papthoma and Dominey-Howes (2003) and Park et al., (2013) simulate the tsunamis run up as a simple contour value. This approach is in contrast to Adriano et al., (2013) who within a GIS modelled the propagation of the waves through the build up environment of Lima, Peru. The output of all these studies, however, remains the same; to provide information for disaster planning and response.

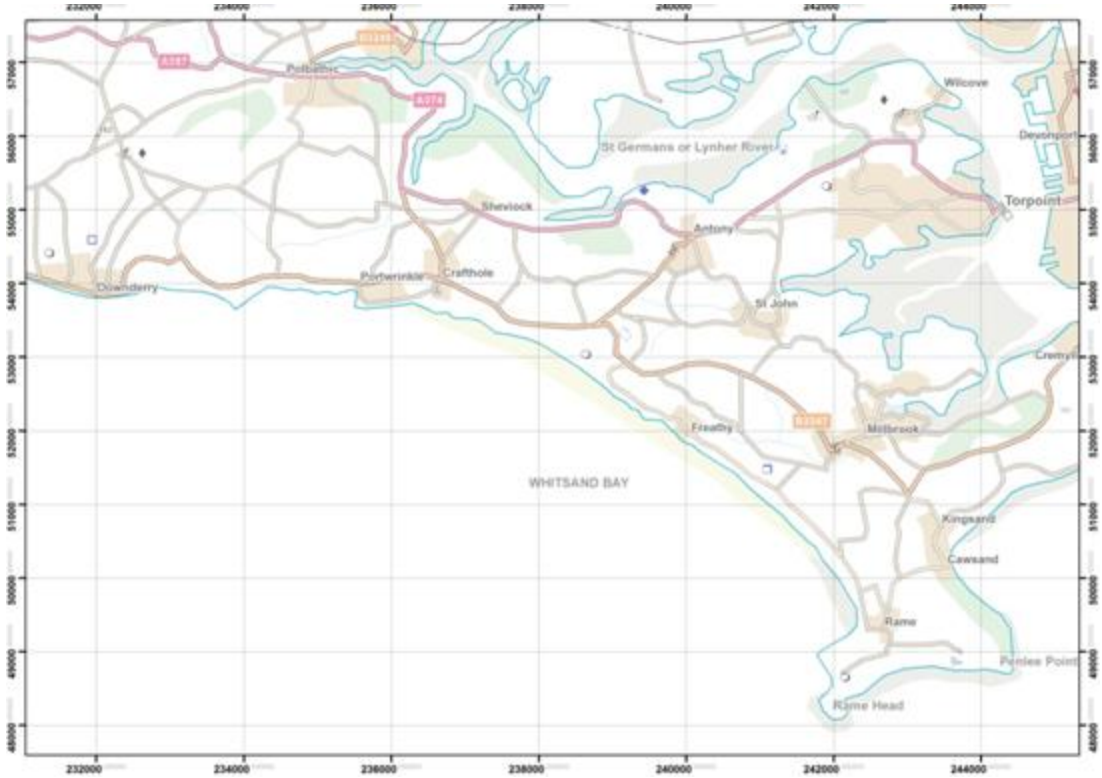

Figure 3.8 Geographical Information System of local infrastructure data highlighting point, line and polygon data types.

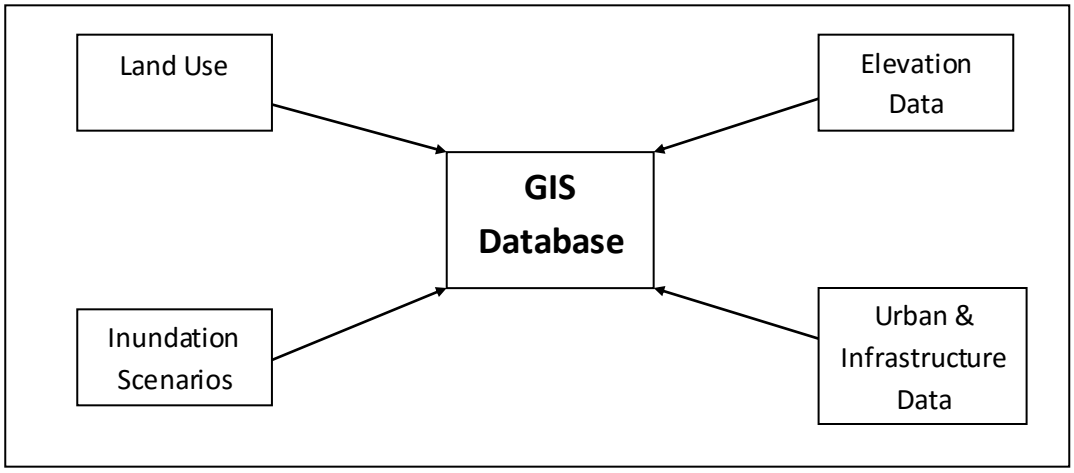

Figure 3.9 Components of the GIS Database utilised within this study.

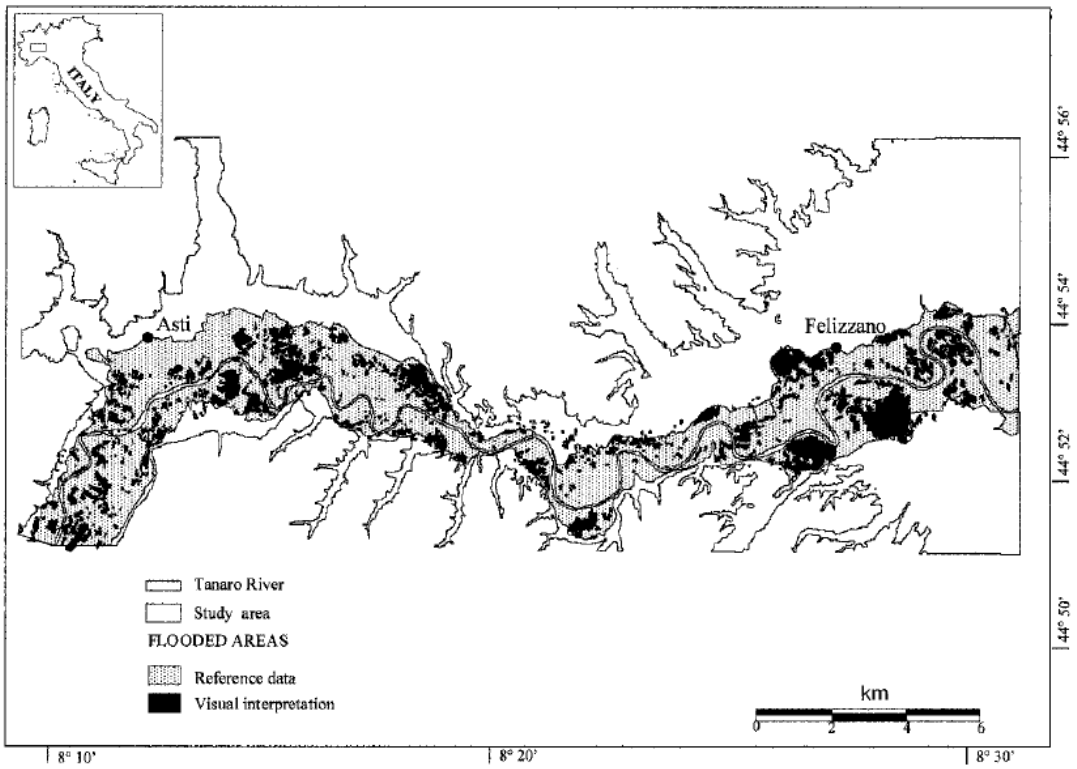

Figure 3.10 Flood map derived from visual interpretation of false colour composite of multitemporal ERS-1 radar images (Brivio et al., (2002). An interpolation of the points was undertaken within GIS to complete the flood map.

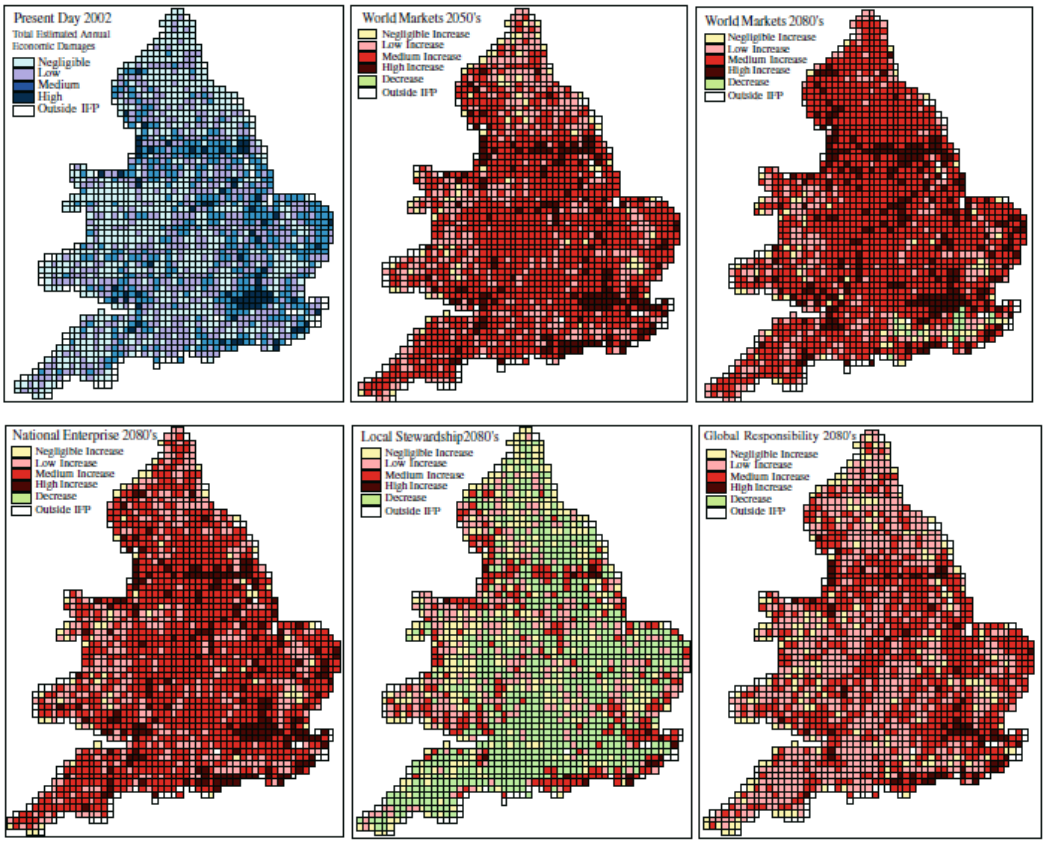

Figure 3.11 Expected annual economic damage for 2002 and future scenarios (Hall et al., (2005).

3.3.2 Two-Dimensional Modelling

The method of overlaying flood events on to spatial data within a Geographical Information system has been criticised as being over-simplistic and frequently over estimating the flood extend (Bates et al., 2005; Mai and von Lieberman, 2001). To combat the simplicity of a GIS approach several authors have developed 2-dimensional models to simulate the flooding (for example Bates et al., 2005, Patro et al., 2009). 2-dimensional modelling uses raster based data to assess the extent of inundation (Horrit and Bates, 2002). The models utilise either a continuity and momentum equation (Horrit and Bates, 2002) or the 2-dimensional shallow water equations of surface flow (Gallend et al., 1992; Bates et al., 1998). These equations are incorporated in to software packages, for example MIKE FLOOD (Patro et al., 2009) and LISFLOOD (Smith et al., 2012; Bates et al., 2005) to model the inundation of specific events. The model effectively involves flooding being treated as a volume filling process (Bates and Roo, 2000), with the software assessing which area to flow to next for the duration of the flood extent. 2-dimesional modelling has proved to be a useful tool in complex areas and can incorporate additional flood parameters including flow velocity, propagation, duration and rate at which water rises (de Moel et al., 2009).

Typically 2-dimensional modelling has been used in the evaluation of fluvial flooding. Several authors have evaluated the effectiveness of 2-Dimensional modelling by comparing the results to historical events. Haider et al., (2003), developed a code to solve 2-Dimensional fluid dynamics, undertaking laboratory calibration and real life simulation of the Nimes, France flood of 1986. Haider et al., (2003) found that in both cases software provided results close to observed measurements, with the model able to effectively take in to account obstacles, i.e. houses. Patro et al., (2009) developed a 1-2 dimensional hydrodynamic model known as MIKE FLOOD to model a river basin in India and compared the results to a known monsoon flood of 2001. Patro et al., (2009) initially calculated the discharge and flow using a 1-Dimensional model and then simulated the event in a 2-Dimensional environment. It was found that when the model was compared to satellite imagery (observed data) there was good correlation, the observed area inundated was of the order of 680km^2 versus the predicted area of inundation of 630km^2. It was hypothesised that the difference was with the model not taking in to account upstream or downstream sinks, i.e. areas that can store flood water leading to the amount of water within the system being reduced.

Horrit and Bates, (2002), and Hunter et al., (2008) have both evaluated the effectiveness of a variety of 2-Dimesional models. Using the River Severn in the U.K. as an example Horrit and Bates, (2002) evaluated the effectiveness of 2-Dimensional models against the flood extent derived from satellite imagery for two separate events that occurred in 1998 and 2000. The first flood event was used for model evaluation while the second was used to evaluate the effectiveness of the models. The study identified that the 2-Dimesnional models effectively predicted the flood extent; however, the models required significant calibration. Hunter et al., (2008) evaluated the effectiveness of six different 2-Dimensional models to predict a small (<0.4 km^2) urban flood in Glasgow. The study showed that the different models predicted the observed flood to +/- 5 cm of a 1 m flood, equivalent to the error within the topographic data and that there was a subtle difference in a variety of parameters of the models including overall flood depth, extent and velocity. The key parameter was understood to be bed friction, which is poorly defined in urban areas. Hunter et al., (2008) found that the LiDAR elevation data was sufficiently accurate to resolve the extent of flooding in urban areas.

Although 2-dimensional modelling has been extensively evaluated for use in fluvial flooding there appears to be limited modelling and evaluation of 2-dimensional modelling in coastal environments. Bates et al., (2005) who developed a 2-Dimensional model, LISFLOOD for coastal flooding from a fluvial flood model, argues that this lack of application is partly due to the frequency of events and the availability of the data to validate the models. However, Bates et al., (2005) established that the 2-dimensional model when applied to a coastal environment can effectively predict the extent of flooding. To validate the applicability of the 2-Dimensional model to the coastal environment Bates et al., (2005) validated the model against three historical coastal floods that occurred in North Wales, Fleetwood and East Anglia in 1990, 1977 and 1953, respectively. The 2-dimensional model performed well, yielding a correlation of between 0.78 and 0.91. At 2 locations a simple planar GIS analysis was performed which yielded a correlation factor as low as 0.11. A comparison of the 2-dimesnional approach and a GIS approach indicated that a GIS significantly over-predicted the extent of flooding, with the 2-dimensional approach slightly under-predicting when compared to the historical observations. Smith et al., (2012) undertook further validation of LISFLOOD for the Somerset Levels, U.K. (Figure 3.12), finding that the 2-dimensional model can effectively simulate real flood events given the availability of high resolution, high accuracy terrain data such as LiDAR.

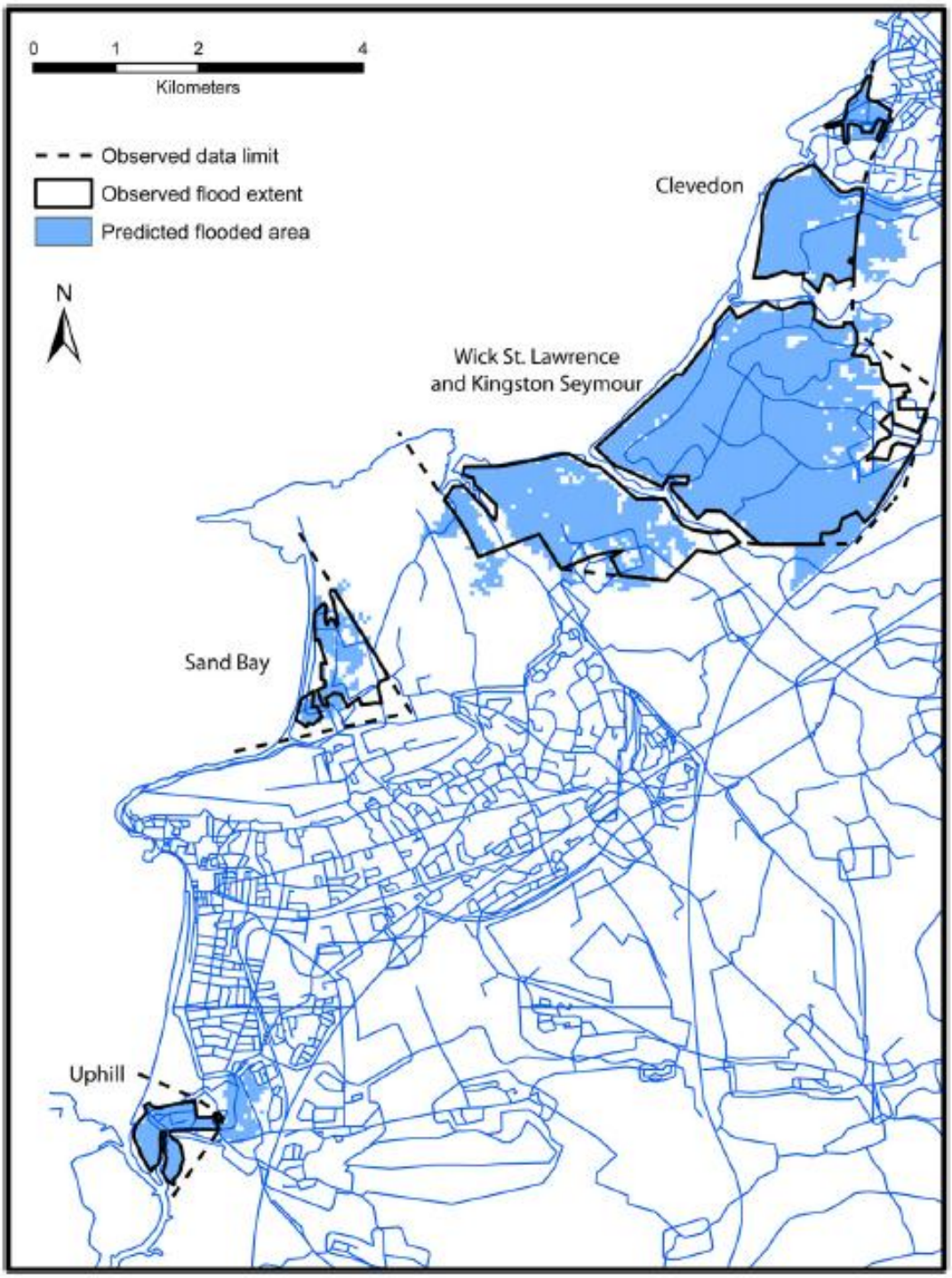

Figure 3.12 Comparison between the observed and predicted flood extent for the 13th December 1981 event along the Somerset Levels (Smith et al., 2012).

3.3.3 Discussion

The two main techniques that allow the representation of inundation levels are a Geographical Information System (GIS) and 2-Dimensional model. A GIS typically evaluates inundation levels on a much broader scale and has the ability to incorporate a range of data sets including digital elevation data, infrastructure data and satellite imagery. From a review of several case studies it has been found to be an effective way to model environmental phenomena. A GIS can model a range of scenario including inundation levels and cliff recession rate and evaluate the overlap. The main limitation of a GIS is that it typically models an inundation level as a simple contour and does not model the dynamic nature of flood events. In comparison, 2-Dimensional models simulate a flood event in a dynamic fashion using 2-dimensions fluid dynamics, calculating the flow volume and direction from each cell within the digital elevation model. The main application of 2-Dimensional models is within a fluvial environment, with limited application within a coastal setting. Furthermore, 2-Dimensional models are typically undertaken on the small scale (<10 km^2). The output from 2-dimensional modelling still needs to be incorporated into a GIS to allow the evaluation of the consequence and to link to other processes.

A Geographical Information System has been selected to evaluate the affect of uncertainties on inundations levels due to the size of the study area and the requirement to incorporate a range of data sets, specifically infrastructure data. The different data sets utilised within this study and the methodology to undertake a GIS analysis is discussed in Section 4.7, the results of the GIS analysis are presented in Chapter 6.

Chapter 4 Methodology

4.0 Introduction

This chapter describes the methodology adopted in analysing the tide gauge records for Newlyn and Devonport. It describes the available data sets that have been used within this study, how these data sets have been compiled and enhanced, and how from these data sets an analysis of both sea-level rise and extreme value analysis of storm surges and waves can be undertaken, identifying the range of uncertainty attributable to different extreme value methodology. From these outputs the chapter illustrates the approaches used in evaluating the implications of the uncertainty related to different storm surge and wave predictions on the coastal environment using a Geographical Information System (GIS), how this is likely to change over time by incorporating sea-level rise scenarios; and enabling a comparison of the level of uncertainty associated with storm surge and sea-level rise predictions.

4.1 Overview of Methodology

The approach adopted within this study is twofold; firstly, using the observed tidal data and extracting a range of data sets including: the annual mean sea level; annual maximum observed sea level; annual maximum observed storm surge level; the 10 largest events of both the annual maximum observed sea level and storm surge level and the frequency distribution of the data sets. From these extracted data sets a range of statistical analysis has been undertaken to evaluate the following:

- Mean Sea Level.
- Storm surge distributions.
- Storm surge frequency-magnitude relationships.

Secondly, these data formed the basis for modelling the inundation in order to evaluate the impact/vulnerability of South-west England to coastal flooding under different sea-level rise and storm surge conditions. This provides a method of measuring each inundation scenario and the sensitivity of the coast line to storm surge predictions and mean sea-level rise.

In addition to the storm surge analysis, wave height and wind data was evaluated to incorporate the main components of inundation; storm surge, tides and wave height. A case study of Devonport Dockyard, Plymouth was used to demonstrate the methodology and the applicability of the approach in the evaluation of coastal structures.

Woodworth et al., (2009) identified that some of the variability observed within the U.K. tide gauge records could be explained by meteorological affects. Therefore, in addition to the tide gauge records, weather data (pressure, wind speed) records were analysed and cross-referenced to the tide gauge records with a view to evaluating and explaining any trends identified within the data sets.

The methodological approach adopted within this study is illustrated in Figure 4.1 and 4.1a.

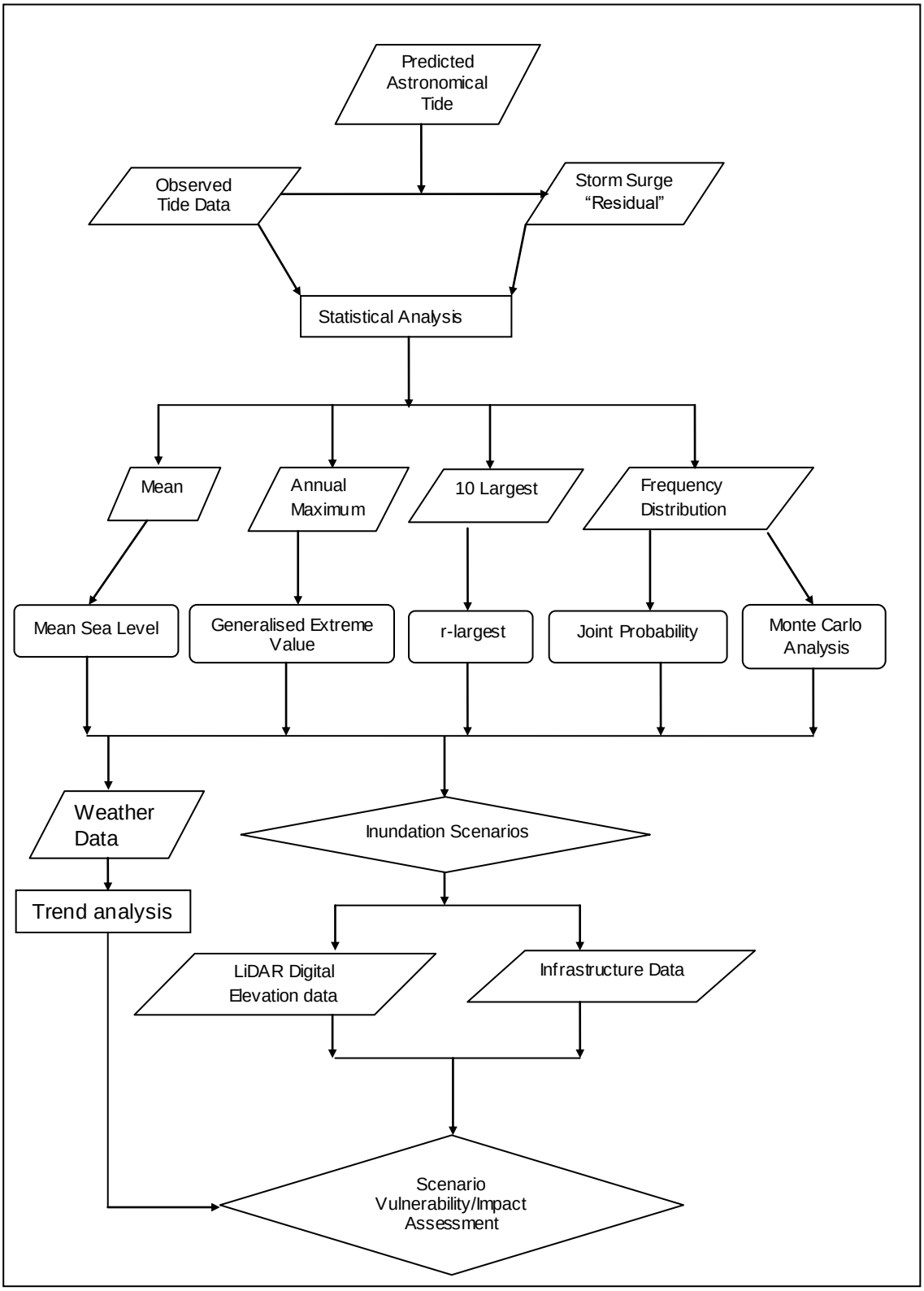

Figure 4.1. Flow diagram of methodological approach adopted within this study.

4.2 Data Sets

A significant amount of data is available to allow an assessment of coastal inundation to be undertaken. The data includes tide gauge, weather and wave data for the evaluation of frequency-magnitude relationships; LiDAR digital elevation data and infrastructure data which allow the visualisation of inundation scenarios.

4.2.1 Tide Gauge Data

Tide gauges, which record the observed sea level at a given point are installed at over 40 locations throughout the U.K. (NTSLF, 2013). The availability of data within the study area is shown in Table 4.1. In total close to 2 million tide gauge data points were utilised within this study, with almost 200,000 data points inputted manually. When considering the individual storm surge, astronomical tidal component, wind and wave data almost 5 million data points have been utilised to evaluate the uncertainty attributed to the evaluation of frequency magnitude relationships.

Location	Period	Description	Data
Devonport	1962-1989	Hourly readings in paper form	8760 per year
	1990-1992	Hourly readings in electronic form	8760 per year
	1993-2012	Readings every 15 minutes in electronic form	~35,000 per year
Newlyn	1915-1992	Hourly readings in electronic form	8760 per year
	1993-2012	Readings every 15 minutes in electronic form	~35,000 per year

Table 4.1 Available Tide Gauge Data for Newlyn and Devonport.

4.2.2 Weather Data

Weather data has been acquired at Mount Batten, Plymouth since 1920, with hourly electronic records available since 1962. The main purpose of acquiring the weather data for the purpose of this research is to attempt to explain any variability observed within the tide gauge data set. The available weather data for Plymouth is shown in Table 4.2.

Location	Period	Description	Data
Plymouth	1960-2008	Daily Average pressure readings	365 per year
		Daily average wind speed readings	365 per year
		Daily average wind direction readings	365 per year

Table 4.2 Available Weather Data for Plymouth.

4.2.3 Wave Data

Wave analysis is an important component in the assessment of coastal flooding and is a required component in the design of coastal structures (Reeves et al., 2012). Waves increase the peak height of the observed water levels and can be the difference between a location being inundated or not. Chapter 2 outlined the formation of waves and how this increases the height of the overall flood level. Compared to the tide gauge data set there is limited availability of wave data for the study area, as shown in Table 4.3, therefore the wave predictions have had to be compared to wave height predictions calculated using the wind speed data. For example Kamphuis, (2010) used wind speeds to calculate wave height in a semi-closed basin. The methodology of Kamphuis (2010) has been used calculating wave height from wind speed to confirm the findings of the predictions of wave height from using only the wave data.

Location	Period	Description
Polperro	2006-2012	Hourly Average wave height data for the period
Looe Bay	2009-2012	Hourly Average wave height data for the period
Porthlevean	2011-2012	Hourly Average wave height data for the period
Port Isaac	2010-2012	Hourly Average wave height data for the period

Table 4.3 Available Wave Data for the Study Area.

4.2.4 LiDAR Data

To allow the visualisation of the inundation scenarios for south-west England requires the incorporation of the levels in to a three dimensional space. As such accurate height data forms an important component of a geospatial assessment. One method for acquiring this data is the use of LiDAR (Light Detection and Ranging). Due to the variety of applications and large number of end users the Environment Agency has been undertaking LiDAR surveys of the UK for over 15 years (Environment Agency, 2013). Aerial LIDAR uses a laser to measure the

distance between the survey aircraft and the ground surface, including buildings and other assets (above ground pipelines, highways, street furniture, power lines, railway tracks). The LiDAR data typically have a vertical accuracy in the range of 5 cm to 15 cm with a spatial resolution of between 25 cm and 2 m (Channel Coast, 2013).

LiDAR data utilised within this study was flown in 2007/2008 by the Environment Agency (Channel Coast, 2013) using the Optech ALTM 2033 and 3100 LiDAR, based on a scan rate 0f 34 Hz, with a swath angle of 25^0 and flight altitude of 1000 m. LiDAR data are available from the Channel Coast Observatory in ASCII Grid file format in tile sizes typically 1 km^2 (Channel Coast, 2013). In total approximately 10,000 individual tiles were acquired for the study area, downloaded in batches of approximately 100 tiles, each of approximately 2 MB in size. These then had to be digitally stitched together and visually assessed to check for calibration errors and anomalies.

4.2.5 Ordnance Survey Data

A variety of infrastructure information is available in digital form (Digimap, 2013). Depending on the requirements of the end user and the spatial extent the user requires determines which Ordnance Survey data set is most applicable.

Within this study two different Ordnance Survey data sets are utilised. The first is a “regional scale” 1:250,000, data set called Strategi (Digimap, 2013a). It is typically used at as a coarse resolution data set for planning purposes. Within this study the data set was aimed at assessing the impact for the whole of the study area. The second is a much high resolution 1:10,000, scale data set called 1:10,000 Raster. Although it contains similar information or layers as the Strategi 1:250,000 data set the level of detail is much greater. For example where Strategi shows an “urban” area as a whole polygon, the 1:10,000 raster data set, breaks up the “urban” area in to individual houses. Therefore where the output from Strategi provides the total urban area inundated, the output for the 1:10,000 raster would be the total number of houses.

More detail on the two different data sets are given in Section 4.7.

4.3 Processing and Analysis of Time Series Tidal Gauge Data

Chapter 2 outlined the main constituents of observed sea level recorded at tide gauges throughout the UK. This includes, mean sea level, storm surge and astronomical tide. Data was acquired from National Tide and Sea Level Facility, (NTSLF, 2013) in electronic form and Taunton Hydrographic Office in analogue form. These analogue readings had to be digitized into the correct format prior to data processing. To extract the relevant data set first required the collation, data entry, checking and quality control of the data. From this the relevant data sets of storm surges, annual maximums and frequency distributions could be extracted to allow analysis of mean sea level and storm surge frequency-magnitude relationships. This phase of data compilation and validation formed a significant, and time consuming component of the work undertaken for this thesis.

4.3.1 Extending the Devonport Observed Tide Gauge Data Set

Originally, the observed data for Devonport existed for the period 1990 to present with some minor gaps (NTSLF, 2013). This data set was small in comparison to the Newlyn data set (1915-Present). Although attempts had been made to utilise the Devonport data set (1990-2012) (Whitworth et al., 2005), there are reservations with regards the quality and length of the data set and therefore its applicability for the analysis of sea level (Woodworth et al., 1999). To improve the length of the Devonport data set an archival search was undertaken which identified hourly observed data for Devonport for the period 1961 to 1989, located in hard copy form at the Hydrographic Office in Taunton. The format of the data is shown in Figure 4.2, and these data had to be manually inputted in to Excel spreadsheets as demonstrated for one month in Figure 4.3. The located hard copy data recorded any datum shifts, highlighted in Figure 4.2, ensuring the data had a uniform datum. These data were then converted in to a text file to enable the data to be quality controlled using both a visual assessment within Excel and a computer algorithm within MATLAB.

The extended record has allowed a better comparison between Newlyn and Devonport and provided greater confidence in the predictions made for both storm surge magnitudes and sea-level trend for the area.

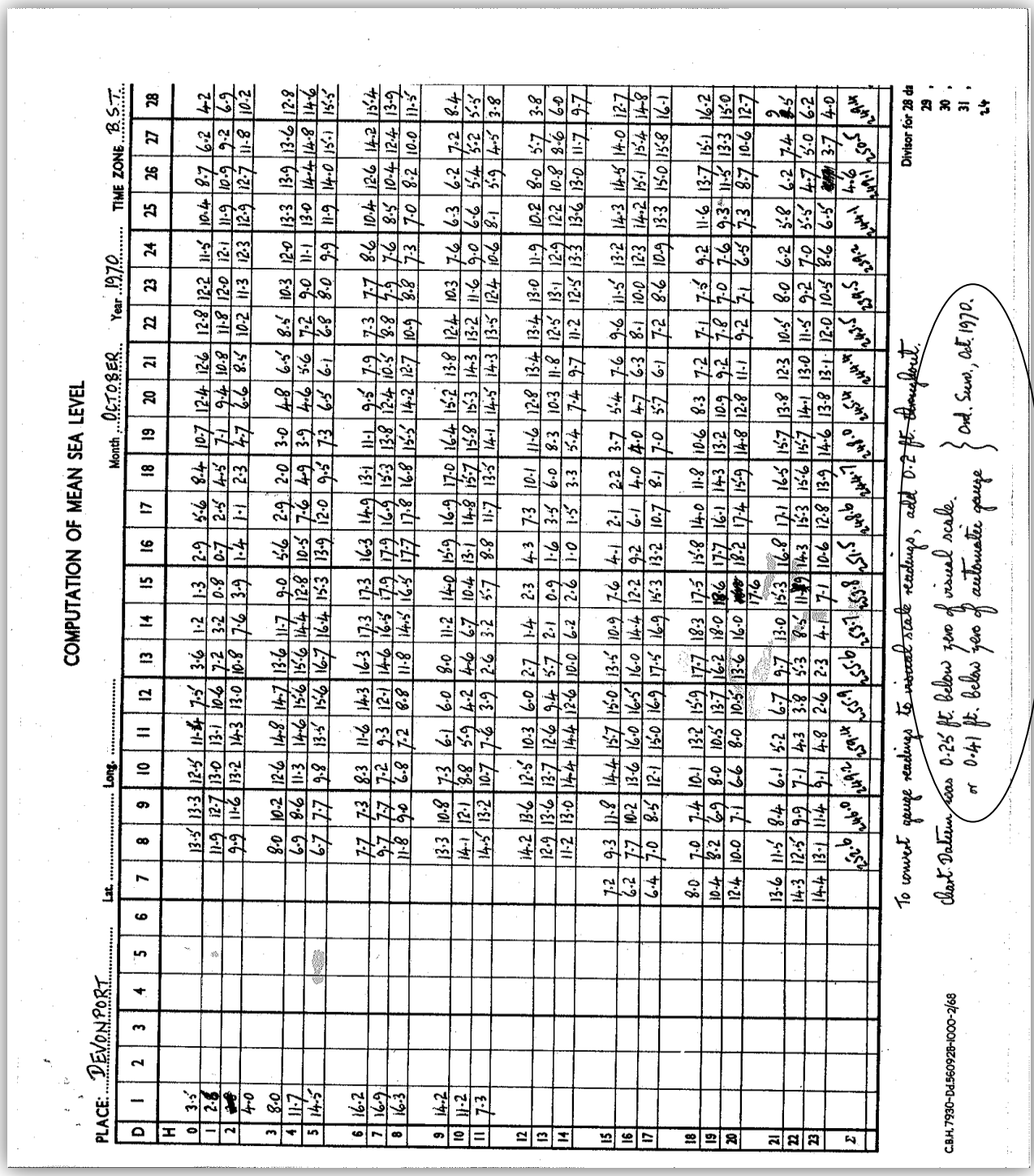

Figure 4.2. Example of the data from 1961 to 1989 which had to be entered manually. The circle text highlights the datum shifts recorded.

Year 1964

JAN	1	2	3	4	5	6	7	8	9	10	11	12	13	14	15	16	17	18	19	20	21	22	23	24	25	26	27	28	29	30	31
0	1.4	3.7	6.2	8.4	10.3	11.6	12.1	12.1	12.0	11.2	9.5	7.4	5.2	3.7	2.3	2.6	3.4	4.8	7.1	9.3	10.8	12.0	12.8	12.7	11.8	9.8	6.6	3.1	0.9	1.0	2.5
1	0.8	1.7	3.3	5.0	7.4	9.4	10.7	11.7	12.3	12.3	11.4	10.2	8.5	6.3	3.8	2.3	2.0	2.6	3.9	6.0	7.9	10.0	11.7	12.7	12.8	11.8	9.9	7.0	3.0	0.7	0.6
2	3.4	1.6	1.8	2.8	4.6	6.9	8.7	10.5	11.9	12.7	12.6	12.1	11.3	9.8	7.2	4.7	2.7	1.9	2.3	3.5	5.0	7.3	9.8	11.9	13.1	13.2	12.4	10.6	7.3	3.5	1.2
3	8.0	4.7	2.5	2.0	3.0	4.8	6.7	8.9	11.0	12.5	13.2	13.4	13.3	12.8	10.8	8.6	6.0	3.7	2.5	2.4	3.0	4.9	7.3	10.2	12.5	13.8	14.0	13.4	11.3	8.2	4.8
4	12.0	9.4	6.1	3.5	2.9	3.9	5.1	7.1	9.5	11.5	12.9	13.8	14.5	14.7	13.4	12.1	10.0	7.7	5.3	3.4	2.5	3.4	5.2	8.0	11.0	13.4	14.9	15.2	13.9	12.0	9.5
5	14.7	13.1	10.3	7.3	5.1	4.3	4.6	5.7	7.7	9.8	11.7	13.4	14.8	15.7	15.1	14.4	13.0	11.4	9.3	6.7	4.1	3.3	4.0	5.9	8.8	11.9	14.5	15.9	15.7	14.6	13.0
6	16.5	15.4	13.4	10.9	8.6	6.5	5.2	5.2	6.3	7.9	9.7	12.8	13.8	15.6	15.8	15.8	15.0	14.1	12.5	10.4	7.5	5.1	3.9	4.5	6.4	9.5	13.0	15.1	16.5	16.4	15.3
7	16.9	16.9	15.3	13.5	11.6	9.6	7.3	5.7	5.5	6.1	7.5	9.4	11.8	14.0	15.0	15.9	16.0	15.7	14.6	13.0	10.8	8.3	5.6	4.3	4.6	6.6	10.1	13.2	15.4	16.7	16.7
8	15.8	16.8	16.2	14.9	13.5	11.9	9.8	7.4	5.9	5.3	5.5	6.8	9.2	11.7	13.1	14.6	15.5	16.2	15.7	14.7	13.0	11.0	8.4	5.6	3.8	4.2	6.7	10.3	13.3	15.1	16.3
9	13.4	15.2	15.8	15.4	14.5	13.3	11.4	9.5	7.4	5.4	4.4	4.6	6.2	8.4	10.2	12.3	13.8	15.1	15.7	15.3	14.3	12.8	10.6	8.0	4.4	2.9	3.8	6.3	10.0	12.6	14.7
10	9.9	12.7	14.0	14.5	14.5	13.8	12.5	11.2	9.3	6.7	4.6	3.5	4.0	5.2	6.6	8.8	11.1	13.0	14.2	14.8	14.7	13.8	12.2	10.3	6.7	3.1	2.1	3.0	5.7	9.1	12.0
11	5.4	9.0	11.3	12.6	13.4	13.6	13.0	12.2	11.1	8.9	6.3	4.2	3.3	3.4	3.7	5.2	7.4	9.9	11.8	13.1	14.0	14.0	13.2	11.8	9.3	5.3	2.2	1.1	2.3	4.5	8.0
12	2.3	4.8	7.5	9.8	11.5	12.4	12.7	12.6	12.2	10.9	8.8	6.3	4.4	2.9	2.2	2.7	3.9	6.2	8.5	10.5	12.3	13.2	13.4	12.9	11.3	8.4	4.7	1.3	0.4	1.2	3.6
13	0.8	2.0	3.9	6.2	8.6	10.4	11.6	12.4	12.7	12.2	11.0	9.2	7.4	5.0	2.7	1.7	1.8	3.2	4.9	7.0	9.5	11.3	12.6	13.4	12.7	10.8	8.4	4.3	1.3	-0.1	1.0
14	1.9	1.0	1.9	3.5	5.7	8.0	9.8	11.5	12.6	12.9	12.3	11.4	10.4	6.3	5.7	3.2	1.9	1.9	2.6	4.1	6.4	8.8	10.9	13.0	13.4	12.6	11.2	8.1	4.7	1.5	0.3
15	5.9	2.9	1.6	2.0	3.7	5.7	7.7	9.9	11.7	12.9	13.1	12.9	12.6	11.4	9.3	6.9	4.4	2.7	1.9	2.3	4.0	6.2	8.7	11.6	13.2	13.7	13.2	11.1	9.0	5.7	2.7
16	10.2	7.0	4.2	2.7	3.0	4.3	5.9	8.1	10.3	12.1	13.2	13.7	14.2	13.4	12.1	10.5	8.4	6.2	3.8	2.3	2.8	4.2	6.3	9.5	12.2	13.9	14.6	13.3	12.0	9.9	7.2
17	13.1	10.7	6.0	5.4	4.1	4.1	4.7	6.4	8.4	10.6	12.2	13.6	14.9	14.8	14.1	12.9	11.5	9.8	7.4	4.5	3.3	3.3	4.5	7.2	10.2	13.0	14.9	14.9	14.2	12.7	11.0
18	15.1	13.3	11.1	8.9	6.8	5.2	4.5	5.3	6.6	8.5	10.4	12.4	14.5	15.1	15.1	14.6	13.6	12.5	10.7	7.9	5.8	4.0	3.6	5.0	7.6	11.0	13.8	15.1	15.5	14.7	13.4
19	16.2	15.0	13.1	11.5	9.8	7.7	5.6	5.0	5.2	6.5	8.1	10.3	12.8	13.9	15.0	15.3	15.0	14.3	11.9	10.8	9.0	6.3	4.2	3.8	5.1	8.1	11.6	13.8	15.4	15.7	15.0
20	15.8	15.8	14.4	13.0	11.6	10.0	7.6	6.0	4.9	5.0	5.9	7.6	10.3	11.8	13.5	14.7	15.1	15.1	14.3	12.6	11.2	9.0	6.1	3.9	3.5	5.2	8.6	11.5	13.8	15.1	15.5
21	14.1	15.0	14.7	13.9	12.7	11.5	9.7	7.7	5.7	4.5	4.2	5.2	7.3	8.9	11.2	12.9	13.9	14.8	14.8	13.7	12.6	11.0	8.6	5.5	3.1	3.1	5.2	8.0	11.2	13.2	14.5
22	11.3	13.0	13.6	13.8	13.3	12.3	10.9	9.6	7.5	5.2	3.8	3.6	4.7	5.7	7.8	10.0	11.7	13.1	14.0	13.9	13.3	12.3	10.6	7.9	4.3	2.3	2.9	4.3	7.4	10.4	12.2
23	7.4	10.1	11.6	12.5	13.0	12.6	11.8	11.0	9.5	7.2	4.9	3.4	3.3	3.2	4.6	6.4	8.4	10.6	12.2	12.4	13.2	13.0	11.9	10.1	7.0	3.3	1.8	1.7	3.5	6.3	9.0
SUM	###	###	###	###	###	###	###	###	###	###	###	###	###	###	###	###	###	###	###	###	###	###	###	###	###	###	###	###	###	###	###
	###	###	###	###	###	###	###	###	###	###	###	###	###	###	###	###	###	###	###	###	###	###	###	###	###	###	###	###	###	###	###
T	9.7	9.6	9.2	8.9	8.9	8.9	8.7	8.9	9.1	9.1	9.1	9.2	9.7	9.7	9.6	9.5	9.4	9.4	9.2	8.9	8.8	8.7	8.6	8.7	8.7	8.8	9.2	9.2	9.3	9.2	9.2

Figure 4.3. Example Excel spreadsheet of the manual input data for one month.

4.3.2 Initial Data Processing

To allow the extraction of the relevant data sets for the computation of sea-level rise (Section 4.3) and Extreme Value Analysis (Section 4.4) required significant levels of data processing. For each year the observed water levels recording the hourly tide gauge readings were imported as a text file in to excel. The astronomical tidal prediction based on the tidal prediction software POLTIPS, (Chapter 2; (POLTIPS, 2008)) was computed for each hour within the specified year and imported as a text file in to the same Excel spreadsheet. To calculate the storm surge component (also known as the residual component) the astronomical component was subtracted from the observed level (Chapter 2, Equation 2.1; Pugh, 1987).

From this computation the Excel spreadsheet three columns were produced, the observed level from the tide gauge, the astronomical tide component and the residual storm surge component. This is illustrated in Table 4.4 showing an example of the Newlyn data for 1992. This process was undertaken for each year of data for both Devonport (1962 to 2012) and Newlyn (1915 to 2012).

From 1993 both Newlyn and Devonport data sets recorded information every 15 minutes. To ensure a homogeneous data set for the period 1915 to 2012 (Newlyn) and 1962 to 2012 (Devonport) the readings between the hour, i.e. 15, 30 and 45 were filtered leaving only the readings recorded on the hour.

Date	hour	observed	tidal	Residual
01/01/1992	00:00:00	3.799	4.0553	-0.2563
01/01/1992	01:00:00	4.278	4.515	-0.237
01/01/1992	02:00:00	4.375	4.6139	-0.2389
01/01/1992	03:00:00	4.147	4.3819	-0.2349
01/01/1992	04:00:00	3.702	3.9293	-0.2273
01/01/1992	05:00:00	3.122	3.3522	-0.2302
01/01/1992	06:00:00	2.497	2.7306	-0.2336

Table 4.4. An example of Excel spreadsheet showing the observed, tidal and residual levels for Newlyn.

4.3.3 Extracting the Annual Maximum and 10 Largest Values

To allow the calculation of storm surge frequency-magnitude relationships required the extraction of the annual maximum and 10 largest values from both the observed sea level and storm surge (residual) data sets (Cole, 2001). Following the calculation of the storm surge component for each hourly reading, the data for each year were sorted from largest to smallest based on the observed data. The top 200 results were copied and for ease of computation pasted in to a separate work sheet. These top 200 readings were then sorted firstly by date and then by the observed maximum reading. This, therefore, grouped the annual maximum readings into days. The maximum observed reading for each day was then copied, thus no two readings were copied from the same day. This ensured that all data was separated by 24 hours and could be assumed to be statistically independent. If 10 independent results were not found within the top 200 results further data was selected until 10 independent readings were obtained. The top 10 readings for the year were copied back in to the original spread sheet with the annual maximum copied in to a separate column.

To extract the maximum and 10 largest residual observations the above process was repeated but by sorting the residual column rather than the observed column. In addition to extracting the 10 largest values, to enable an analysis utilising the Generalised Pareto Distribution and to provide an understanding of the change in storm frequency over time all independent observations above 5.4 m CD and 0.4 m for observed and residual observations, respectively, were also extracted.

An example of the extracted data for Newlyn for 1992 is given in Table 4.5. In total for both Newlyn and Devonport over 2,000 (1000 for each: annual maximum and storm surge maximum) independent results were extracted to enable an analysis to be undertaken utilising the GEV and the r-largest methodology. For the GPD methodology approximately 8000 independent results were extracted from the tide gauge data.

4.3.4 Frequency Distribution

To enable a joint probability analysis to be produced as detailed in Section 4.4.5, a frequency analysis was undertaken of the data set. A data range was created at intervals of 0.1 m between the maximum and minimum values for the residual component, tidal component and observed component. The “Frequency

Distribution" function within Excel was then used to calculate the number of occurrences within this interval.

The Monte Carlo methodology can model the frequency distribution utilised by the Joint Probability approach as a discrete data set, or the individual hourly tide gauge records can be imported and modelled within the appropriate software package. This means within the Monte Carlo analysis almost 4 million data points were modelled to evaluate the frequency magnitude relationships.

An example of the calculated values for 1992 is given in Table 4.6

Observed Annual Maximum (mCD)	Observed Residual Maximum (m)	10 Observed Maximum (mCD))	10 Observed Residual (m)	Residual Above 0.4 m	Observed Above 5.4 mCD
6.164	0.3927	6.164	0.3927	-	6.164
		6.108	0.3858		6.108
		6.053	0.3853		6.053
		5.951	0.3771		5.951
		5.932	0.3529		5.932
		5.917	0.3361		5.917
		5.9	0.3258		5.9
		5.895	0.3006		5.895
		5.884	0.286		5.884
		5.865	0.2825		5.865

Table 4.5 An example from Newlyn for 1992 showing the extracted values for the annual maximum, residual maximum, 10 largest annual maximum, 10 largest residual maximum and values above a threshold for both the residual and observed. N.B Not all values for Observed above 5.4 m are given.

Observed Level		Residual		Astronomical	
Interval (mCD)	Count	Interval (m)	Count	Interval (mCD)	Count
5.60	0	0.50	0	6.2	0
5.50	0	0.40	50	6.1	2
5.40	3	0.30	170	6	8
5.30	5	0.20	535	5.9	12
5.20	22	0.10	1661	5.8	29
5.10	77	0.00	2727	5.7	29
5.00	126	-0.10	2570	5.6	48
4.90	181	-0.20	990	5.5	72
4.80	193	-0.30	37	5.4	114

Table 4.6. Example of Frequency analysis of Observed, residual and Astronomical levels for Newlyn, 1992. N.B Not all data is shown.

4.3.5 Sea-level Rise Analysis

To calculate the sea-level rise for both Newlyn and Devonport the observed sea-level values for each year have to be averaged to give a mean annual observed level. This was undertaken for each year, with a plot of the mean annual observed sea level plotted against time. To ensure that the annual mean is representative of the overall sea-level rise component, the tidal component and storm surge component were also analysed. The gradient of the graph provided the rate of sea-level rise for both Newlyn and Devonport for the period 1915-2012. In addition, an analysis was undertaken to see if there were any changes in the average rate over various decades of the data set.

A comparison of the sea-level trend of Newlyn and Devonport provided an indication as to the quality of the Devonport data set.

4.4 Statistical data analysis

An outline of the main methods of statistical analysis that utilise real time data to evaluate frequency-magnitude relations was given in Chapter 3. These included, Generalised Extreme Value Analysis (Cole, 2001, Reeve et al., 2012) r-largest (Cole, 2001) and Joint Probability (Dixon and Tawn, 1989). The following section outlines the methodology of each approach, and how it utilises the data sets. Results of the statistical analysis are given in Chapter 5.

4.4.1 Generalised Extreme Value Analysis

If we consider a series of independent random variables X_1, X_2, …. X_n, with a cumulative distribution function $F_x(x)$ with a maximum value of $M_n = \max\{X_1,\ldots,X_n\}$, then the cumulative density function of M_n can be obtained as:

$$\Pr(M_n<x) = Fx(x)\}^n \qquad (4.1)$$

As n tends to infinity the distribution function of M_n can be approximated by a member of the generalized extreme value (GEV) family of distributions (An and Pandey, 2007; Kotz and Nadarajah, 2005; Cole, 2001):

$$G(z) = \exp\{-[1+\xi(\frac{z-\mu}{\sigma})]^{-\frac{1}{\xi}}\} \qquad (4.2)$$

The three parameters of the distribution are:

- A location parameter (μ).
- A scale parameter (σ).
- A shape parameter (ξ).

As $\xi \rightarrow 0$, the type 1 (Gumbel) distribution is obtained, as $\xi>0$, the GEV is known as the Type 2 (Frechet) distribution and as $\xi<0$ the GEV is known as the Type 3 (Weibull) distribution.

The Weibull distribution has a finite value which means it decays to a point where the maximum value cannot be exceeded. The Gumbel distribution has no upper bound meaning that it can take on infinitely high values. The Frechet distribution has no upper bound but due to the shape of the distribution can lead to high values with greater probability than would be obtained with the Gumbel distribution. Examples

of the three distributions and representative return level plots are shown in Figure 3.1.

For many situations it is difficult to extract the relevant information from the cumulative density function, as natural hazard studies are typically interested in the recurrence level or frequency level of a particular magnitude event.

Pugh, (1987) stated that if the probability of a level (Z_p) being exceeded in any given year is p, the level is often said to have a return period of 1/p years. Therefore

$$Z_p = \{\mu - \frac{\sigma}{\xi}[1 - \{-\log(1-p)\}^{-\xi}]\}, \; for \xi \neq 0$$
$$Z_p = \{\mu - \sigma \log\{-\log(1-p)\}\}, \; for \xi = 0 \qquad (4.3)$$

where G(z) = 1-p.

It is common to present the return level against the return period on a logarithmic scale. A comparison of the raw data and the return level plot produced by the GEV analysis allows a visual assessment and validation of the model.

4.4.2 Modelling the Generalised Extreme Value Distribution

Section 4.3.3 outlined the methodology of extracting the individual annual maximum for each year from the observed data set. For each site the annual maximum for all years (Devonport 1962-2012, Newlyn 1915-2012) was compiled in to a new Excel spreadsheet. This gave a total of 50 annual maximum for Devonport and 98 annual maximum for Newlyn. To undertake a GEV analysis the Excel spreadsheet containing the annual observed maximum for each site was converted in to a text file. The text file was then imported in to a software package called “Extremes” based on the R software language (Gilland and Katz 2005). Within the “Extremes” software programme the annual maximum data for each site was selected and analysed using a Generalised Extreme Value Distribution. This process is illustrated in Figure 4.4. The GEV analysis was then undertaken, with the output illustrated in Figure 4.5. The software can then be interrogated to evaluate the precise return level and return period with the required confidence limits. This process is then repeated for the storm surge annual maximum and sub sets of the both data sets.

The goodness of fit of the input data and the output from the GEV model can be undertaken by reviewing the probability, quantile and density plots as shown in Figure 4.5.

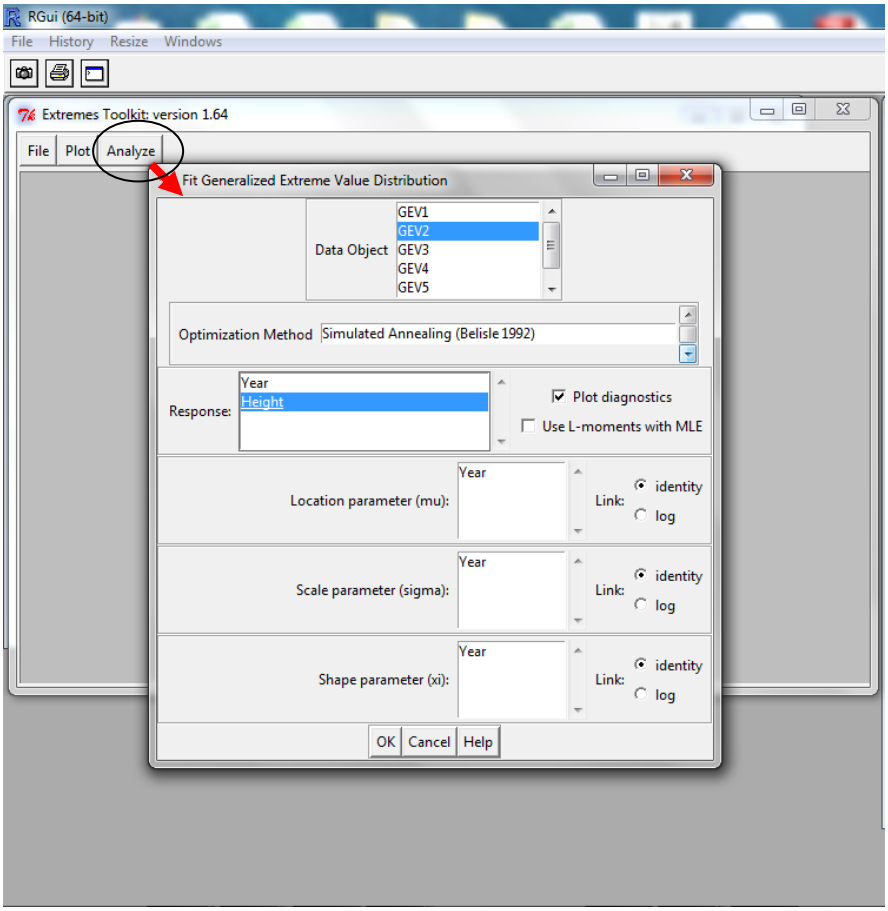

Figure 4.4 Methodology of inputting the data set in to Extremes software package. The left panel highlights the selection of relevant data set, the chosen optimisation method and the required parameter within the relevant data set.

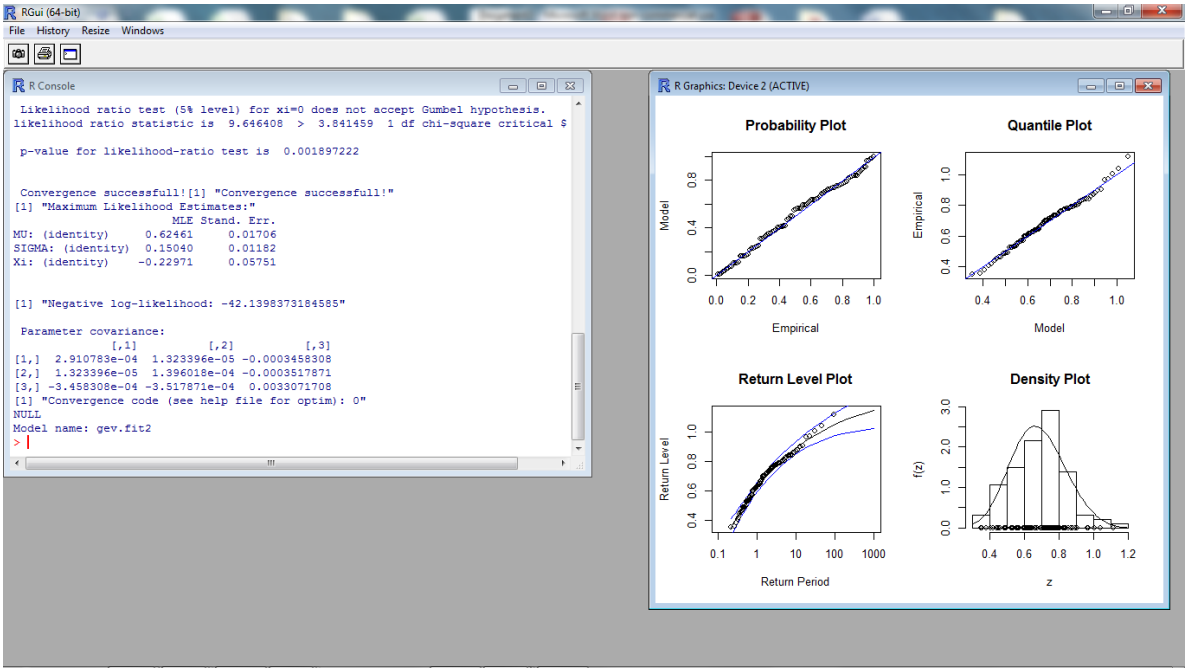

Figure 4.5 Initial output from a Generalised Extreme Value Distribution based on the input from Figure 4.4. The left hand panel gives details of whether the model satisfies the Gumbel model and the shape parameters. The right hand panel shows the data in a series of plots of predicted against the raw data, allowing an evaluation of the effectiveness of the model.

4.4.3 Generalised Extreme Value Distribution Validation

Several authors (e.g. Cole, 2001; An and Pandley, 2007) note that due to the sensitivity of the Generalised Extreme Value Distribution the Gumbel distribution is not always selected despite theoretically being the best fit. Therefore it is often neccesary to undertake further evaluation to test whether the GEV is modelled by $\xi \rightarrow 0$. From equation 4.2 as $\xi \rightarrow 0$ the Gumbel Distribution is given by:

$$Z_p = P = e^{-e^{\frac{-(x-u)}{\xi}}} \quad (4.4)$$

Taking logarithms of both sides of equation 4.4 twice gives:

$$-\ln\left(-Ln(P)\right) = \frac{x-u}{\xi} \quad (4.5)$$

Where:

$$P = \frac{M}{N+1} \quad (4.6)$$

P=Probability.

M=Rank of each individual event.

N=Number of events.

Plotting x against –ln(-ln(P) (known as the Gumbel Variate) should retrieve a straight line with slope ξ and intercept u. These values can then be put back into equation 4.5 and for any given probability a magnitude can be calculated **(**Reeve et al., 2012)**.**

From equation 4.2 as $\xi<0$ the GEV Weibull distribution is given by:

$$Z_p = P = 1 - e^{-\left(\frac{x-\phi}{\lambda}\right)^K} \quad 4.7$$

Taking logarithms of both sides of equation 4.7 gives:

$$(ln\frac{1}{1-P})^{\frac{1}{k}} = \frac{x-\phi}{\lambda} \quad 4.8$$

If in Excel x is plotted against (ln (1/1-P))$^{1/K}$ (known as the Weibull Variate) a straight line with slope λ and intercept ϕ should be achieved. These values can then be put back into equation 4.7 and for any given probability a magnitude can be calculated (Reeve et al., 2012). A comparison of the Gumbel and Weibull plots provides a test as to whether or the "Extreme" software package has selected the correct distribution when undertaking a GEV analysis.

4.4.3 r-Largest

One of the main drawbacks of the Generalised Extreme Value distribution is that in only using the annual maximum it wastes a significant amount of data (Reeve et al 2012). To combat this limitation the r-largest approach was developed by Smith, (1986). In an extension to the Generalised Extreme Value Distribution the r largest values for each year, z = ($z^{(1)}$, …., $z^{(r)}$) where r ≥ 1, are extracted from each year and ordered. The joint probability density function is then of the form:

$$f(z) = \exp[-\{1+\xi(\frac{x^{(r)}-\mu}{\sigma})\}^{-\frac{1}{\xi}}]\prod_{k=1}^{r}\frac{1}{\sigma}\{1+\xi(\frac{x^{(k)}-\mu}{\sigma})\}^{-\frac{1}{\xi}-1} \qquad 4.9$$

The three parameters (μ,σ,ξ) correspond to the parameters of the GEV model (Butler et al., 2006) and have been calculated using the "extremes" software programme. For each year the selected r values must be selected from independent storm events.

4.4.4 Modeling the r-Largest

To undertake a r-largest analysis, the 10 (r) largest observed maximum for each year of the data set were compiled in to an excel spreadsheet and then converted in to a text file. The text file was then imported in to a software package called "Extremes" (Gilland and Katz, 2005). The file was chosen to be analysed with an r-largest distribution. The model was then run with the output similar to that of the GEV in Figure 4.4. The value of r (2 to 10, a value of 1 equates to the GEV) was then varied to identify the value of r that provided the best fit to the data by evaluating the various plots. The software was then interrogated to evaluate the precise return level and return period with the required confidence limits. This

process was then repeated for the storm surge annual maximum and sub sets of the both data sets.

4.4.5 Generalised Pareto Distribution

The Generalised Pareto Distribution (GPD) requires the selection of data above a specified threshold (Section 3.1). To model within the “extremes” software package the data must be converted from Excel format in to a text file with all data contained within one column. The text file is then imported in to “extreme” and selected to be analysed using the GPD approach. Figure 4.6 shows the GPD analysis screen highlighting the file to be selected, the individual response. An optimization method is selected and the specific threshold above which all data is modeled inputted. To enable return level plots to be produced requires the average number of observations in one year to be specified. The output from the GPD analysis is the same for the GEV, with a series of probability plots and return level plots as shown in Figure 5.

4.4.6 Joint Probability

To utilise the complete hourly records for observed sea level to predict return periods for extreme events, Tawn and Vassie (1980) developed the Joint Probability Method by considering the surge and astronomical tidal functions separately. At any given time the observed sea level $\zeta(t)$ has three components; mean sea level $Z_o(t)$, tidal level X(t) and meteorologically induced level Y(t) (Pugh and Vassie, 1980).

$$\zeta(t) = Z_o(t) + X(t) + Y(t) \qquad 4.10$$

Section 4.3.4 described the methodology of calculating the frequency of occurrence of a specific observed, storm surge or astronomical tidal level. The data is illustrated in Table 4.6. The probability of a specific tidal height was calculated by dividing the number of observations of a specific tidal height by the total number of observations. The surge probabilities were calculated in much the same manner. The joint probabilities were then calculated for each possible combination of tide and surge, by multiplying the tidal probability by the storm surge probability. For example a tidal height of 1.1 m with a probability of 0.15 combined with a surge height of 0.1 m with a probability of 0.1 gives an overall observed height of 1.2 m with a probability of 0.015. An example of this process is illustrated in Table 4.7 As different combinations of tide and surge will give the same overall height the probabilities for each specific height were then combined to calculate the overall probability. An example of this is given in the Table 4.8 below.

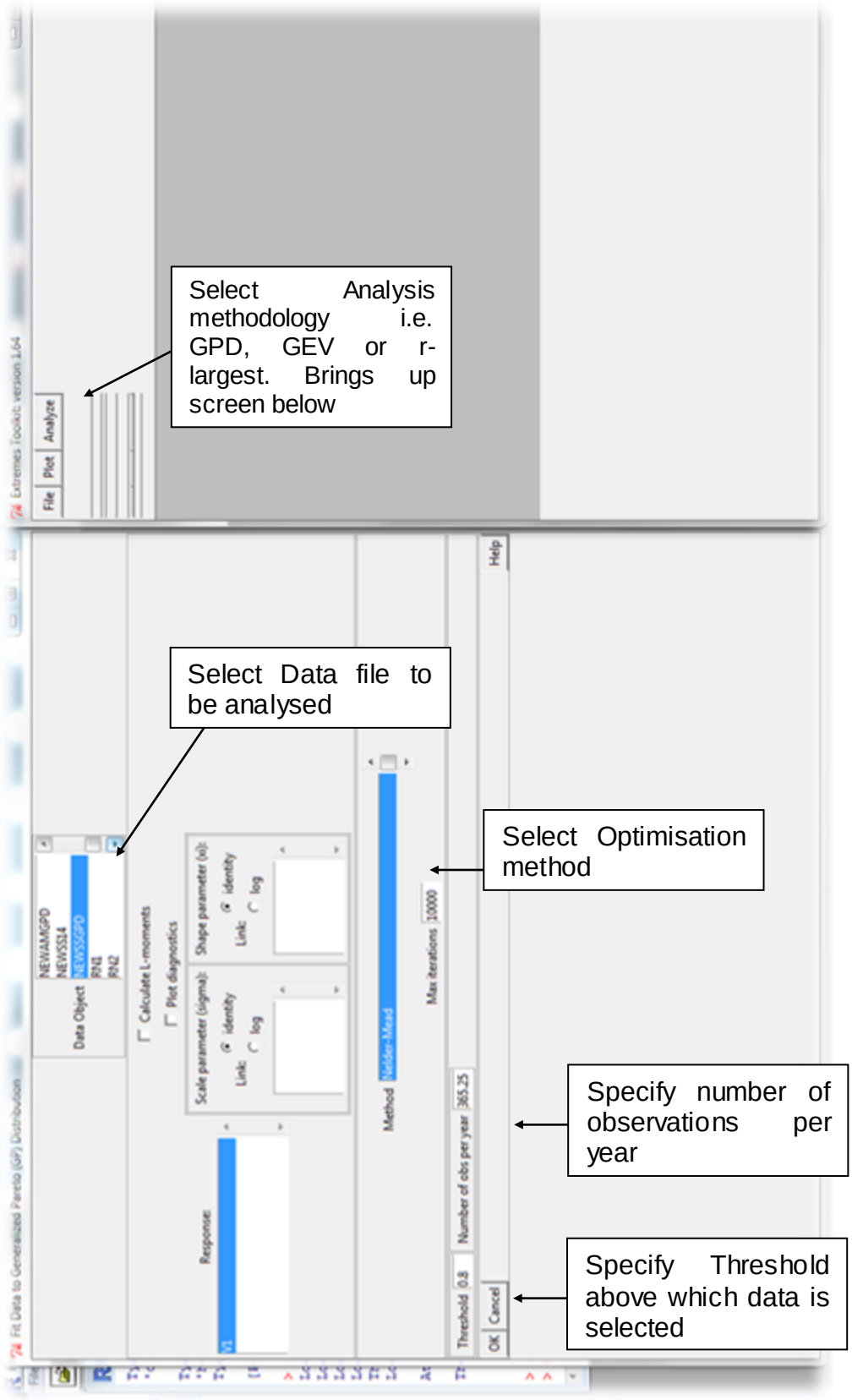

Figure 4.6 Generalised Pareto Distribution Analysis undertaking within the "Extremes" software package.

			Surge				
Tide		Height (m)	0.1	0.2	0.3	0.4	0.5
Height (m)	Probability	Probability	0.1	0.15	0.5	0.15	0.1
1	0.1		0.01	0.015	0.05	0.015	0.01
1.1	0.15		0.015	0.0225	0.075	0.0225	0.015
1.2	0.5		0.05	0.075	0.25	0.075	0.05
1.3	0.15		0.015	0.0225	0.075	0.0225	0.015
1.4	0.1		0.01	0.015	0.05	0.015	0.01

Table 4.7 Example calculation of the probability of surge and tidal heights. Cells with the same colour give the same overall height when tide and surge are combined. See Table 4.8.

Overall Height (m)	Colour (see Table 4.)	Probability
1.1		0.01
1.2		0.03
1.3		0.1225
1.4		0.18
1.5		0.315
1.6		0.18
1.7		0.1225
1.8		0.03
1.9		0.01

Table 4.8. Example calculation of combining surge and height to calculate the overall probability of a given observed height. The probabilities of each cell with the same colour (Table 4.7) and thus the same overall height are added together to give a probability for the specific height.

4.4.6 Probabilistic Scenarios

For a coastal planner or designer the resolution of an inundation map may not always be sufficient to answer two fundamental questions; for a given return period will the area be flooded; if the area is flooded what level does an area need to be raised to mitigate against it. Furthermore, a deterministic approach may not be sufficient for design purposes when a range of scenarios need to be considered.

The following Section outlines a probabilistic approach, using a Monte Carlo simulation (Section 3.1 & 3.2.3) to determine inundation levels based on the existing data sets of storm surge, astronomical tide, wave height and sea-level rise to undertake an assessment of the probability of inundation from all four components.

4.4.7 Modeling the Data Sets

If you have a range of outcomes and the frequency, or probability of occurrence are known, as has been created within Section 4.3 (frequency distributions of the storm surge, wind, wave and tide data), then the data can be modelled as a probability distribution. The software package @Risk (Palisade, 2013) uses probability distributions to describe uncertain values, i.e. values at the extremal end of a data set or data that are possibly unseen. Using the @Risk add on package to Excel the distributions modeled describe a range of values and their probability of occurrence, based on a fitted distribution. Using the calculated frequency distributions outlined in Section 4.3 it was possible to model the distributions for storm surge, observed levels, tidal data and wave data within @ risk. Within Excel the frequency data set was selected and using the @Risk function “Distribution Fitting” the actual data was modeled against up to 30 possible distributions (Palisade, 2013).

Figure 4.6 shows an excel work book with the @Risk package. Highlighted is the data modeled (input data), the output and the distribution models that fit the data set ordered according to the r^2 values (goodness of fit). The blue data represents the actual data set, with the lines representing the modeled distributions.

Figure 4.7 shows two distributions, logistic and loglogistic that according to the r^2 value are the best fit to the actual data set of one year of storm surge data. It is possible to compare more than one distribution against the actual data, although the logistic distribution fits the actual data better according to the r^2 value, the loglogistic distribution has a better fit at the upper extremal end of the data. The requirements

of the end user depends on the choice of distribution. In the case of this study the research concentrated on the upper extreme of the data. As an example, for this study the loglogistic probability distribution would be chosen, based on a comparison of the upper tail of the modeled distribution with the actual data.

The modeled distribution has a series of shape parameters as highlighted in Figure 4.6, which define the distribution and allow the determination of a probability of a given event, in this case storm surge heights.

Confidence intervals have also been established within the modeling of the data sets. Within @Risk, the “bootstrap-Confidence interval” was selected with a confidence interval of 95%. The output from @Risk was a mean, upper and low bound value for each of the distribution shape parameters.

To evaluate the sensitivity of the @Risk software both the modeling of the data sets and the establishment of confidence intervals was undertaken several times to ensure consistency was achieved.

4.4.7 Probability of Inundation

From Section 4.4.7 modeled distributions have been established for storm surge, wave height, astronomical tide and sea-level rise. By combining the different components it was possible to produce a range of probabilities of inundation.

Taking the individual distributions calculated within @risk it was possible to combine them using the “simulation” function. The individual distributions were the inputs with the outputs being a summation of the individual distributions. This process is illustrated in Figure 4.8, where the two inputs are the storm surge and astronomical tide levels with the output being a probability distribution of a inundation level. To calculate the output distribution @risk runs a Monte Carlo simulation, randomly sampling each input distribution to calculate a probability for each output. Undertaking this numerous times, up to 10,000 iterations gives a probability distribution for the output. The probability distribution can then be plotted on a curve of inundation level against probability as illustrated in Figure 4.9 below. It is then possible from this to look at the affect of other components on the probability that cannot easily be modeled such as sea-level rise.The following combination of Monte Carlo simulations was undertaken for both Newlyn and Devonport data sets:

1. Astronomical tide and storm surge height distributions
2. Astronomical tide, storm surge and wave height distributions
3. Astronomical tide, storm surge height and sea-level distributions
4. Astronomical tide, storm surge, wave height and sea-level distributions

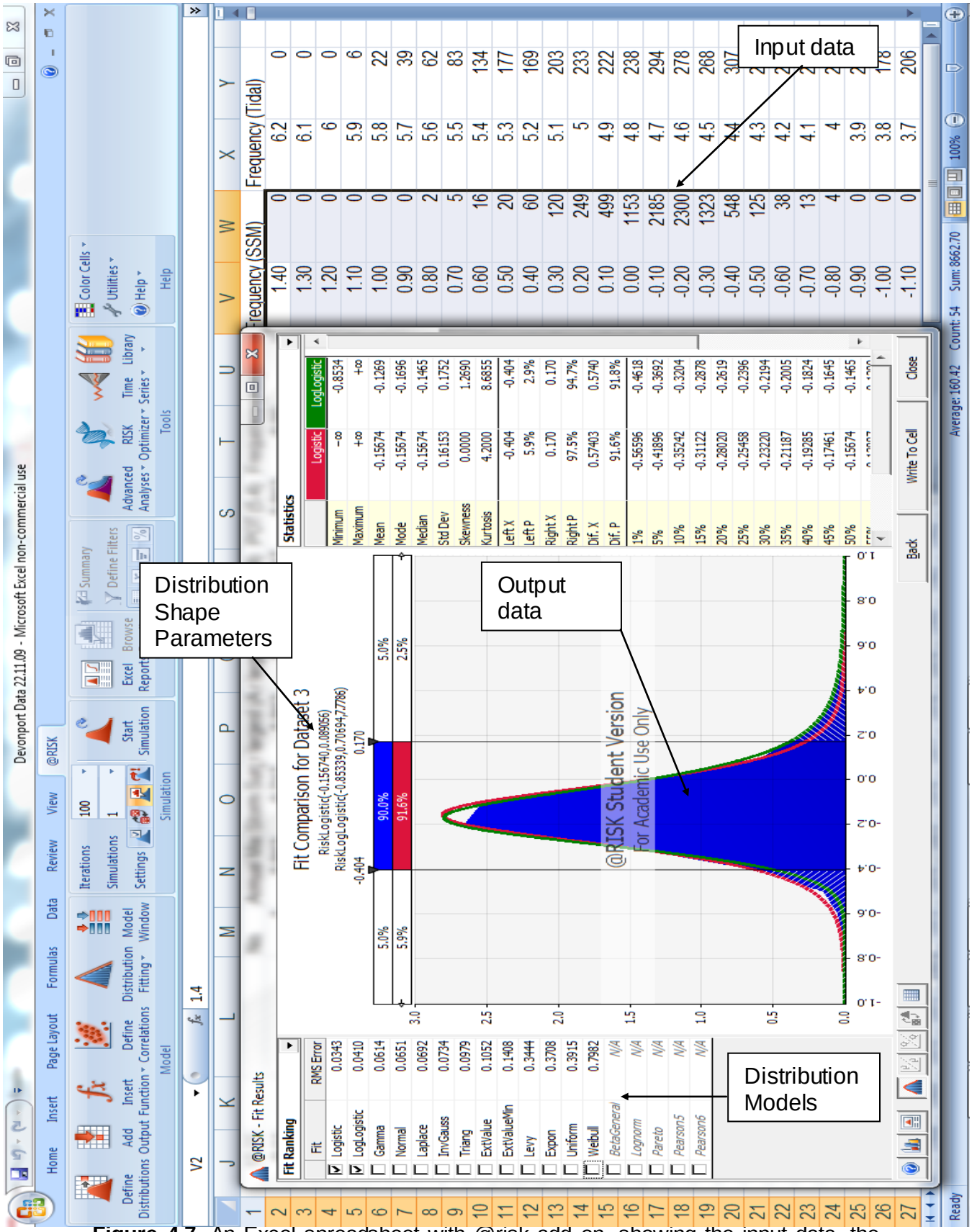

Figure 4.7. An Excel spreadsheet with @risk add on, showing the input data, the modeled distributions and a comparison of the modeled distribution with the input data.

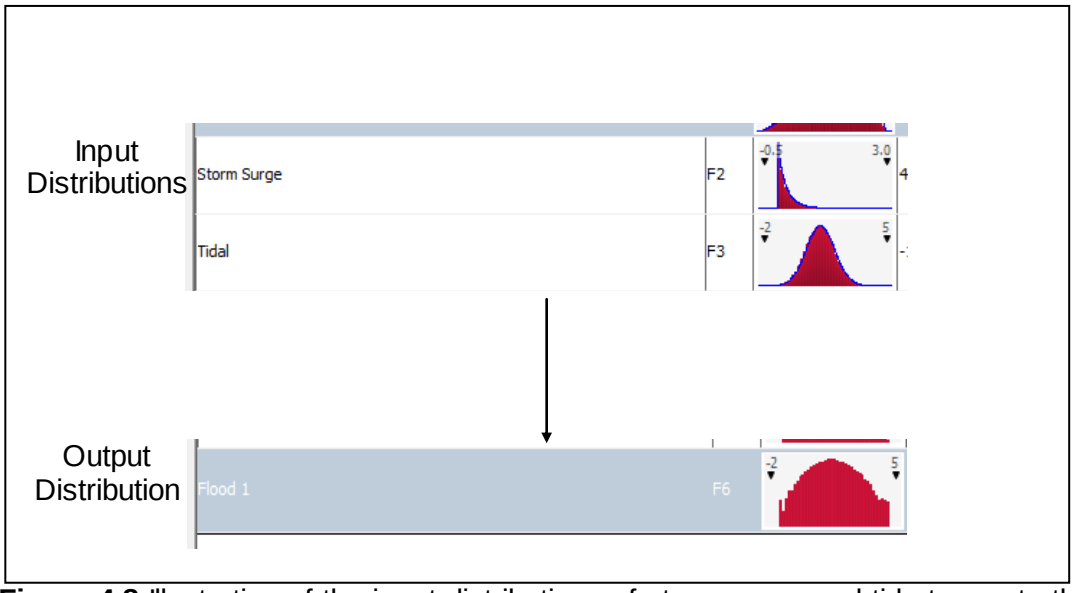

Figure 4.8 Illustration of the input distributions of storm surge and tide to create the output distribution of inundation levels.

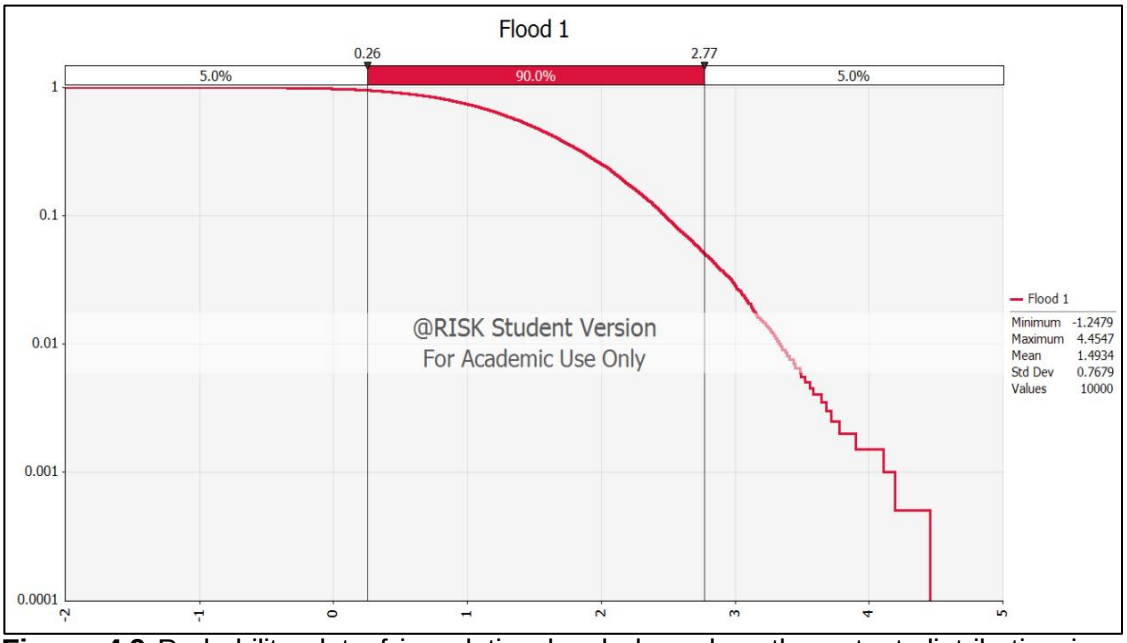

Figure 4.9 Probability plot of inundation levels based on the output distribution in Figure 4.7.

4.5 Devonport Weather Data

In an attempt to resolve the trends observed in the tide gauge records for Newlyn and Devonport and identify fluctuations in the data due to natural phenomena, weather data for Mountbatten (Plymouth) were obtained from the Meteorological Office. The data were in the form of a text file containing daily average readings of pressure, wind speed and wind direction for the period 1962-2008. An example of the data set is given in Table 4.6.

For the daily pressure and wind speed readings the annual mean, maximum and minimum were calculated and the graphs plotted in Excel. For wind direction the data was interrogated to identify any significant changes over the time period.

In addition to analysing the weather data to evaluate any observed trends, a frequency analysis was undertaken to allow the data to be converted to wind speed using the charts of Kamphuis, (2010). This allowed the data to be incorporated in to the evaluation of inundation levels for Devonport using a Monte Carlo simulation.

Day	Month	Year	Pressure at Mean Sea Level (hPa/mb) at 0900Z	Wind - Daily Mean Speed (knots)	Wind - Mean Direction at 0900Z
1	1	1969	1036.1	3.9	30
2	1	1969	1037.7	6.9	350
3	1	1969	1034.4	1.8	0
4	1	1969	1025.8	2.6	0
5	1	1969	1013.2	4.5	20
6	1	1969	1006.8	12.1	100
7	1	1969	985.5	22.5	160
8	1	1969	998.5	10.8	250
9	1	1969	1008.2	15.4	150

Table 4.9 Example of weather data for Mountbatten Plymouth.

4.6 Calculation of Wave Height

A component of inundation that cannot be easily modelled within GIS but is of significant importance to coastal planners and designers is wave height. To design a structure or to evaluate the likelihood of flooding requires an understanding of the relationship between the frequency of wave and their heights (Reeve et al., 2012; Kampuis, 2010). To model the possible wave heights and their frequency the following data sets of wave height and wind speed as outlined earlier in this chapter were utilised.

Chapter 3 showed the applicability of the statistical analysis methods in evaluating frequency-magnitude relations not only for storm surges but also for wind and wave data. Using the methodology of extracting the relevant data sets from the observed sea-level data (Section 4.4), the annual maximum and 10 largest values were extracted from the wave and wind data. In addition, a frequency analysis was undertaken of both wind and wave data sets.

As discussed in Chapter 3, a Generalised Extreme Value assessment is limited to longer data sets. As the wave data is limited to only 7 years an analysis of the wave data will be undertaken using the r-largest methodology (Section 4.4.4). The output from the analysis was a return period plot, evaluating the frequency-magnitude relations for wave height. The extreme value analysis was then compared with the probability distributions calculated using @risk, which are discussed in Section 4.4.5.

Devonport Dockyard, a specific case study within south-west England is located within an area of the Tamar Estuary known as the Hamoaze. This area can be classified as being within an enclosed or semi-enclosed basin (Kamphuis, 2010), therefore the wave height predictions for the main coastline are not applicable as the predictions are made for a fully developed sea (Kamphuis, 2010). Therefore a different approach needs to be adopted to evaluate wave height at Devonport Dockyard.

Kampuis, (2010) developed methodology for converting wind data to wave height:

Assuming a fetch limited body of water:

$$H_{mo} = \frac{H^*_{mo} U^2}{g} \qquad 4.11$$

Where:

$H_{mo} = Wave\ Height\ (m).$
$H^*_{mo} = Dimensionless\ wave\ Height.$
$U = Wind\ Speed\ (m/s).$
$g = acceleration\ due\ to\ gravity\ (m/s^2).$

And

$$H^*_{mo} = 0.0016\ (F^*)^{1/2} \qquad 4.12$$

$$\boldsymbol{F}^* = \frac{gF}{U^2} \qquad 4.13$$

$F = Fetch\ length\ (m).$
$\boldsymbol{F}^* = Dimensionless\ Fetch\ Length.$

For example, from a wind speed of 20m/s, over a fetch of 100km, F^* =2451.5 (eq 4.13, using equation 4.12 gives a H^*_{mo} = 0.079, which gives a value of 3.2 m for H_{mo}. These values can be confirmed from Figure 4.10 at the intersection of 20 m/s and 100km.

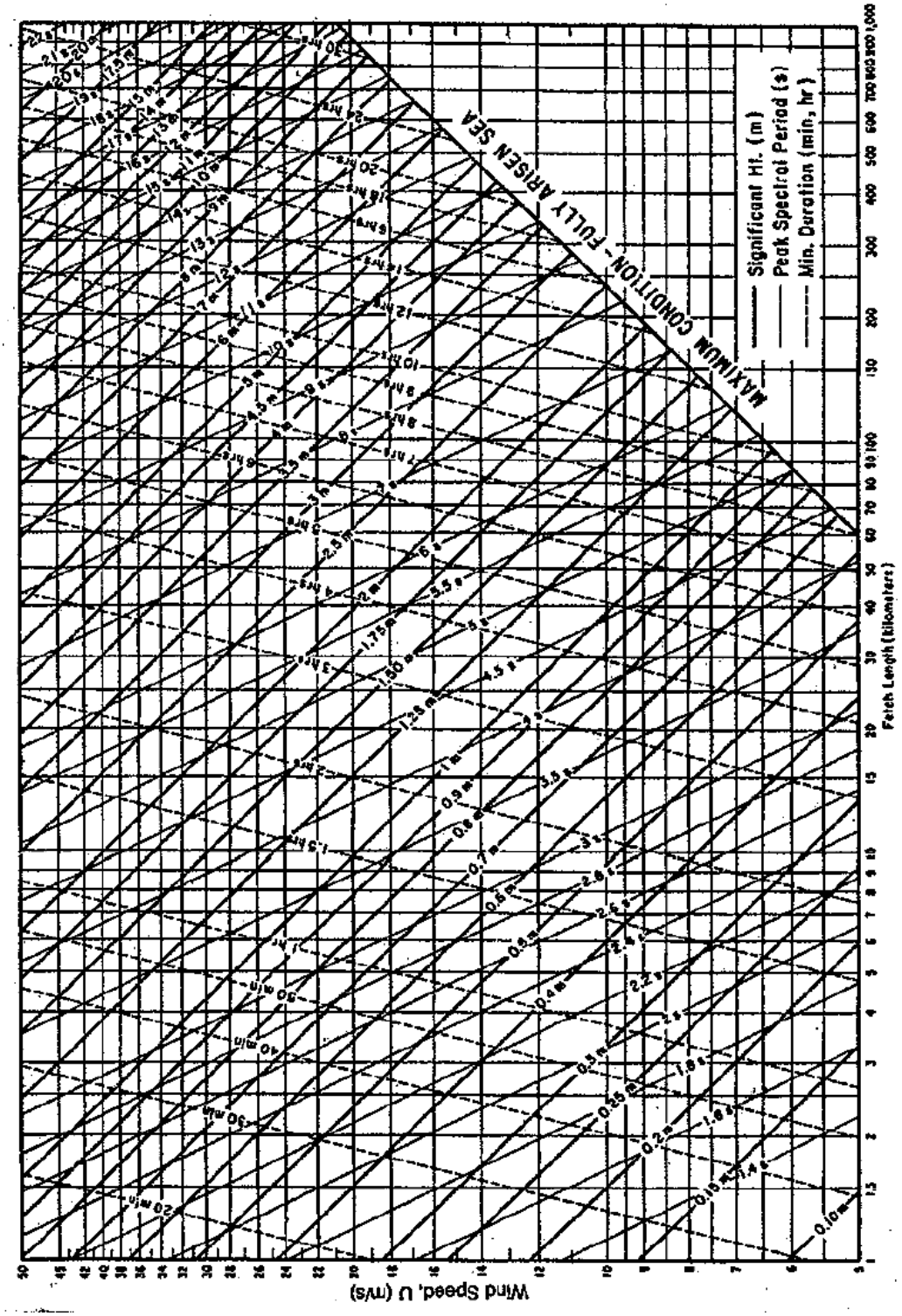

Figure 4.10 Wind Hindcasting Nomogram for the estimation of wave height and period for a given wind speed and fetch (Kamphuis, 2006).

4.7 Tsunami Modelling

Based on historical data and the assessment of potential sources of an earthquake creating a tsunami that could affect south-west England, the most likely point of origin is the Gibraltar-Azores plate boundary (DEFRA, 2007; DML, 2002; Horsburgh et al., 2008). The maximum magnitude of earthquake and subsequent tsunami is evaluated to be of a similar order to the Lisbon earthquake and tsunami of 1755. However, there is discrepancy between historical accounts (Section 2.5) and modelling (Horsburgh et al., 2008) regarding the maximum tsunami amplitude to have affected south-west England. To attempt to resolve the conflicting amplitudes a finite difference tsunami model which attempts to resolve the 2-D shallow water equations was developed in conjunction with Imperial College London (Per Comm. Jon Hill). The model is similar to Horsburgh et al., (2008) and adopts the same source parameters. However, the model undertaken by Imperial College London attempts to create a higher resolution grid size down to 150 m, compared to a typical grid size of Horsburgh et al., (2008) of between 1 km and 10 km. The updated model attempts to resolve the complex coastline of south-west England to provide more representative results. The overall bathymetry remains as the tsunami model undertaken by Horsburgh et al., (2008).

Within the model, 56 receptors are placed along the south-west England, providing details of wave amplitude and period. The wave amplitude will be compared to the potential inundation levels of storm surges and the potential inundation levels modeled within a Geographical Information System (Chapter 6).

4.8 Past, Present and Future Scenarios

4.8.1 Introduction

As outlined in Chapter 3, for this research it was decided that a Geographical Information System (GIS) analysis was required to fully understand past, present and future sea-level scenarios based on the predictions from tide gauge record and to determine the spatial impact of different inundation scenarios. Chapter 3 reviewed the applicability of a GIS analysis for evaluating the hazard and risk of natural events. Creating a GIS analysis incorporating the inundation levels on to the digital elevation data and infrastructure data will allow a visual representation of the different sea-level scenarios and their possible implications. This technique rather than just producing a series of numbers provided additional information as well as an effective communication tool for potential end users. The different inundation levels may be mathematically significant but spatially the effects may be quite small, or conversely a small difference in inundation levels may spatially be significant. This approach allowed a more detailed comparison of the scenarios and provided an understanding of the sensitivities of the south-west coastline to storm surges, waves and sea-level rise by giving an insight in to which component was the driving force for future inundation levels.

4.8.2 Building the GIS Data Base

The GIS database consisted of two main layers; the first layer comprised a digital elevation model developed from LiDAR (Light Detection and Ranging data as detailed in Section 4.1). These data came in the form of ESRI ASCII raster grid format, downloaded from the Channel Coast Observatory (www.channelcoast.org). The individual tile sizes ranged between 0.25 km^2 and 4 km^2. In total for the study area there are between 8000 and 10,000 individual tiles, each of approximately 2 MB in size. The LiDAR data was flown for the study area at various dates between 2007 and 2008 by the Environment Agency. Typically the data had a resolution in both the horizontal and vertical of 0.001 m, with an accuracy in the order of 0.1 m to 0.2 m (Channel Coast, 2013).

To combine the individual raster tiles in to a complete Digital Elevation Model (DEM) for the study area (Penzance to Plymouth) each individual ASCII grid file was imported in to ARC GIS 10.1 (ESRI, 2013). Due to the processing speed the individual tiles were stitched in batches of 10 using the “Mosaic to new raster”

function within ARC Catalog (ESRI, 2013). These new rasters were then combined in further batches until all individual tiles were combined in to one raster. Several smaller raster files were created for the Plym and Tamar estuary to allow a more detailed analysis of this area to be undertaken. To visualise the data, the complete raster file was imported in to ARC Map, the raster were then visually checked to ensure the tiles have joined correctly without any gaps in the image.

An example of the Digital Elevation Model for the Tamar and Plym Estuary is given in Figure 4.11. The full data set is presented in Appendix B1, in ARC GIS 10.1.

4.8.3 Vulnerability/Impact Assessment

A second data set was compiled that represented the infrastructure and population for the study area. Chapter 3 outlines the various methods used in undertaking vulnerability/impact assessments of natural hazards. The aim of this assessment is not just to provide a visual representation of the different inundation scenarios, but also to measure the impact the various scenarios had on the study area.

Various sources and types of data are available which covered the study area (see http://digimap.edina.ac.uk). From the available data sets “Strategi” (Ordnance Survey, 2006) was chosen to provide a low resolution overview for the whole study area, with a higher resolution data set of 1:10,000 digital raster maps (Ordnance Survey, 2006) for a more detailed assessment of the impact of the scenarios on the Tamar and Plym Estuaries. Strategi is classified as a regional data set which can be used in the planning and decision making process (Ordnance Survey 2006).

Strategi is a database of geographic features represented as points and lines in vector format. The data above is available as individual layers, so that the user can select the required information or as a complete data set. The data contained within the complete data set is given below:

1. Settlements:
    a. Cities.
    b. Towns.
    c. Other built up areas.
2. Communication:
    a. Airports.
    b. Motorway and Road Network.

    c. Railways.
3. Water Features:
    a. Coastline.
    b. Rivers
    c. Lakes
4. Administrative Boundaries.
5. Land use.
6. Tourist Features.

The required data or complete data set was imported in to ARC Map and could be either overlain on to the DEM or visualised on its own.

An example of the complete Strategi data set overlain on to the DEM for the Plym and Tamar Estuaries is shown in Figure 4.12. The full data set is presented in Appendix B1, in ARC GIS 10.1.

The 1:10,000 raster Ordnance Survey data is part of the OS MasterMap series which was provided at three resolutions, 1:2,500; 1:5,000 and 1:10,000 (Digimap 2013). The data was used to undertake a detailed assessment and came in the form of a GIS layer that contained features that represented different components (i.e. buildings, fields and roads). Each feature was in the form of either a point, line or polygon came with a series of attribute data that allowed the data to be further queried or represented in different ways. Due to the structure of the data it allowed a complex analysis to be undertaken, for example to evaluate the number of houses affected by a specific inundation scenario.

4.8.4 Inundation Scenarios

From the methodology outlined previously within this chapter, the output (Chapter 5) will be a series of predictions for sea-level rise, storm surge, wave height and wind speed frequency magnitude relationships and the identification of uncertainties within each component. Based on the predictions for these different components the following scenarios will be modelled within ARC GIS (Chapter 6) to allow the dominant uncertainty with coastal processes to be identified.

Component	Present day	2050	2100
Storm Surge (1 in 250 and 1 in 1000 return period	Lowest Prediction and Highest prediction	(a) Low (b) Medium (c) High	(a) Low (b) Medium (c) High
Wave Set up (Looe, Cornwall)	Dependent upon return period of storm surge	Dependent upon return period of storm surge	Dependent upon return period of storm surge
Wave Height (Devonport)	Same return period as that evaluated for storm surge	Same return period as that evaluated for storm surge	Same return period as that evaluated for storm surge
Sea-level Rise	None	(a) As for 20th Century (this study) (b) IPCC/UKCP 09 rates (c) UKCP 09 H++ Scenario	(a) As for 20th Century (this study) (b) IPCC/UKCP 09 rates (c) UKCP 09 H++ Scenario

Table 4.10 Summary of inundation scenarios to be modelled in ARC GIS.

4.7.4 Inundation Scenario Comparison

Using “raster calculator” within ARC MAP an individual inundation level was simulated by separating out the contours above and below the inundation level, for example for a hypothetical flood level of 4.1 m ODN, the raster calculator created a new raster with two separate layers, one layer had all values 4.1 m ODN and below while the other contained all values above. This raster is then converted to a polygon using “convert raster to polygon”. This initially kept the two components of

the original raster. Typically the values 4.1 m and below are assigned a code within ARC Map of 1 and the values above a code of 0. To separate out the polygon of 4.1 mODN and below, all values assigned a code of 1 were selected within the attribute table of the polygon. The selected data was then exported to a new layer using the function “convert selection to new layer”. This layer was then saved as a new polygon and contained only the values 4.1 mODN and below, therefore simulating an inundation level of 4.1 mODN.

A simulated hypothetical inundation layer of 4.1m overlain on to the DEM and Strategi data set obtained from this analysis is shown in Figure 4.13.

To allow a comparison between different inundation scenarios the polygon that represented the specific inundation level was queried against the infrastructure data by using the “overlay-intersect” function in ARC MAP (ESRI, 2013). This produced a new polygon that represented only the areas were the inundation level and infrastructure overlaped. From this layer using the information contained within the attribute table the area was calculated to give, for example, the total urban area or the total area of roads that would be flooded.

Figure 4.14 is an example of this process showing the polygon intersection of a hypothetical 4.1m ODN inundation level and the urban areas (subset of Strategi data set).

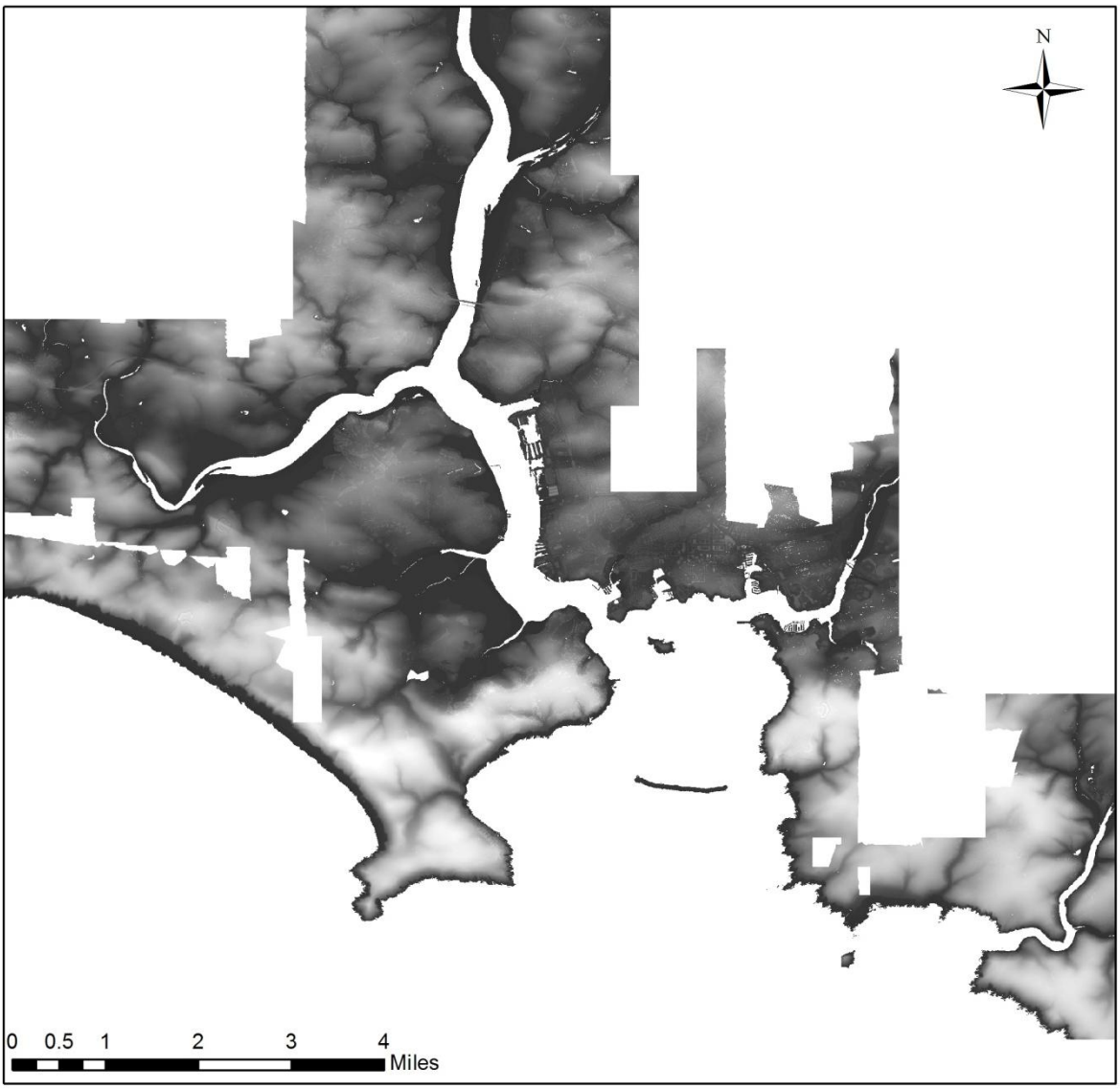

Figure 4.11 Digital Elevation Model (DEM) for the Tamar and Plym Estuaries based on LiDAR data downloaded from the Channel Coast Observatory (Channel Coast, 2013).

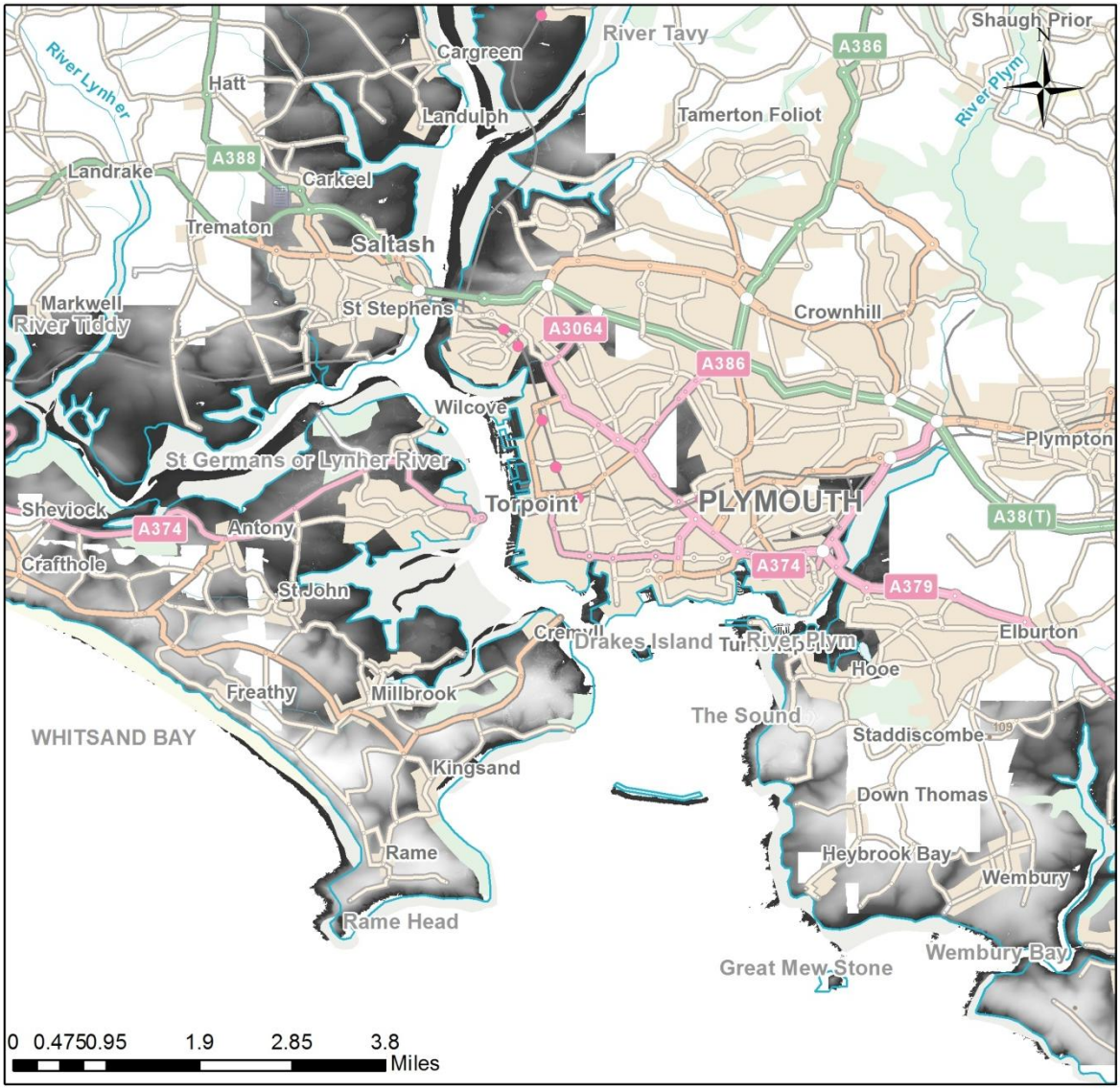

Figure 4.12 Urban and Infrastructure Data (Edina, 2014) overlain on to the Digital Elevation Model.

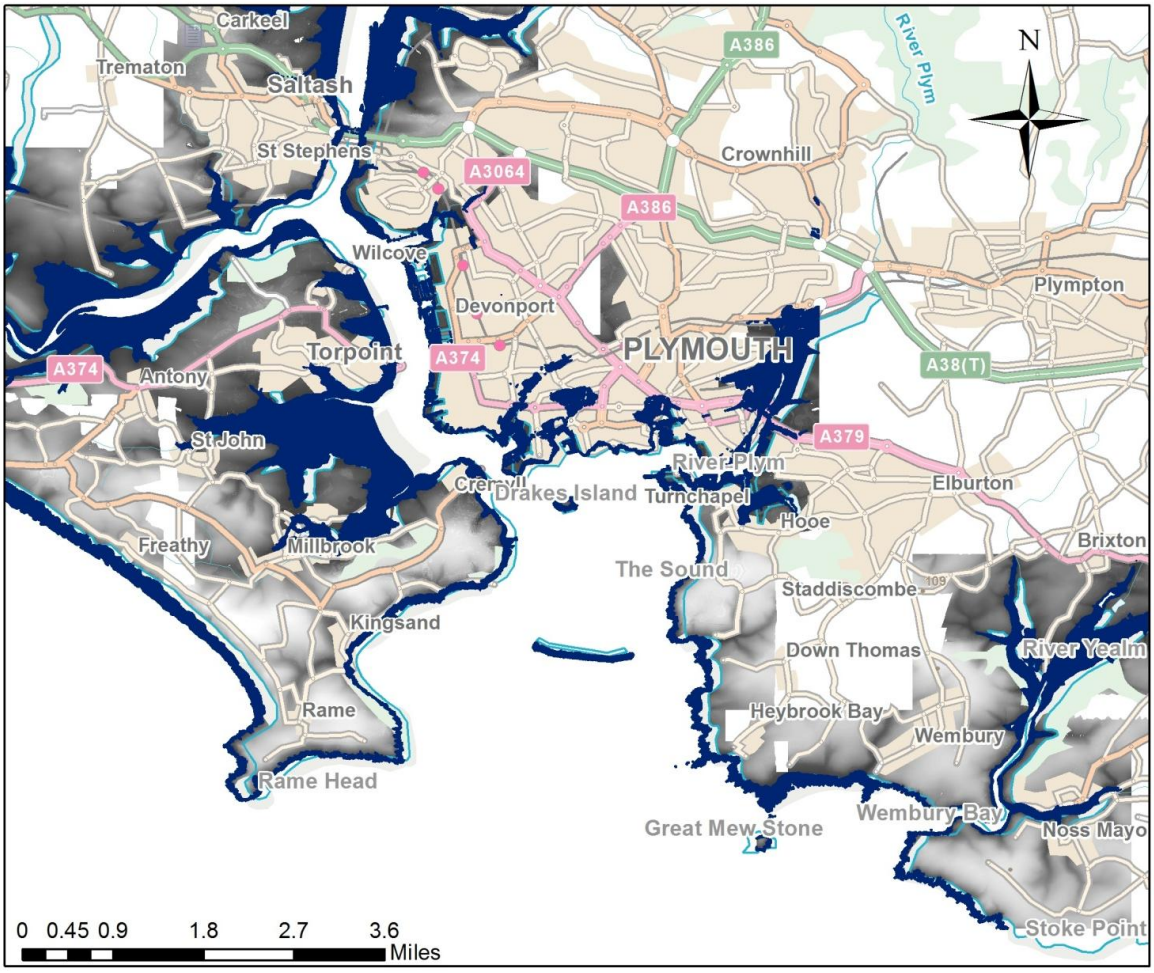

Figure 4.13 Hypothetical 4.1 m flood layer (blue) overlain on the DEM and Strategi Infrastructure data set.

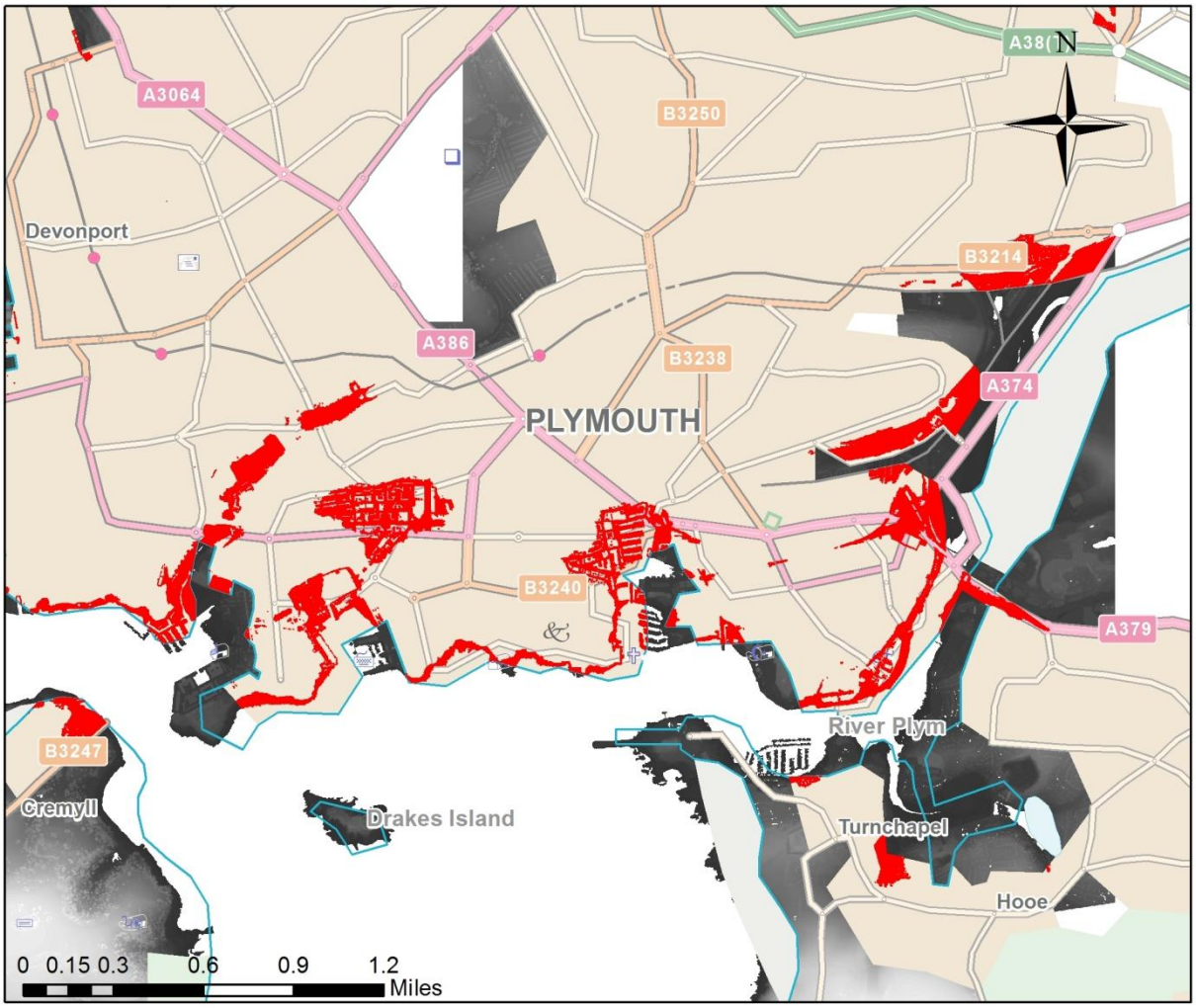

Figure 4.14 The union of a hypothetical 4.1 m flood layer and urban areas (Subset of Strategi data). The area shown in red is only areas were the flood level intersects the urban area.

Chapter 5 Statistical Analysis Results

5.1 Introduction

This chapter describes the results from the statistical analysis undertaken on observed sea level, storm surge, weather and wave data sets, using the methodology described within Chapter 4. Initially the extracted data sets of the annual maximum, r-largest, threshold and frequency distributions are illustrated in Section 5.2. Section 5.3 discusses trends identified within the data, with Section 5.4 focusing on the statistical analysis, establishing frequency-magnitude relations for observed sea levels, storm surge levels, wind speed and wave height for a range of statistical techniques. Chapter 6, based on the range of predictions and uncertainties produces a range of scenarios for the whole study area and two case studies; Devonport Dockyard (Plymouth) and Looe (Cornwall). The scenarios include predicted inundation levels, wave height and sea-level rise scenarios. The impact of these different scenarios are analysed within a Geographical Information System (GIS), presented in Chapter 6.

5.2 Data Sets

Section 4.3.2 and Section 4.3.5 describe the data sets and the methodologies used to extract the relevant information from the Newlyn and Devonport tide gauge data sets, the Plymouth weather data and the Polperro wave data. From the Devonport and Newlyn tide gauge records the following data sets were extracted: the annual mean sea level; the ten largest independent observed levels including the annual maximum; the ten largest observed and storm surge levels above a 5.5 mCD and 0.4 m threshold, respectively; and the frequency distribution of the observed astronomical tide and storm surge levels. From the Plymouth weather data the annual mean and ten largest events were extracted from daily average pressure and wind speed records. In addition, pressure readings were separated into annual average frequencies above and below the mean. This will enable the evaluation of any changes in high and low pressure systems over the study area. Furthermore, the largest independent wave heights, including the annual maximum and the frequency distribution of wave height, were extracted from the Polperro wave data.

Figure 5.1 and Figure 5.2 show the ten largest independent observed sea levels extracted from the Devonport and Newlyn tide gauge data. Both data sets show a trend of increasing observed levels over time. At the beginning of the series, Devonport has a range of values from 5.6 mCD to 6.1 mCD, by 2012 this range has increased to 5.8 mCD to 6.25 mCD. Over the same time period Newlyn gives a similar range of 5.7 mCD to 6.1 mCD in 1962 to 5.8 mCD to 6.2 mCD in 2012. It is interesting to note that both data sets have a maximum value of 6.4 mCD. Figure 5.3 and Figure 5.4 show the ten largest independent storm surge levels extracted from the tide gauge data for Devonport and Newlyn. The Devonport data shows a downward trend in the height of the storm surge data over time, compared to Newlyn that shows an upward trend. When compared over the same time period (1962-2012), the range in the data for Newlyn and Devonport are similar for both at 0.3 m to 0.95 m. For the period 1915-2012, Newlyn has a range in storm surge magnitude between 0.2 m and 0.97 m. The maximum storm surge recorded for Devonport and Newlyn is of a similar magnitude, 0.93 m and 0.97 m respectively.

Figure 5.5 to Figure 5.7 shows the frequency distribution for observed sea levels, astronomical tide and storm surge levels for Devonport. Figure 5.6 shows that the tide at Devonport is represented by a binomial distribution diurnal, with a range of 0.0 mCD to 6.2 mCD. The observed level is dominated by the diurnal nature of the tides (Section 2.2) with a range between 0 mCD to 6.4 mCD. The storm surge frequency distribution closely approximates a normal distribution with a range of -1.0 m to 1.0 m. The data for Newlyn (Figures 5.8 to 5.10) shows the same relationship between observed sea levels, astronomical tide and storm surge levels. Figure 5.11 represents the observed sea level, astronomical tide and storm surge levels as a probability plot, demonstrating that the observed levels only deviate from the astronomical tide component at the upper and lower extremes of the data.

As discussed in Chapter 4, the weather data record from Plymouth has been utilised to evaluate any trends within the data sets, with wind speed data converted to wave height data to evaluate potential overtopping at Devonport Dockyard. Figure 5.12 and Figure 5.13 show the ten highest and ten lowest pressure readings for Plymouth. The range in high pressure is between 1030 mb to 1047 mb, with the range in low pressure between 955 mb to 997 mb. Figure 5.14 shows that the ten largest annual wind speed readings for Plymouth have a range from 18 to 36 knots.

The longest wave record for the study area comes from Polperro (Cornwall), this however only spans 7 years. The results of the ten largest annual wave heights ranging between 6.5 m to 10 m are shown in Figure 5.15. Typically the annual

maximum lies between 9.5 m and 10 m. Figure 5.17 illustrates the frequency distribution of the wave data. The shape is typical of a log normal distribution, with a skewed peak and a heavy tail.

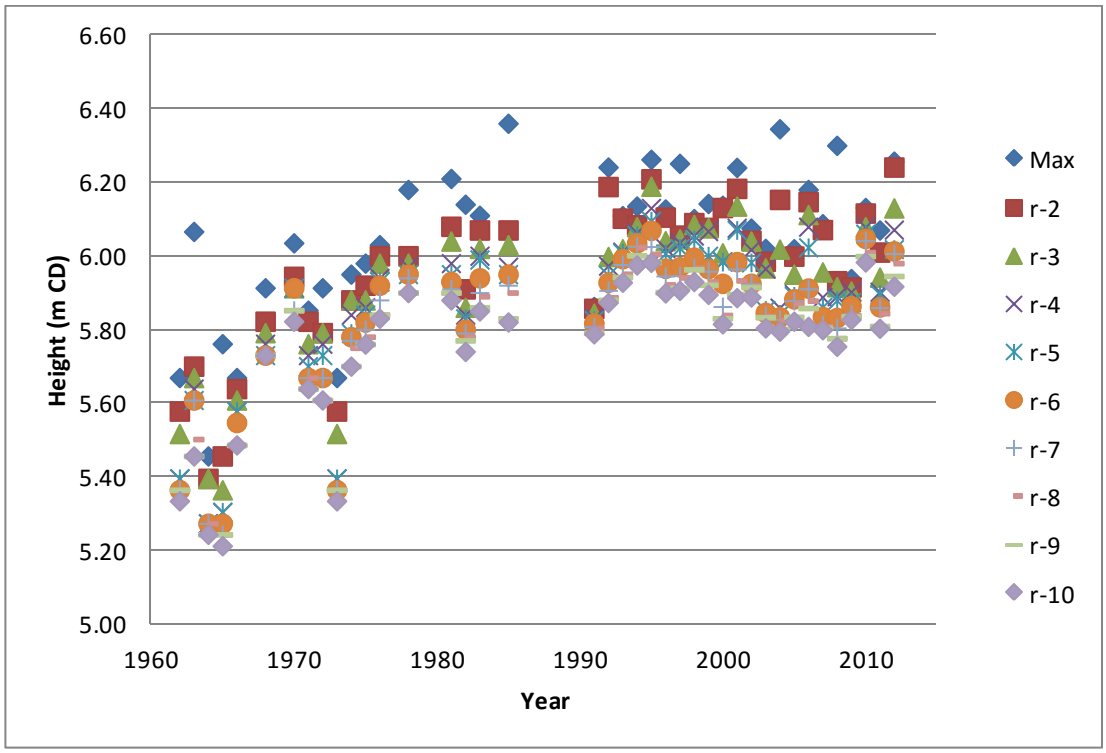

Figure 5.1 Ten largest independent annual maximum observed water levels for Devonport for the period 1962-2012.

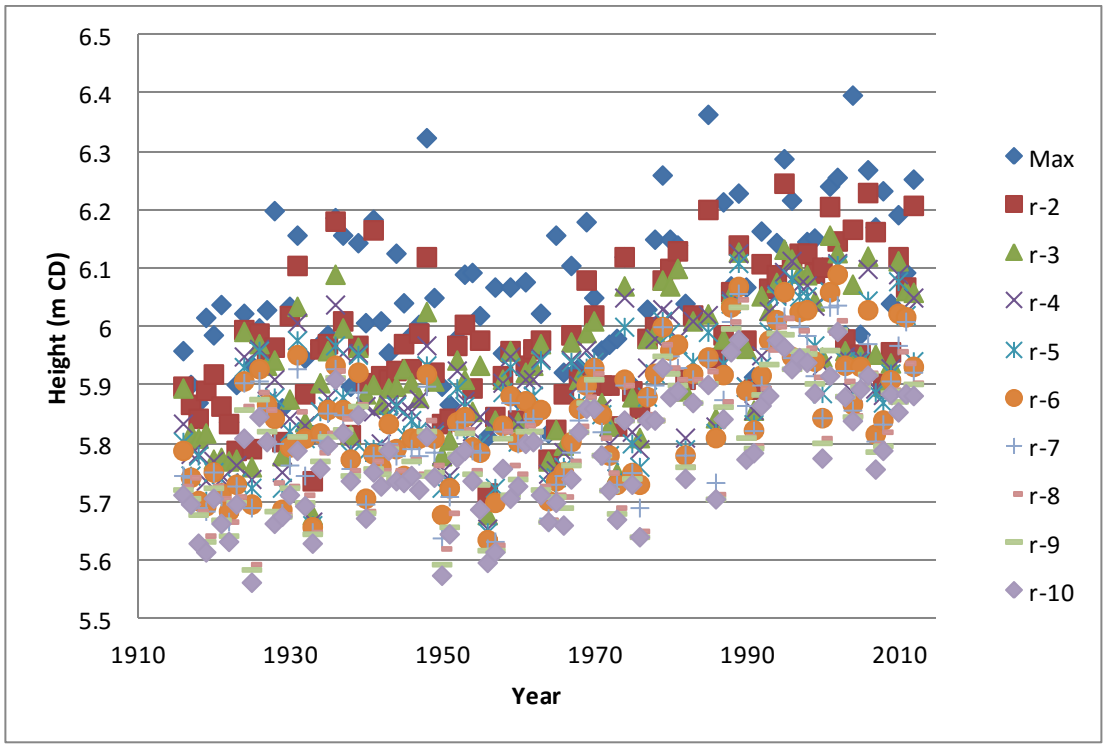

Figure 5.2 Ten largest independent annual maximum observed water levels for Newlyn for the period 1915-2012.

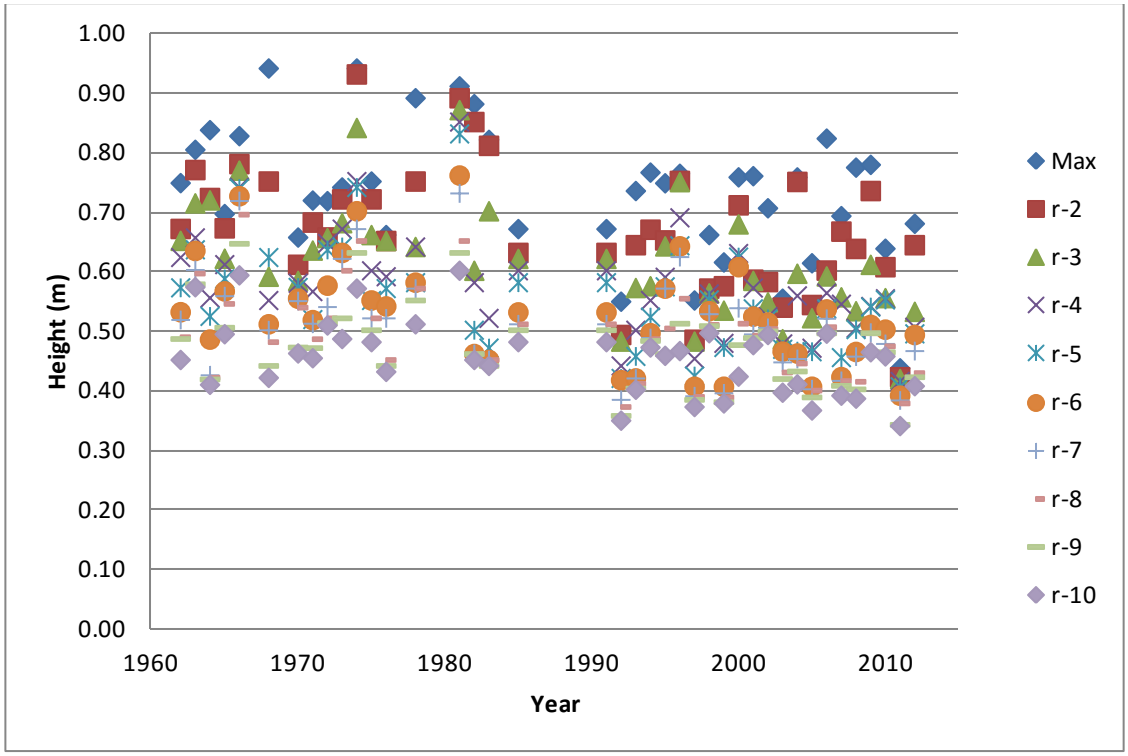

Figure 5.3 Ten largest independent storm surge maximum for Devonport for the period 1962-2012.

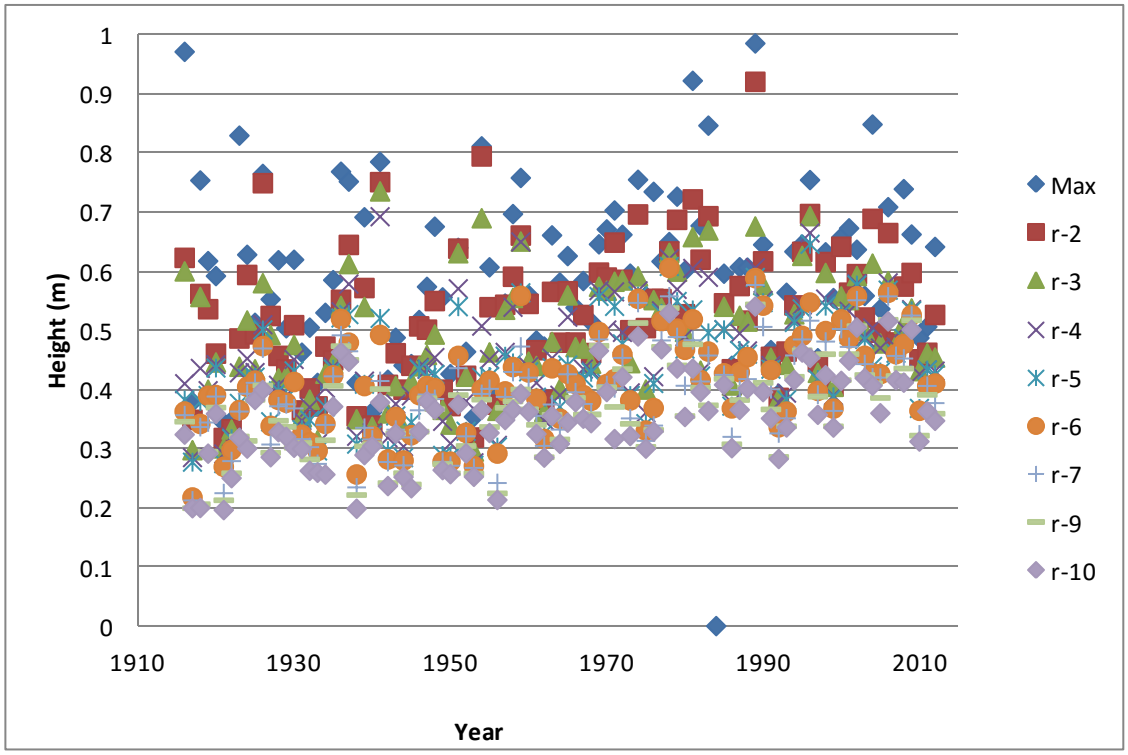

Figure 5.4 Ten largest independent storm surge maximum for Newlyn for the period 1915-2012.

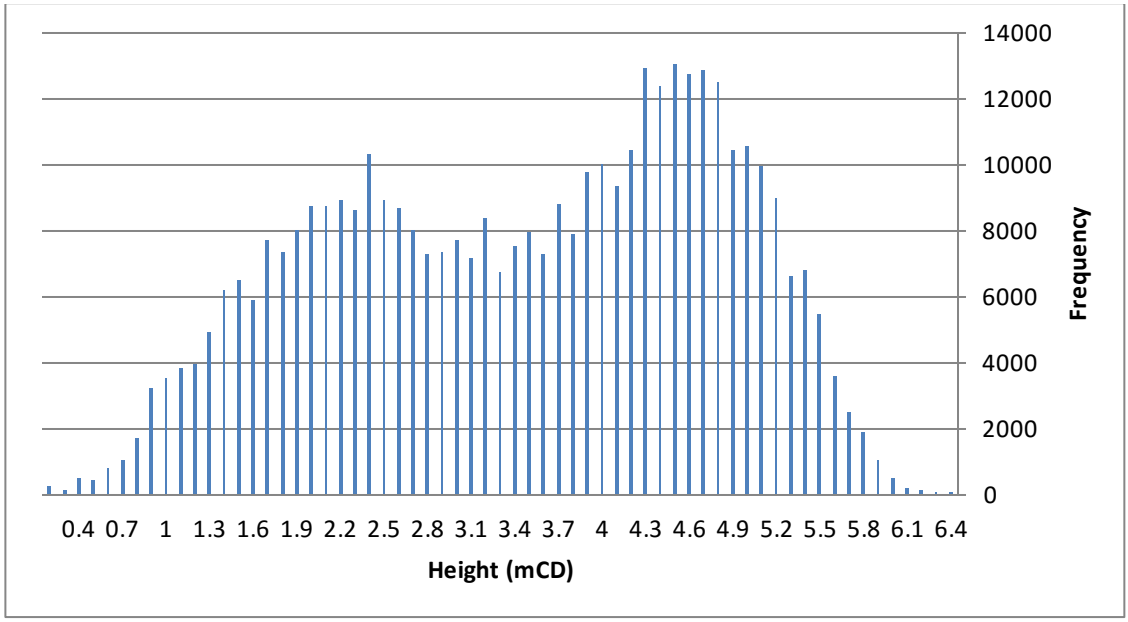

Figure 5.5 Still water level frequency distribution plot for all hourly observations for Devonport 1962-2012.

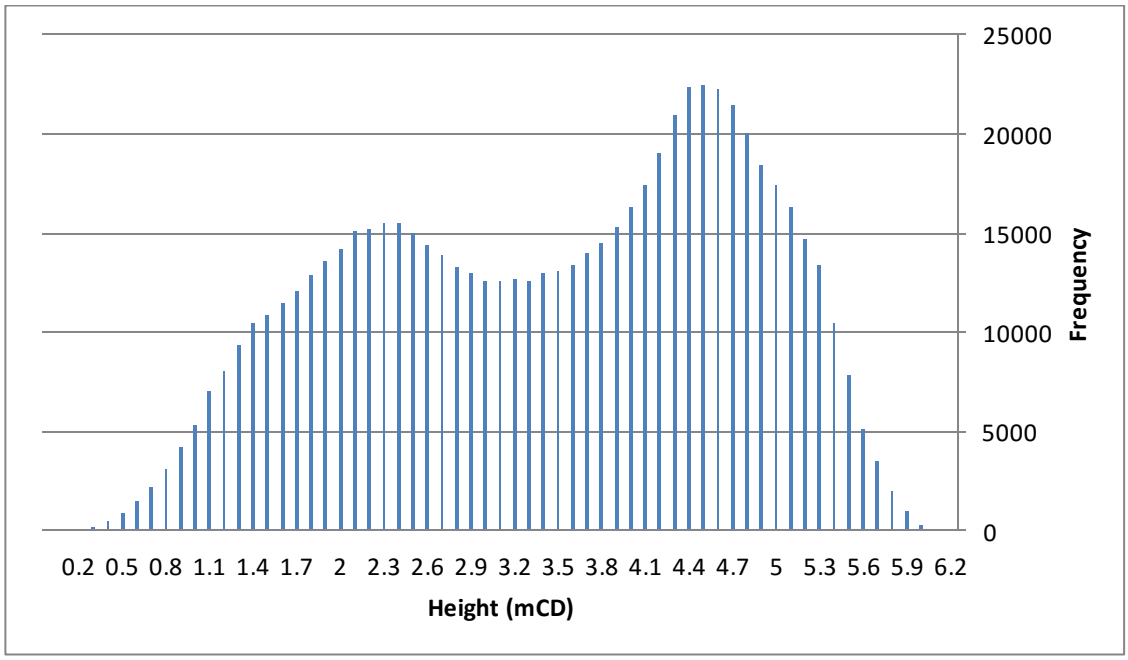

Figure 5.6 Astronomical tide frequency distribution plot for all hourly observations for Devonport 1962-2012.

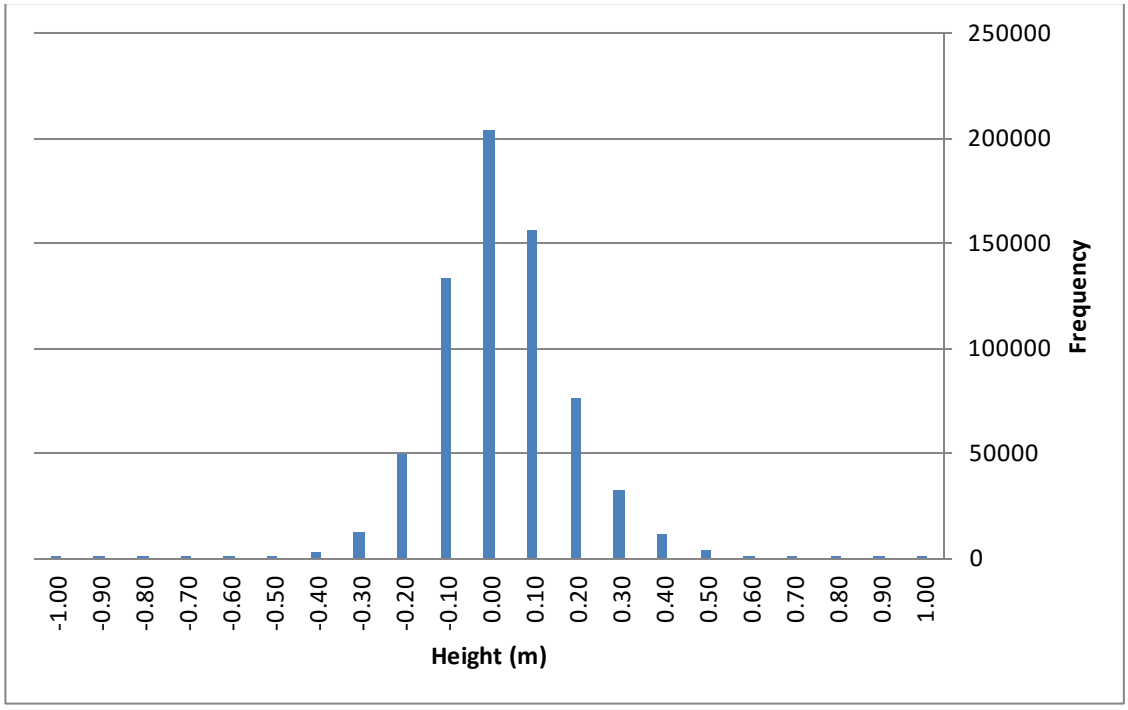

Figure 5.7 Storm Surge Frequency Distribution plot for all hourly observations for Devonport 1962-2012.

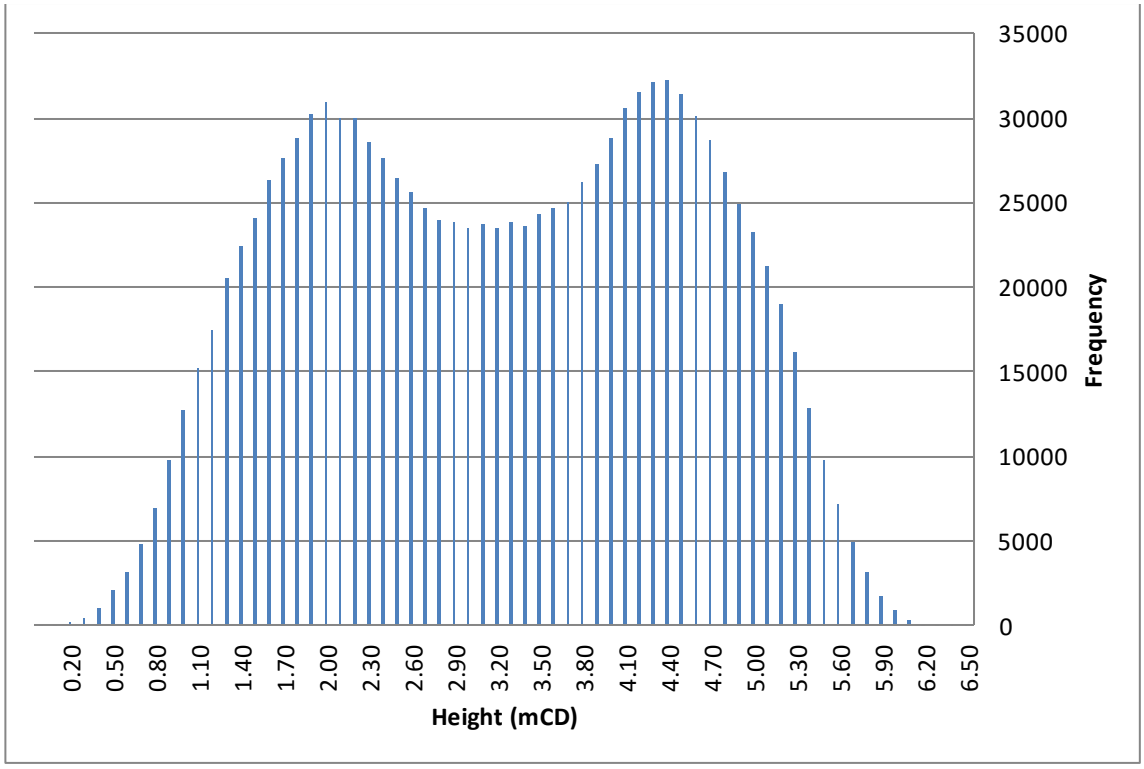

Figure 5.8 Observed still water level frequency distribution plot for all hourly observations for Newlyn 1962-2012.

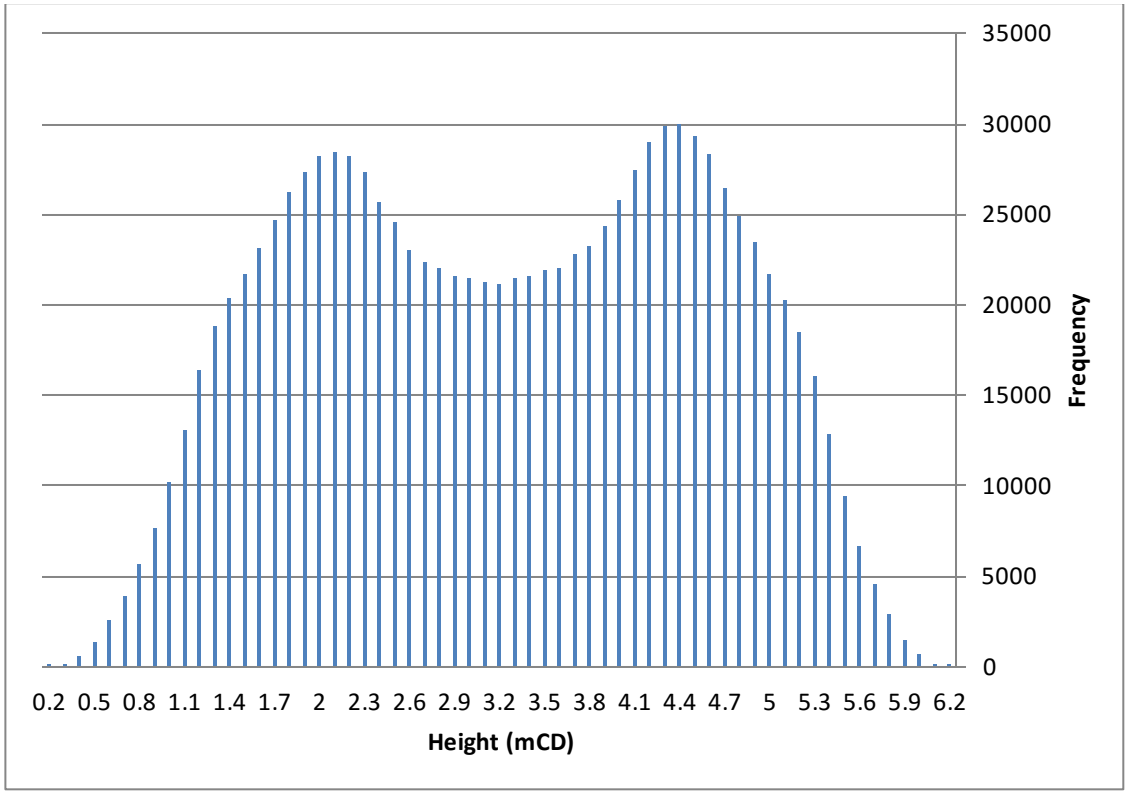

Figure 5.9 Astronomical tide frequency distribution plot for all hourly observations for Newly 1915-2012.

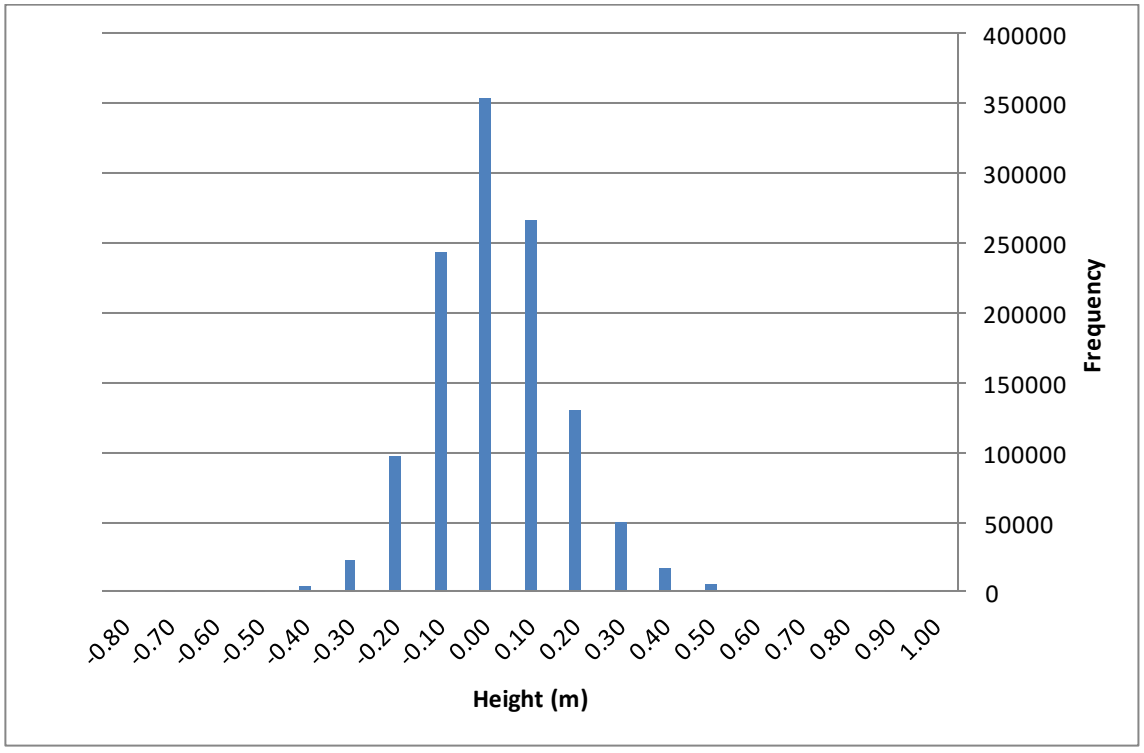

Figure 5.10 Storm Surge Frequency Distribution plot for all hourly observations for Newlyn 1915-2012.

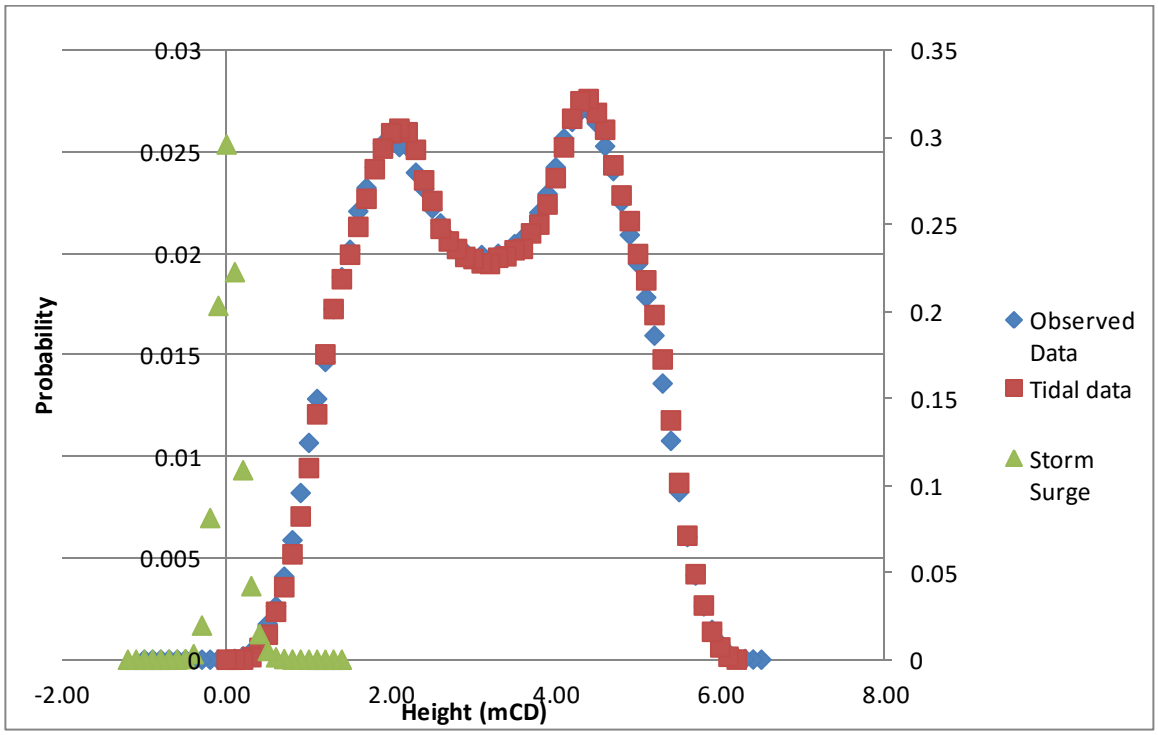

Figure 5.11 Comparison of Observed data, Storm Surge and Tidal Data Probabilities for Newlyn 1915-2012.

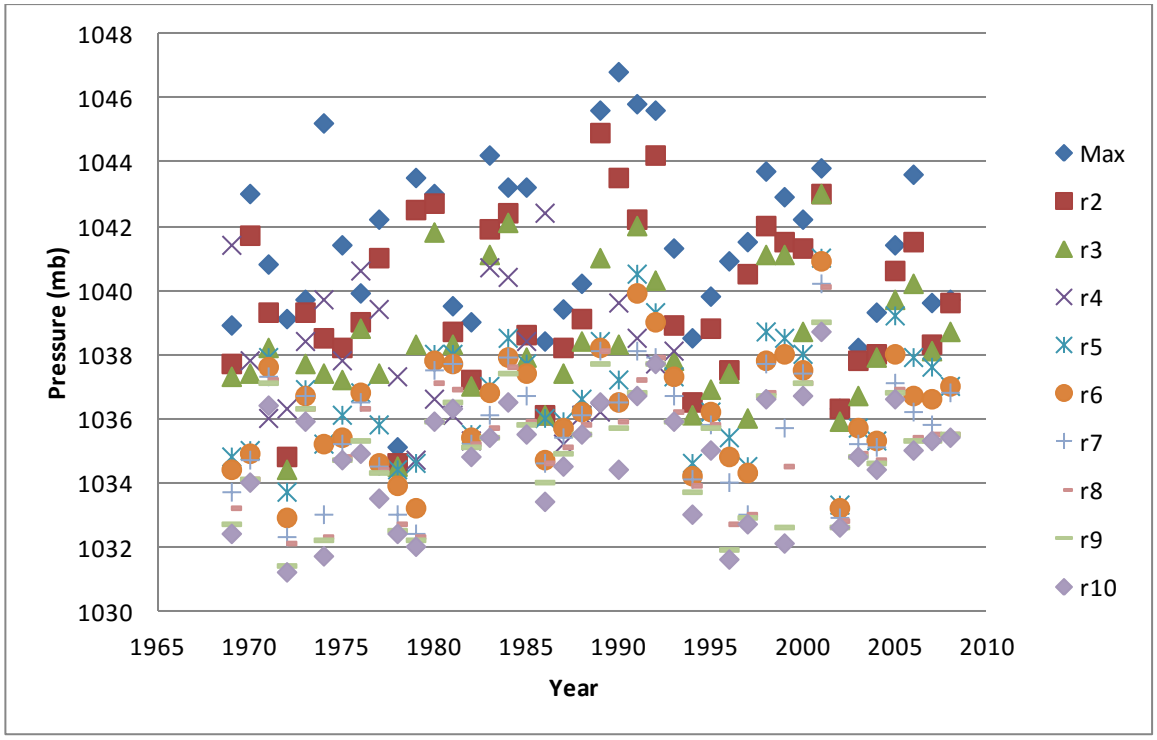

Figure 5.12 Ten highest independent pressure readings for Plymouth 1969-2008 based on mean daily pressure readings.

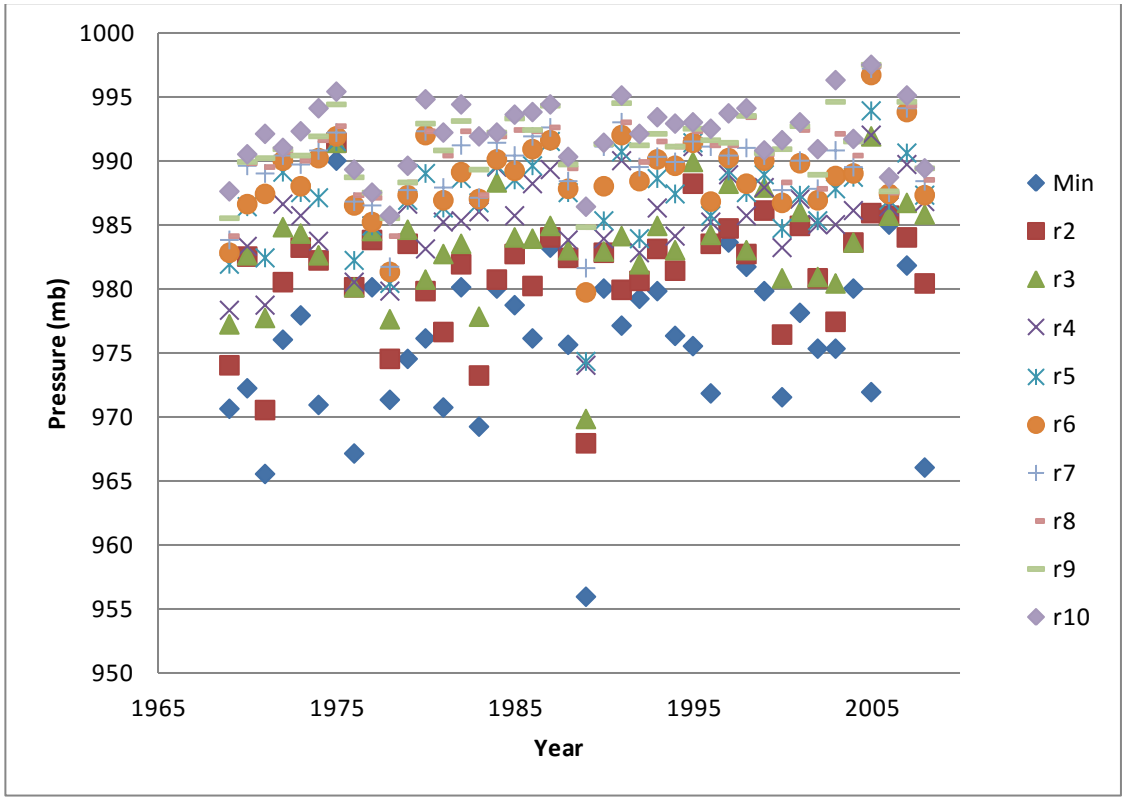

Figure 5.13 Ten lowest independent pressure readings for Plymouth 1969-2008 based on mean daily pressure readings.

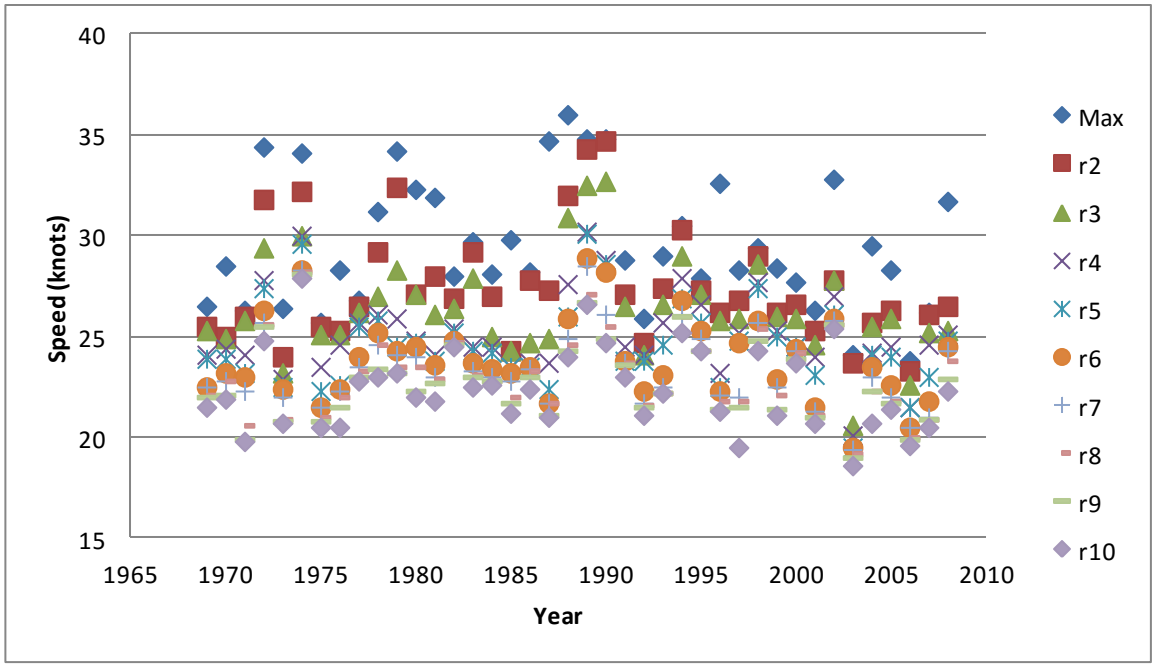

Figure 5.14 Ten largest independent wind speed readings for Plymouth 1969-2008 based on mean daily pressure readings.

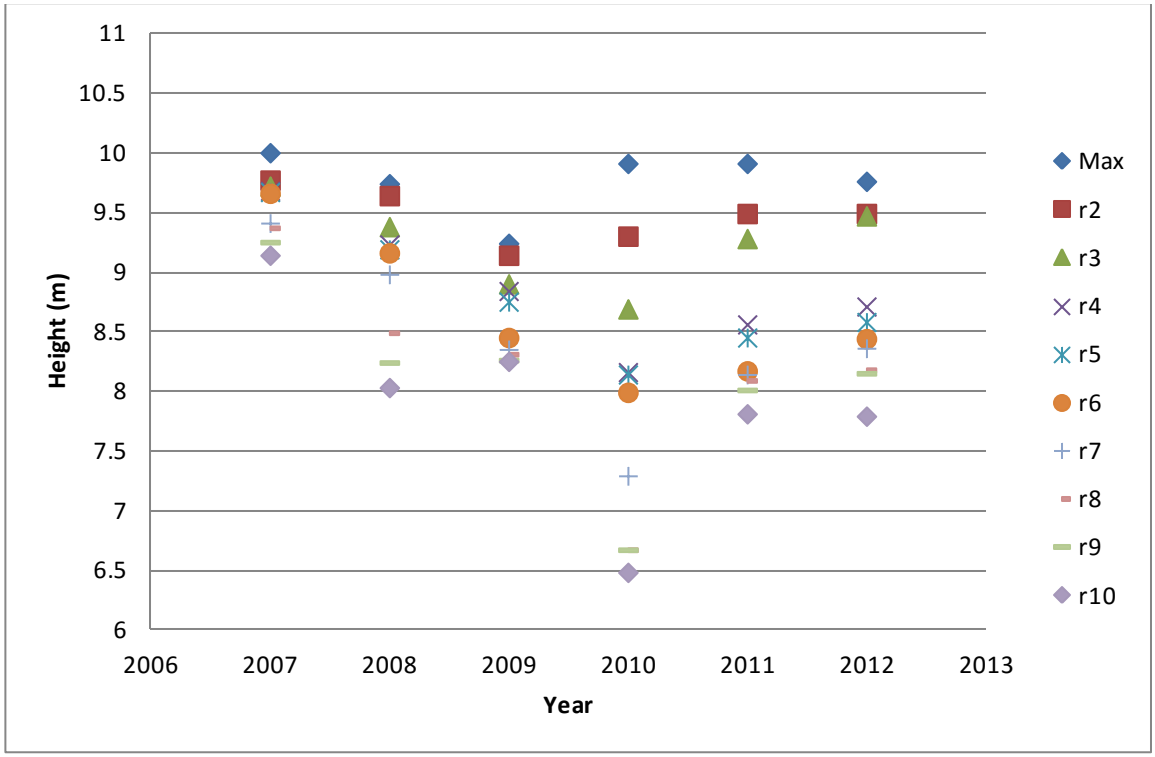

Figure 5.15 Ten largest independent wave heights for Polperro, Cornwall for 2007-2012.

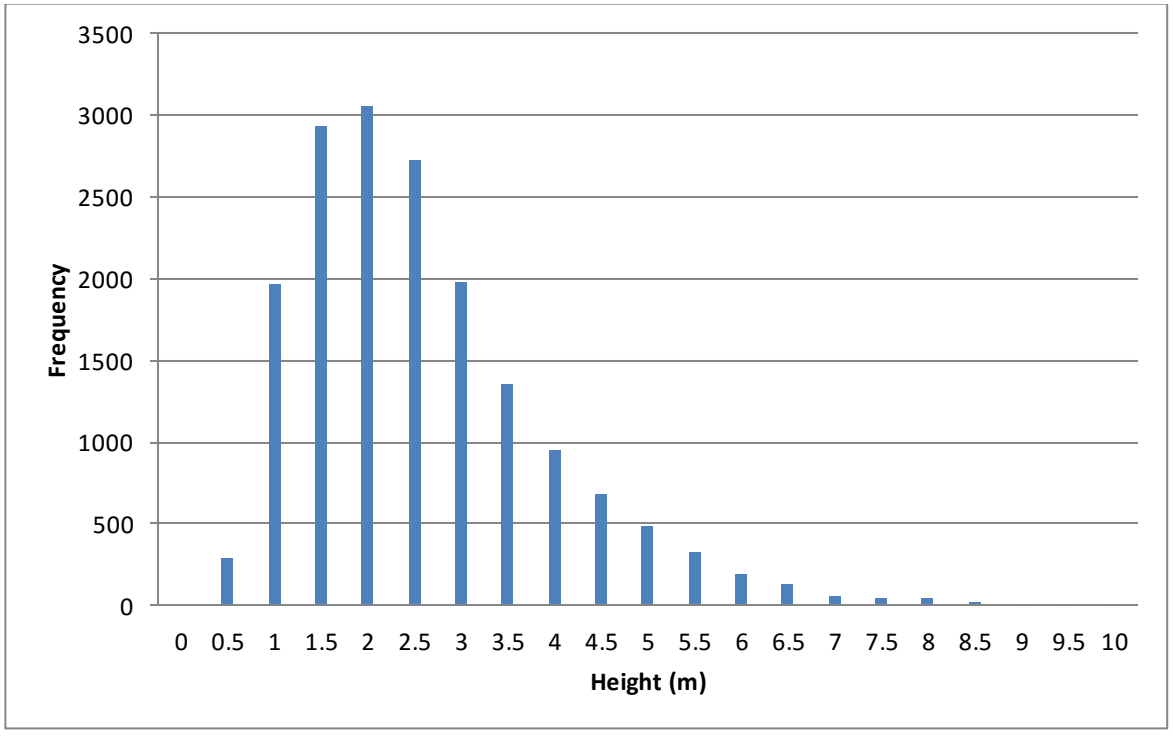

Figure 5.16 Wave height frequency distribution plot for all hourly observations for Polperro, 2007-2012.

5.3 Observed Trends

The following section looks at observed trends over time within the various data sets, focussing initially on the annual mean and frequency of the data and comparing the trends to phenomena that are known to influence changes in the data set. Due to the short Polperro data set no trend analysis has been undertaken on the wave data.

5.3.1 Sea-level Rise

To evaluate the change in mean sea level over time, the annual average of the observed levels is calculated, as described in Section 4.3.5. The annual mean is plotted against time as illustrated in Figure 5.17 and Figure 5.18 for Devonport and Newlyn, respectively. Also plotted to aid in the identification of any trends in the data is the 5-year rolling average.

The linear trend of the data indicates an increasing trend in mean sea level of 2.1+/- 0.3 mm/yr (95% confidence) and 1.8+/- 0.2 mm/yr (95% confidence) for Devonport (Figure 5.17) and Newlyn (Figure 5.18), respectively. An exponential trend plotted for the data indicates a rate of between 0.001 to 0.002 mm/yr^2 acceleration within the data set. Initial rates of sea-level rise for Newlyn in 1915 of 1.9 mm/yr, and for 1962 for Devonport of 2.2 mm/yr. By 2010 this rate of sea-level rise had increased to 2.05 mm/yr for Newlyn and 2.3 mm/yr for Devonport. A comparison between the r^2 values indicates that an exponential growth trend plotted to the data provided a better fit when compared to a linear trend; 0.78 compared to 0.59 for Devonport and, 0.90 compared to 0.75 for Newlyn. The rolling average indicates an oscillation within the data set, with annual sea-level rise, above and below the overall mean value of the data set. The peaks in the data centre around 1965 and 2000 for Devonport and 1930, 1950, 1960, 1970, 1985 and 2000 for Newlyn. For Newlyn this indicates a cyclicity of 10 to 15 years. Due to missing data in the Devonport record between 1985 and 1990, it is not possible to identify any trends between 1980 and 1995. A decadal analysis, looking at 20 year trends of sea-level rise within the data, indicates varying trends between 3.8 mm/yr centred around 1950 and 1990 and, -1.1 mm/yr centred around 1965-70.

5.3.2 Storm Surges

Figure 5.19 and Figure 5.20 show a plot of frequency of observed independent tide gauge levels greater than 5.4 mCD against time for Devonport and Newlyn. Both Devonport and Newlyn show an upward trend in the frequency of observed levels over time with an increase from 40 events to approximately 100 events from 1915 to 2012. This increase in frequency of events is confirmed when looking at non-independent events. Figures 5.21 and Figures 5.22 show the change in frequency of non-independent observed events >5.0 mCD; >5.4 mCD and, >5.7 mCD for Devonport and Newlyn. The data indicates for >5.7 mCD an increase in frequency from 50 events per year to 150 events per year for both the Newlyn and Devonport data. Figures 5.23 and 5.24 show the change in frequency of storm surge events >0.4 m and >0.6 m. Above a threshold of 0.4 m the data indicates an increase in frequency from approximately 50 to between 250 and 350 events per year (Newlyn 1915-2012). The number of these events can be seen to increase over time, with a potential exponential increase observed in the storm surge frequency (Figure 5.24). A similar oscillation observed in the mean sea-level trend can also be identified in the records of observed and storm surge levels. The overall trends observed are clear within the Newlyn data, showing peaks in the frequency centred around 1925, 1935, 1950, 1960, 1970, 1980, 1990, 2000 and 2010, but due to missing data between 1985 and 1990 the trends for Devonport are not quite as clear.

5.3.3 Weather Data

Figure 5.25 shows the annual average pressure readings calculated from the daily averages at Mount Batten, Plymouth for the period 1969 to 2008. Figure 5.26 shows the frequency of high pressure (>1013mb) and low pressure (<1013mb). The results of the daily average indicate a scatter of data around a mean value of approximately 1016 mb with a range from 1014mb to 1020mb, and no overall trend. The rolling average shows an oscillation in the data with peaks centred around 1960-1970, 1985-1995 and 2005, with troughs in the data centred around 1980 and 2000. The frequency of high and low pressures shown in Figure 5.26 shows no significant trend with the number of high pressures per year typically around 250 and low pressure frequencies typically around 100 for the duration of the observations.

Daily average wind speed and daily average wind direction is illustrated in Figures 5.27 and 5.28, respectively. From Figure 5.27 it can be seen that there is a slight downward trend in average wind speed over time. Although not as pronounced as for the pressure reading (Figure 5.26), there are slight oscillations in the wind speed data centred around 1980, 1990 and 2005. For an analysis of wind direction a frequency analysis of the occurrence of a northerly (315-045°), easterly (045-135°), southerly (135-225°) and, westerly (225-315°) wind direction was undertaken (Figure 5.28). The data shows that Plymouth is dominated by easterly and westerly winds. There is a slight oscillation in the data with a peak in the westerly direction centred around 1980 and a trough centred around 1997. An interesting occurrence happens between 1995 and 2000 where there is a reduction in the westerly wind and a peak in the northerly direction.

5.3.4 Storminess and the North Atlantic Oscillation

Figure 5.29 is a comparison plot of low pressure frequency for Mount Batten, Plymouth, and storm surge frequency for Devonport (Y axis has been adjusted to allow both data sets to plot on the same graph). This shows that the peak in the frequency of storms surges coincides closely with a peak in the frequency of low pressures. However, there is a slight lag of 3-4 years, which can be partly attributed to the different length of the data sets, with the weather data commencing in 1969 and the storm surge data set commencing in 1962. Highlighted on Figure 5.29 are the spikes in the North Atlantic Oscillation (NAO) (Woodworth et al., 2012). A comparison between the NAO positive spikes and the peaks in the storm surge and pressure data shows there is a correlation between the data sets. Although a peak in the NAO between 1985 and 1995 is not highlighted in Figure 5.29, peaks in the storm surge data around this time are picked up in Figures 5.20 to 5.22.

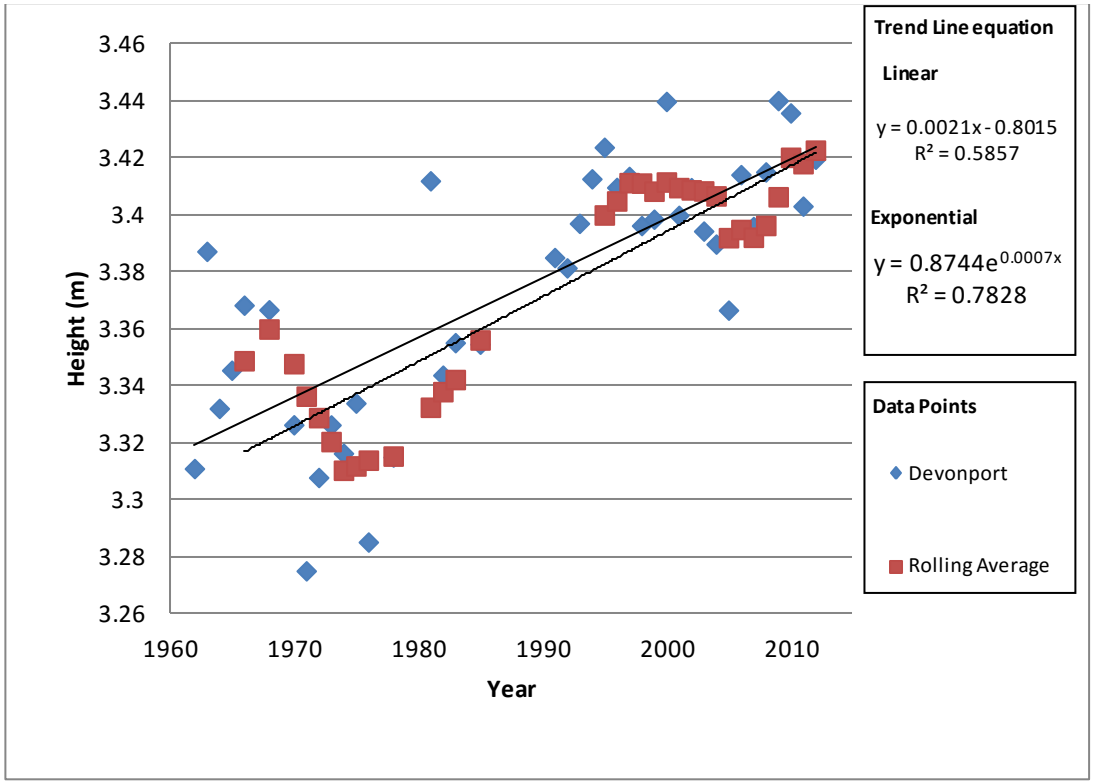

Figure 5.17 Sea-level rise trend for Devonport for the period 1962-2012.

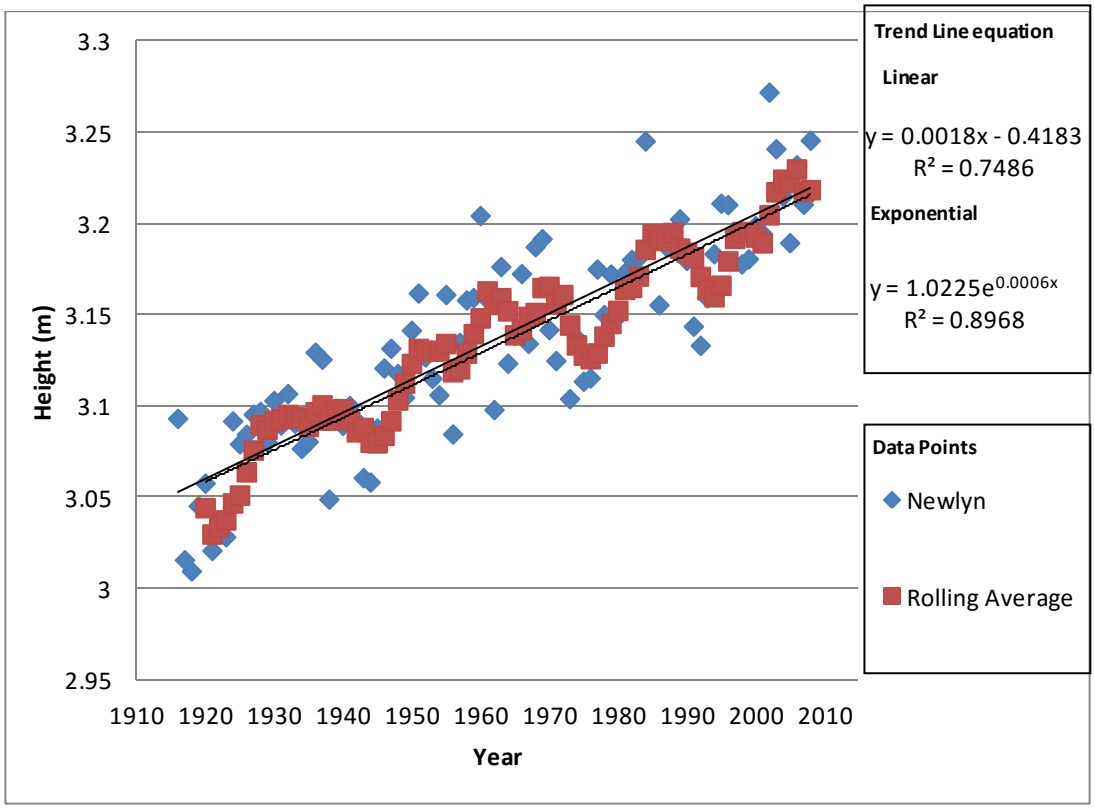

Figure 5.18 Sea-level rise trend for Newlyn for the period 1915-2012.

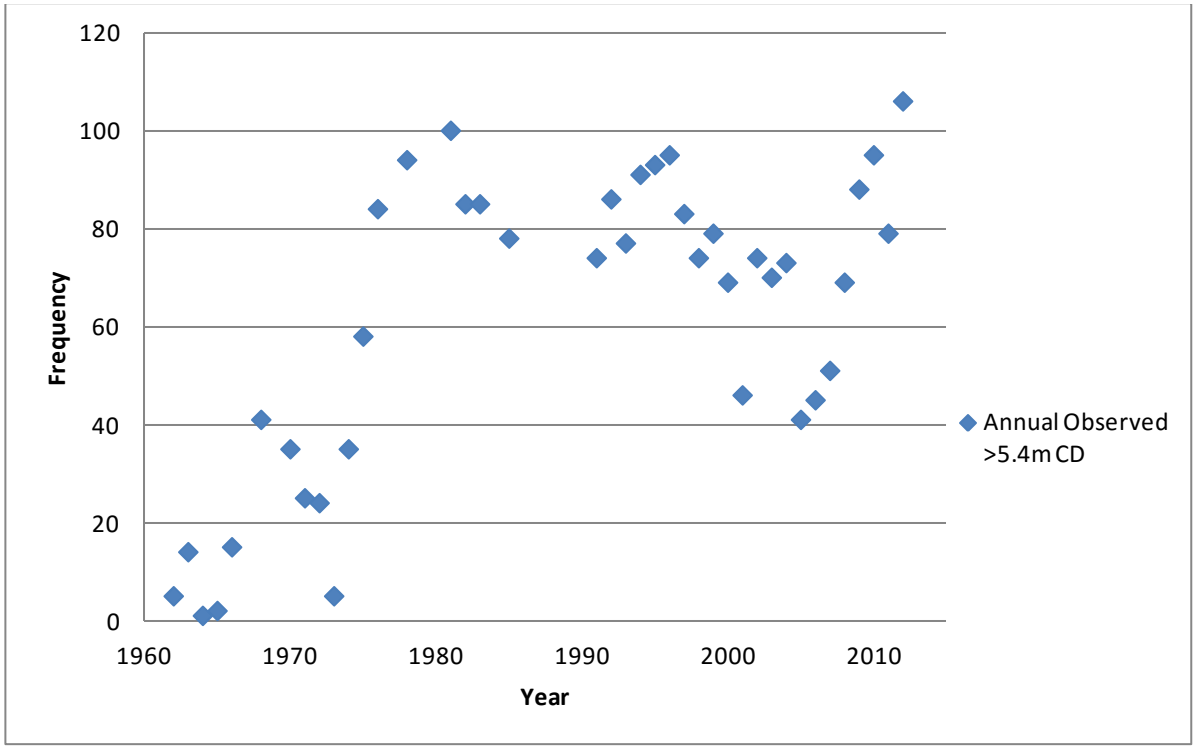

Figure 5.19 Trend Analysis of data greater than 5.4m CD observed levels for Devonport 1962-2012**.**

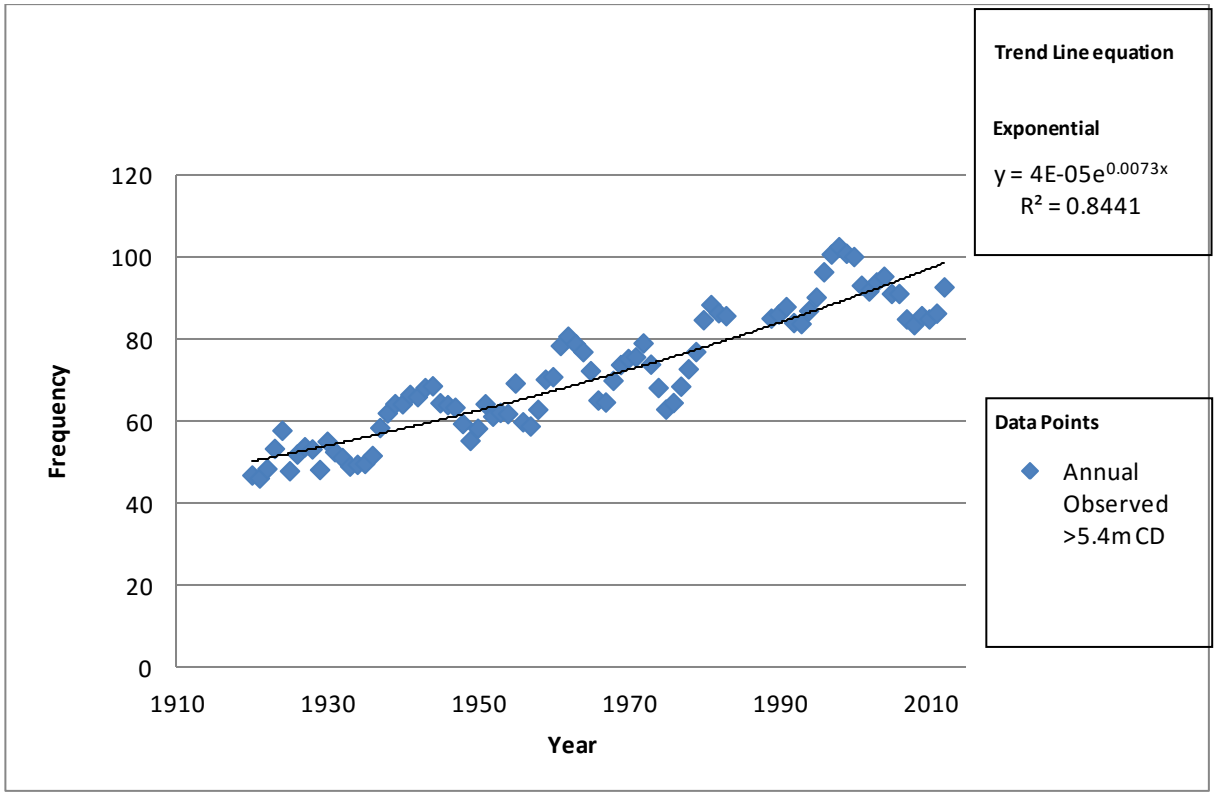

Figure 5.20 Trend Analysis of data greater than 5.4m CD independent observed levels for Newlyn 1915-2012.

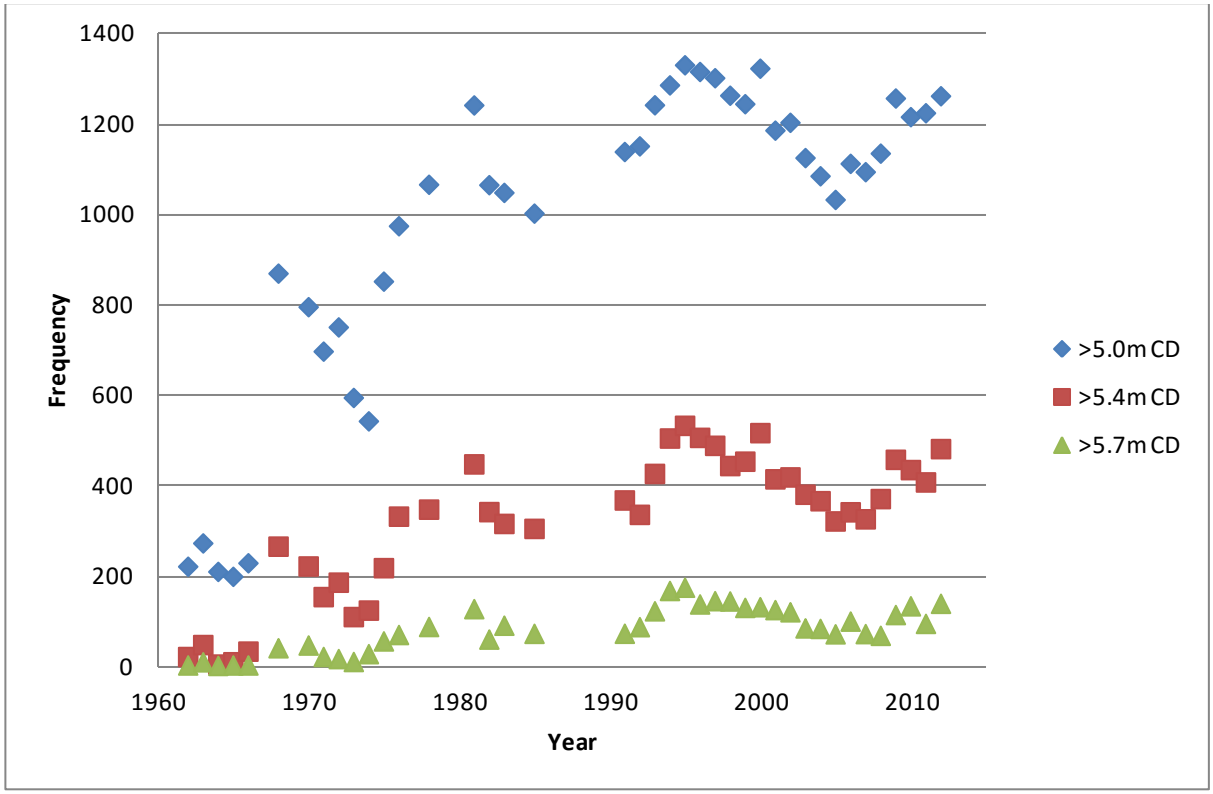

Figure 5.21 Trend Analysis of non-independent observed levels for Devonport 1962-2012.

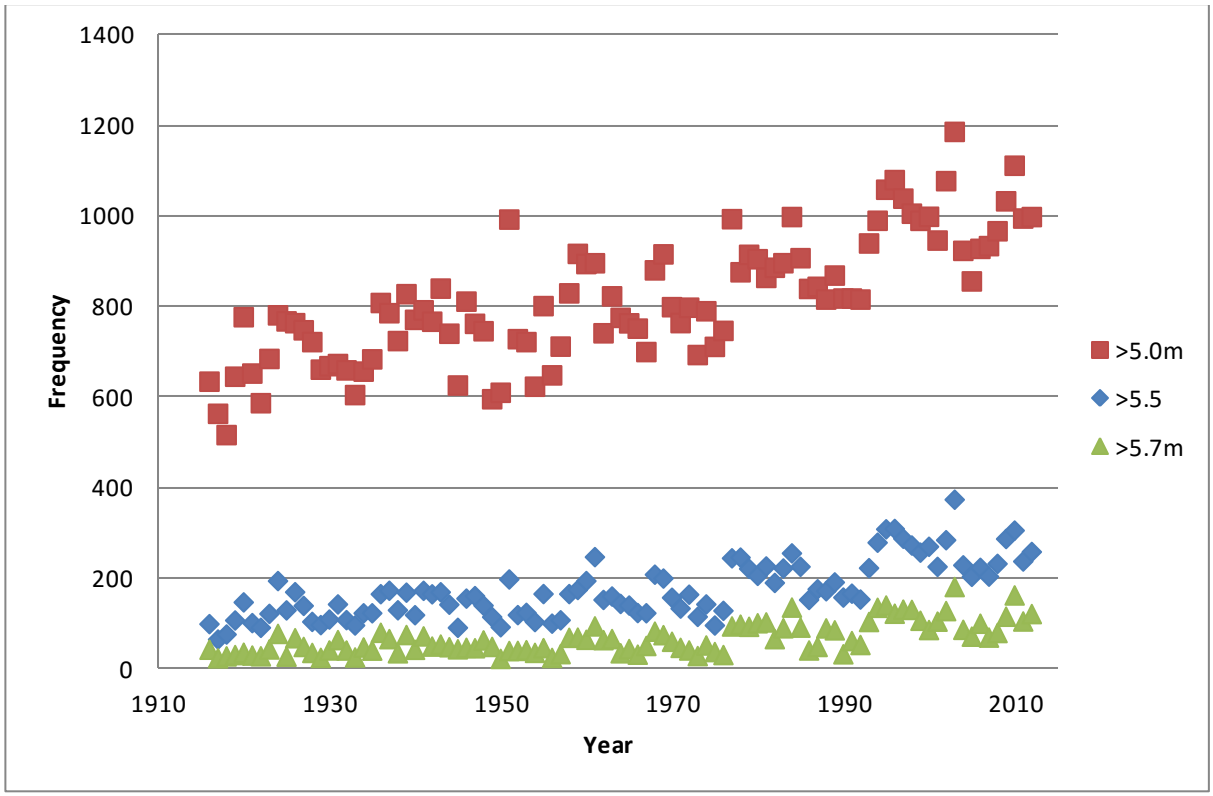

Figure 5.22 Trend Analysis of non-independent observed levels for Newlyn 1915-2012.

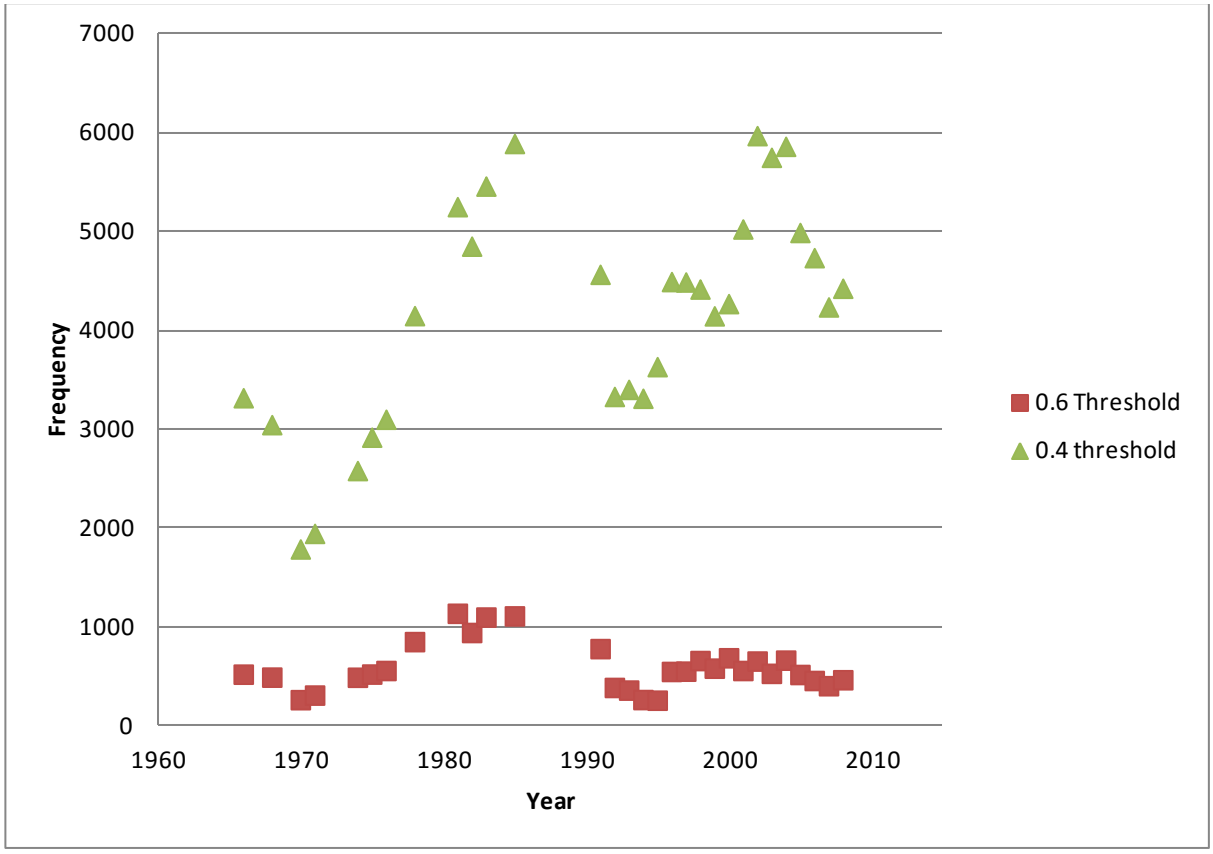

Figure 5.23 Trend Analysis of non-independent storm surge events levels for Devonport 1962-2012.

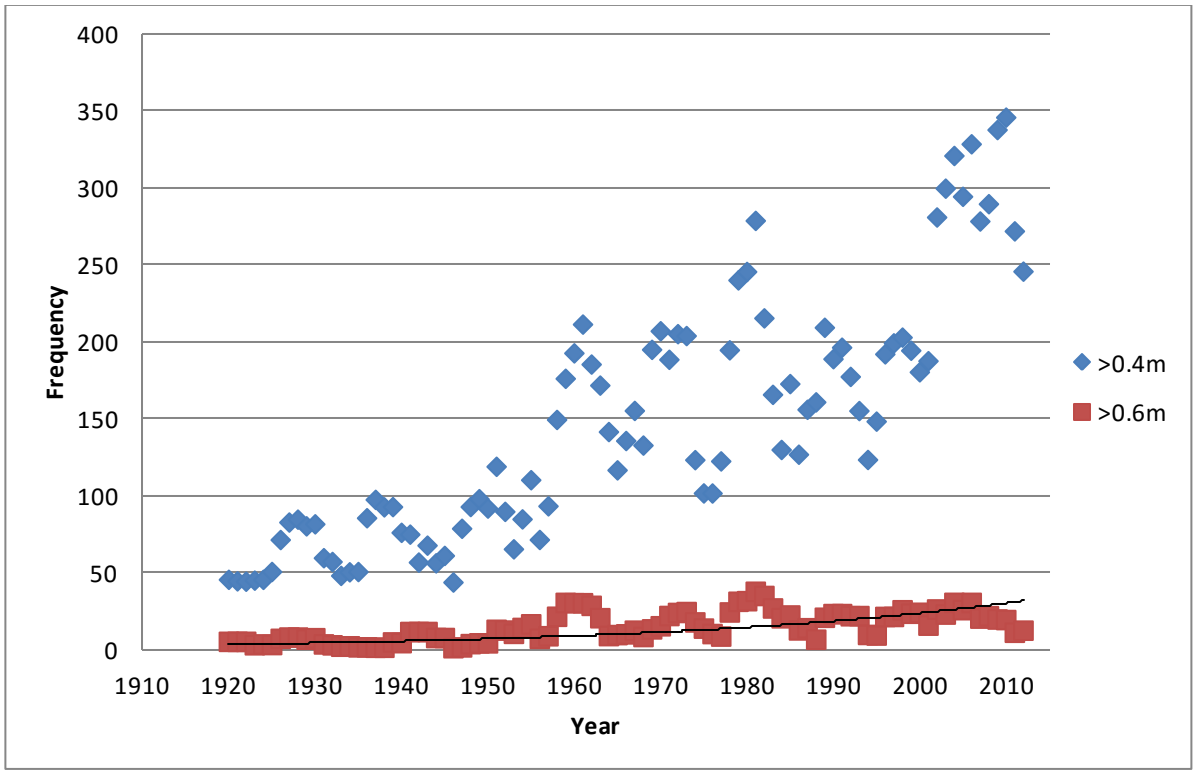

Figure 5.24 Trend Analysis of non-independent storm surge events for Newlyn 1915-2012.

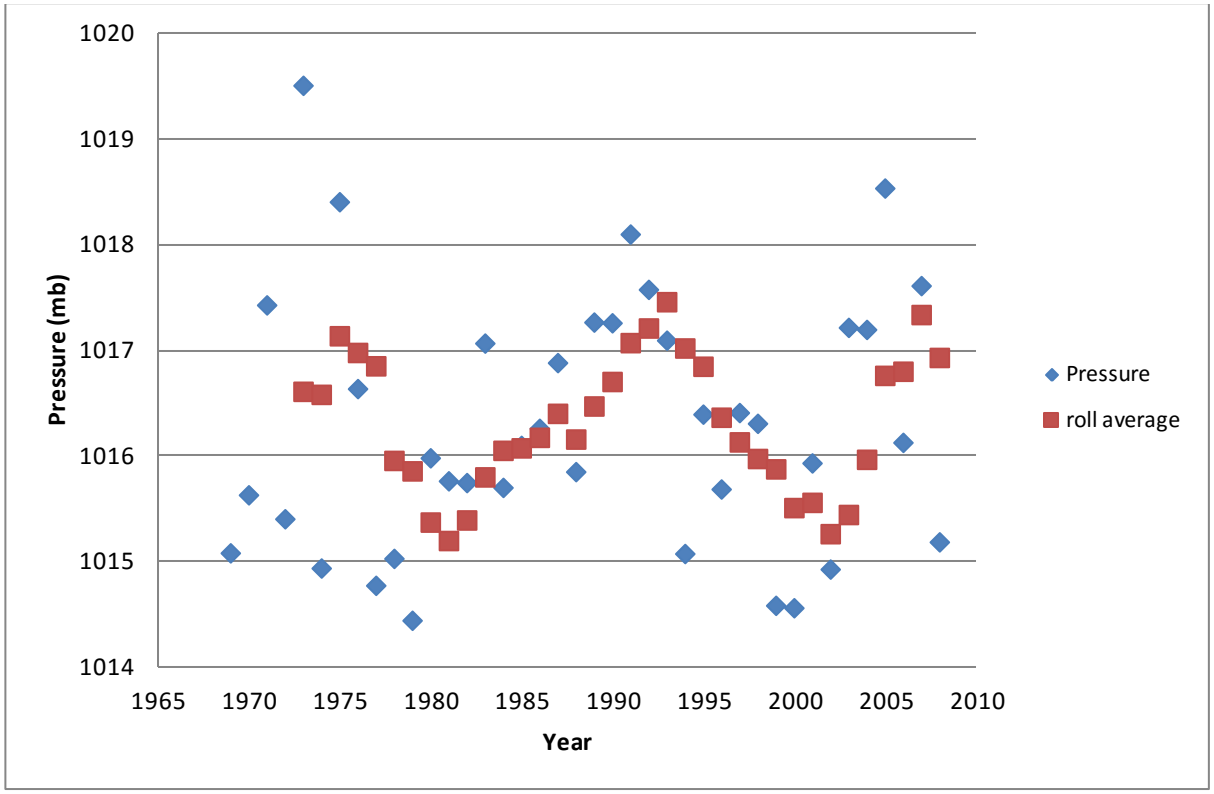

Figure 5.25 Trend Analysis of annual average pressure readings for Plymouth for the period 1969-2008.

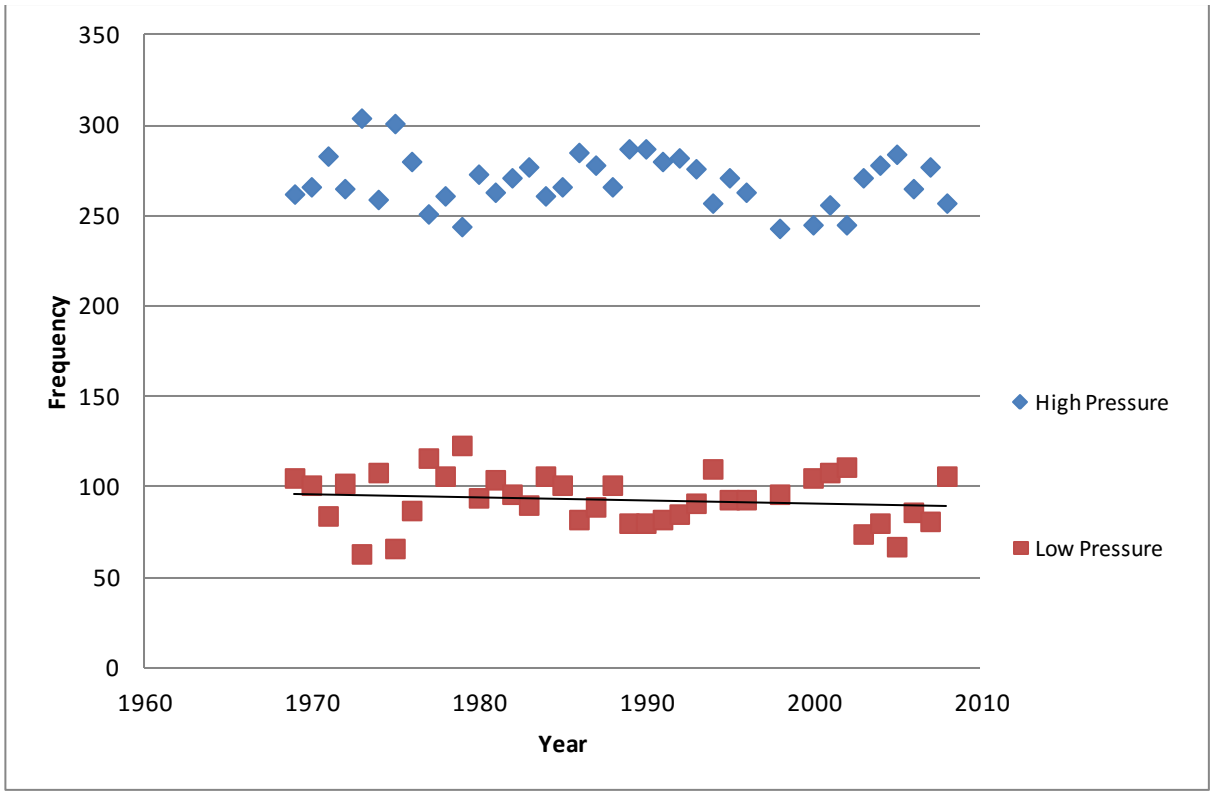

Figure 5.26 Trend Analysis of annual average pressure readings above (high pressure) and below (low pressure) 1013mb for Plymouth for the period 1969-2008.

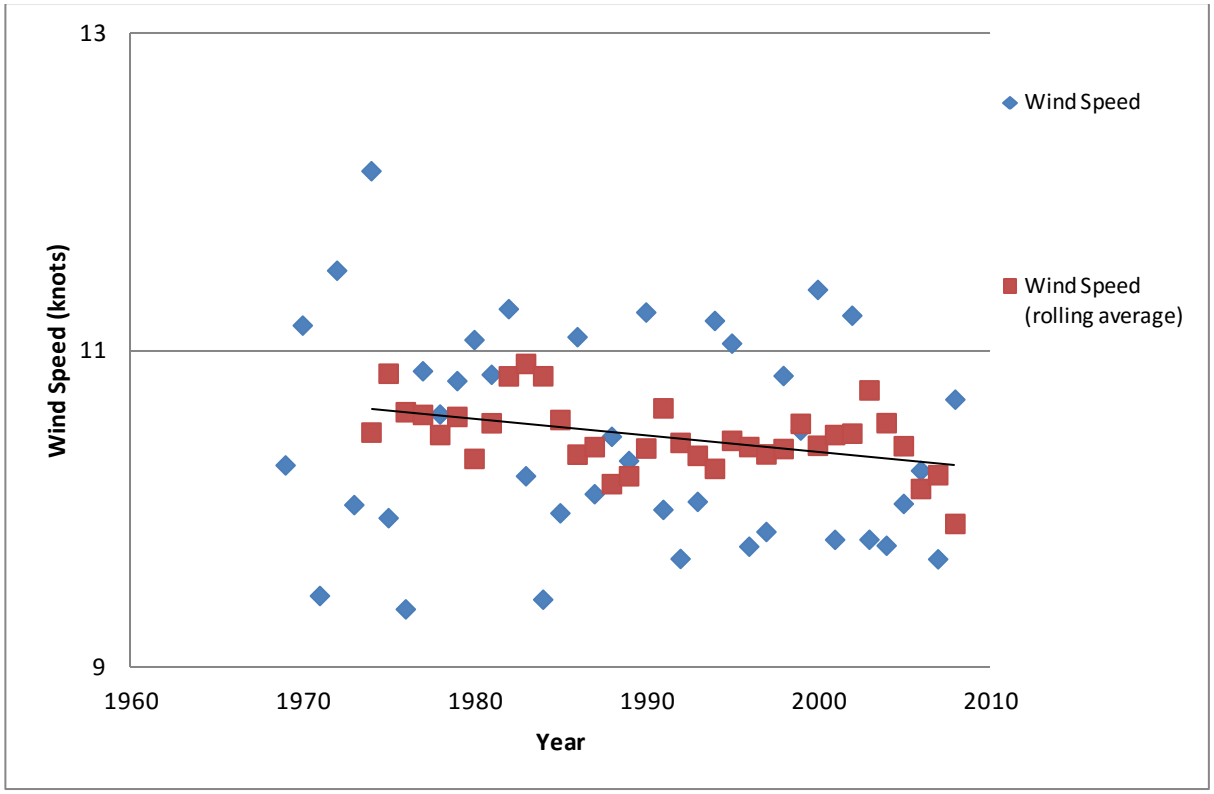

Figure 5.27 Trend Analysis of annual average wind speed readings for Plymouth for the period 1969-2008.

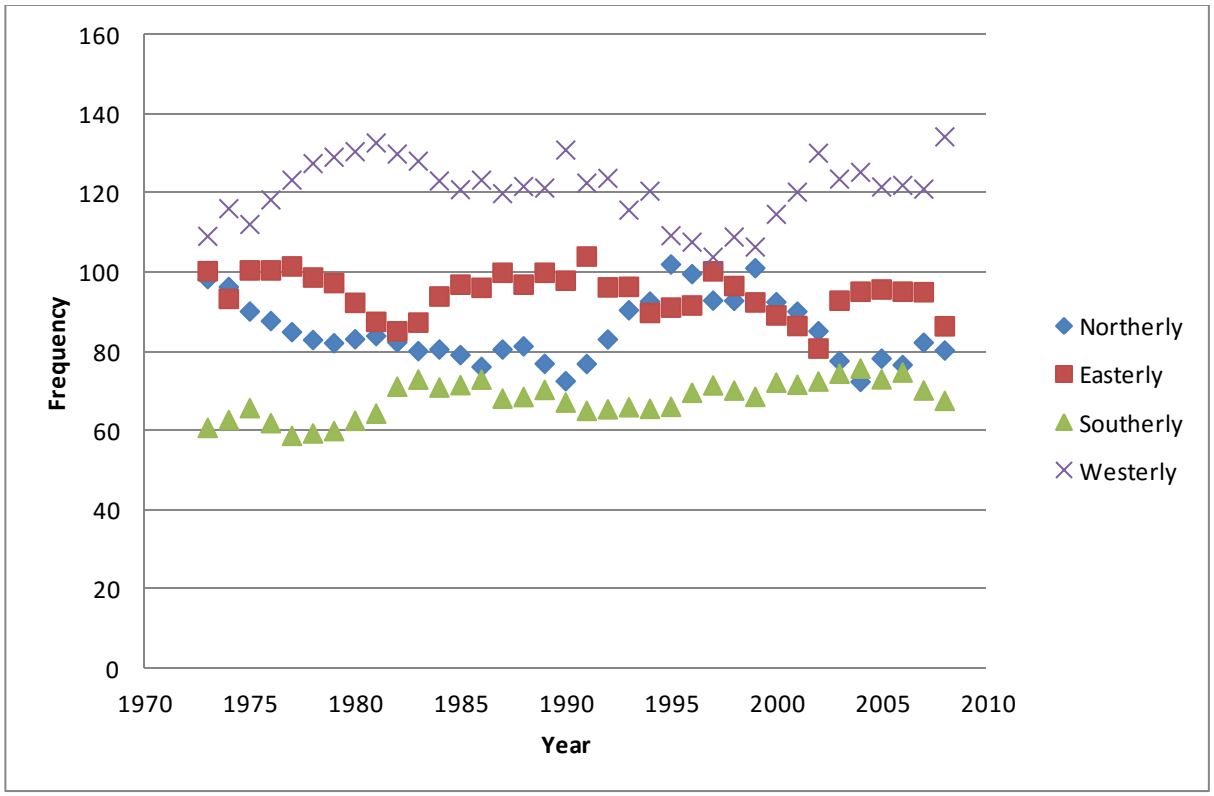

Figure 5.28 Trend Analysis of daily average wind speed direction readings for Plymouth for the period 1969-2008.

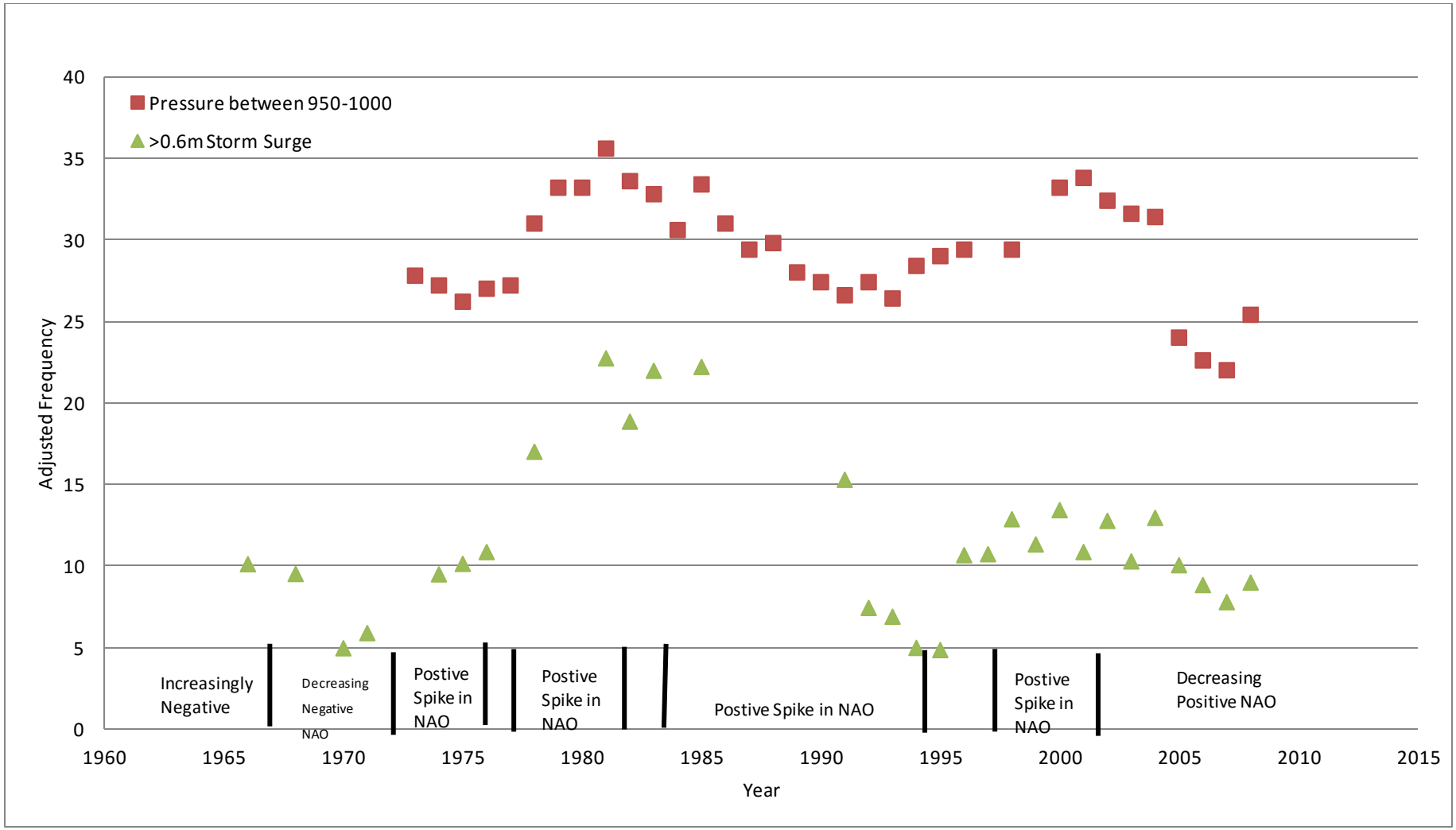

Figure 5.29 Comparison of low pressure frequency against storm surge frequency for Devonport, with general trend of the North Atlantic Oscillation.

5.4 Statistical Results

The following section describes the results from the statistical analysis of observed tide gauge levels including the analysis of extracted storm surge data. The section corresponds to the methodology detailed in Section 4.4.

5.4.1 Generalised Extreme Value

An outline of the Generalised Extreme Value (GEV) methodology is given in Section 4.4.1 to 4.4.3. To undertake a GEV analysis the annual maximum for each year of the observed and storm surge levels were extracted as illustrated in Section 5.2. These data were imported into the “extremes” software package and an analysis undertaken. The results for the annual maximum are given in table 5.1 and 5.2 for Devonport and Newlyn, respectively. A GEV return level and diagnostic plot are given in Figures 5.30 and 5.31. For Devonport based on the observed annual maximum the mean value for a 1 in 10 year event is 6.28 mCD, for a 1 in 1000 year event the value is 6.37 mCD. Overall the prediction based on the GEV has a maximum uncertainty range of 0.09 m at the 95% confidence limit (1 in 1000 year). For Newlyn the mean value for a 1 in 10 year event is 6.22 mCD, for a 1 in 1000 year event the value is 6.46 mCD. Overall the prediction based on the GEV for Newlyn has a maximum uncertainty range of 0.29 m (1 in 1000 year).

The results based on the GEV undertaken on the extracted storm surge maximum are given in table 5.3 and 5.4 for Devonport and Newlyn, respectively. With the GEV return level and diagnostic plot are given in Figures 5.32 and 5.33. For Devonport based on the extracted storm surge maximum the mean value for a 1 in 10 year event is 0.87 m, for a 1 in 1000 year event the value is 0.98 m. Overall the prediction based on the GEV has a maximum uncertainty range of 0.16 m at the 95% confidence limit (1 in 1000 year). For Newlyn the mean value for a 1 in 10 year event is 0.78 m, for a 1 in 1000 year event the value is 1.06 m. Overall the prediction based on the GEV for Newlyn has a maximum uncertainty range of 0.35 m (1 in 1000 year).

A review of the return level and diagnostic plots shows that both the annual maximum and storm surge data fit a Weibull distribution (Figure 5.34 and 5.35). This observation has been confirmed by undertaking a validation as described in Section 4.4.3. By comparing the results for Devonport and Newlyn, it can be seen that for

both the annual maximum and storm surge maximum the Devonport return level plot reaches a plateau, where for an increase in return period there is only a slight increase in the amplitude. For Newlyn no plateau is reached, and a positive relationship is observed showing that an increase in return period gives an increase in amplitude. This leads to narrower confidence intervals for Devonport, when compared to Newlyn. The diagnostic plots (Figures 5.30 and 5.31) shows that the Devonport annual maximum data has a skewed distribution, compared to a more normal distribution for Newlyn (Figure 5.31). For the storm surge maximum (Figures 5.32 and 5.33) both data sets closely approximate a normal distribution although Newlyn is slightly skewed towards lower values. Based on a comparison between the predicted GEV model and the empirical data, both data sets, for both sites, have a good agreement (Figures 5.30 and 5.31).

Furthermore, there is a good agreement between the mean predicted values for Devonport and Newlyn for both the observed annual maximum and the storm surge maximum, with all return periods being within +/-0.1 m (tables 5.1 to 5.4). However due to the nature of the curves of the Devonport and Newlyn distributions at the upper 95% confidence there is a difference of 0.23 m and 0.21 m for a 1 in 1000 year observed annual maximum and storm surge maximum event respectively.

The Literature Review (Chapter 3) highlighted that to undertake a meaningful GEV analysis 20 years or more of data are required. To undertake an assessment of the length of data set required to undertake a GEV analysis, 5, 10 and 20 years subsets of the Devonport data were analysed, with the results compared to the results for the full data set (40 years). The results for the 5 and 10 year analysis data sets produced no output, (i.e. the program was unable to resolve the GEV and evaluate the frequency-magnitude relationship). Two sets of 20 years worth of data (i.e. (1962-1982 and 1992-2012) was assessed, with 1992-2012 analysis evaluating the frequency magnitude relationship close to (+/- 0.10 m) the prediction made for the complete data set. The second data set (1962-1982), instead of choosing the Weibull distribution (reaches a plateau) to fit the data, chose the Gumbel distribution (linear relationship between return period and magnitude). This led to comparable predictions for lower return periods (up to 1 in 200 years), but for the higher return periods (1 in 500 and 1 in 1000) led to significantly higher magnitude events for the higher return periods (+0.6 m for 1 in 1000), when compared to the prediction made for the complete data set using 40 years worth of data (1962-2012).

	Height (mCD)			
Return Period	95% Lower	Middle	95% Upper	Range (m)
10	6.25	6.28	6.33	0.08
25	6.29	6.32	6.37	0.08
50	6.32	6.34	6.39	0.07
100	6.33	6.36	6.41	0.08
250	6.34	6.36	6.42	0.08
500	6.35	6.37	6.43	0.08
1000	6.35	6.37	6.44	0.09

Table 5.1 Results of GEV analysis for Devonport annual maximum for the period 1962-2012.

	Height (mCD)			
Return Period	95% Lower	Middle	95% Upper	Range (m)
10	6.19	6.22	6.27	0.08
25	6.25	6.29	6.36	0.11
50	6.29	6.34	6.43	0.14
100	6.32	6.37	6.49	0.17
250	6.35	6.41	6.57	0.22
500	6.36	6.44	6.62	0.26
1000	6.38	6.46	6.67	0.29

Table 5.2 Results of GEV analysis for Newlyn annual maximum for the period 1915-2012.

	Height (mCD)			
Return Period	95% Lower	Middle	95% Upper	Range (m)
10	0.84	0.87	0.92	0.08
25	0.88	0.91	0.97	0.09
50	0.90	0.93	1.00	0.10
100	0.91	0.95	1.03	0.12
250	0.93	0.96	1.06	0.13
500	0.93	0.97	1.08	0.15
1000	0.94	0.98	1.10	0.16

Table 5.3 Results of GEV analysis for Devonport storm surge maximum for the period 1962-2012.

	Height (mCD)			
Return Period	95% Lower	Middle	95% Upper	Range (m)
10	0.74	0.78	0.83	0.09
25	0.81	0.86	0.94	0.13
50	0.85	0.91	1.02	0.17
100	0.89	0.95	1.09	0.20
250	0.92	1.00	1.18	0.26
500	0.95	1.03	1.24	0.29
1000	0.96	1.06	1.31	0.35

Table 5.4 Results of GEV analysis for Newlyn storm surge maximum for the period 1915-2012.

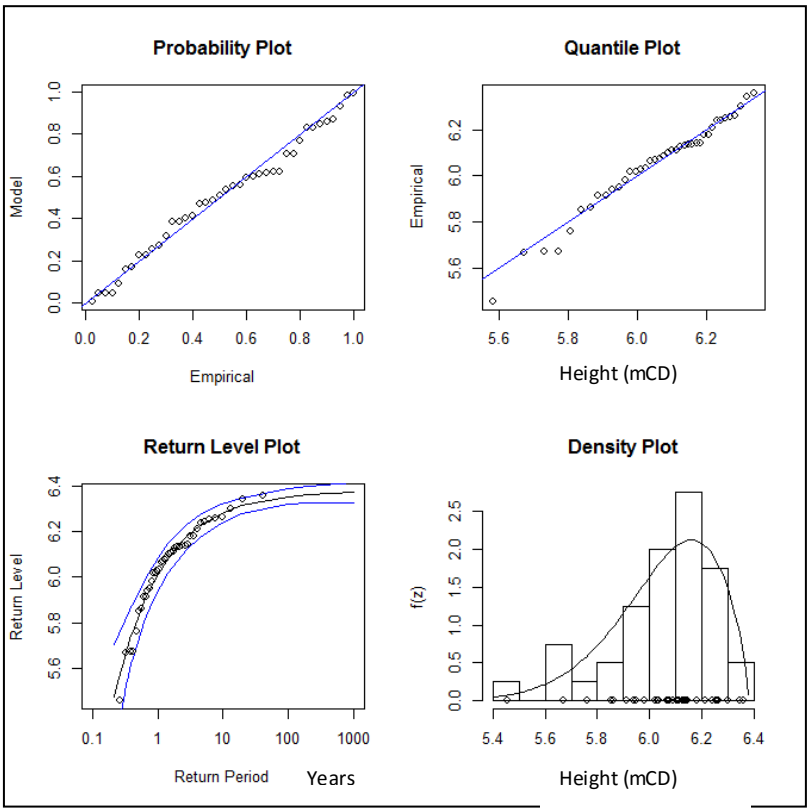

Figure 5.30 Generalised Extreme Value distribution return level and diagnostic plots for Devonport annual observed maximum data for the period 1962-2012.

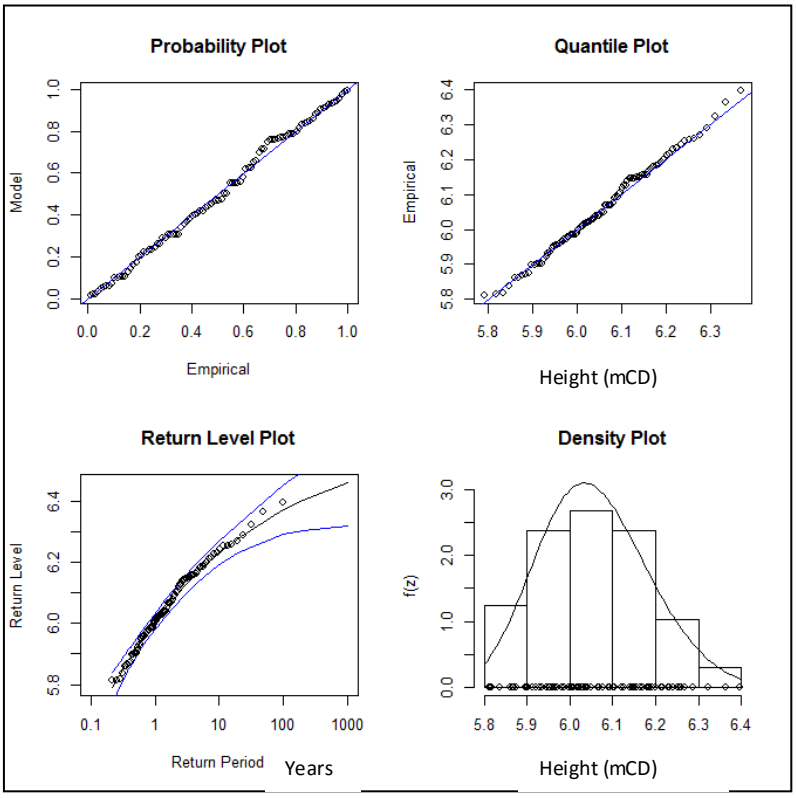

Figure 5.31 Generalised Extreme Value Distribution return level and diagnostic plots for Newlyn Annual Observed Maximum data for the period 1915-2012.

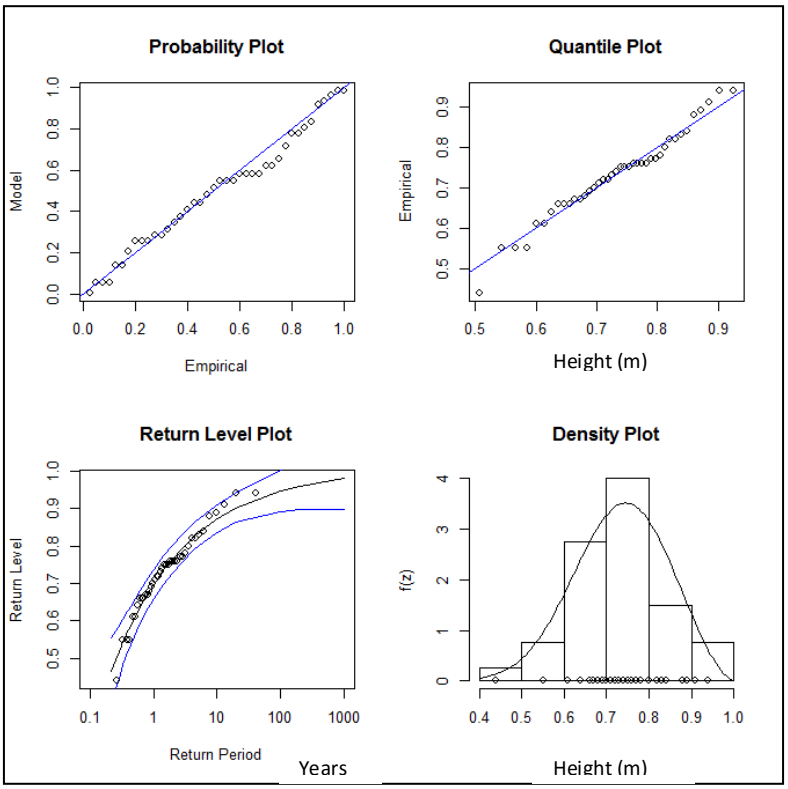

Figure 5.32 Generalised Extreme Value distribution return level and diagnostic plots for Devonport storm surge maximum data for the period 1962-2012.

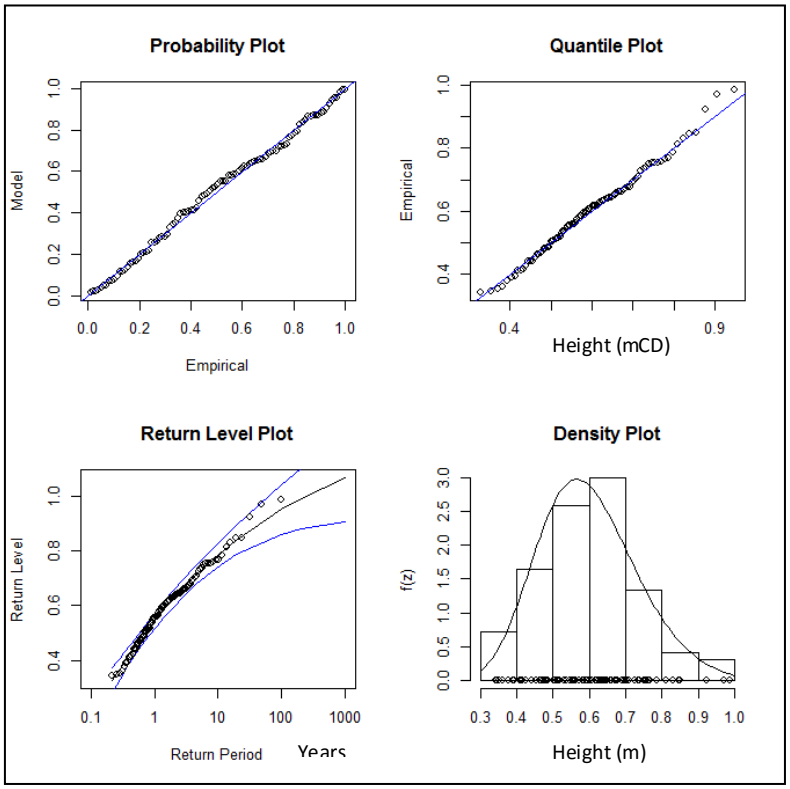

Figure 5.33 Generalised Extreme Value distribution return level and diagnostic plots for Newlyn storm surge maximum data for the period 1915-2012.

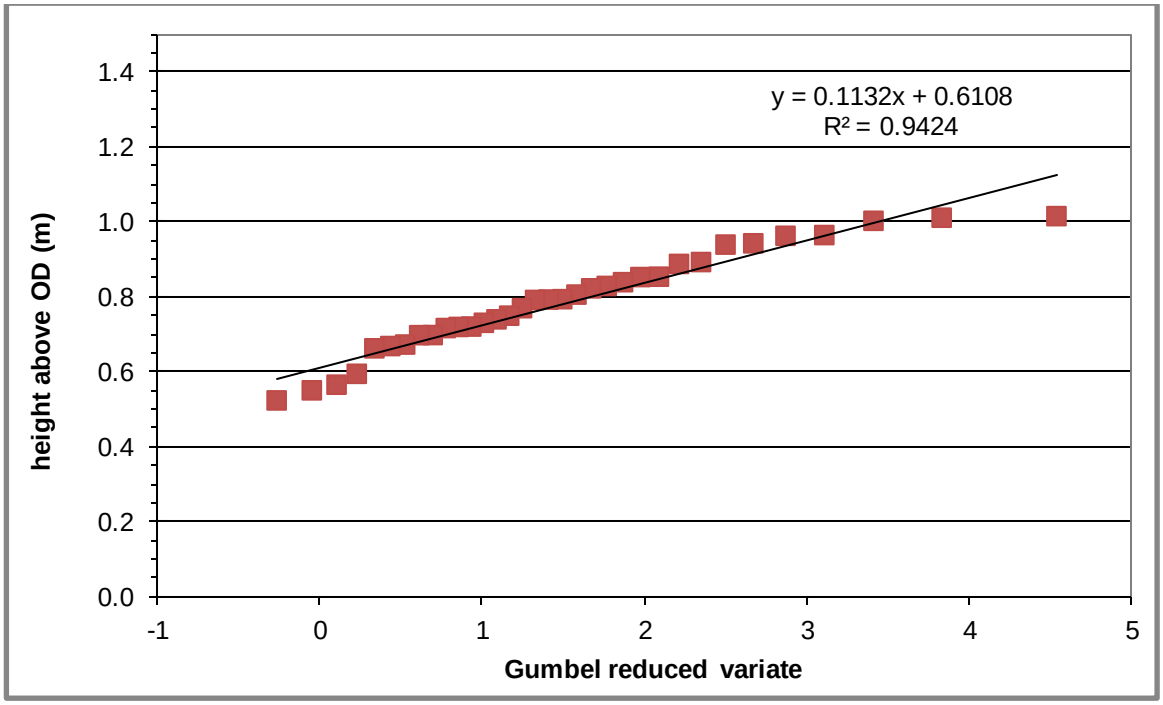

Figure 5.34 Gumbel Plot of storm surge against the Gumbel reduced Variate for Devonport for the period 1962-2012.

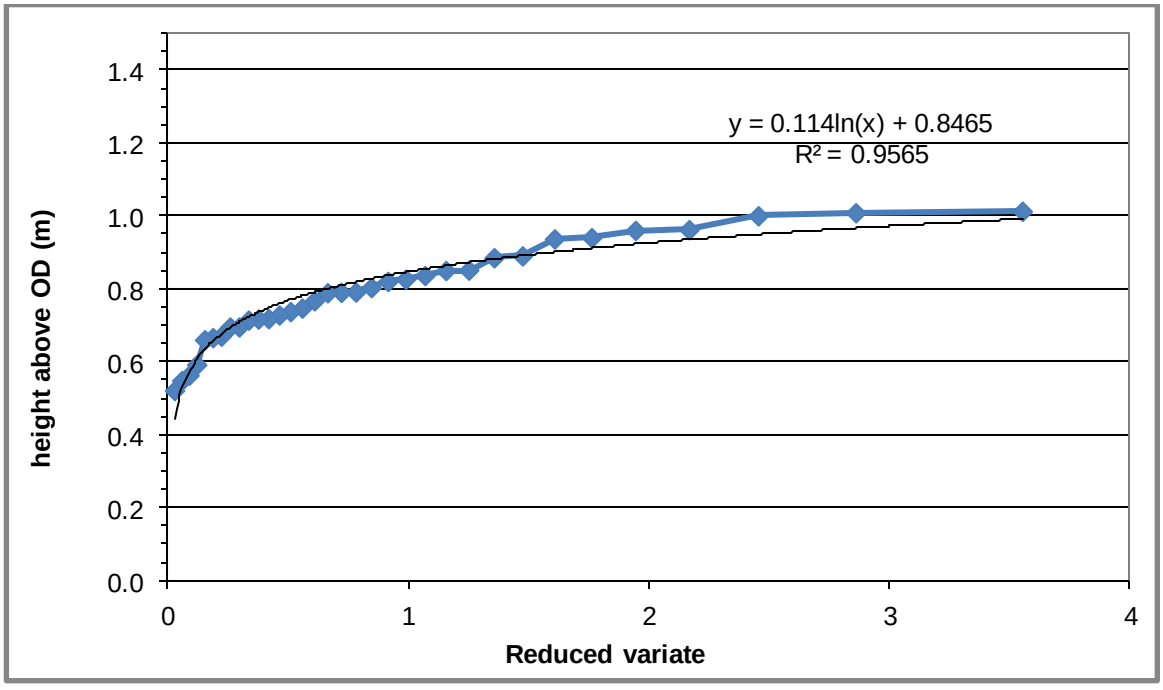

Figure 5.35 Weibull Plot of storm surge against the Gumbel reduced Variate for Devonport for the period 1962-2012.

5.4.2 r-largest

An outline of the r-largest methodology was given in Sections 4.4.4 and 4.4.5. Rather than using either the observed annual maximum or storm surge maximum, the r-largest methodology utilises a series of independent values extracted from the data sets. Within this study up to 10 values from each year were extracted and analysed. The ten largest annual maximum and storm surge maximum are illustrated in Figure 5.1 to 5.4. These data were imported into the "extremes" software package and analyses undertaken. The r-largest results for the annual maximum are given in Table 5.5 and Table 5.6 for Devonport and Newlyn, respectively, with r-largest return level and diagnostic plots given in Figures 5.36 and 5.37. For Devonport based on the observed ten largest annual maximum the mean value for a 1 in 10 year event is 6.31 mCD, for a 1 in 1000 year event the value is 6.40 mCD. Overall the prediction based on the r-largest has a maximum uncertainty range of 0.23 m at the 95% confidence limit (1 in 1000 year). For Newlyn the mean value for a 1 in 10 year event is 6.24 mCD, for a 1 in 1000 year event the value is 6.42 mCD. Overall the prediction based on the r-largest for Newlyn has a maximum uncertainty range of 0.29 m (1 in 1000 year).The results for r-largest based on the extracted storm surge values are given in tables 5.7 and 5.8 for Devonport and Newlyn, respectively. r-largest return level and diagnostic plot are given in Figures 5.38 and 5.39. For Devonport based on the ten largest extracted storm surge maximum the mean value for a 1 in 10 year event is 0.90 m, for a 1 in 1000 year event the value is 1.14 m. Overall the prediction based on the r-largest has a maximum uncertainty range of 0.26 m at the 95% confidence limit (1 in 1000 year). For Newlyn the mean value for a 1 in 10 year event is 0.80 m, for a 1 in 1000 year event the value is 1.10 m. Overall the prediction based on the r-largest for Newlyn has a maximum uncertainty range of 0.35 m (1 in 1000 year).

From a review of the return level and diagnostic plots it can be seen that both the observed annual and storm surge data fit a Weibull distribution. By comparing the results for Devonport and Newlyn (Figures 5.36 to 5.39), it can be seen that for both the annual maximum and storm surge maximum the Devonport return level plot reaches a plateau, where for an increase in return period there is only a slight increase in the amplitude. For Newlyn no plateau is reached, and a positive relationship is observed showing that an increase in return period gives an increase in amplitude. Also the diagnostic plots show that the Devonport observed data has a skewed distribution towards the higher values compared to a more normal distribution for Newlyn. For the storm surge maximum both data sets closely

approximate a normal distribution (Figures 5.1 to 5.4). This finding is comparable to the findings of the GEV analysis undertaken. Furthermore a comparison between the r-largest model and empirical data (Figures 5.36 to 5.39) fit suggests that the r-largest does not fit the data as well as the GEV analysis (Figures 5.30 to 5.34).

There is a good agreement between the predicted values for Devonport and Newlyn for both the observed annual and the storm surge data, with all return periods being within +/-0.05 m, at the 95% upper confidence interval (table 5.7 and 5.8).

The Literature Review (Chapter 3) highlights that a r-largest analysis can be undertaken with < 20 years of data. In an assessment similar to that undertaken for the GEV methodology, 5, 10 and 20 year subset of the Devonport data were analysed, with the results compared to the results for the full data set. With only 5 years of data, no output was possible. Both 10 and 20 years worth of data produced an output including a confidence interval. As with the GEV analysis, some subsets of the full data set chose the Gumbel distribution, leading to higher magnitude events at higher return periods, when compared to the prediction made for the complete data set.

In addition to assessing the applicability of the r-largest to predict frequency-magnitude relationships with short data sets, the value of r was varied from 10 to 2 to identify the optimum value of r. Figure 5.34 shows a comparison between a value of r of 5 and 2 for Devonport. However, when high r values (e.g. r=5) are chosen the methodology struggles to accurately model the data (Figure 5.36).

	Height (mCD)			
Return Period	95% Lower	Middle	95% Upper	Range (m)
10	6.28	6.31	6.35	0.07
25	6.31	6.35	6.40	0.09
50	6.34	6.37	6.44	0.10
100	6.34	6.38	6.48	0.14
250	6.36	6.39	6.54	0.18
500	6.36	6.39	6.57	0.21
1000	6.36	6.4	6.59	0.23

Table 5.5 Results of r-largest analysis for Devonport annual maximum for the period 1962-2012.

	Height (mCD)			
Return Period	95% Lower	Middle	95% Upper	Range (m)
10	6.22	6.24	6.28	0.06
25	6.26	6.28	6.34	0.08
50	6.28	6.32	6.39	0.11
100	6.3	6.36	6.45	0.15
250	6.32	6.38	6.53	0.19
500	6.33	6.41	6.58	0.25
1000	6.34	6.42	6.63	0.29

Table 5.6 Results of r-largest analysis for Newlyn annual maximum for the period 1915-2012.

	Height (mCD)			
Return Period	95% Lower	Middle	95% Upper	Range (m)
10	0.86	0.9	0.94	0.08
25	0.90	0.94	1.02	0.12
50	0.92	0.97	1.06	0.14
100	0.96	1	1.15	0.19
250	0.99	1.07	1.2	0.21
500	1.01	1.11	1.25	0.24
1000	1.04	1.14	1.30	0.26

Table 5.7 Results of r-largest analysis for Devonport storm surge maximum for the period 1962-2012.

	Height (mCD)			
Return Period	95% Lower	Middle	95% Upper	Range (m)
10	0.78	0.8	0.83	0.05
25	0.83	0.87	0.95	0.12
50	0.86	0.92	1.03	0.17
100	0.88	0.95	1.1	0.22
250	0.93	1	1.2	0.27
500	0.96	1.03	1.26	0.30
1000	0.98	1.1	1.33	0.35

Table 5.8 Results of r-largest analysis for Newlyn storm surge maximum for the period 1915-2012.

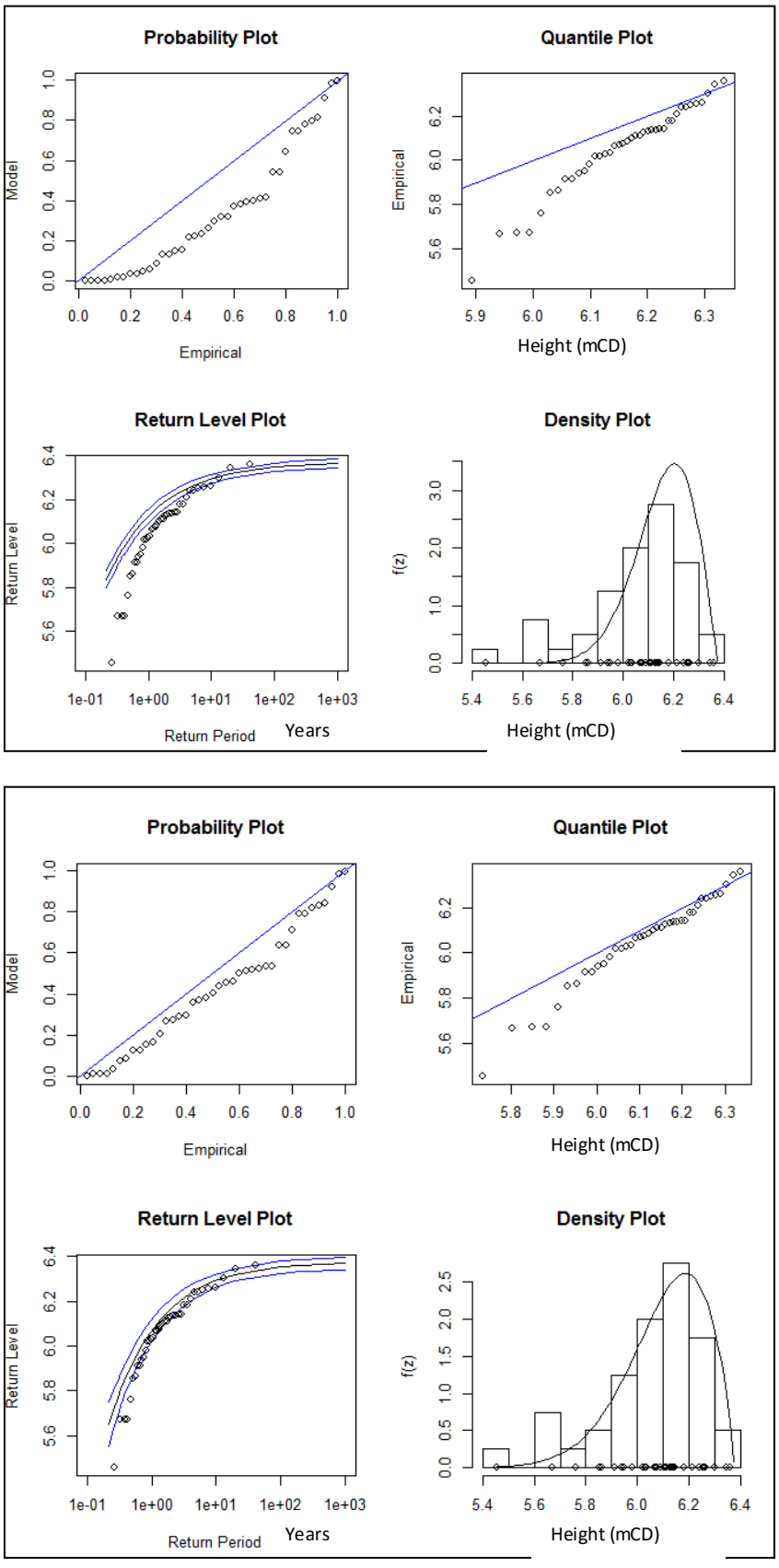

Figure 5.36 r-largest distribution return level and diagnostic plots for Devonport annual observed maximum data for the period 1962-2012. Top r=5, bottom r=2.

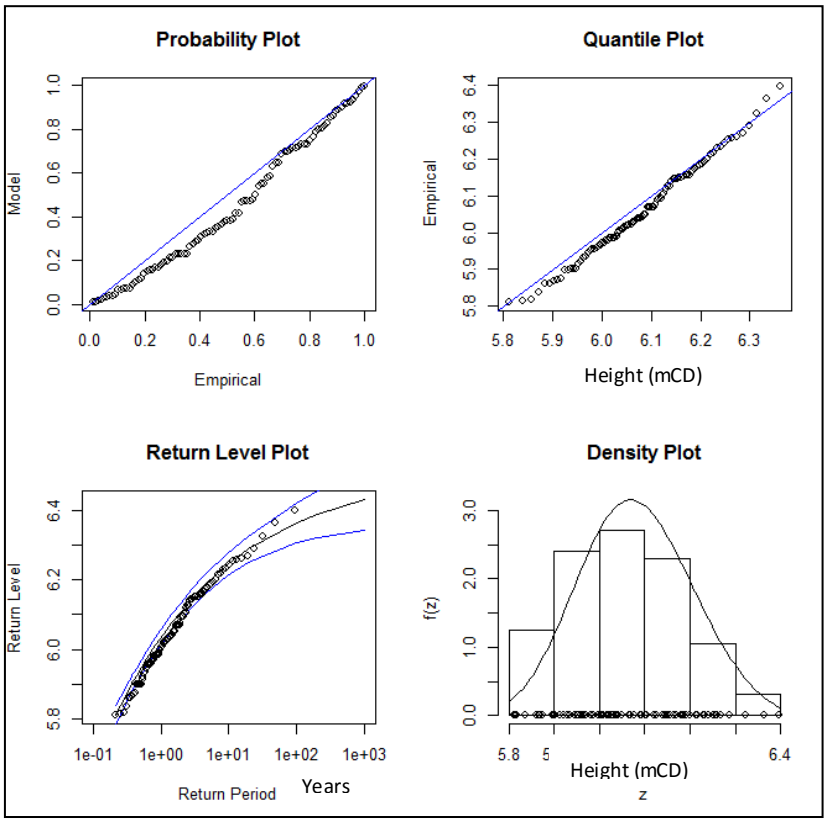

Figure 5.37 r-largest distribution return level and diagnostic plots for Newlyn annual observed maximum data for the period 1915-2012. r=2.

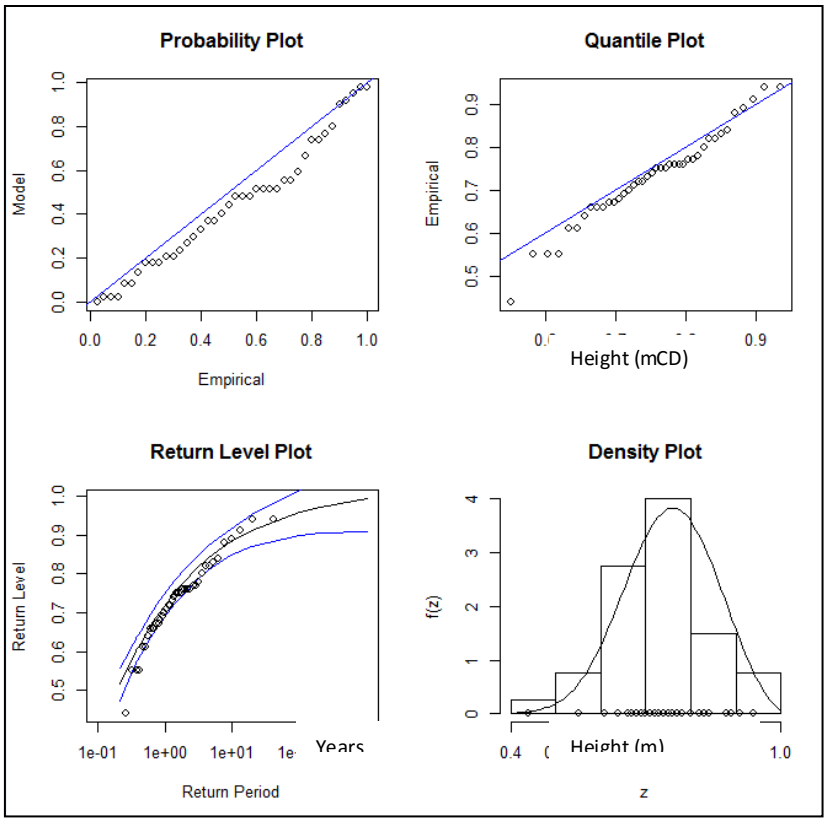

Figure 5.38 r-largest distribution return level and diagnostic plots for Devonport storm surge maximum data for the period 1962-2012. r=2.

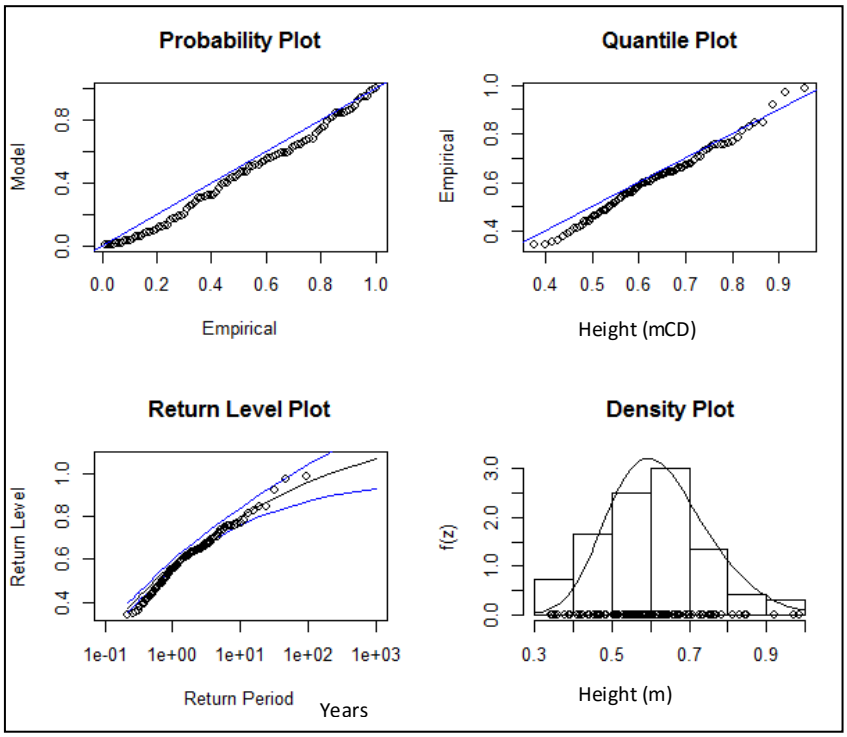

Figure 5.39 r-largest distribution return level and diagnostic plots for Newlyn storm surge maximum data for the period 1915-2012. r=2.

5.4.3 Generalised Pareto Distribution

An outline of the Generalised Pareto Distribution (GPD) methodology was given in Section 4.4.6 and 4.4.7. The GPD methodology is also known as the Peak Over Threshold (POT) methodology, as instead of utilising the annual maximum or the ten largest values as undertaken for the GEV and r-largest methodology, all values above a certain threshold are selected. This means that several results may be selected from one year, while other years no results could be selected. For the observed data set the threshold was set at 5.5 mCD, leading to approximately 2000 observations for Devonport, equating to an average of 40 observations per year, and for Newlyn over 4000 observations, also equating to approximately 40 observations per year. All observations were separated by at least 24 hours and can be considered independent. For the extracted storm surge data the threshold was set at 0.50 m, leading to approximately 750 observations for Devonport equating to on average approximately 15 observations per year. For Newlyn the threshold gave approximately 1000 observations, giving an average of 11 observations per year.

The GPD data was imported into the “extremes” software package (Section 4.4.5) and an analysis undertaken. The GPD results for the annual maximum are given in table 5.9 and 5.10 for Devonport and Newlyn, respectively, with return level and diagnostic plots given in Figures 5.40 and 5.43. For Devonport based on the analysis undertaken on values above a threshold the mean value for a 1 in 10 year event is 6.24 mCD, for a 1 in 1000 year event the value is 6.38 mCD. Overall the prediction based on the GPD has a maximum uncertainty range of 0.11 m at the 95% confidence limit (1 in 1000 year). For Newlyn the mean value for a 1 in 10 year event is 6.22 mCD, for a 1 in 1000 year event the value is 6.41 mCD. Overall the prediction based on the GPD for Newlyn has a maximum uncertainty range of 0.13 m (1 in 1000 year). The results for GPD based on the extracted storm surge values are given in Table 5.11 and 5.12 for Devonport and Newlyn, respectively, with return level and diagnostic plots given in Figures 5.44 and 5.45. For Devonport based on the extracted storm surge maximum above a threshold the mean value for a 1 in 10 year event is 0.90 m, for a 1 in 1000 year event the value is 1.07 m. Overall the prediction based on the GPD has a maximum uncertainty range of 0.21 m at the 95% confidence limit (1 in 1000 year). For Newlyn the mean value for a 1 in 10 year event is 0.79 m, for a 1 in 1000 year event the value is 1.09m. Overall the prediction based on the GPD for Newlyn has a maximum uncertainty range of 0.26 m (1 in 1000 year).

Using this methodology both observed and storm surge data fit a Weibull distribution (Figures 5.40 to 5.45). This is similar to the GEV and r-largest methodologies. By comparing the results for Devonport and Newlyn (Figures 5.40 to 5.45), it can be seen that for both the annual maximum and storm surge maximum the Devonport return level plot reaches a plateau, where for an increase in return period there is only a slight increase in the amplitude. For Newlyn no plateau is reached, and a positive relationship is observed showing that an increase in return period gives an increase in amplitude. A visual of the diagnostic plots shows a good fit for all data sets, when comparing the GPD model and empirical data (Figures 5.40 to 5.45).

There is a good agreement between the predicted values for Devonport and Newlyn for both the observed annual and the storm surge data, with all return periods being within +/-0.05 m. This includes results at the 95 % upper confidence interval (Tables 5.9 to 5.11).

Chapter 3 highlighted that the GPD methodology can be sensitive to the choice of threshold. Within this study the threshold was increased from 5.5 mCD to 5.8 mCD and then to 6.0 mCD, reducing the number of observations from approximately 2000 to 500 and then to 100. When reviewing the diagnostic plots (Figures 5.40 to 5.42) it was identified that the low threshold (5.50 mCD ~2000 observations) gave the poorest fit based on a visual assessment of the return level plots, despite an excellent fit when viewing the probability plot of empirical data against the GPD model data. Nevertheless the predictions of the frequency-magnitude relationships based on the three different thresholds are within +/-0.05 m of each other, indicating the choice of threshold has little impact on the predictions made.

	Height (mCD)			
Return Period	95% Lower	Middle	95% Upper	Range (m)
10	6.22	6.24	6.28	0.06
25	6.26	6.29	6.32	0.06
50	6.28	6.31	6.36	0.08
100	6.30	6.33	6.39	0.09
250	6.32	6.36	6.42	0.10
500	6.33	6.37	6.43	0.10
1000	6.34	6.38	6.45	0.11

Table 5.9 Results of GPD analysis for Devonport Observed data for the period 1962-2012.

	Height (mCD)			
Return Period	95% Lower	Middle	95% Upper	Range (m)
10	6.20	6.22	6.25	0.05
25	6.25	6.28	6.31	0.06
50	6.28	6.31	6.36	0.08
100	6.30	6.34	6.40	0.10
250	6.33	6.37	6.44	0.11
500	6.35	6.39	6.47	0.12
1000	6.36	6.41	6.49	0.13

Table 5.10 Results of GPD analysis for Newlyn Observed data for the period 1915-2012.

	Height (m)			
Return Period	95% Lower	Middle	95% Upper	Range (m)
10	0.86	0.90	0.95	0.09
25	0.91	0.95	1.02	0.11
50	0.94	0.98	1.07	0.13
100	0.96	1.00	1.12	0.16
250	0.98	1.04	1.17	0.19
500	0.99	1.05	1.19	0.20
1000	1.00	1.07	1.21	0.21

Table 5.11 Results of GPD analysis for Devonport storm surge data for the period 1962-2012.

	Height (m)			
Return Period	95% Lower	Middle	95% Upper	Range (m)
10	0.76	0.79	0.83	0.07
25	0.82	0.85	0.93	0.11
50	0.85	0.91	1.00	0.15
100	0.89	0.95	1.06	0.17
250	0.93	1.00	1.13	0.2
500	0.95	1.05	1.18	0.23
1000	0.97	1.09	1.23	0.26

Table 5.12 Results of GPD analysis for Newlyn storm surge data for the period 1915-2012.

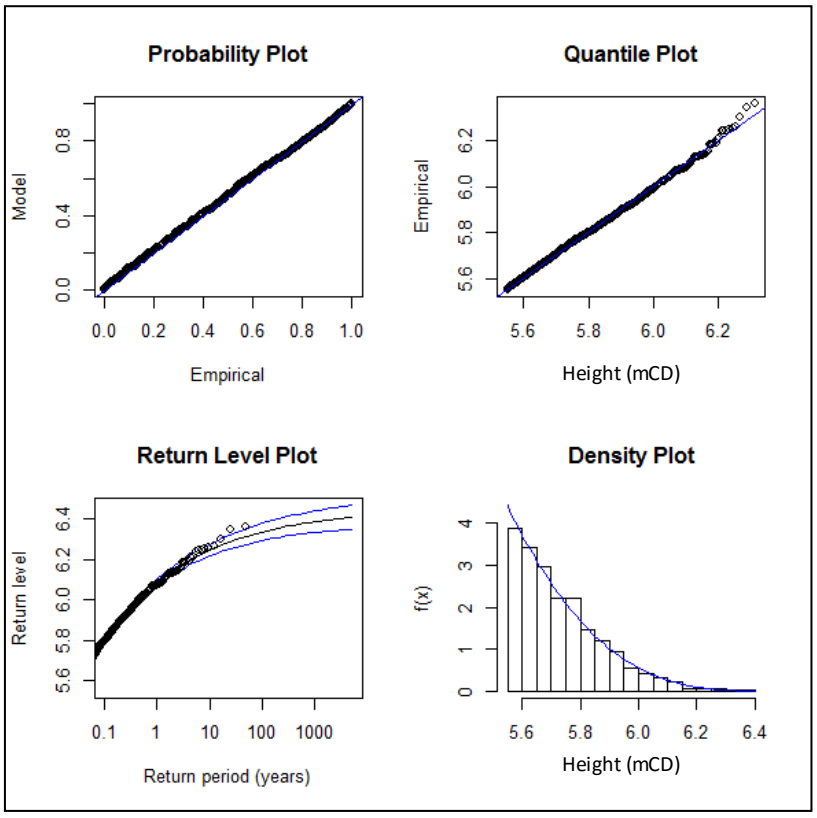

Figure 5.40 GPD distribution return level and diagnostic plots for Devonport Observed data for the period 1962-2012. Threshold=5.55m CD equating to approximately 2000 observations.

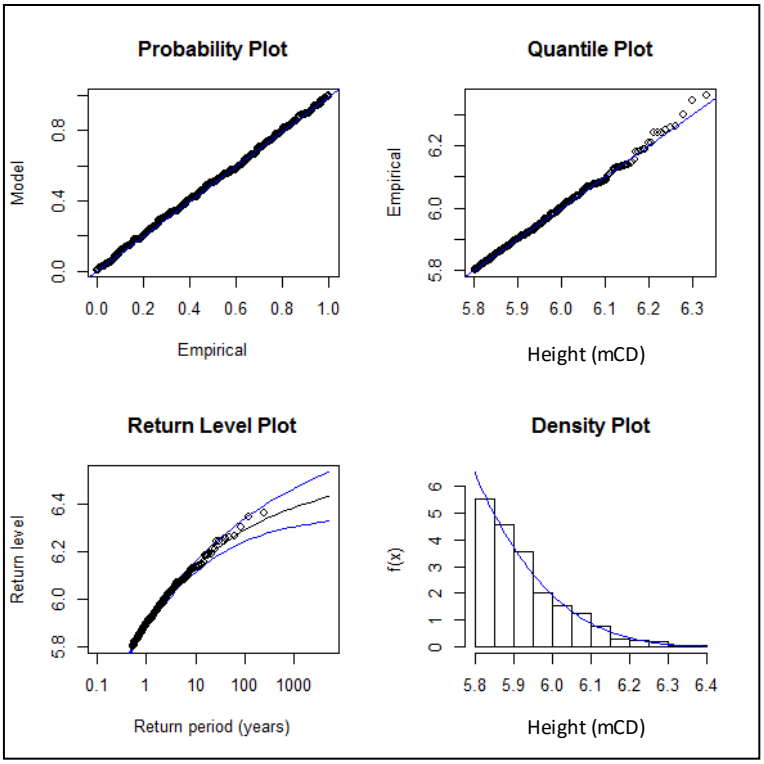

Figure 5.41 GPD distribution return level and diagnostic plots for Devonport Observed data for the period 1962-2012. Threshold=5.80mCD equating to approximately 500 observations.

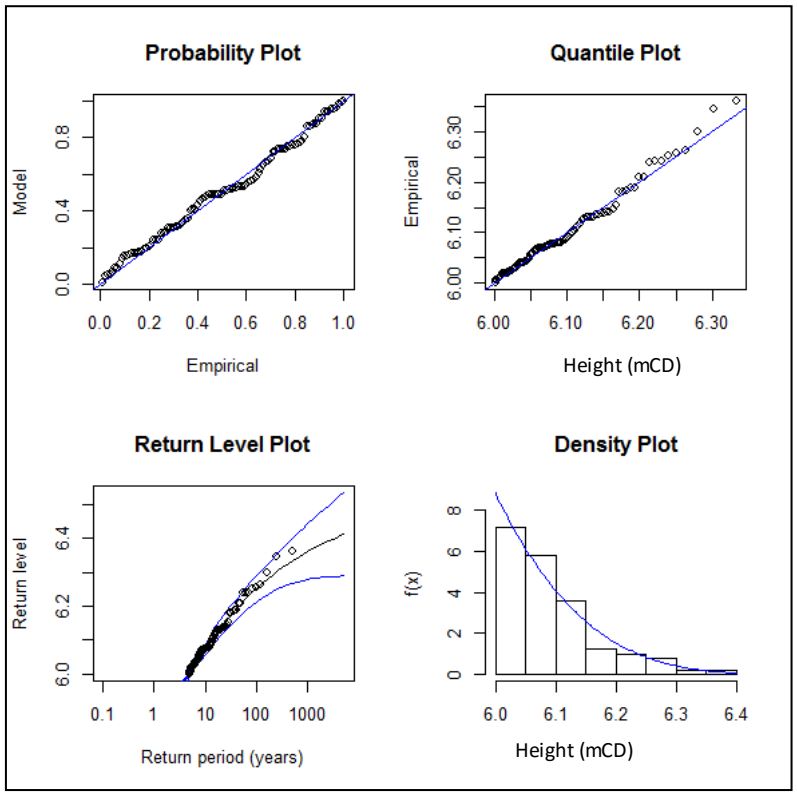

Figure 5.42 GPD distribution return level and diagnostic plots for Devonport Observed data for the period 1962-2012. Threshold=6.00mCD equating to approximately 100 observations.

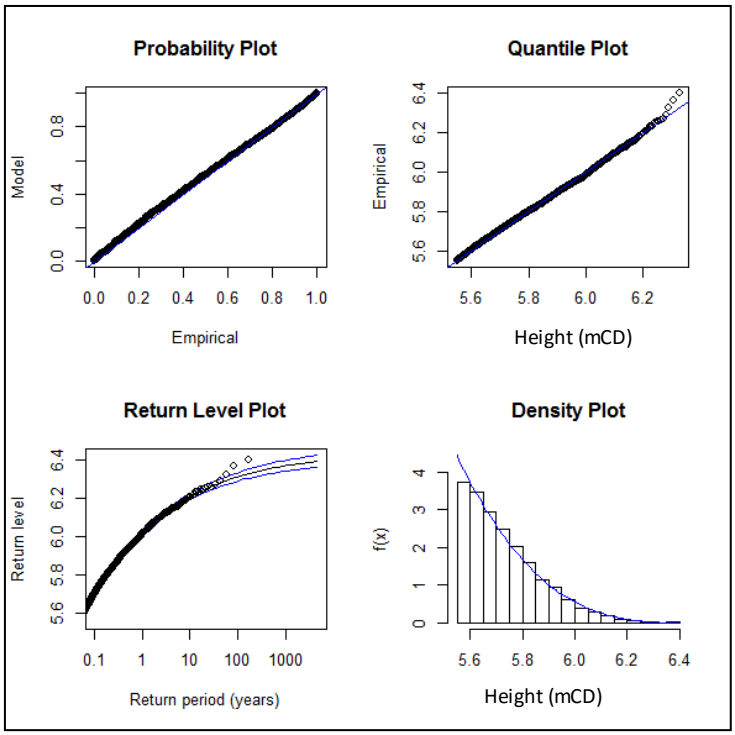

Figure 5.43 GPD distribution return level and diagnostic plots for Newlyn Observed data for the period 1915-2012. Threshold=5.55 mCD equating to approximately 4000 observations.

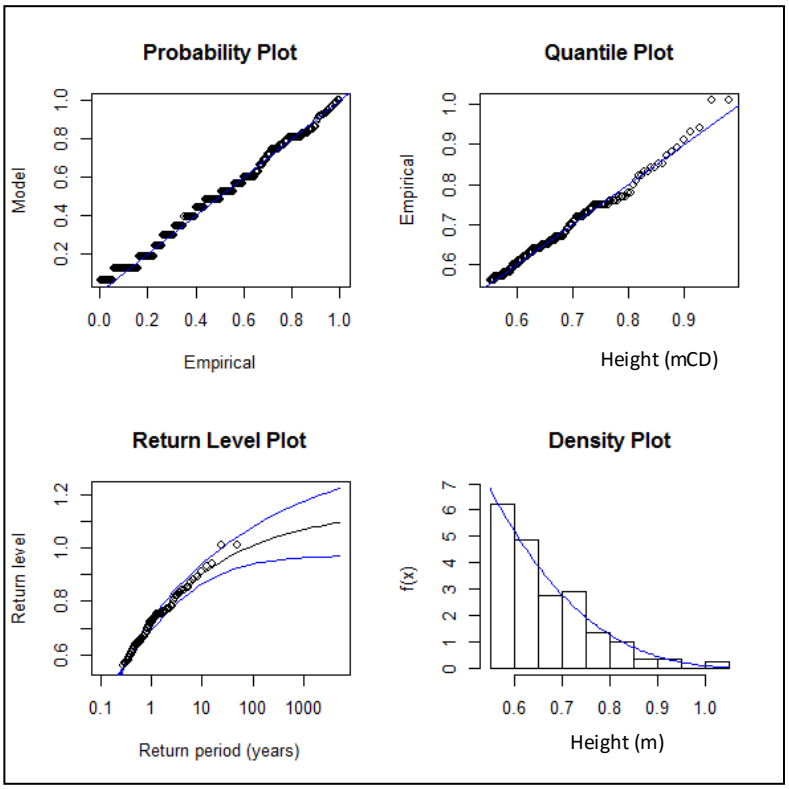

Figure 5.44 GPD distribution return level and diagnostic plots for Devonport storm surge data for the period 1962-2012. Threshold=0.55m equating to approximately 400 observations.

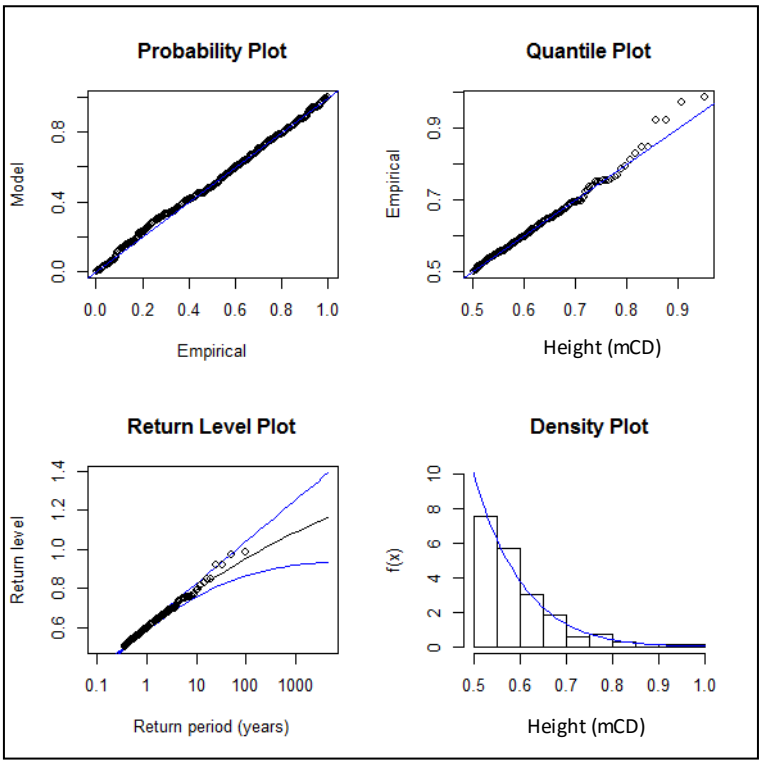

Figure 5.45 GPD distribution return level and diagnostic plots for Newlyn storm surge data for the period 1915-2012. Threshold=0.55m equating to approximately 700 observations.

5.4.3 Joint Probability

A Joint Probability (JP) analysis was undertaken as outlined in Section 4.4.8. In comparison to utilising only part of the data set, the JP methodology utilises all hourly observations. As described in Section 4.4.8 the astronomical and tidal component are separated from the observed levels. The data are then counted in intervals or bins of 0.1 m. For each astronomical and storm surge height the probability of occurrence is calculated (i.e. Figure 5.11). The astronomical tide and storm surge levels are recombined and a joint probability calculated (Table 4.7 and 4.8).

The results from the JP analysis for Devonport and Newlyn are given in Tables 5.13 and 5.14 respectively, and illustrated in Figures 5.46 and 5.47. For Devonport based on the JP analysis undertaken on frequency distribution data set the mean value for a 1 in 10 year event is 6.60 mCD, for a 1 in 1000 year event the value is 7.0 mCD. Overall the prediction based on the JP has a maximum uncertainty range of 0.20 m at the 95% confidence limit (1 in 1000 year). For Newlyn the mean value for a 1 in 10 year event is 6.50 mCD, for a 1 in 1000 year event the value is 6.85 mCD. Overall the prediction based on the JP for Newlyn has a maximum uncertainty range of 0.20 m (1 in 1000 year). For both Devonport and Newlyn there is a linear relationship between magnitude and Log (Return period). There is a strong correlation between the predictions made for Devonport and Newlyn, with a maximum difference in predictions of 0.15 m (Tables 5.13, 5.14 and Figure 5.49).

The ability of the JP to predict accurately the frequency-magnitude relations based on a limited data sets has been assessed by utilising 1, 5, 10 and 20 years worth of the Devonport data set. Figure 5.48 shows a comparison between the predictions made based on these data sets. For lower return periods there are close agreements between the different data sets. Beyond this the predictions diverge, with a significant difference at the higher return periods, and at 1 in 1000 return period the predictions vary by up to 0.15 m. It can be seen that 20 years worth of data compares favourably to the complete data set. This is potentially linked to the 18.6 years required to simulate a complete tidal cycle (Chapter 2 Section 2.2).

	Height (mCD)			
Return Period	95% Lower	Middle	95% Upper	Range (m)
10	6.5	6.6	6.7	0.2
25	6.55	6.65	6.75	0.2
50	6.6	6.7	6.8	0.2
100	6.7	6.8	6.9	0.2
250	6.75	6.85	6.95	0.2
500	6.8	6.9	7.0	0.2
1000	6.9	7.0	7.1	0.2

Table 5.13 Results of Joint Probability analysis for Devonport for the period 1962-2012.

	Height (mCD)			
Return Period	95% Lower	Middle	95% Upper	Range (m)
10	6.4	6.5	6.6	0.2
25	6.45	6.55	6.65	0.2
50	6.5	6.6	6.7	0.2
100	6.55	6.65	6.75	0.2
250	6.6	6.7	6.8	0.2
500	6.7	6.8	6.9	0.2
1000	6.75	6.85	6.95	0.2

Table 5.14 Results of Joint Probability analysis for Newlyn for the period 1915-2012.

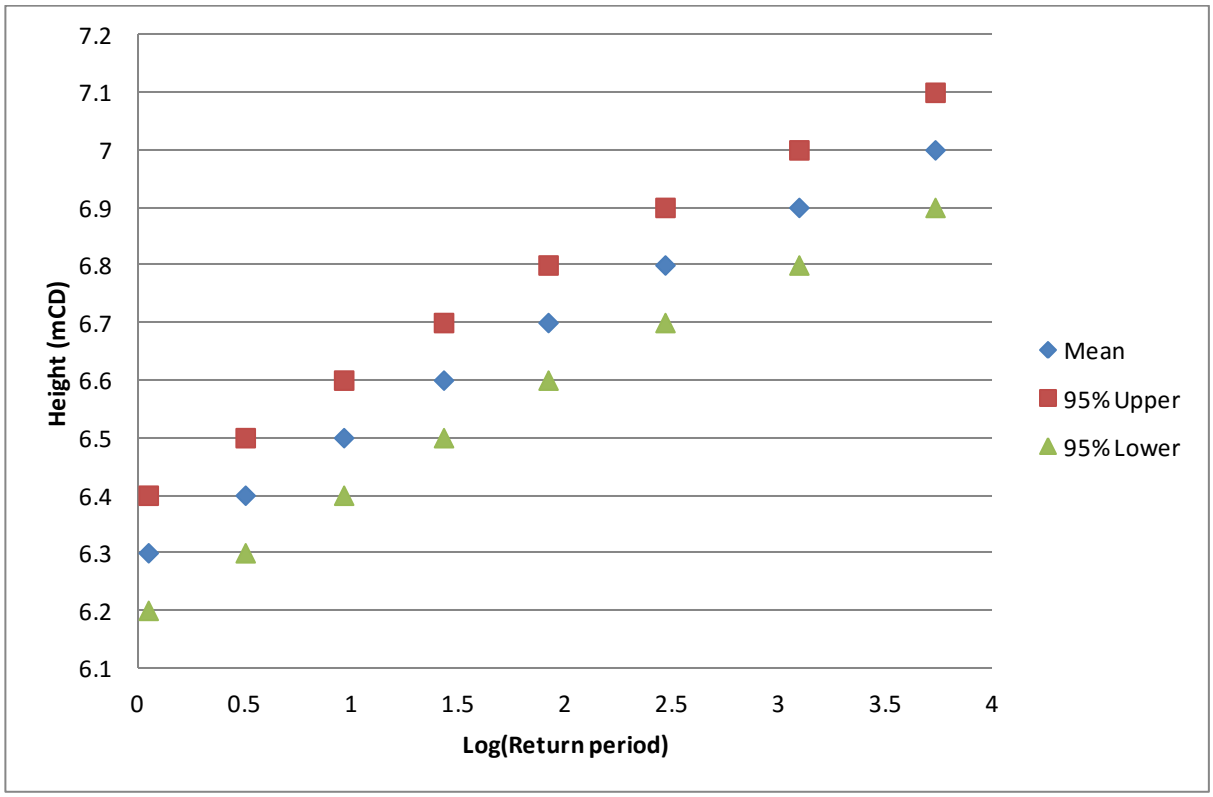

Figure 5.46 Joint probability plot for Devonport for the Period 1962-2012.

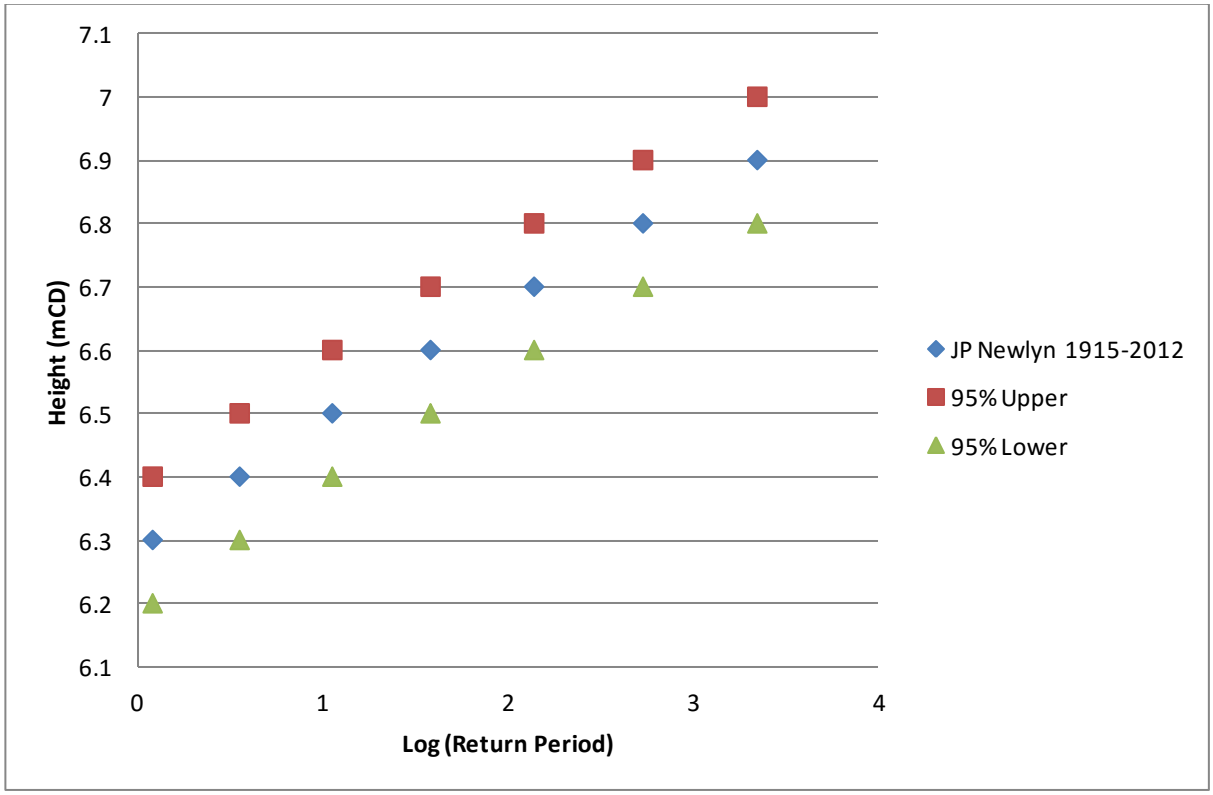

Figure 5.47 Joint Probability plot for Newlyn for the Period 1915-2012.

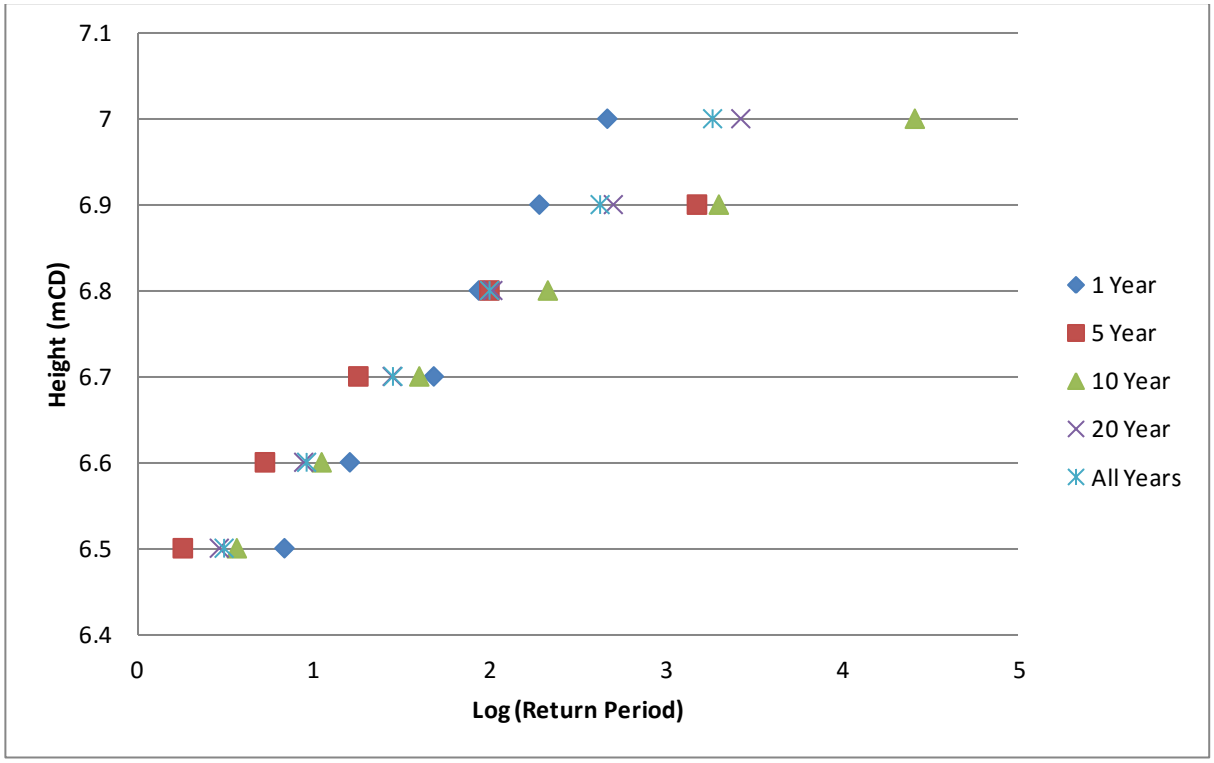

Figure 5.48 Comparison of prediction for the Joint Probability based on the number of years used within the analysis.

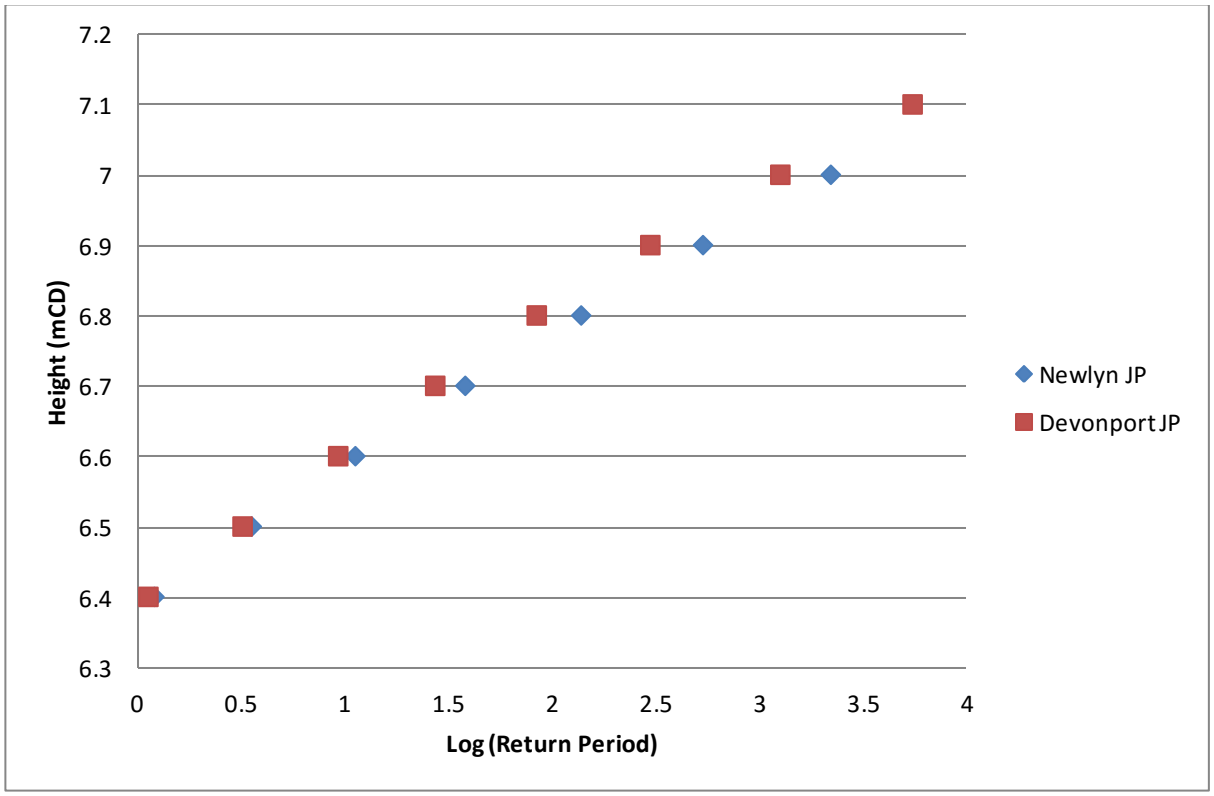

Figure 5.49 Comparison between the joint Probability Predictions made for Devonport and Newlyn.

5.4.4 Monte Carlo Simulation

An outline of the methodology to undertake a Monte Carlo analysis is discussed in Section 4.4.8 to Section 4.4.10. In a similar manner to the Joint Probability methodology, a Monte Carlo analysis utilises all the hourly data. The approach can utilise either the frequency distribution data modelled by the JP method, or each hourly reading can be imported in to a relevant software package, with the software calculating the frequency of the data on the user's behalf. In this study both approaches have been employed.

Figure 5.50 and Figure 5.51 shows a comparison with the input data (blue histogram) and the modelled Probability Density Function (PDF) (Red Line) for the storm surge and astronomical tidal data for Devonport. The data was modelled within the software package @risk (Palisade, 2013). Figure 5.50 shows that the storm surge distribution is close to a normal distribution and can be modelled by several different PDFs. The @risk software package fails to fully define a diurnal tide (Figure 5.51) as within the software package a bimodal distribution PDF is not available. The closest approximation is a BetaGeneral distribution; however, this distribution underestimates the probability of occurrence of the tidal component between a height of 4 mCD and 5.5 mCD. This would lead to an under-prediction of the tidal component between the height of 4.0 mCD and 5.5 mCD, leading to an under prediction for the larger inundation events when the tidal component is combined with the storm surge component. In an attempt to combat this under prediction, a Monte Carlo analysis is undertaken using only the positive storm surge data, between 0 m and 1 m in Figure 5.51 (i.e. combining the Betageneral model of the astronomical tidal component and the storm surge model between 0 and 1 m).

To recombine the astronomical tidal component and a storm surge component a Monte Carlo simulation is undertaken recombining the PDFs (Figures 5.50 and 5.51. The simulation was set to undertake 10000 iterations a total of 10 times. In addition confidence intervals were set at 95%, which requires the software program to run additional simulations. Typically this simulation took approximately 48 hours on a 2.2GHz processor with 3.0GB of RAM. In total approximately 50 of these simulations were undertaken.

Figure 5.52 shows the result of the Monte Carlo simulation that recombines the storm surge and astronomical tidal data. A plot of the return period against inundation height is shown in Figure 5.53. The same process was repeated for Newlyn and Figures 5.54 to 5.57 present the results. For Devonport based on the

Monte Carlo analysis of the complete hourly data set the mean value for a 1 in 10 year event is 6.50 mCD, for a 1 in 1000 year event the value is 6.15 mCD. Overall the prediction based on the GPD has a maximum uncertainty range of 1.0 m at the 95% confidence limit (1 in 1000 year). For Newlyn the mean value for a 1 in 10 year event is 6.45 mCD, for a 1 in 1000 year event the value is 7.10 mCD. Overall the prediction based on the GPD for Newlyn has a maximum uncertainty range of 0.10 m (1 in 1000 year).

Both Devonport and Newlyn data sets can be represented by similar PDFs. The storm surge data approximates the LogLogistic PDF, with a BetaGeneral PDF modelling the astronomical tidal component. The shape of recombining the PDFs within a Monte Carlo simulation provides comparative results (Figure 5.51). The main difference between Devonport and Newlyn is that the established confidence interval for Newlyn are extremely small. The Monte Carlo simulation significantly underestimates the magnitude of events for all return periods for both Devonport and Newlyn when compared to the other statistical methods (tables 5.15 and 5.16). This is most likely due to the underestimation of the astronomical tidal component between 4.0 and 5.5 mCD. However, utilising only the maximum storm surge values compensates for this with comparative results produced, when compared to the Joint Probability method.

The ability of a Monte Carlo simulation to predict accurately the frequency-magnitude relations based on a limited data sets has been assessed by utilising 1, 5, 10 and 20 years worth of the Devonport data set, in a similar process to the Joint Probability methodology. As the 1, 5, and 10 year data sets approximate the same PDFs as the full data set, the Monte Carlo methodology is able to evaluate the frequency–magnitude relationship up to approximately a 1 in1000 year event with as little as 1 years worth of data to an accuracy of (+/-0.15m) (Figure 5.59) when compared to the complete data set (+ve storm surge values).

	Height (mCD)			
Return Period	95% Lower	Middle	95% Upper	+ve Values (95% Upper
10	5.0	5.5	6.0	6.50
25	5.2	5.7	6.2	6.55
50	5.4	6.0	6.5	6.65
100	5.7	6.3	6.8	6.8
250	5.8	6.4	6.85	6.95
500	5.9	6.5	6.9	7.05
1000	6.0	6.60	7.0	7.15

Table 5.15 Results of Monte Carlo analysis for Devonport for the period 1962-2012.

	Height (mCD)			
Return Period	95% Lower	Middle	95% Upper	+ve Values
10	5.27	5.35	5.35	6.45
25	5.45	5.5	5.6	6.60
50	5.65	5.75	5.8	6.70
100	5.9	6.0	6.05	6.80
250	6.1	6.15	6.15	6.90
500	6.2	6.25	6.25	7.00
1000	6.27	6.35	6.35	7.10

Table 5.16 Results of Monte Carlo analysis for Newlyn for the period 1915-2012.

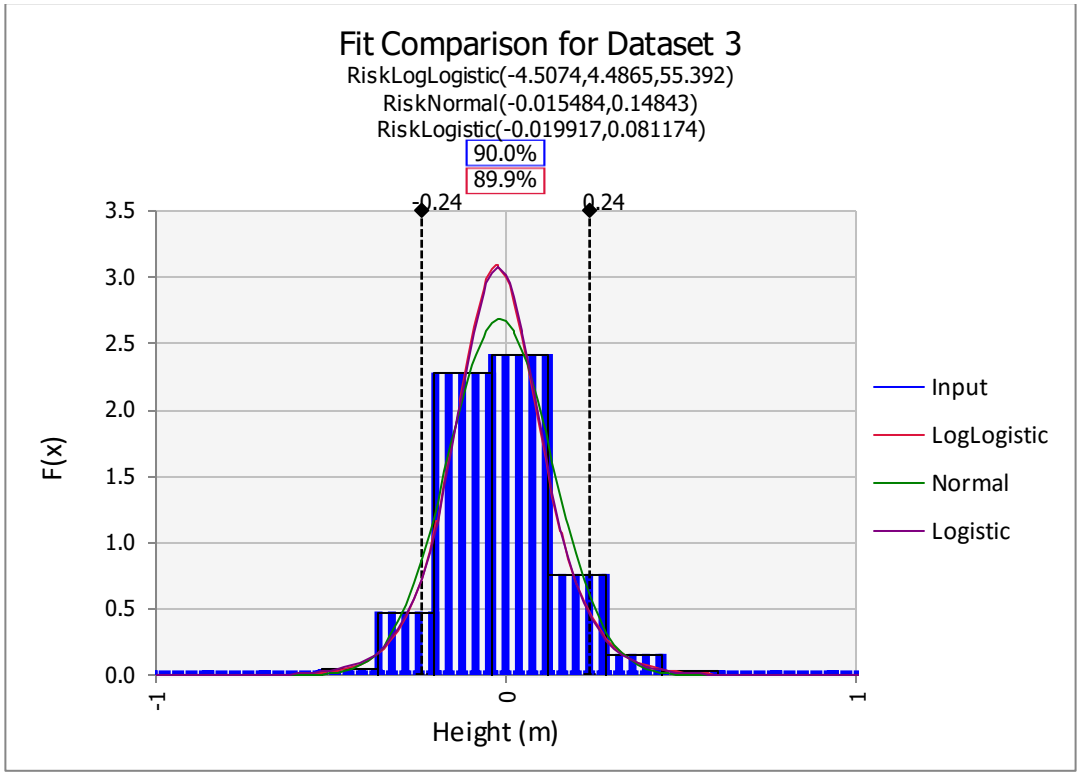

Figure 5.50 Comparison between input storm surge data for Devonport 1962-2012 and 3 different Probability Density Function modelled in @risk.

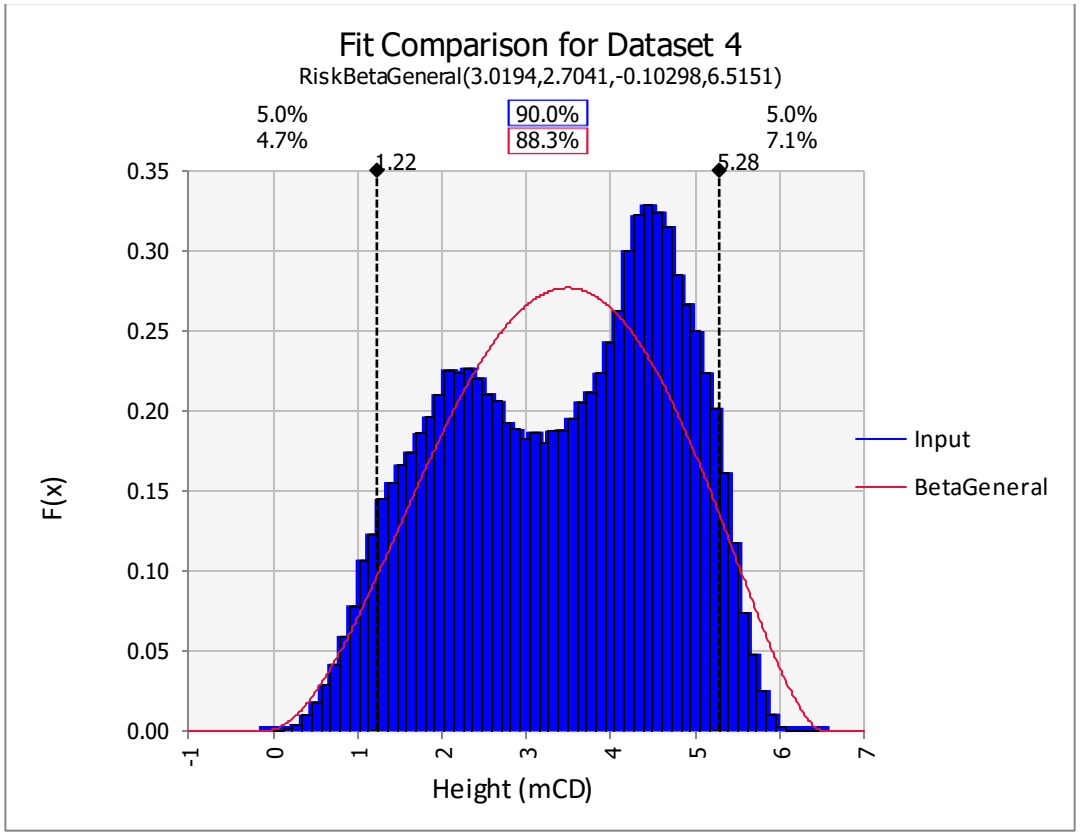

Figure 5.51 Comparison between input astronomical tidal data for Devonport 1962-2012 and BetaGeneral Probability Density Function modelled in @risk.

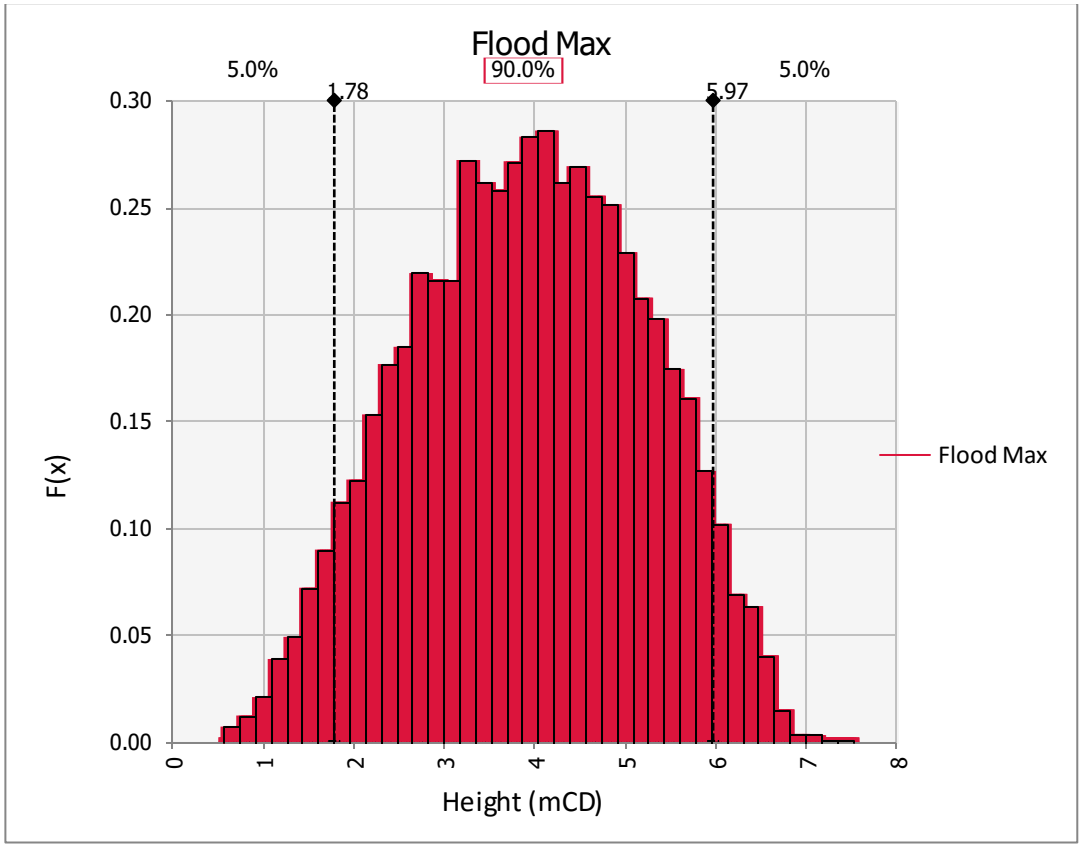

Figure 5.52 Monte Carlo simulation to produce inundation levels for Devonport based on the input PDFs from Figures 4.43 and Figures 4.44.

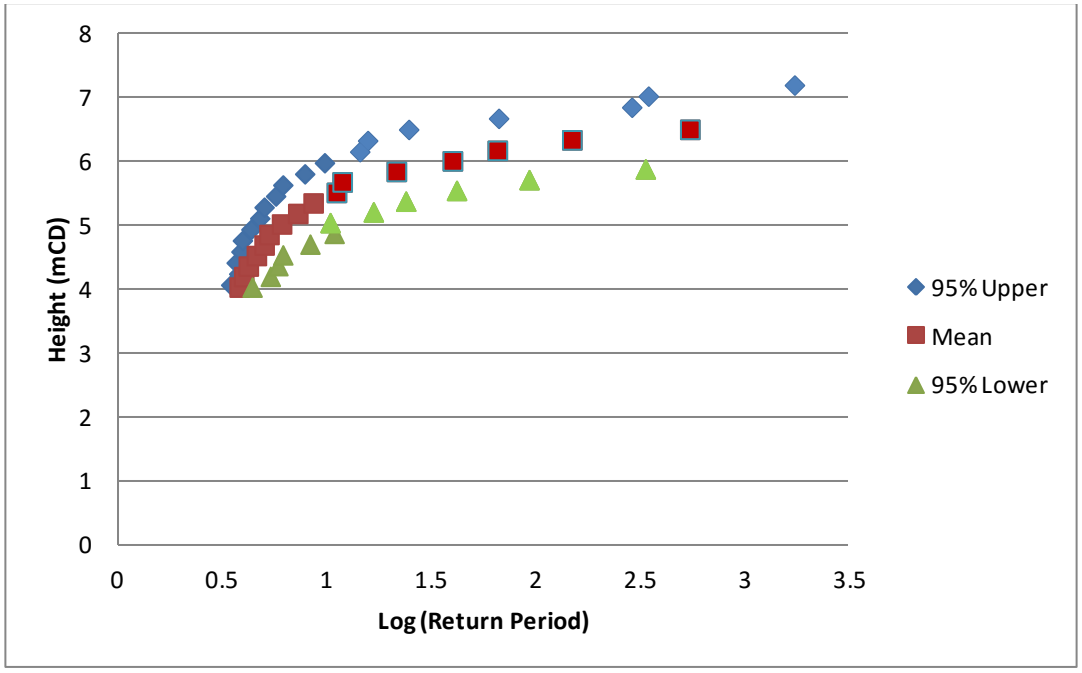

Figure 5.53 Return Level plot of Log (Return period) vs inundation level for Devonport based on the output from the Monte Carlo simulation in Figure 5.45.

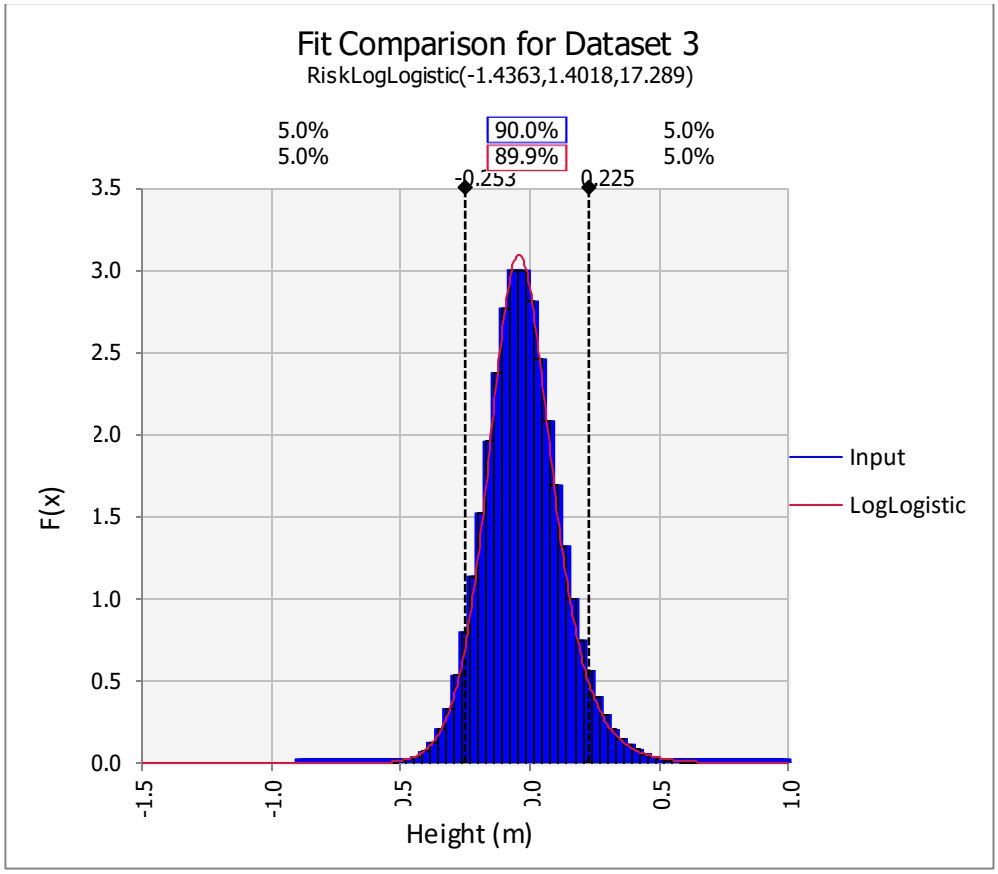

Figure 5.54 Comparison between input storm surge data for Newlyn 1915-2012 and Loglogistic Probability Density Function modelled in @risk.

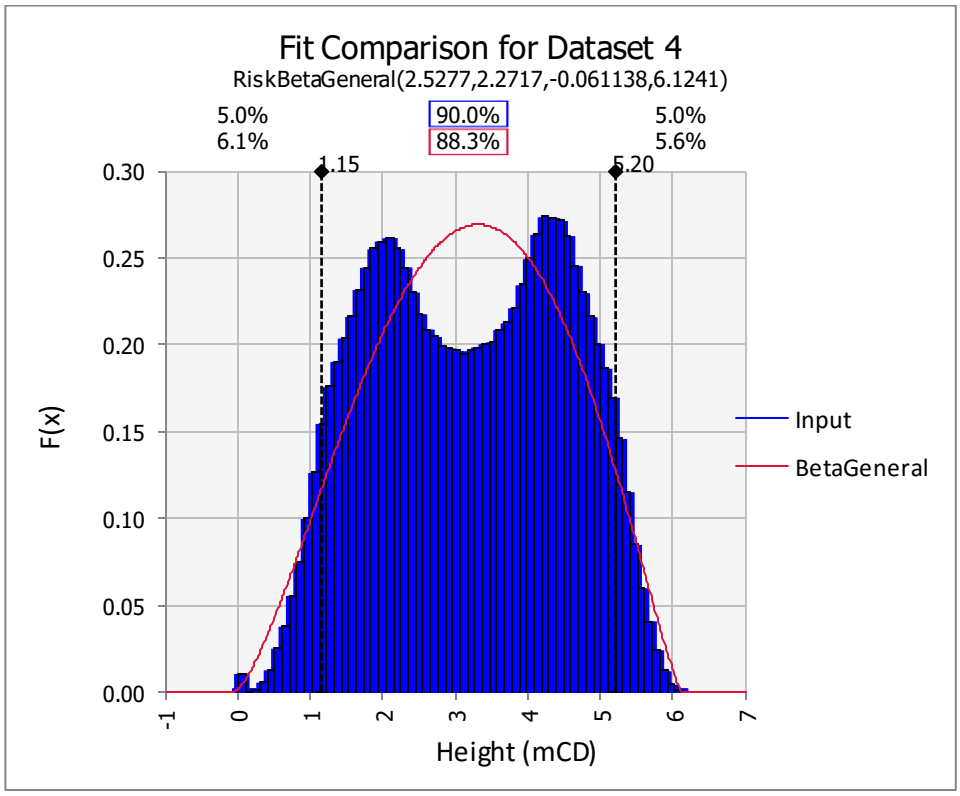

Figure 5.55 Comparison between input astronomical tidal data for Newlyn 1915-2012 and BetaGeneral Probability Density Function modelled in @risk.

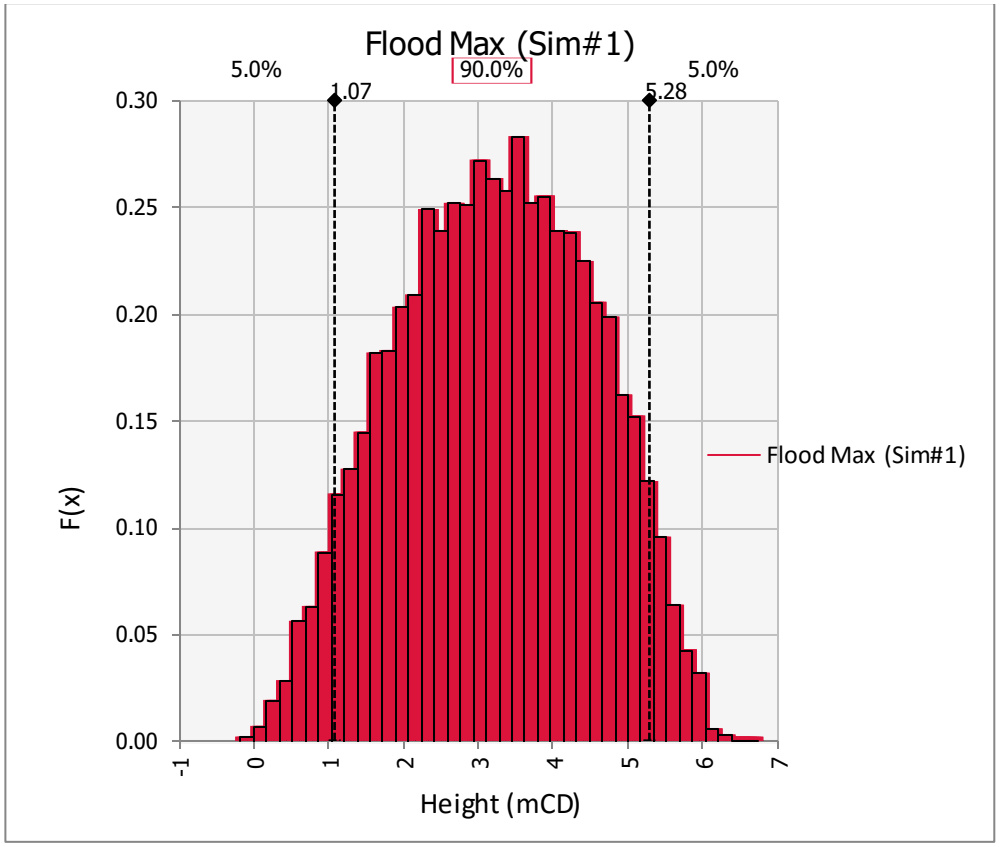

Figure 5.56 Monte Carlo simulation to produce inundation levels for Newlyn based on the input PDFs from Figures 4.47 and Figures 4.48.

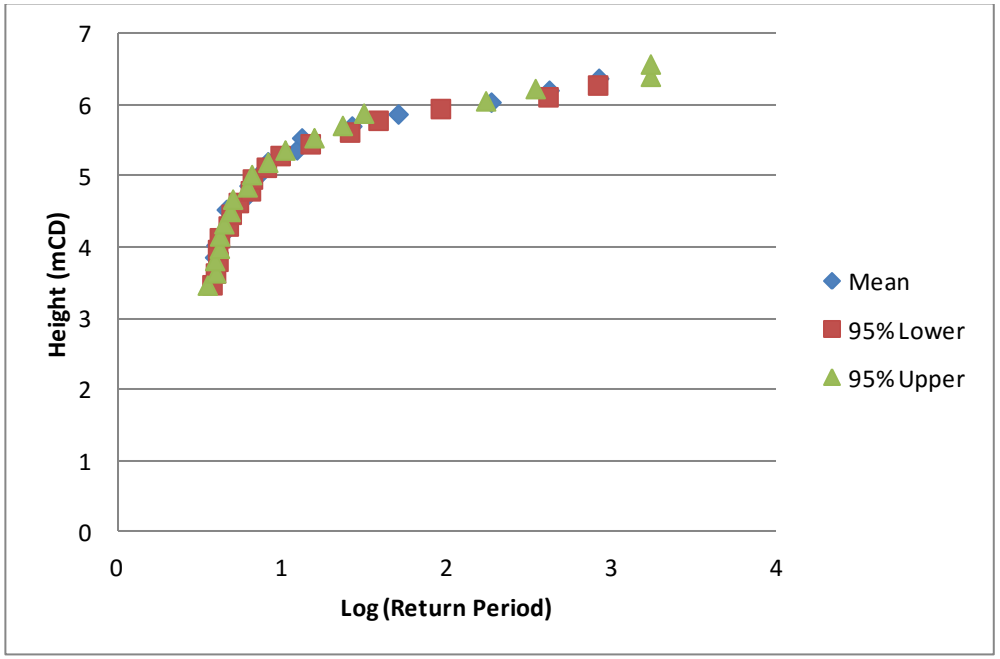

Figure 5.57 Return Level plot of Log (Return period) vs inundation level for Newlyn based on the output from the Monte Carlo simulation in Figure 5.49.

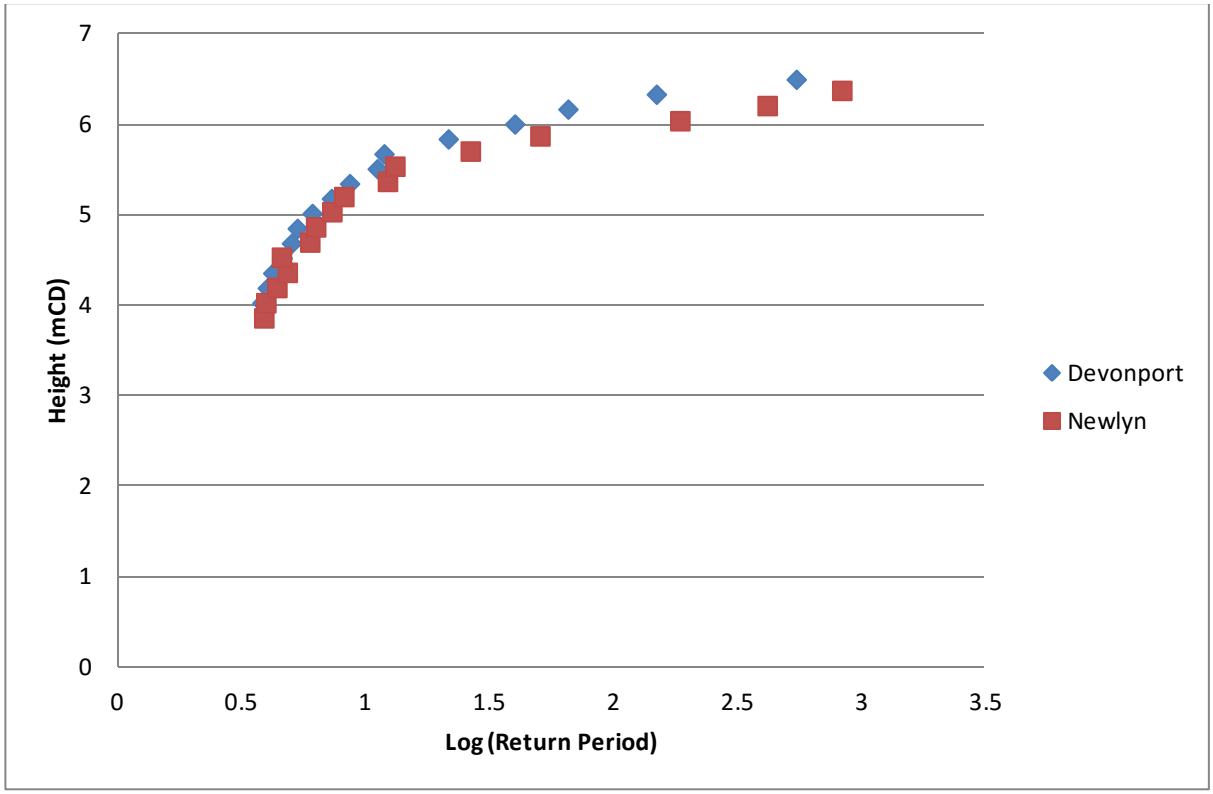

Figure 5.58 Comparison between the Monte Carlo Predictions for Devonport and Newlyn.

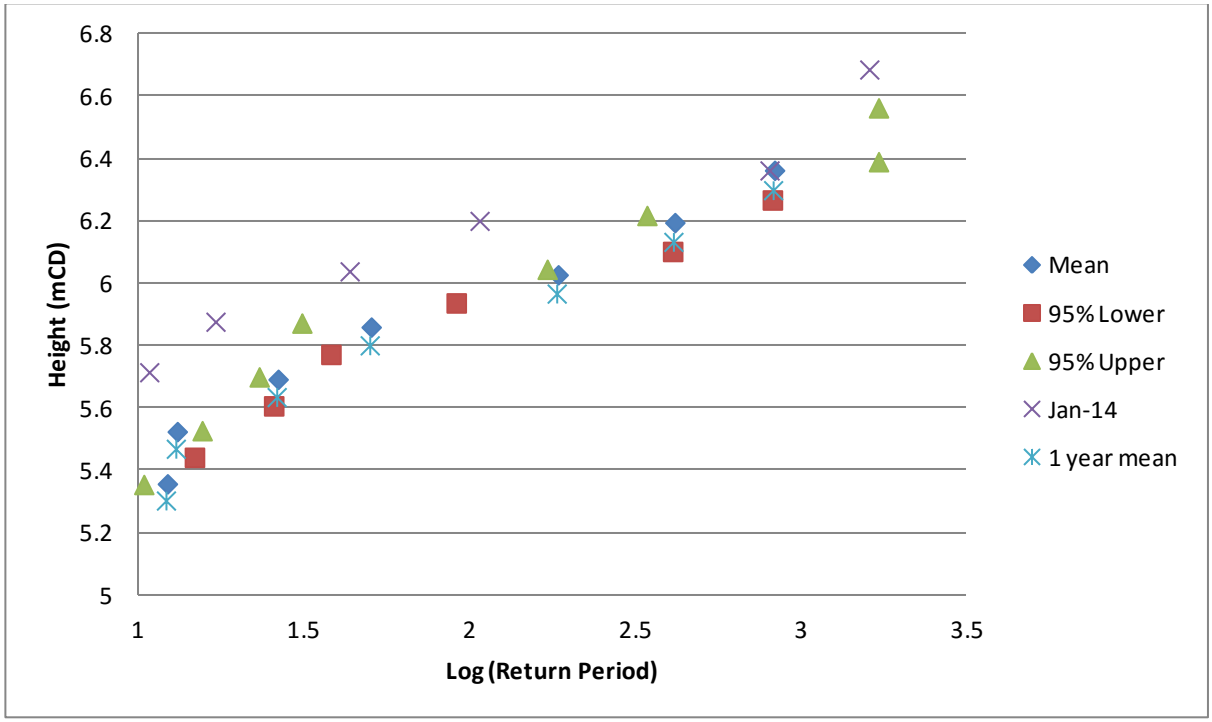

Figure 5.59 Comparison between the Monte Carlo Predictions for Newlyn for the complete data set, for one year of the data set and one month of data (January 2014) and Newlyn. N.B. The January 2014 output is discussed in Chapter 7.

5.4.5 Statistical Analysis Comparison

In total five different statistical techniques have been utilised to evaluate the frequency- magnitude relationship of both the observed levels and the storm surge levels. These statistical techniques utilise the data in different ways, from considering only the annual maximum, to considering the ten largest annual events, to utilising the complete hourly data.

Table 5.17 and 5.18, Figure 5.60 and 5.61 show the results for all statistical techniques compared to the raw data. The raw data has been converted to a probability based on formula 4.6 (P=M/(N+1)). As the analysis of the storm surge data does not represent an overall inundation level, the data has been combined with; firstly, a Mean High Water Spring (MHWS) tide and, secondly a 1 in 1 year tide, calculated by averaging the 10 largest tides between the period 2012-2021.

The predictions made typically have an uncertainty range of 0.30 m for a 1 in 1000 year event, with an increase in uncertainty when utilising shorter data sets, up to 0.6 m for the GEV methodology when utilising a data set of only 20 years. These analyses indicate that there is a range in the predictions for Devonport of between 6.40 mCD and 7.0 mCD for a 1 in 100 year event, for a 1 in 1000 year event there is a range of between 6.45 mCD and 7.15 mCD at the 95% confidence limit. A similar range in the results can be seen for Newlyn (6.5 mCD and 7.2 mCD for a 1 in 1000 year event). Typically the methodology that utilises the observed annual maximum values gives the lowest magnitude, with the highest magnitude for those that utilise the complete data set (i.e. the Joint Probability and the Monte Carlo methods). Combining the storm surge with MHWS provides comparable results to the raw data, while combing the storm surge data with a 1 in 1 year tide is comparable to the predictions made using the Joint Probability and the Monte Carlo methods.

It is noted that when comparing the predictions made by the GEV, r-largest and GPD to the raw data that, at the higher return periods the raw data drifts from the mean and is modelled more closely by the upper 95% confidence limit. When analysing just the storm surge component, the three different methods used to analyse the data (GEV, r-largest, GPD), evaluate the same magnitude-frequency relationship and provide a good approximation to the raw data with a range of +/- 0.05 m for a 1 in 50 year event for all statistical techniques (Figure 5.62).

	Statistical Technique Height (mCD)										
Return Period	GEV AM	GEV SSM[1]	r-Largest AM	r-Largest SSM[1]	r-Largest SSM[2]	GPD AM	GPD SS[1]	Joint Probability	Monte Carlo	Raw Data	Range (m)
10	6.33	6.5	6.35	6.4	6.8	6.28	6.4	6.7	6.50	6.45	0.5
25	6.37	6.6	6.40	6.5	6.9	6.32	6.5	6.75	6.55	-	0.6
50	6.39	6.65	6.44	6.55	6.95	6.36	6.55	6.8	6.65	-	0.6
100	6.41	6.65	6.48	6.6	7.0	6.39	6.6	6.9	6.8	6.55	0.6
250	6.42	6.7	6.54	6.7	7.1	6.42	6.7	6.95	6.95	-	0.7
500	6.43	6.7	6.57	6.75	7.15	6.43	6.75	7.0	7.05	-	0.7
1000	6.44	6.75	6.59	6.8	7.2	6.45	6.8	7.1	7.15	6.65	0.75

Table 5.17 Comparison of results for the various statistical techniques for Devonport 1962-2012. All results based on upper 95% confidence interval. [1] Storm surge prediction added to Mean High Water Springs astronomical tide. [2] Storm surge prediction added to average of ten highest tides over the next ten years.

	Statistical Technique (Height (mCD))										
Return Period	GEV AM	GEV SSM[1]	r-Largest AM	r-Largest SSM[1]	r-Largest SSM[2]	GPD AM	GPD SS[1]	Joint Probability	Monte Carlo	Raw Data	Range (m)
10	6.27	6.33	6.28	6.33	6.73	6.25	6.33	6.6	6.45	6.25	0.5
25	6.26	6.44	6.34	6.45	6.85	6.31	6.43	6.65	6.60	-	0.55
50	6.43	6.52	6.39	6.53	6.93	6.36	6.5	6.7	6.70	-	0.6
100	6.49	6.59	6.45	6.6	7	6.40	6.56	6.75	6.80	6.45	0.6
250	6.57	6.68	6.53	6.7	7.1	6.44	6.63	6.8	6.90	-	0.65
500	6.62	6.74	6.58	6.76	7.16	6.47	6.68	6.9	7.00	-	0.7
1000	6.67	6.81	6.63	6.83	7.23	6.49	6.73	6.95	7.10	6.60	0.75

Table 5.18 Comparison of results for the various statistical techniques for Newlyn 1915-2012. All results based on upper 95% confidence interval. [1] Storm surge prediction added to Mean High Water Springs astronomical tide. [2] Storm surge prediction added to average of ten highest tides over the next ten years.

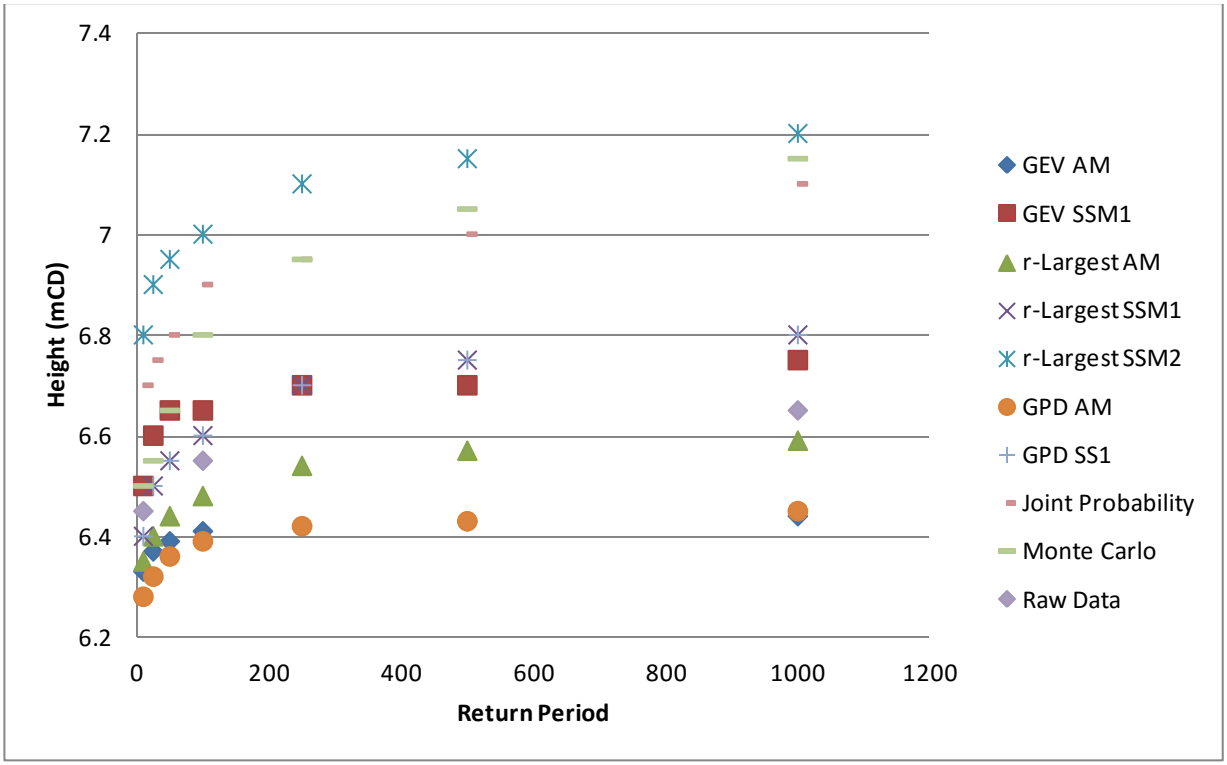

Figure 5.60 Comparison of the different statistical predictions for Devonport. (GEV AM-Generalised Extreme Value Distribution Annual Maximum, GEV SS-Generalised Extreme Value Distribution storm surge, R AM-r-largest Annual Maximum, R SS r-largest storm surge maximum, JP-Joint Probability, MC-Monte Carlo Maximum predictions).

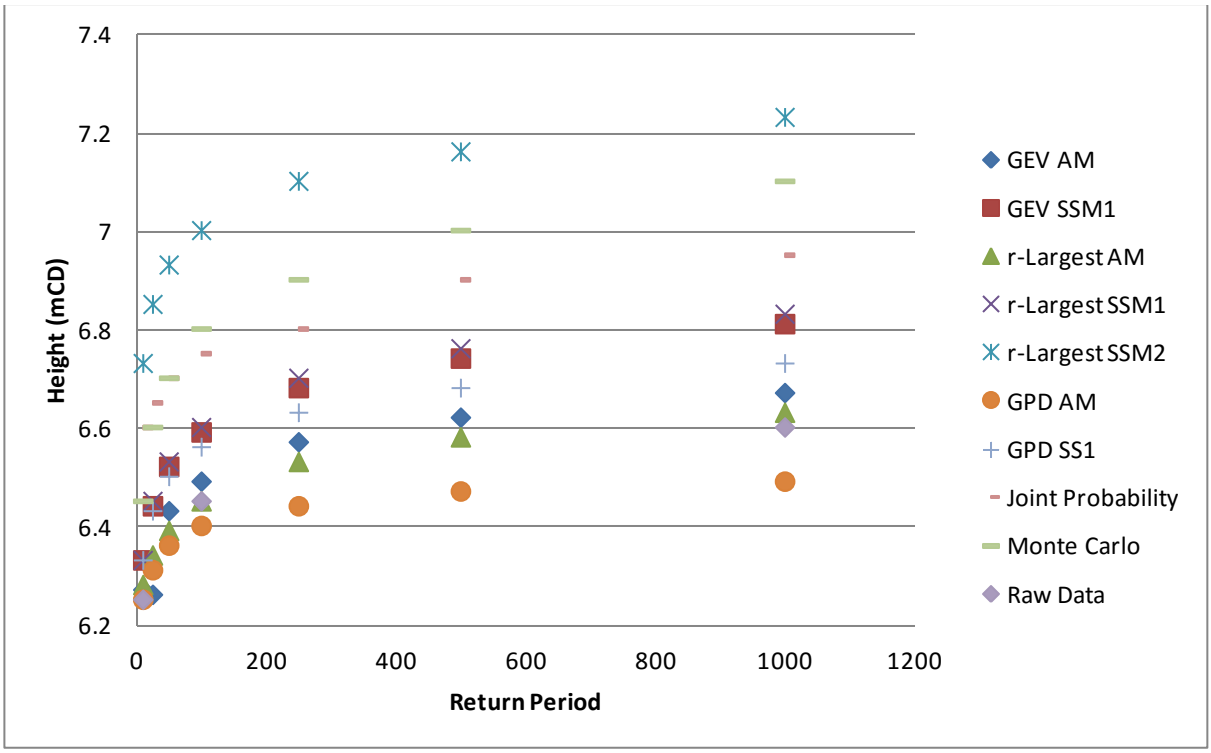

Figure 5.61 Comparison of the different statistical predictions for Devonport. (GEV AM-Generalised Extreme Value Distribution Annual Maximum, R AM-r-largest Annual Maximum, JP-Joint Probability, MC-Monte Carlo, MC Positive-Monte carlo simulation using only positive storm surge values).

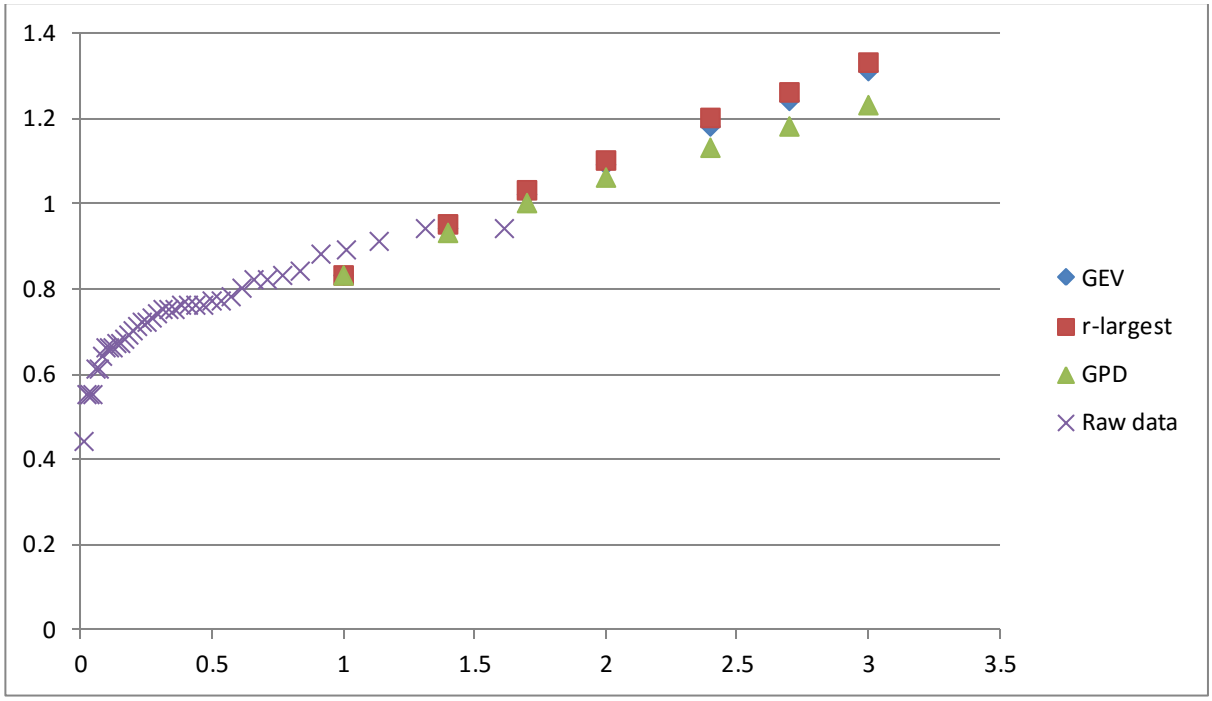

Figure 5.62 Comparison of the different statistical predictions for the storm surge component for Devonport.

5.4.6 Weather Data

The same approach was adopted to evaluate the wind data from Mount Batten, Plymouth as that utilised for observed sea levels and storm surge data. The statistical methods adopted for evaluating wind speed included the Generalised Extreme Value (GEV), r-largest and Monte Carlo analysis. The results of these analyses are given in Table 5.19, Table 5.20 and Figures 5.63 to 5.67. The GEV methodology evaluates a wind speed of 33.7 knots at a 1 in 10 year event, for a 1 in 1000 year event the prediction is 40.2 knots with a maximum uncertainty range 16.8 knots. The r-largest evaluates a 1 in 10 year event at 33.0 knots and a 1 in 1000 year event at 39.0 m with a maximum uncertainty range of 9 knots. Compared to the other methods the Monte Carlo analysis significantly underestimates the mean wind speed, for a 1 in 10 year event the mean wind speed is 8.5 knots and for a 1 in 1000 year event is 29 knots.

The GEV and r-largest methods both approximate the Weibull distribution for these data, with no upper limit reached. However, both methods struggle to adequately fit the mid-order return periods (5-20 years). The GEV copes well with the lower order data, where r-largest does not model the data as well, but both models predict the upper return period well. A comparison between the empirical data and the model data shows that the GEV methodology provides the better fit to the data. However for both methods the Probability Density Function (PDF) fails to take in to account the increased frequency of events at the high values of wind speed (34-36 knots) and as such over-estimates the probabilities of wind speeds between 30 and 34 knots (Figures 5.56 to 5.57). From a visual review of Tables 5.19 and 5.20, it can be seen that there is good agreement in the predictions made for the mean wind speed for all return periods between the GEV and r-largest. However, the GEV has much greater confidence intervals and as such the upper bound 95% confidence interval is significantly higher when compared to the r-largest; as much as 8 knots at the 1 in 1000 return period.

The results of fitting a Monte Data set to the daily mean wind speed are shown graphically in Figure 5.64 and numerically in table 5.20. The wind speed data are skewed towards the lower wind speeds and fits both an inverse Gaussian and a Pearson PDF. A comparison between the return periods calculated from the Monte Carlo PDFs and the r-largest shows the Monte Carlo significantly underestimates the wind speed for all return periods (table 5.19 and 5.20).

	Speed (Knots)		
Return Period	95% Lower	Middle	95% Upper
10	32.3	33.7	36.0
25	33.8	35.4	39.0
50	34,6	36.5	41.6
100	35.1	37.6	44.2
250	35.6	38.7	47.6
500	35.9	39.5	50.2
1000	36.0	40.2	52.8

Table 5.19 Results of GEV analysis for Plymouth wind speed data for the period 1969-2008.

	Speed (Knots)			
Return Period	95% Lower	Middle	95% Upper	Monte Carlo
10	32.0	33.0	34.0	8.5
25	-	34.0	35.0	14.5
50	32.5	35.0	36.5	18.5
100	33	36.0	38.0	21.0
250	34	37	40.0	24.5
500	34.5	38.5	42.0	27.0
1000	35	39	44.0	29.0

Table 5.20 Results of r-largest and Monte Carlo analysis for Plymouth wind speed data for the period 1969-2008.

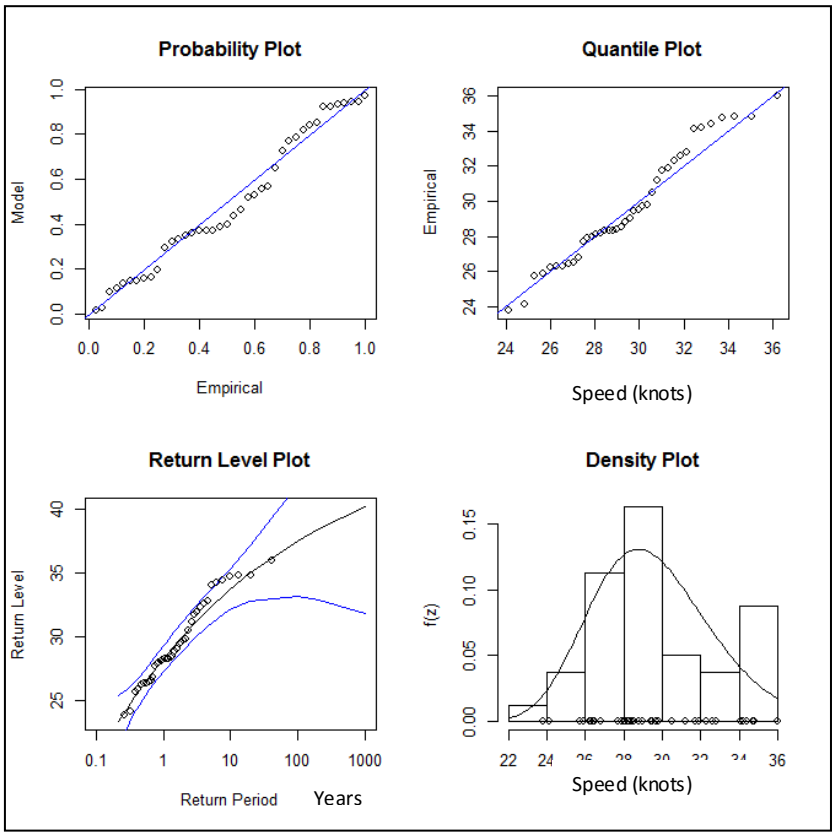

Figure 5.63 Generalised Extreme Value Distribution return level and diagnostic plots for Plymouth Annual Observed wind speed based on daily mean for the period 1969-2008.

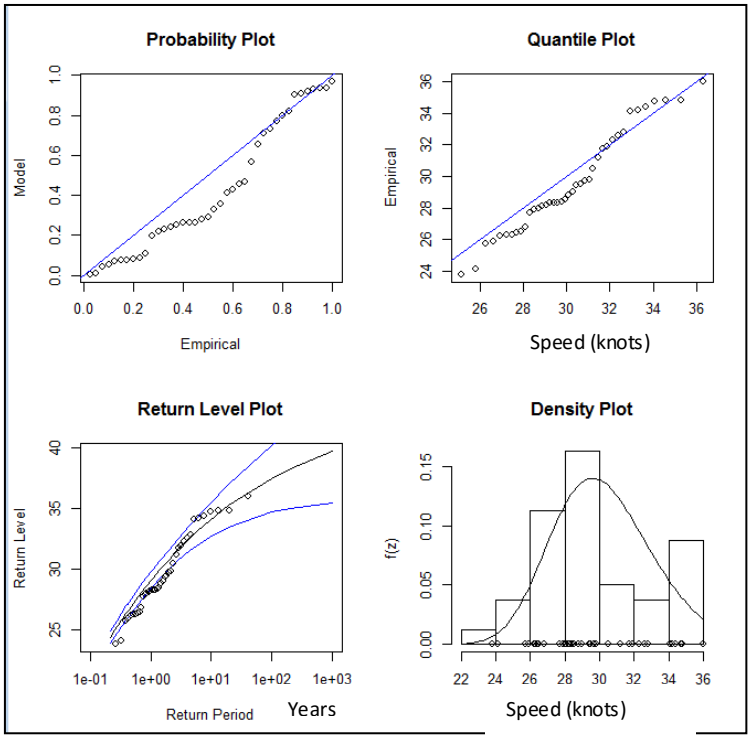

Figure 5.64 r-largest return level and diagnostic plots for Plymouth Annual Observed wind speed based on daily mean for the period 1969-2008.

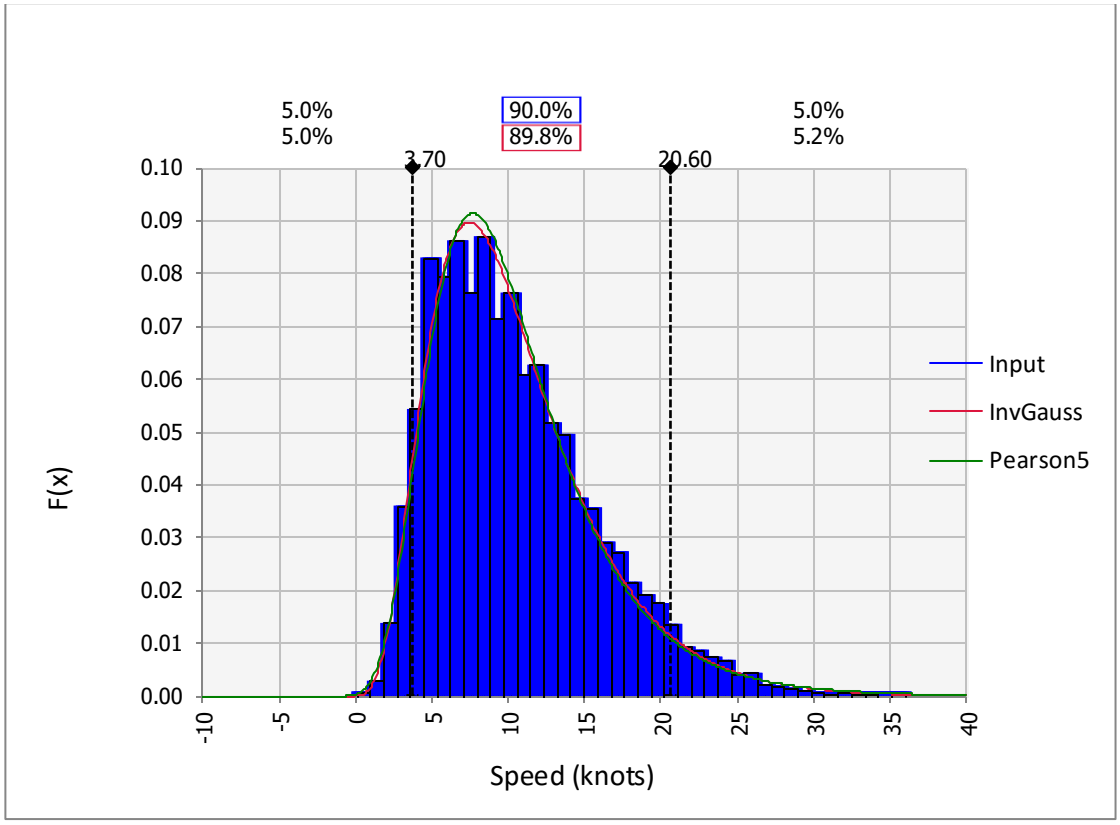

Figure 5.65 Comparison between input daily mean wind speed data for Plymouth 1969-2008 and two Probability Density Functions modelled in @risk.

5.4.7 Wave Data

Due to the limited number of years of wave data (7 years) it is not possible to undertake an analysis using all statistical techniques. The results of the r-largest and Monte Carlo analysis are shown in Figure 5.66, 5.67 and Table 5.21. Due to the limited amount of data the r-largest fails to fully resolve the magnitude-frequency relationship, with a peak in the Weibull distribution reached at the maximum wave height observed of 10 m. There is a difference of only 0.1 m between a 1 in 10 year event and a 1 in 1000 year event (table 5.21). The modelling of the data to different PDFs within a Monte Carlo modelling software are shown in Figure 5.67. However, the Monte Carlo method significantly underestimates the frequency-magnitude relationship (table 5.21, Figure 5.68). For a 1 in 1000 year event the Monte Carlo PDFs give a value of 10.5 m, this is close to the maximum wave height observed over a 7 year period.

In addition to the statistical analysis of wave height magnitude-frequency relationships, an analysis has been undertaken to evaluate the coincidence of wave height and storm surges. This was undertaken by plotting all positive surge heights against the coincidence wave height (Figure 5.69), and plotting the coincident wave height for all independent storm surges >0.4 m (Figure 5.70). There is no direct correlation between storm surge and wave height, with a wave height of 9.5 m coinciding with a 0.4 m storm surge and a 6 m wave coinciding with a 0.8 m storm surge. However, from the data it is possible to infer “average” conditions of the coincidence of a specific wave occurring for a given storm surge height. This is illustrated as a straight line on Figures 5.69 and 5.70.

	Height (m)			
Return Period	95% Lower	Middle	95% Upper	Monte carlo
10	-	9.9	-	3.8
25	-	-	-	5.0
50	-	-	-	6.0
100	9.9	9.9	10.0	7.0
250	-	-	-	8.5
500	-	-	-	9.5
1000	10.0	10.0	10.0	10.5

Table 5.21 Results of r-largest and Monte Carlo analysis for Polperro wave height data for the period 2006-2012.

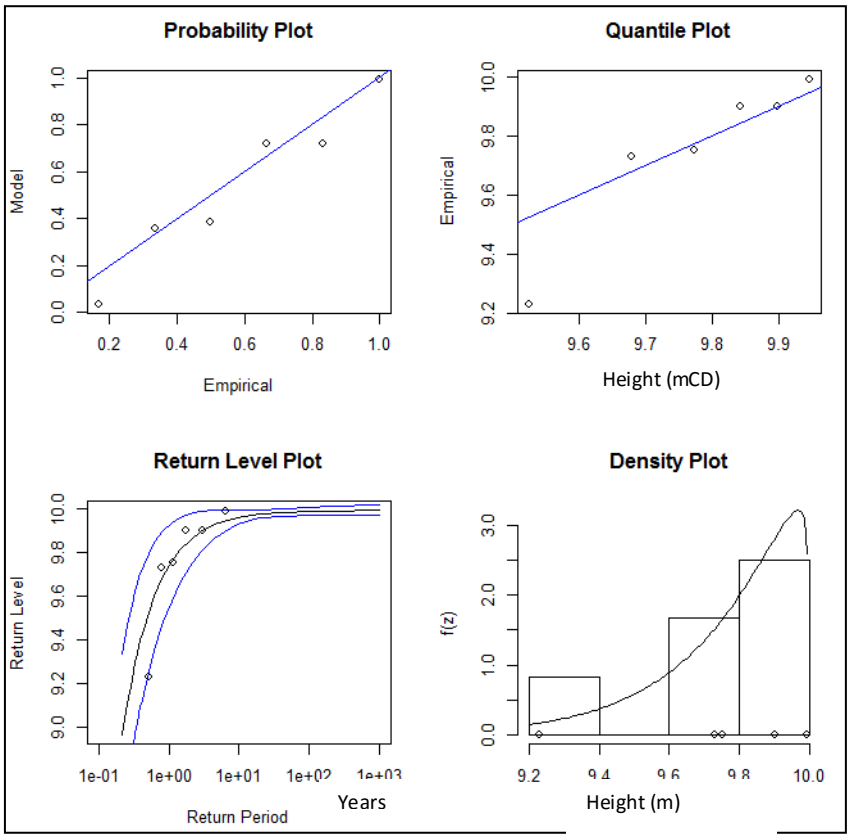

Figure 5.66 r-largest return level and diagnostic plots for Polperro wave data 2006-2012.

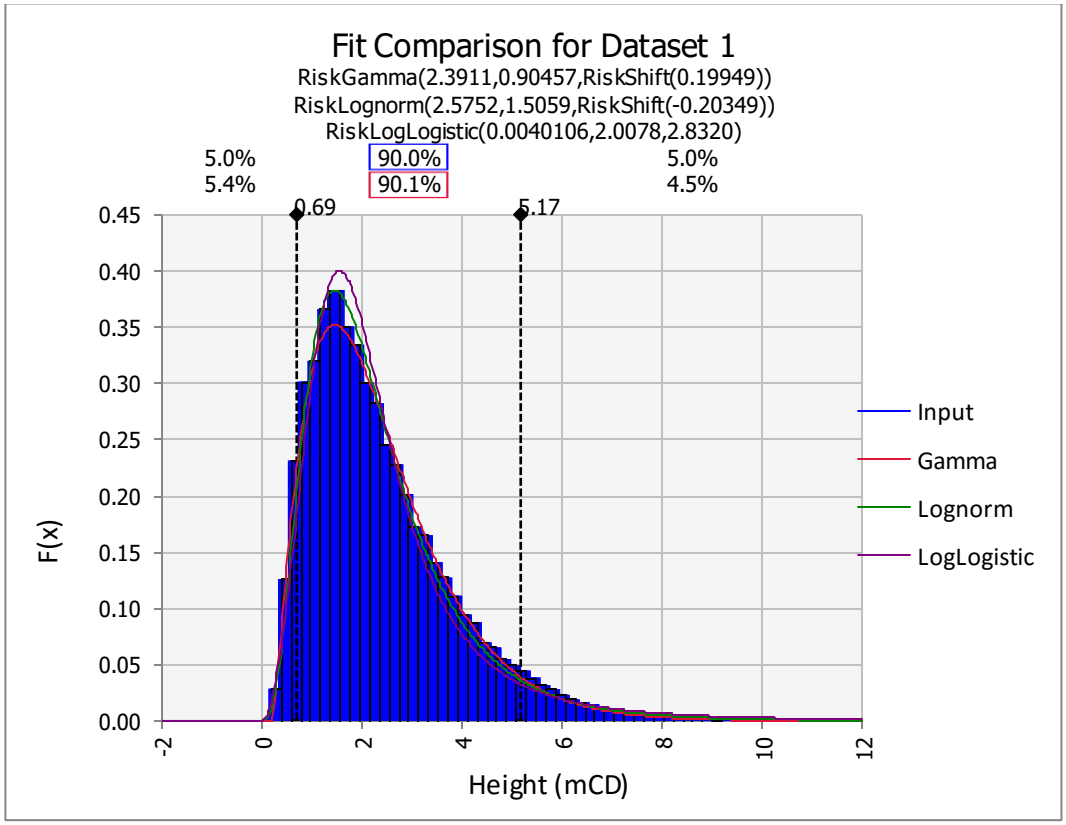

Figure 5.67 Comparison between input wave data for Polperro 2006-2012 and three Probability Density Functions modelled in @risk.

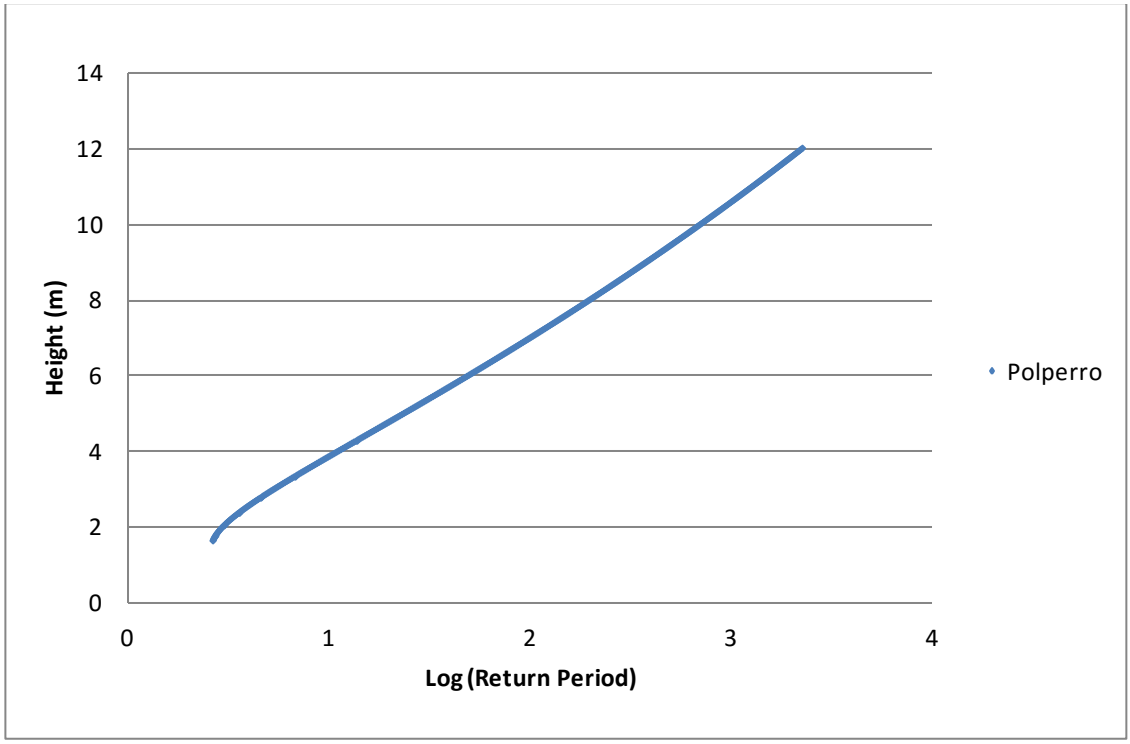

Figure 5.68 Monte Carlo Analysis output in the form of a return level plot for wave height at Polperro 2006-2012.

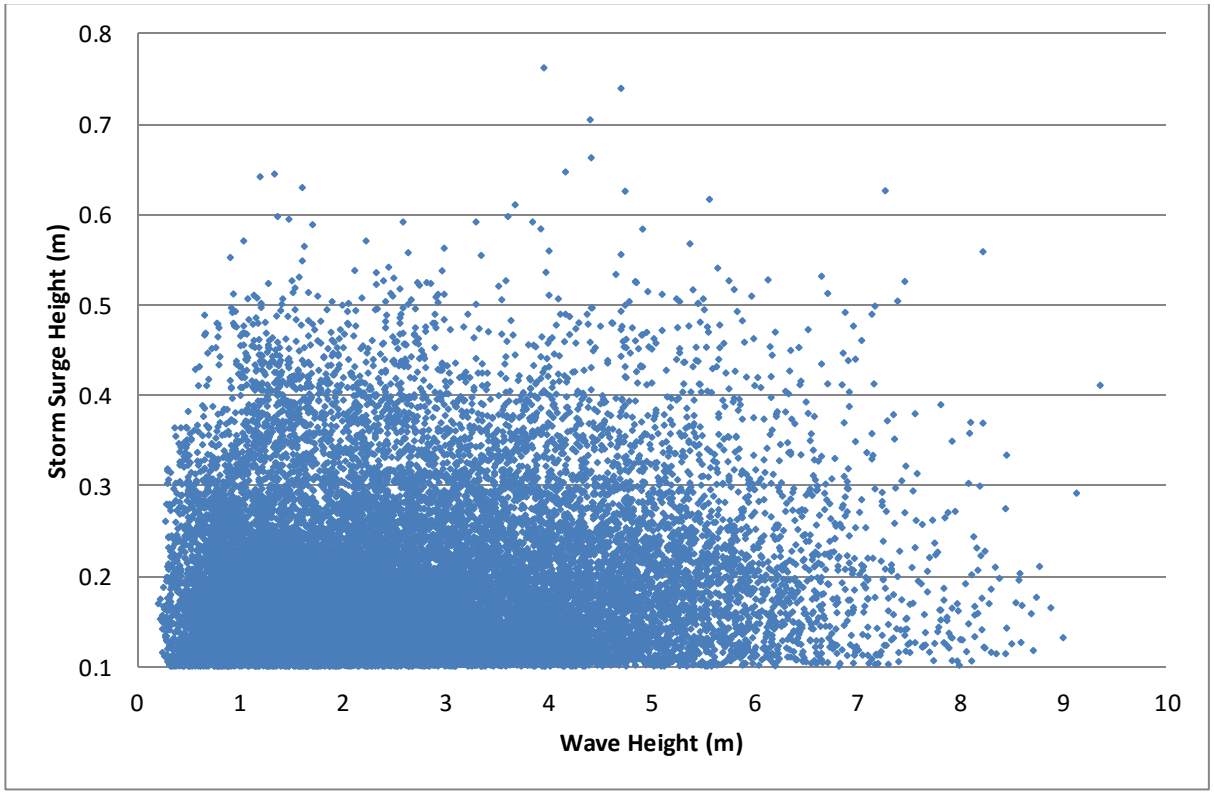

Figure 5.69 Plot of coincidence of storm surges and wave height.

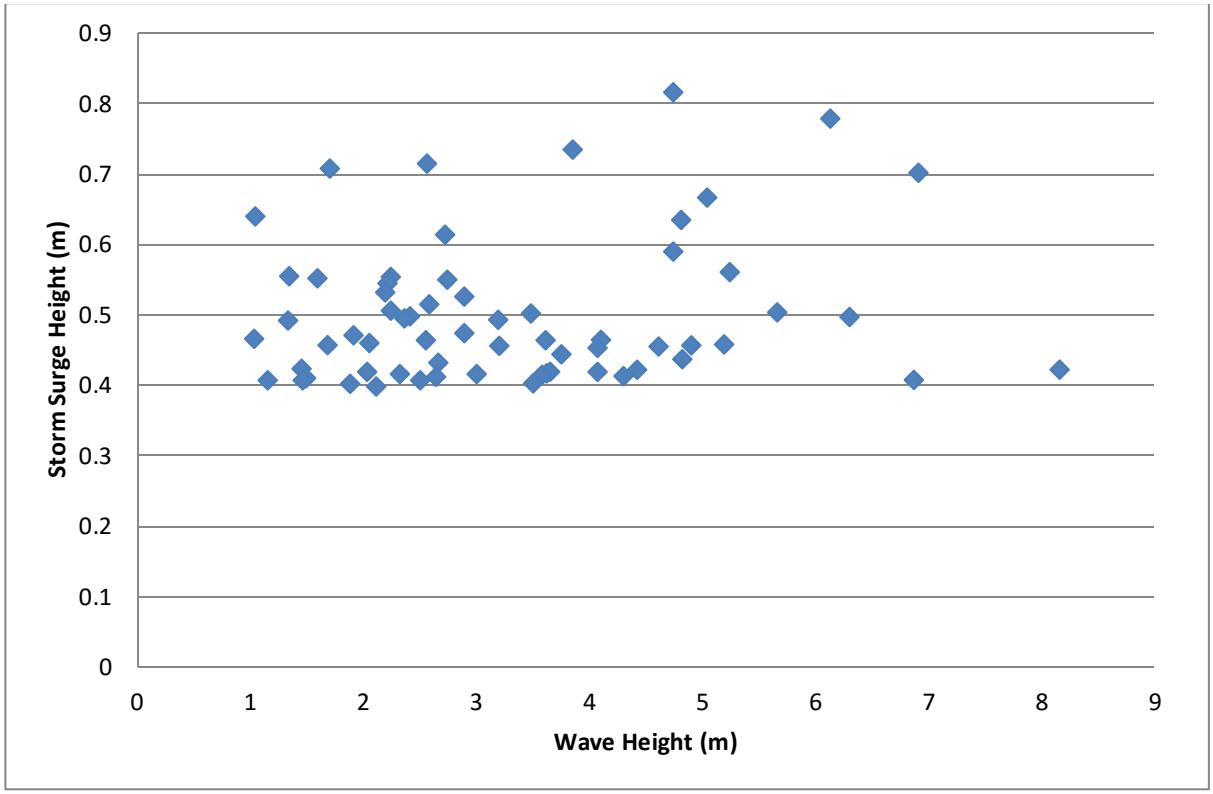

Figure 5.70 Plot of independent storm surges events >0.4 m and coincident wave height at Polperro .

5.4.8 Tsunami Modelling

As described in Section 4.7, in conjunction with Imperial College London (Per Comm. Jon Hill) a finite difference tsunami model of the 1755 Lisbon earthquake was created based on the source parameters of Horburgh et al., (2008), with an improved spatial resolution. 56 receptors were placed only the coast line of the study area to record the wave amplitude. The model identified that the maximum wave amplitude along the study area would be 1 m, from peak to trough, commensurate with the predictions made by Horburgh et al., (2008). However, no amplification due to the shape and bathymetry of the coastline was identified. It is felt that the resolution of the model is sill insufficient to resolve the shape of the coastline and the bathymetry. Therefore at present it is not possible to resolve the difference in magnitude between historical observations and present day modelling of the 1775 tsunami. Therefore, within this research no specific modelling of a tsunami event will be undertaken, however, due to the magnitude of the predictions for storm surges and wave set up, the magnitude of a tsunami event will be covered by the GIS modelling of inundation from storm surges and waves.

5.5 Summary

Chapter 5 presented the results of the observed trends including sea-level rise and storminess based on the observed tidal gauge records from Devonport and Newlyn; the results from the evaluation of frequency magnitude relation of inundation levels from five different statistical techniques and the evaluation of wind and wave frequency magnitude relationships.

The Chapter has identified a sea-level rise of 2.1 mm/yr +/- 0.3 (95%) and 1.8 mm/yr +/- 0.2 (95%) for Devonport and Newlyn respectively. An acceleration component equivalent to between 0.001 to 0.002 mm/yr^2. The observed increase in frequency of storm surges can be attributed to the increase in mean sea level, with an increase and decrease in rates of sea-level rise and storminess linked to the North Atlantic Oscillation. The different statistical techniques have identified different frequency-magnitude relationships dependant on the choice of techniques. Those that utilise a sample of the hourly tide gauge records (i.e. the GEV utilises the annual maximum), provide a good representation of the raw historical data, where those techniques that utilise the complete hourly record (Joint Probability and Monte Carlo methods), over predict and can be considered a conservative “what if” methodology. The difference in predictions for inundation levels indicates a level of uncertainty to be as much as 0.8 m for a 1 in 1000 year event.

For wind speed, it was found that both the GEV and the r-largest effectively modelled the frequency-magnitude relationship. In comparison the Monte Carlo analysis significantly under predicted the frequency magnitude relationship. The Monte Carlo analysis also failed to evaluate the frequency magnitude relationship for wave height; however, due to the limited amount of data (7 years), the r-largest also failed to evaluate the relationship.

Chapter 6 Geographical Information System-Scenario Modelling

6.1 Introduction

Chapter 5 evaluated a range of inundation levels for the study area based on the different predictions made for storm surges. Chapter 6 develops a range of inundation scenarios based on the different predictions made for inundation scenarios and incorporating different sea-level predictions for the study area. In addition to the affect of these predictions for the study area, two case studies have been evaluated to incorporated wave height. For the first case study, Devonport Dockyard, Plymouth, (Section 6.2.2) the wave height was added to the inundation levels to evaluate the point at which the area would be overtopped . For the second study area, Looe, Cornwall, (Section 6.2.3) wave height was converted to wave set up, evaluating the affect of wave set up on inundation levels. These inundation scenarios are then modelled within a Geographical Information System (GIS). The methodology to create a GIS database, model the different inundation levels and evaluate the effects on the study area was described in Chapter 4 Section 4.7. The results for the GIS modelling of the whole study area are presented in Section 6.3. For case study 1, Devonport Dockyard, the results are presented in Section 6.4 and for case study 2, Looe, Cornwall, the results are presented in Section 6.5. Section 6.7 provides details of the GIS database contained within Appendix B, and how the reader can access the database and view the individual components.

6.2 Scenario Development

The aim of this section is to draw together the different statistical analyses, the different data sets and to develop a series of scenarios for the whole study area and two case studies. The different scenarios will then be analysed within a GIS presented in Sections 6.3 to 6.5 to evaluate the potential inundation on the coastline of south-west England and the sensitivity to different components of inundation.

6.2.1 Study Area

For the whole of the study area (Chapter 1) the aim was to evaluate the implications of different storm surge predictions and sea-level rise scenarios at three different points in time; the present day; 2050 and 2100. At each of the two return periods evaluated (1 in 250 and 1 in 1000), the lowest inundation level and the highest inundation level estimate has been assessed to evaluate the affect of uncertainty due to different frequency magnitude relationships. This equates to 6.4 mCD for a 1 in 250 year event based on the predictions made utilising the Generalised Pareto Distribution (GPD), compared to 6.9 mCD based on the prediction made for a 1 in 250 year event based on the Joint Probability and Monte Carlo methodology, giving an uncertainty of 0.50m at the 95% confidence limit. For a 1 in 1000 year event the uncertainty range is 0.7 m based on the difference between the GPD prediction (6.5 mCD) and the Joint Probability/Monte Carlo methodology (7.2 mCD). For an evaluation of the change in inundation levels over time, and to allow a comparison of the affect of uncertainty due to sea-level rise and the affect of frequency magnitude prediction, three sea-level rise scenarios have been modelled based on the predictions of the United Kingdom Climate Change Programme (UKCP, 2009). A low prediction of 0.3 m, a mid range prediction of 0.45 m, and high prediction of 0.78 m (up to 2100). For the time period, 2100 a further sea-level rise scenario named as H++ (1.8 m) in UKCP (2009), which defines a high magnitude but low probability sea-level rise, is also modelled. The H++ event can also be considered to model a “Dragon King” event, equivalent to approximately 2 times a 1 in 1000 storm surge event.

	Timescale					
Component	Present day		2050		2100	
	1:250	1:1000	1:250	1:1000	1:250	1:1000
Inundation Level	Low-6.40m CD (GPD) High-6.9mCD (JP/MC)	Low-6.5m CD (GPD) High-7.2mCD (JP/MC)	Low-6.40m CD (GPD) High-6.9mCD (JP/MC)	Low-6.5m CD (GPD) High-7.2mCD (JP/MC)	Low-6.40m CD (GPD) High-6.9mCD (JP/MC)	Low-6.5m CD (GPD) High-7.2mCD (JP/MC)
Wave Height	None	None	None	None	None	None
Dragon King Event	An Event equivalent to the H++ sea-level rise scenario is modelled to simulate the effect of a potential Dragon King. Equates to approximately 2 times a 1 in 1000 year event.					
Seal Level Rise	None	None	Low-0.15m Mid-0.23m High-0.40m	Low-0.15m Mid-0.23m High-0.40m	Low-0.30m Mid-0.46m High-0.78m H++ 1.8m	Low-0.30m Mid-0.46m High-0.78m H++ 1.8m

Table 6.1 The range of scenarios to be modelled within the GIS for the whole study area.

6.2.2 Case Study 1-Devonport Dockyard

Devonport Dockyard, Plymouth, was selected as a case study as it represents the most critical infrastructure within the study area. The input of the inundation levels and the sea-level rise scenarios remain the same as for the whole study area. In addition to these levels wave height is added to the scenarios to evaluate at what point the cope edge at Devonport Dockyard will be overtopped, leading to the potential flooding of nuclear installations.

To calculate wave height, the wind speed magnitude evaluated in Section 5.4.6 is converted from knots to m/s. As the Mount Batten (Plymouth) weather data only recorded the daily mean, a conversion factor to convert to “daily peak” of 1.75 is used based on the guidance of the World Meteorological Association (WMA, 2012). This process converts the frequency-magnitude relationship based on daily averages to “daily peak” wind speeds in m/s. To convert wind speed to wave height Figure 4.9 is used based on a maximum fetch of 1.5 km. The result of this process is shown in

Figure 6.2, which illustrates the relationships between wave height and return period based on the relationship between wind speed and wave height within a closed basin. It is assumed, partly due to the nature of the infrastructure and partly due to the likely underestimation of "peak daily" wind speed that the frequency of a specific wave will be coincident with a storm surge of the same frequency (i.e. a 1 in 100 wave will coincide with a 1 in 100 storm surge). Therefore a wave height of 0.25 m coincides with a 1 in 250 year storm surge and a 0.5 m wave height coincides with a 1 in 1000 year storm surge. A summary of the scenarios to be modelled for Devonport Dockyard to evaluate the point at which the facility is overtopped is given in Table 6.2.

	Timescale					
Component	Present day		2050		2100	
	1:250	1:1000	1:250	1:1000	1:250	1:1000
Storm Surge	Low-6.4 mCD High-6.9 mCD	Low-6.5 mCD High- 7.2 mCD	Low-6.4 mCD High-6.9mCD	Low-6.5 mCD High- 7.2 mCD	Low-6.4 mCD High-6.9mCD	Low-6.5 mCD High- 7.2 mCD
Wave Height (m)	0.25 m	0.5 m	0.25 m	0.5 m	0.25 m	0.5 m
Sea-level Rise	None	None	Low-0.15 m Mid-0.23 m High-0.40 m	Low-0.15 m Mid-0.23 m High-0.40 m	Low-0.30 m Mid-0.46 m High-0.78 m H++ 1.8 m	Low-0.30 m Mid-0.46 m High-0.78 m H++ 1.8 m

Table 6.2 The range of scenarios to be modelled within the GIS for Devonport Dockyard, Plymouth.

6.2.3 Case Study 2-Looe, Cornwall

Looe, Cornwall has been chosen to evaluate the effect of wave set up (Section 2.5) on the coastal environment. Looe, provides several components of interest; firstly it has been in the news due to the damage caused by the January/February 2014 storms (BBC, 2014), secondly the author was present during a flooding event on the 4th February (Chapter 1), and finally there are several components of vulnerability

including a coastal road, and a local town, and, finally it represents an example within the study area that is not dominated by a steep cliff line.

For Looe the input of the inundation levels and the sea-level rise scenarios remain the same as for the whole study area and Devonport Dockyard. In addition to these levels wave set up is added on to the scenarios to evaluate its effect on the overall inundation levels. Wave setup is calculated based on the examples given by Reeve et al., (2012) and the wave height frequency-magnitude evaluation undertaken in Section 5.4.7. The resultant wave set up against return period is given in Figure 6.3. To incorporate wave set up in the inundation and sea-level rise scenarios it is assumed that the frequency of wave set up that occurs with an inundation level is an order of frequency less (i.e. a wave set up with a return period of 1 in 10 years occurs during an inundation of 1 in 100 years). Therefore a wave height of 0.25 m coincides with a 1 in 250 year storm surge and a 0.5 m wave height coincides with a 1 in 1000 year storm surge. A summary of the scenarios to be modelled for Looe is given in Table 6.3.

	Timescale					
Component	Present day		2050		2100	
	1:250	1:1000	1:250	1:1000	1:250	1:1000
Storm Surge	Low-.4 mCD High- 6.9 mCD	Low-6.5 mCD High- 7.2 mCD	Low-6.4 mCD High-6.9mCD	Low-6.5 mCD High- 7.2 mCD	Low-6.4 mCD High- 6.9 mCD	Low-6.5 mCD High- 7.2 mCD
Wave set up	0.5 m	2.5 m	0.5 m	2.5 m	0.5 m	2.5 m
Seal Level Rise	None	None	Low-0.15 m Mid-0.23 m High-0.40 m	Low-0.15 m Mid-0.23 m High-0.40 m	Low-0.30 m Mid-0.46 m High-0.78 m H++ 1.8 m	Low-0.30 m Mid-0.46 m High-0.78 m H++ 1.8 m

Table 6.3 The range of scenarios to be modelled within the GIS for Looe, Cornwall.

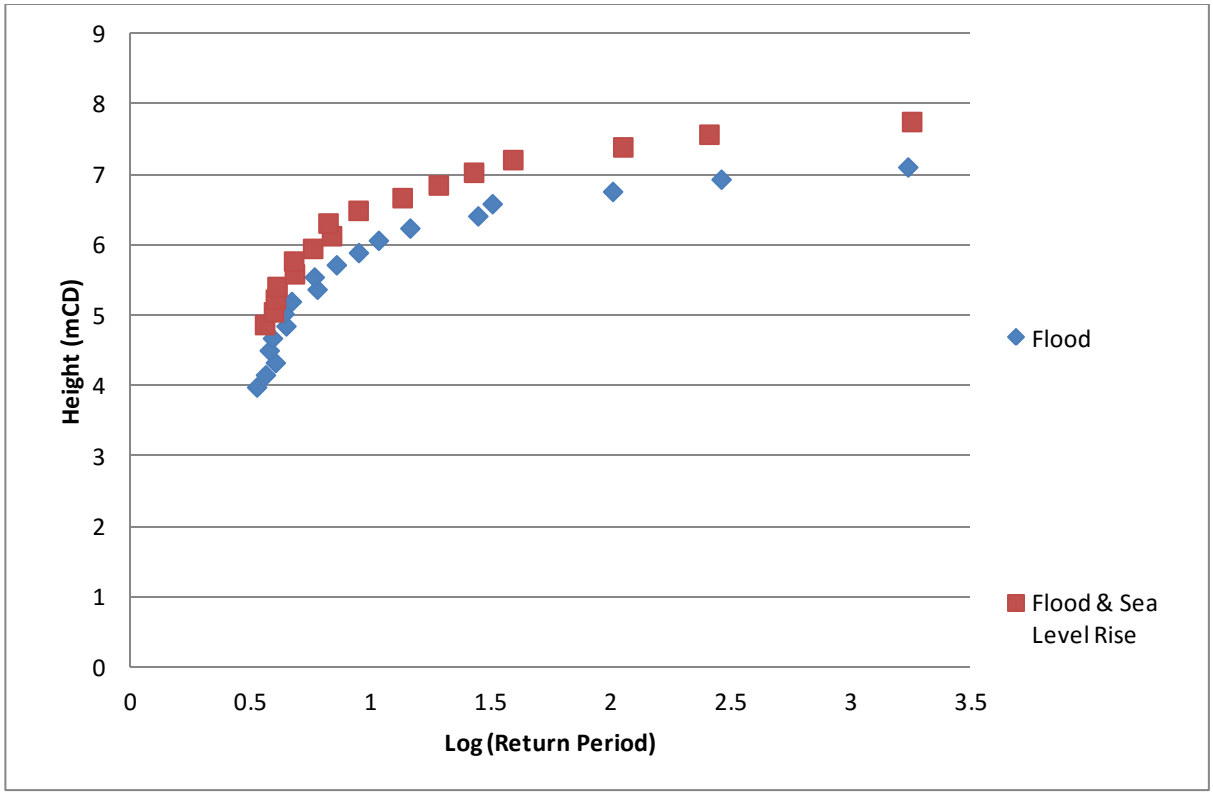

Figure 6.1 Monte Carlo Simulation return level plot combining storm surge, sea-level rise and waves PDFs in a variety of combinations.

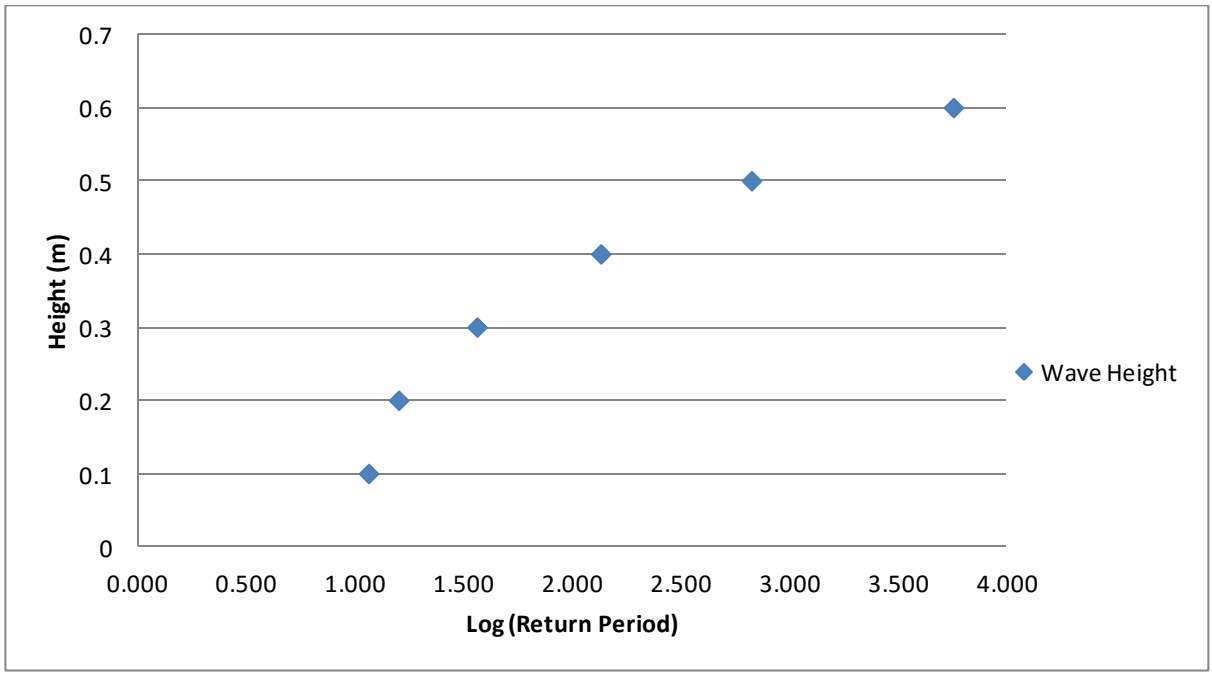

Figure 6.2 Wave Height vs return period for Devonport Dockyard based on converting the wind speed data for Plymouth (Figure 5.53-5.55) to wave height in a closed basin using Figure 4.9.

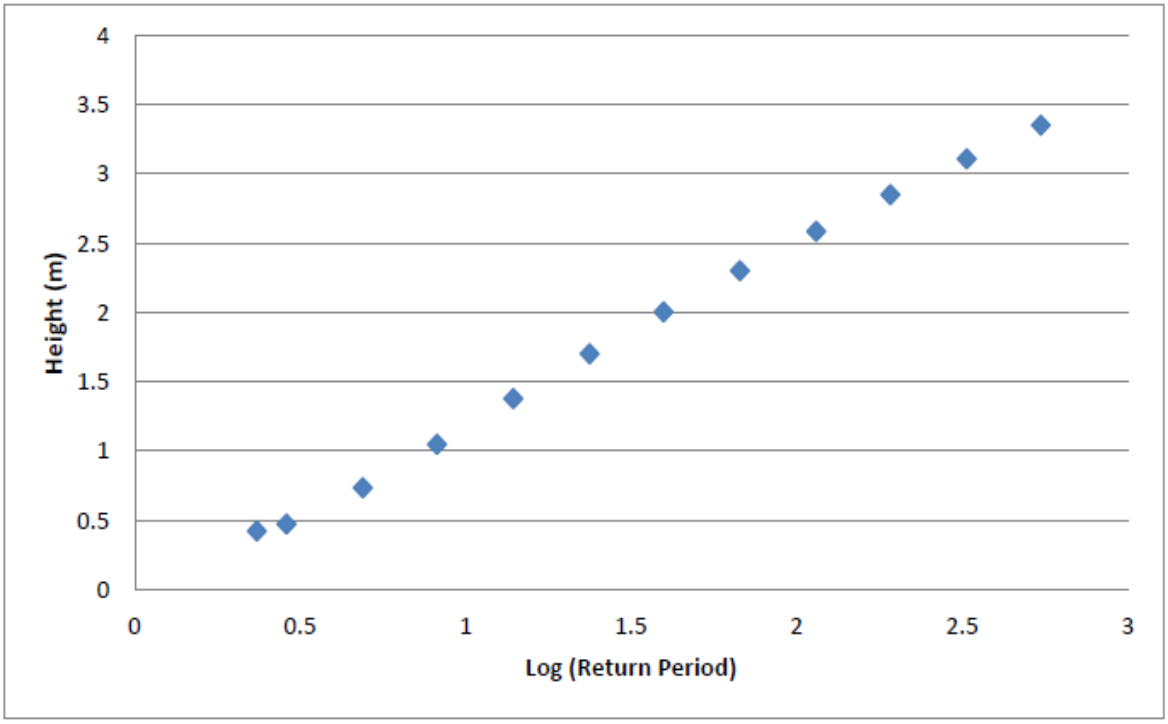

Figure 6.3 Calculation of wave set up based on Figure 5.58 and the example calculations of Reeve et al., (2012).

6.3 Study Area

The full study area (Chapter 1) stretches from Plymouth, Devon, the location of the Devonport tide gauge and the Mt Batten Weather station, to Penzance, Cornwall, the location of the Newlyn tide gauge. For this stretch of coastline LiDAR Digital Elevation Model (DEM) was acquired from Channel Coast Observatory (Channel Coast, 2013) and imported in to ARCGIS as detailed in Section 4.7. The DEM for the whole of the study area is shown in Figure 6.4. Infrastructure was acquired from Edina Digimap (Edina, 2013) and overlain on to the DEM within ARCGIS as detailed in Section 4.7. The infrastructure data for the whole of the study area is illustrated in Figure 6.5. Due to the resolution of the infrastructure data it covers a greater area than the DEM. Inundation levels have been generated by creating a polygon between 0 mCD and the specific flood inundation level (i.e. 6.4 mCD for a 1 in 250 year event). This polygon represents the area that would be affected by a specific event (Section 4.7.4). Due to the resolution of the data sets and generated inundation levels it is not possible to visually represent the levels at a scale covering the whole study area. This is illustrated in Figures 6.6 and 6.7, which show the inundation levels for the Plym and Tamar estuaries and just the Tamar estuary, respectively. From Figure 6.6 it is not possible to see the affect of all inundation levels due to the scale of the image however, when zoomed in to view at a higher resolution the different inundation levels can be more easily resolved (Figure 6.7). In total 23 inundation levels between 6.4 mCD and 9.0 mCD were modelled in ARCGIS. Due to the relatively small difference between the individual scenarios (0.1 to 0.2 m), and the topography of the study area, it was found that between the individual scenarios there was little change. Therefore, within Figures 6.6 to 6.14 only inundation scenarios 6.4 mCD, 7.2 mCD, 8.0 mCD and 9.0 mCD have been represented. The four different inundation levels represent:

- 6.4 mCD corresponds to the lowest prediction for a 1 in 250 inundation level.
- 7.2 mCD corresponds to the following:
    - highest prediction for a 1 in 1000 inundation level.
    - The lowest prediction for a 1 in 250 year event and a 0.8m allowance for sea-level rise.
    - The highest prediction for a 1 in 250 year event and a 0.4m allowance for sea-level rise.

    - Corresponds closely to the lowest prediction of a 1 in 1000 inundation level with a mid range sea-level rise.
- A level of 8.0 mCD corresponds to the highest prediction for a 1 in 1000 inundation level with a high range of sea-level rise and corresponds closely with the lowest prediction for a 1 in 1000 inundation level with a H++ sea-level rise.
- A level of 9.0 mCD corresponds to the highest prediction for a 1 in 1000 inundation level with a H++ sea-level rise i.e. the worst case scenario and models the potential effect of a “Dragon King” event.

To enable visual representation and comparison of the different inundation levels, the figures have been created to show the inundation level that flooded an area first. This means it is possible to evaluate which scenario flooded an area first. For example if the area in Figures 6.6 to 6.14 is red, it means the area was not flooded by a 6.4 mCD level (blue) but was flooded by a 7.2 mCD level (red). Figures 6.6 to 6.14 represent snapshots of the whole study area and have been identified as locations that are affected by the uncertainty within both sea-level rise and frequency magnitude predictions.

To provide a comparison between the inundation models the total area of land and buildings affected by the four different scenarios has been evaluated. This process is illustrated in Figures 6.15 to 6.20 which highlights the intersection between the infrastructure layers of land, buildings and roads with the inundation level of the 9.0 mCD scenario. The calculated values for the four inundation levels are given in Table 6.4.

- A 6.4 mCD scenario effects 8.6 km^2 of land and 0.2 km^2 of buildings.
- A 7.2 mCD scenario effects 13.0 km^2 of land and 0.4 km^2 of buildings. An increase of 50% and 100% respectively.
- An 8.0 mCD scenario effects 17.1 km^2 of land and 0.7 km^2 of buildings. An increase of 100% and 250% respectively when compared to a 6.4 mCD scenario.
- A 9.0 mCD scenario effects 21.1 km^2 of land and 1.1 km^2 of buildings. An increase of 145% and 450% respectively when compared to a 6.4 mCD scenario.

When considering the affect of different prediction methodologies and sea-level rise the following was identified:

- The different predictions for a 1 in 250 year event ranged between 6.4 mCD and 6.9 mCD. The difference between the two scenarios gives an 80% increase in the area of buildings affected and a 40% increase in the area of land affected.
- The different predictions for a 1 in 1000 year event ranged between 6.5 mCD and 7.2 mCD. The difference between the two scenarios gives an 120% increase in the area of buildings affected and a 60 % increase in the area of land affected.
- Comparing the affect of sea-level rise, there is a 50 % and a 25 % increase in the buildings and land between a low prediction of 0.3 m and a high prediction of 0.8 m in 2100 (sea-level rise superimposed on a 1 in 250 year event).
- The increase between the low sea-level rise prediction (0.3 m and the H++ (1.8 m) prediction is similar in magnitude to the change for the inundation predictions for a 1 in 1000 year event. There is an increase of 120 % of buildings affected with an increase of 50 % for the area of land affected. (sea-level rise superimposed on a 1 in 250 year event).

An interesting point is that an inundation level of 7.2 mCD equates approximately to either the lowest prediction for a 1 in 250 year event and a 0.8 m allowance for sea-level rise; or the highest prediction for a 1 in 250 year event and a 0.4 m allowance for sea-level rise. Therefore, depending upon which prediction is correct for a 1 in 250 inundation level, the time at which a location might be inundated due to sea-level rise changes from 2050 to 2010 (high allowance for sea-level rise).

	Area Affected km^2		% Change from 6.4 mCD		% Change factored by change in inundation level	
Inundation Level (mCD)	**Land**	**Buildings**	**Land**	**Buildings**	**Land**	**Buildings**
6.4	8.6	0.2	-	-	-	-
7.2	13.0	0.4	50	100	62.5	125
8.0	17.1	0.7	100	250	125	312.5
9.0	21.1	1.1	145	450	145	450

Table 6.4 Comparison of the total area and buildings affected for the study area under 4 different inundation scenarios.

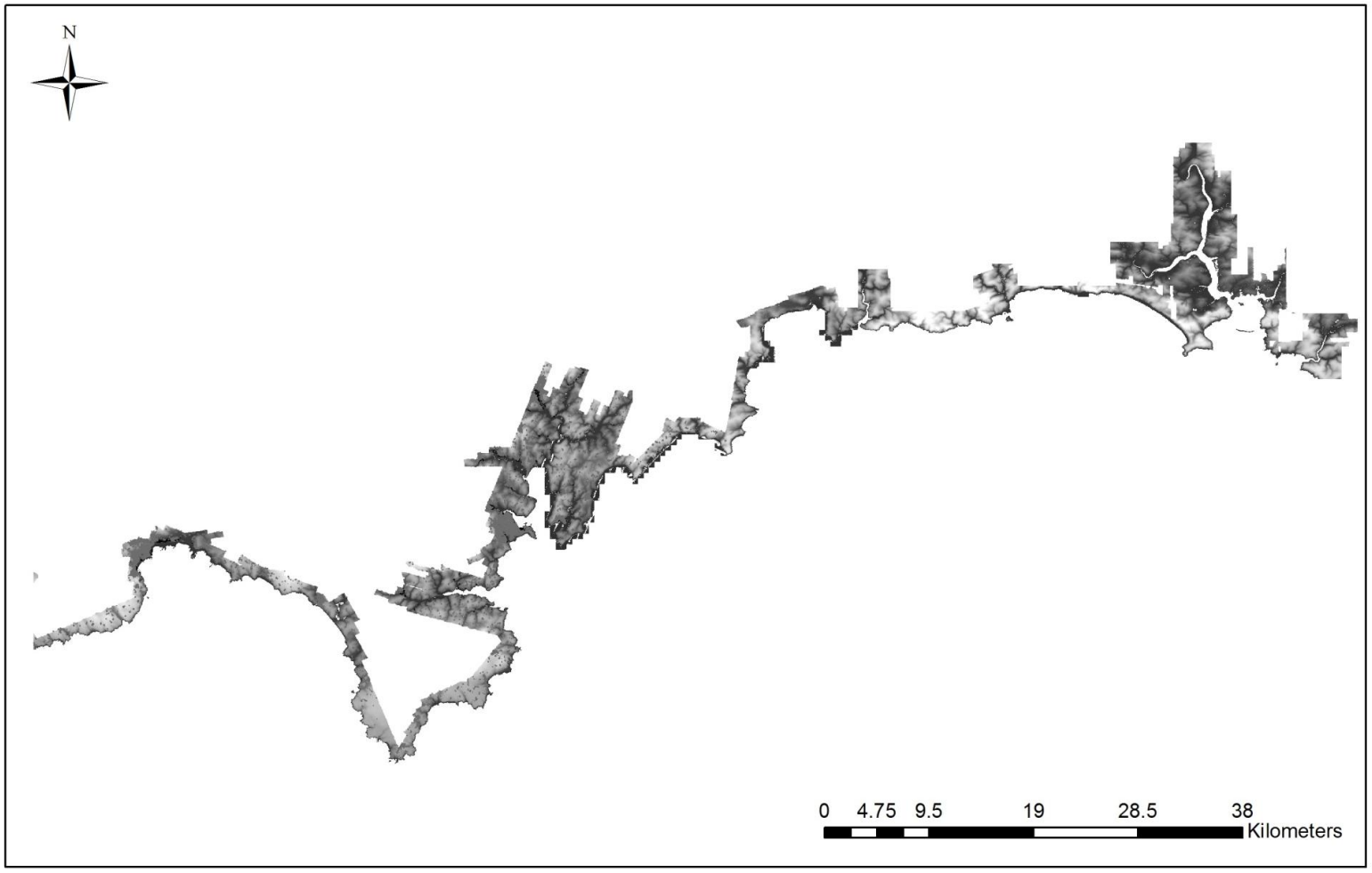

Figure 6.4 LiDAR Digital Elevation Model for the whole of the study area.

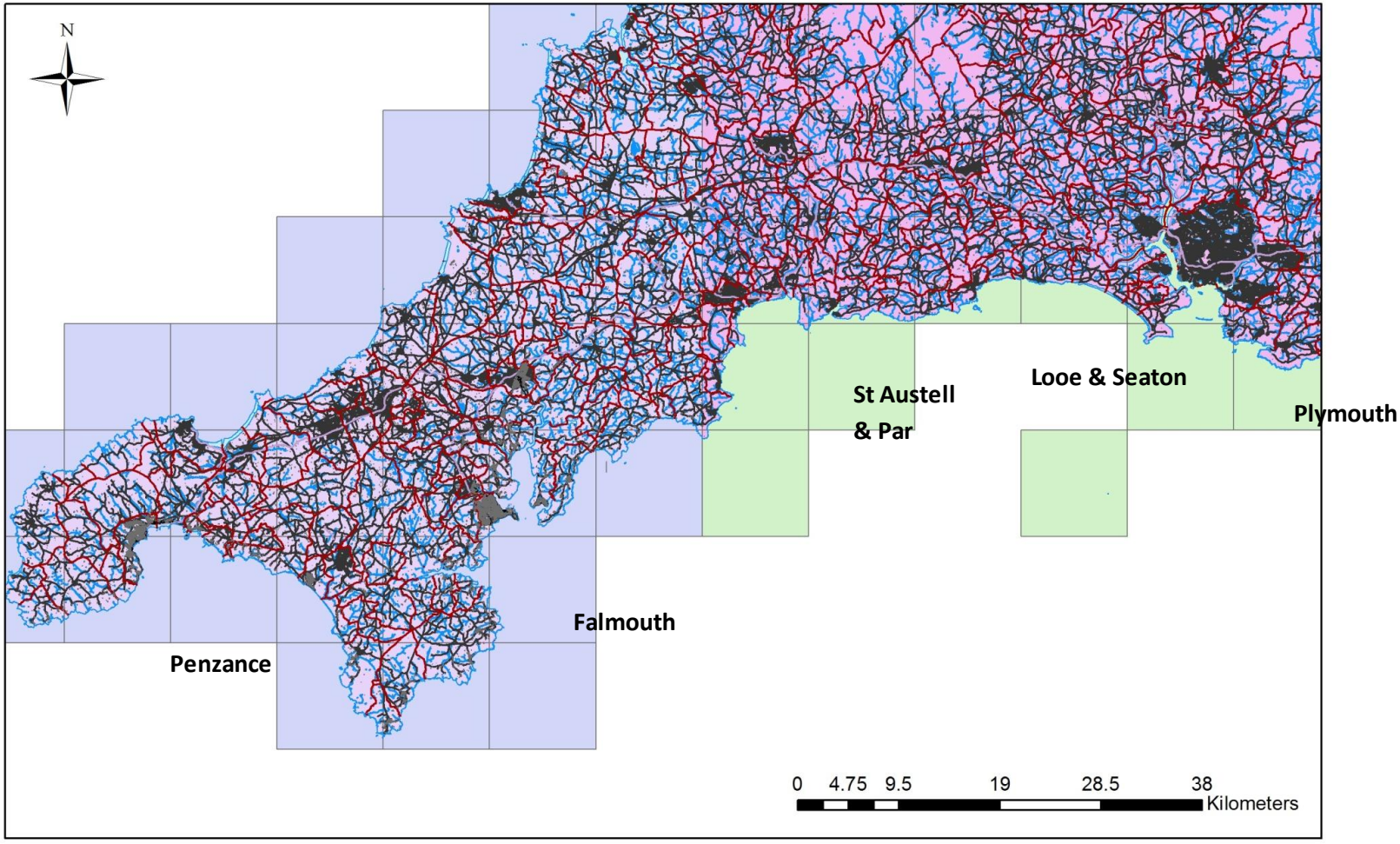

Figure 6.5 LiDAR Digital Elevation Model and Infrastructure Data for the whole of the study area, with locations of zoomed in areas in subsequent figures.

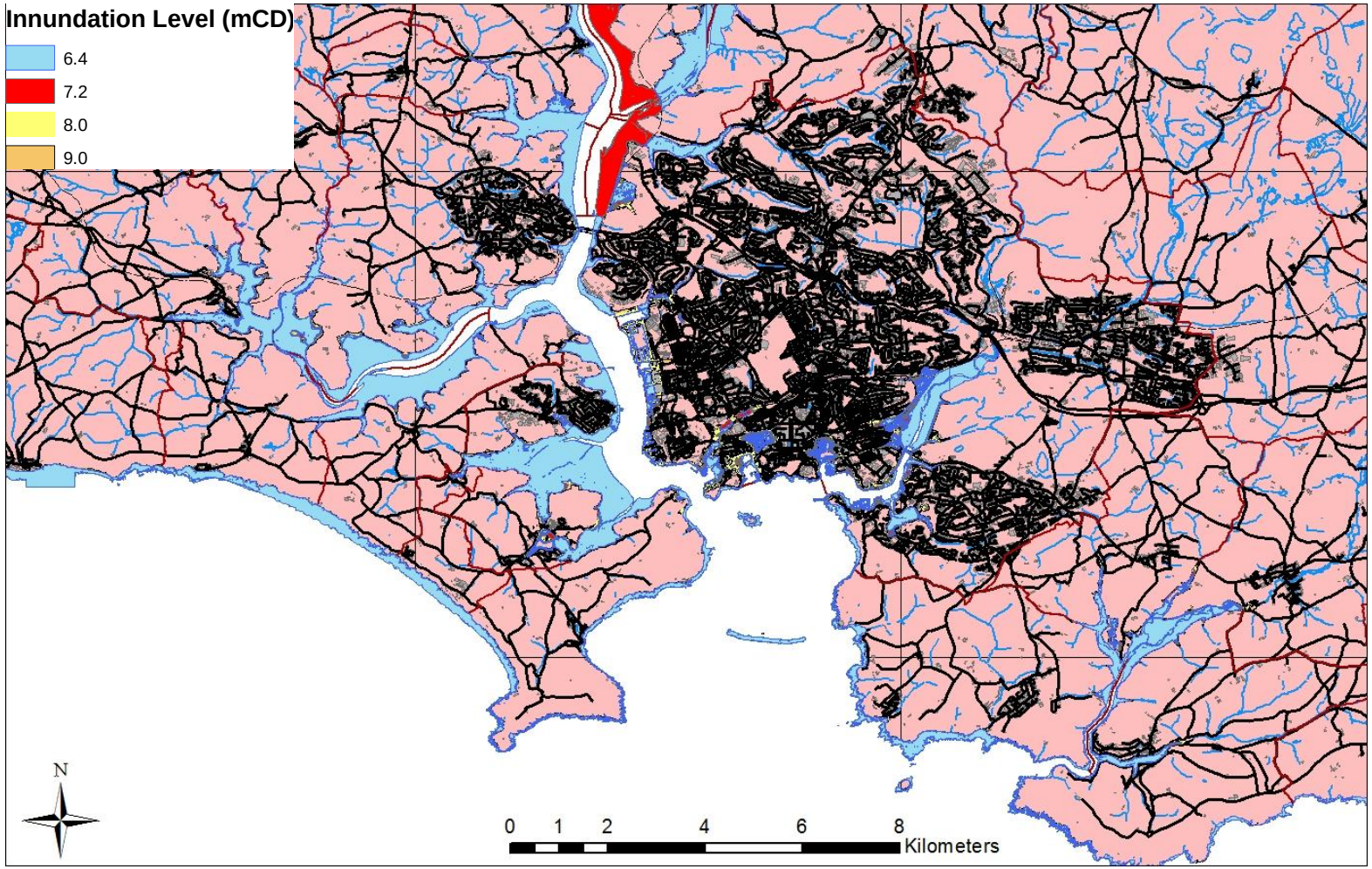

Figure 6.6 LiDAR Digital Elevation Model and Infrastructure Data with Inundation overlay of 6.4, 7.2, 8.0 and 9.0 mCD for the Plym and Tamar Estuaries.

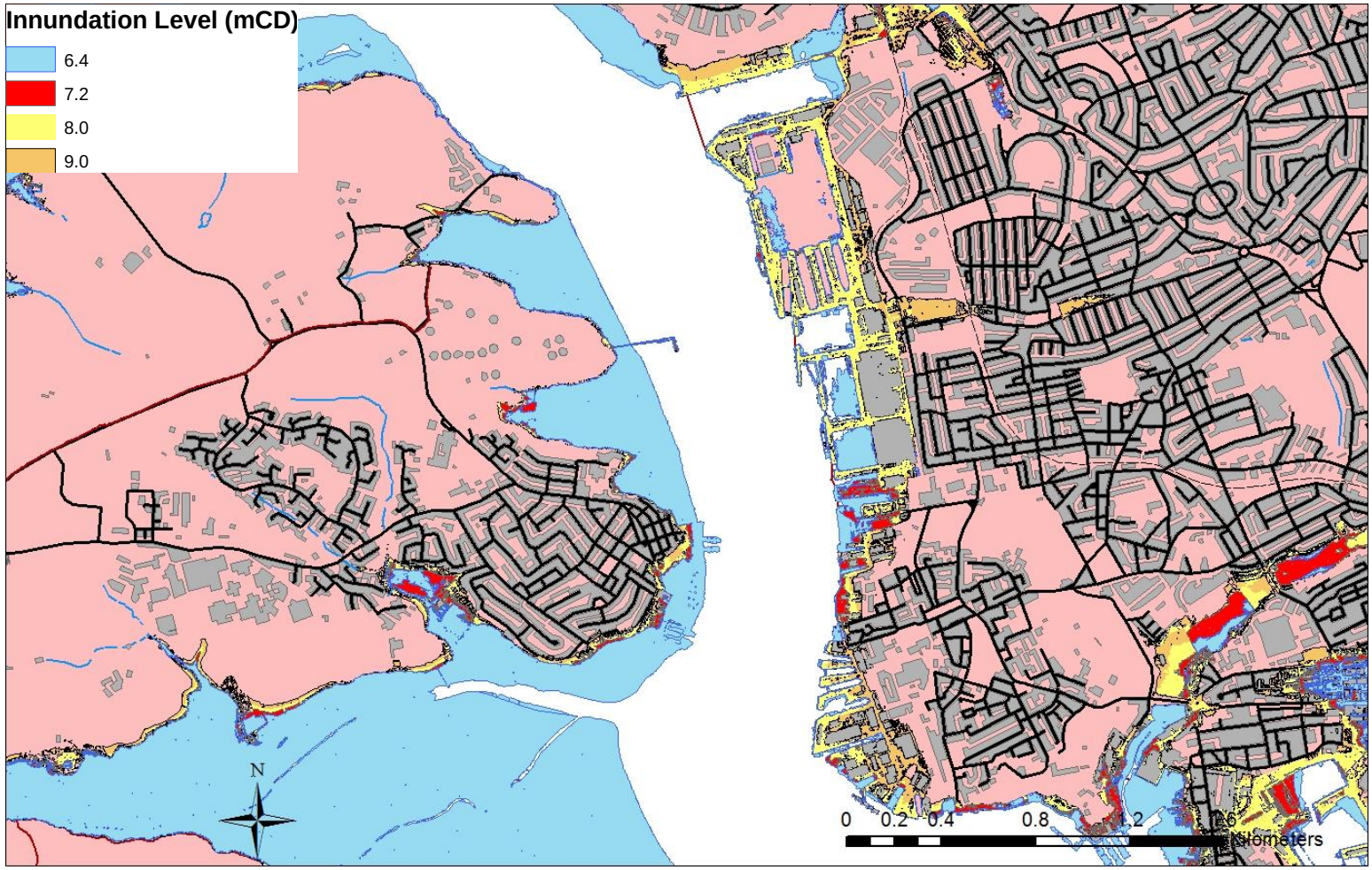

Figure 6.7 LiDAR Digital Elevation Model and Infrastructure Data with Inundation overlay of 6.4, 7.2, 8.0 and 9.0 mCD for the Devonport Dockyard and Tamar Estuary.

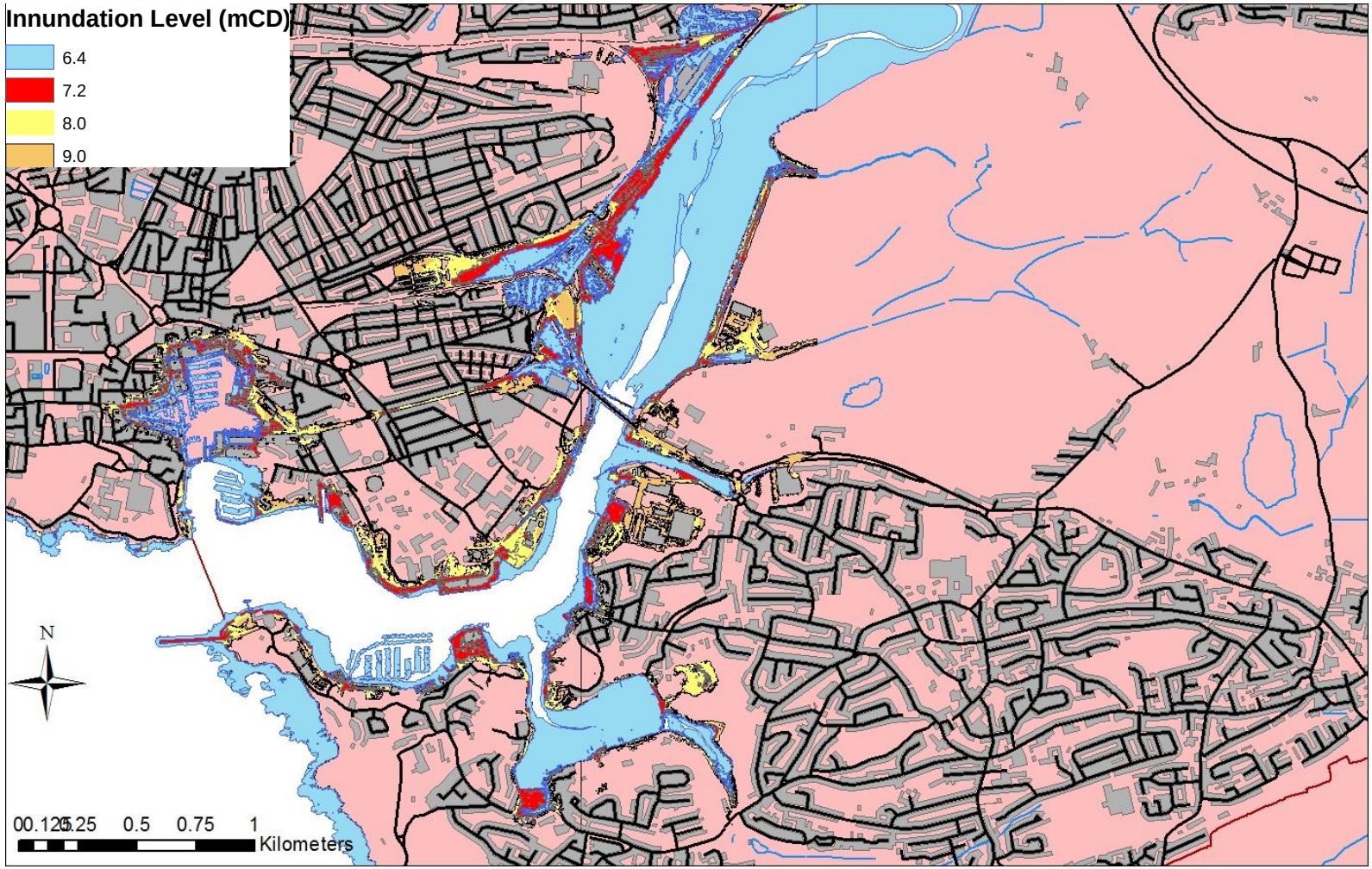

Figure 6.8 LiDAR Digital Elevation Model and Infrastructure Data with Inundation overlay of 6.4, 7.2, 8.0 and 9.0 mCD for the Plym Estuary.

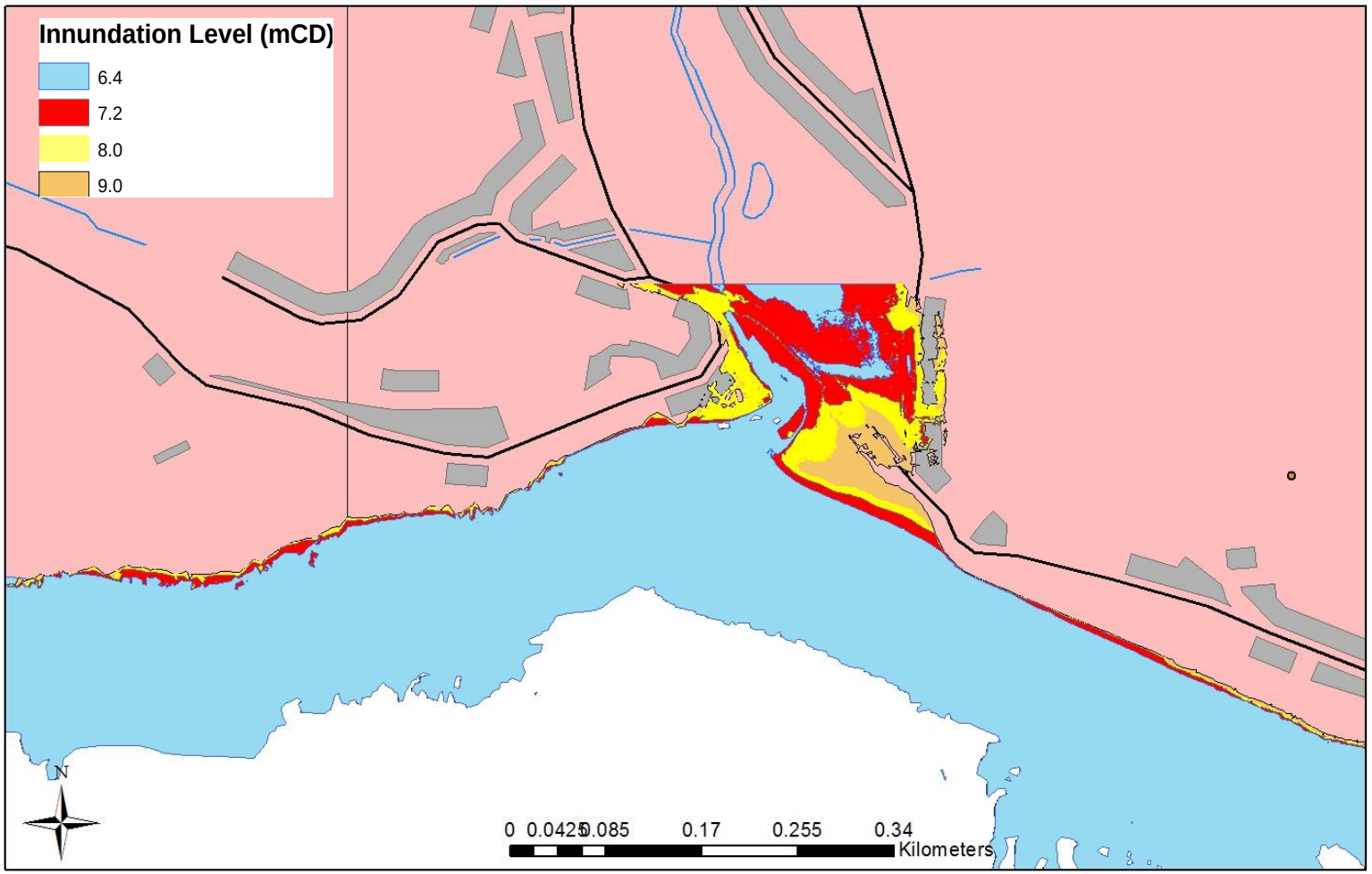

Figure 6.9 LiDAR Digital Elevation Model and Infrastructure Data with Inundation overlay of 6.4, 7.2, 8.0 and 9.0 mCD for the Seaton, Cornwall. The extent of the LiDAR Digital Elevation Model means the inundation extent cannot be fully resolved.

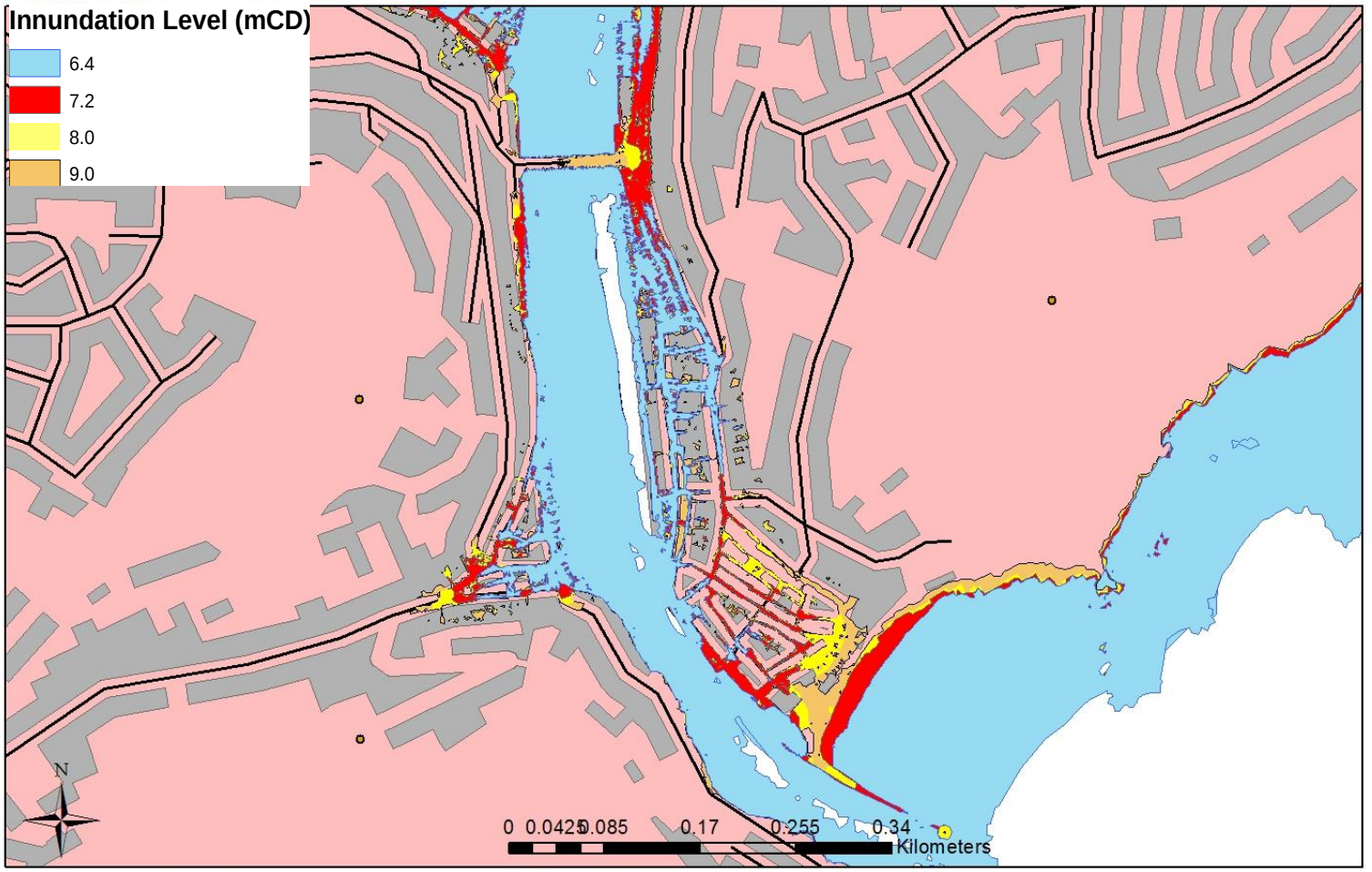

Figure 6.10 LiDAR Digital Elevation Model and Infrastructure Data with Inundation overlay of 6.4, 7.2, 8.0 and 9.0 mCD for Looe, Cornwall.

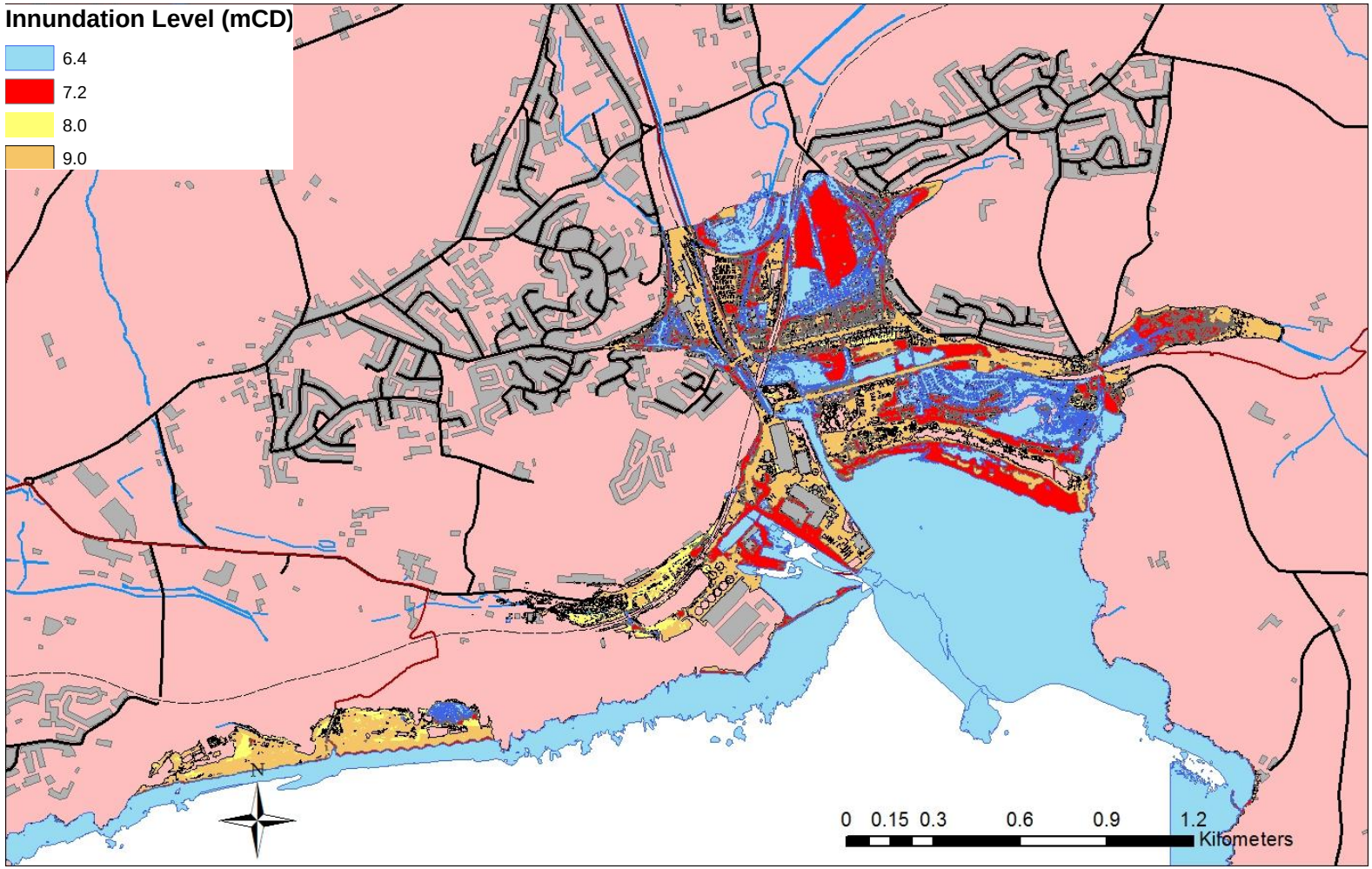

Figure 6.11 LiDAR Digital Elevation Model and Infrastructure Data with Inundation overlay of 6.4, 7.2, 8.0 and 9.0 mCD for Par, Cornwall.

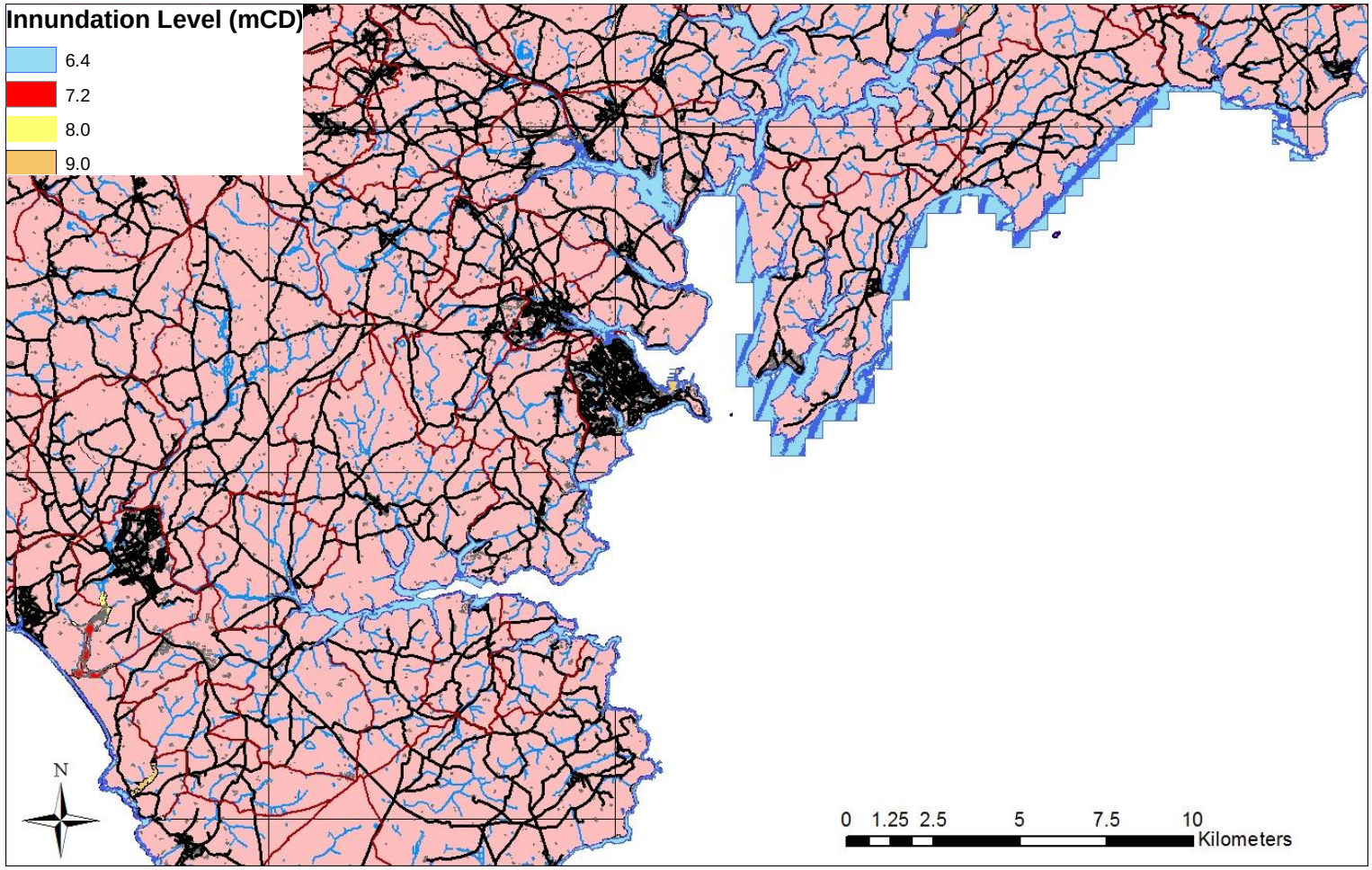

Figure 6.12 LiDAR Digital Elevation Model and Infrastructure Data with Inundation overlay of 6.4, 7.2, 8.0 and 9.0 mCD for Falmouth Bay, Cornwall. At this scale the inundation extent is difficult to visually resolve.

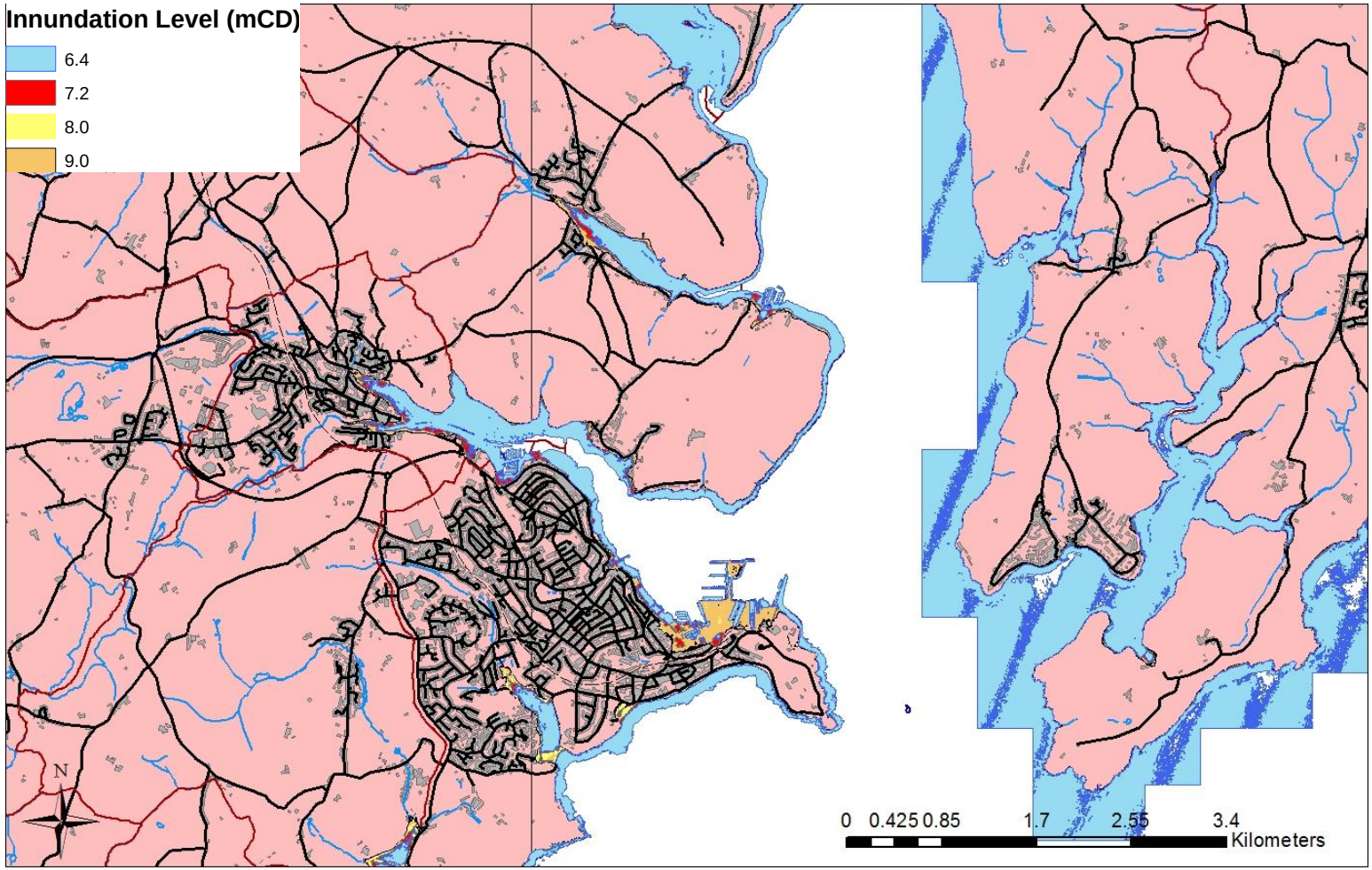

Figure 6.13 LiDAR Digital Elevation Model and Infrastructure Data with Inundation overlay of 6.4, 7.2, 8.0 and 9.0 mCD for Falmouth, Cornwall.

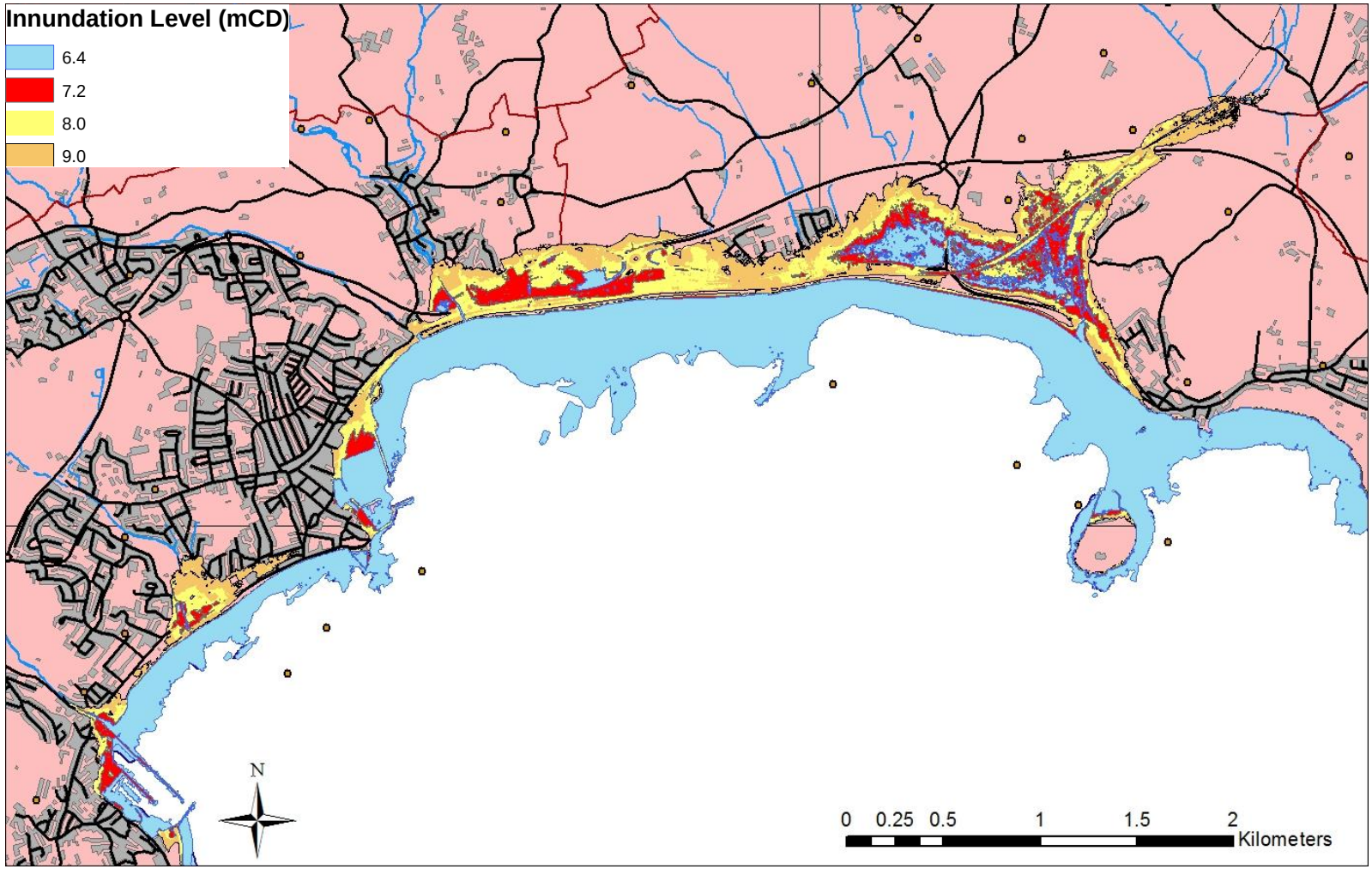

Figure 6.14 LiDAR Digital Elevation Model and Infrastructure Data with Inundation overlay of 6.4, 7.2, 8.0 and 9.0 mCD for Penzance, Cornwall.

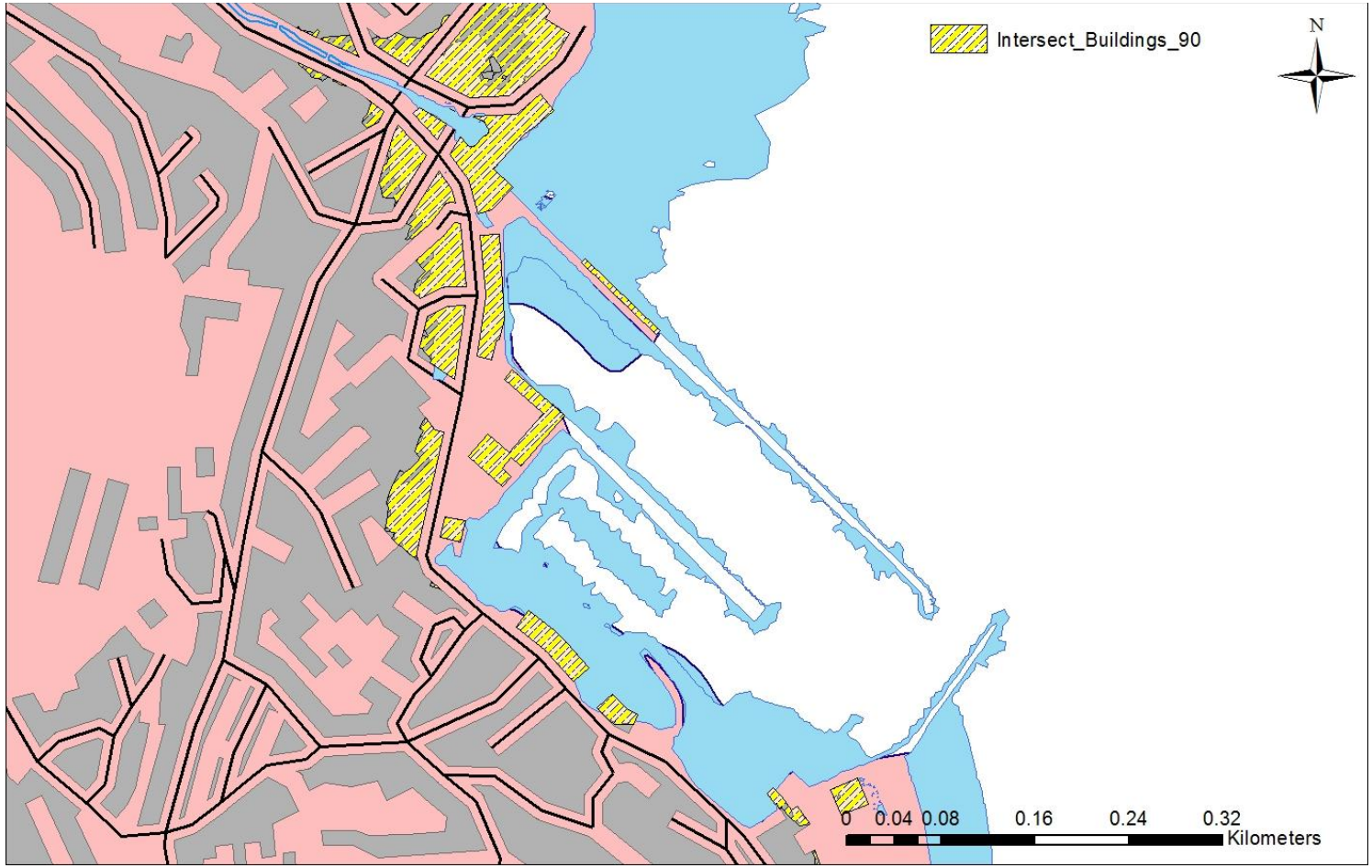

Figure 6.15 Example for Falmouth, Cornwall of the output of the intersection of 9.0 mCD inundation level and the building polygon within the infrastructure data.

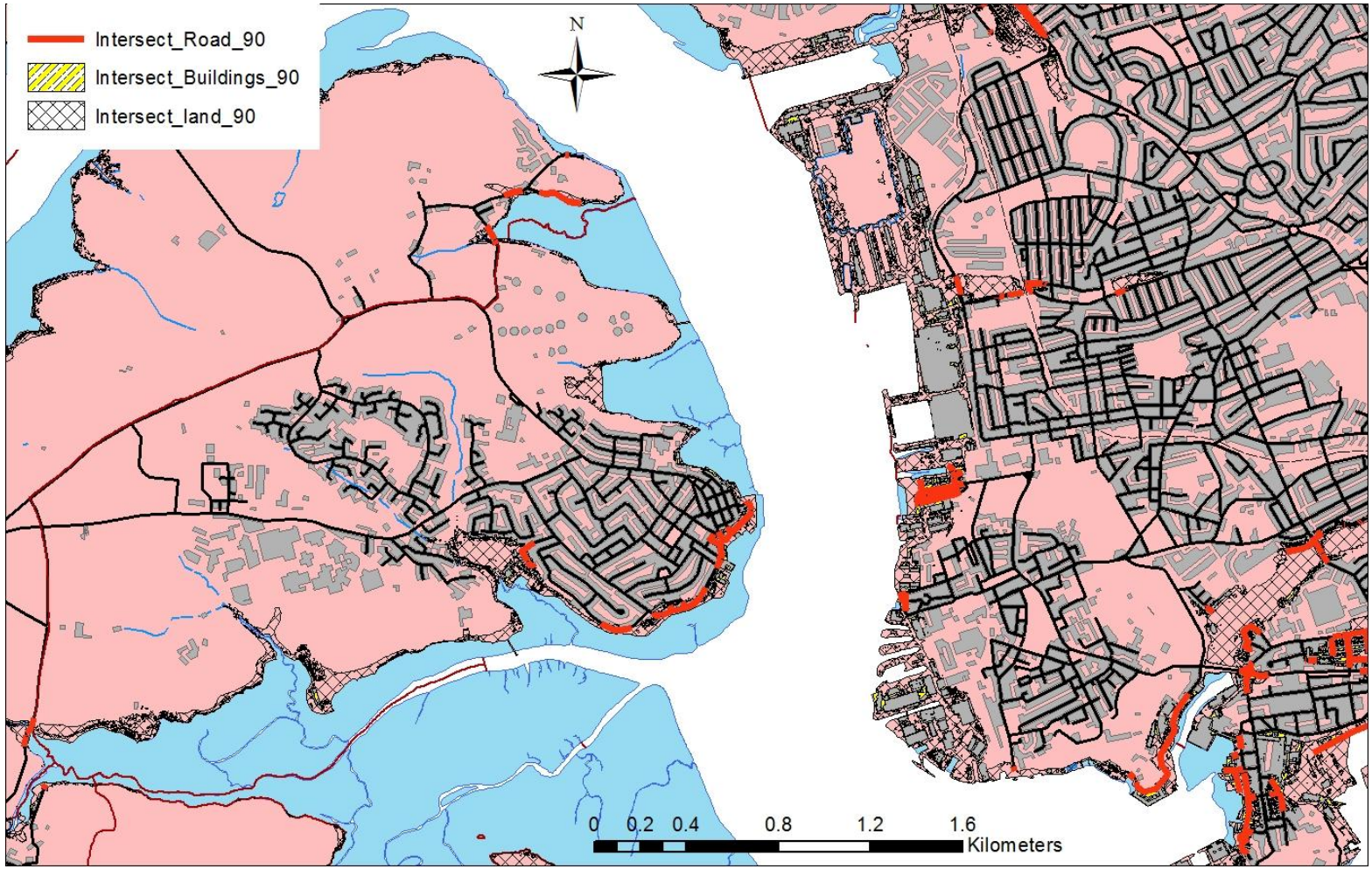

Figure 6.16 Output of the intersection of 9.0 mCD inundation level with the building, roads and land polygons within the infrastructure data for the Tamar estuary.

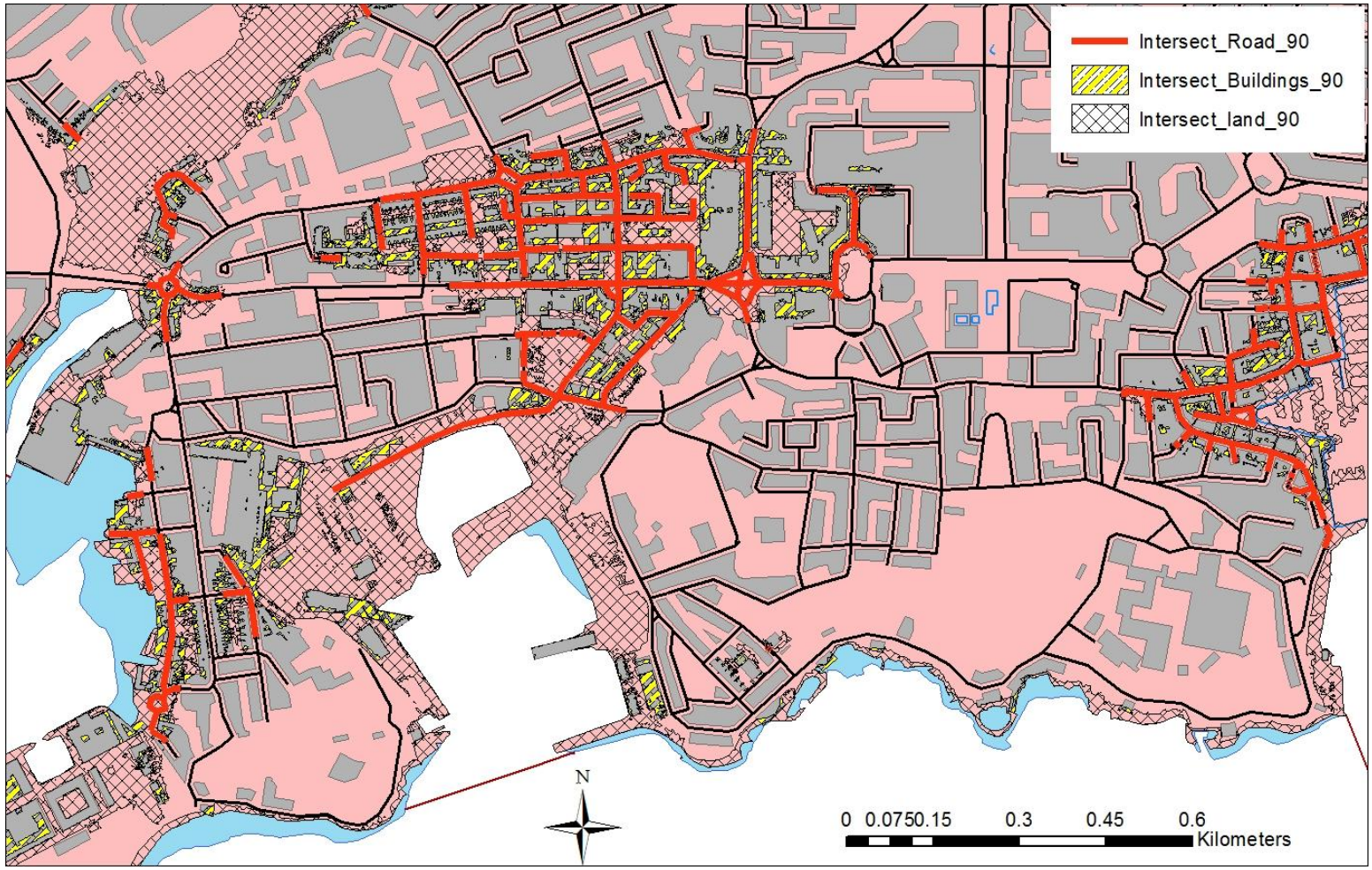

Figure 6.17 Output of the intersection of 9.0 mCD inundation level with the building, roads and land polygons within the infrastructure data for Millbay, Plymouth.

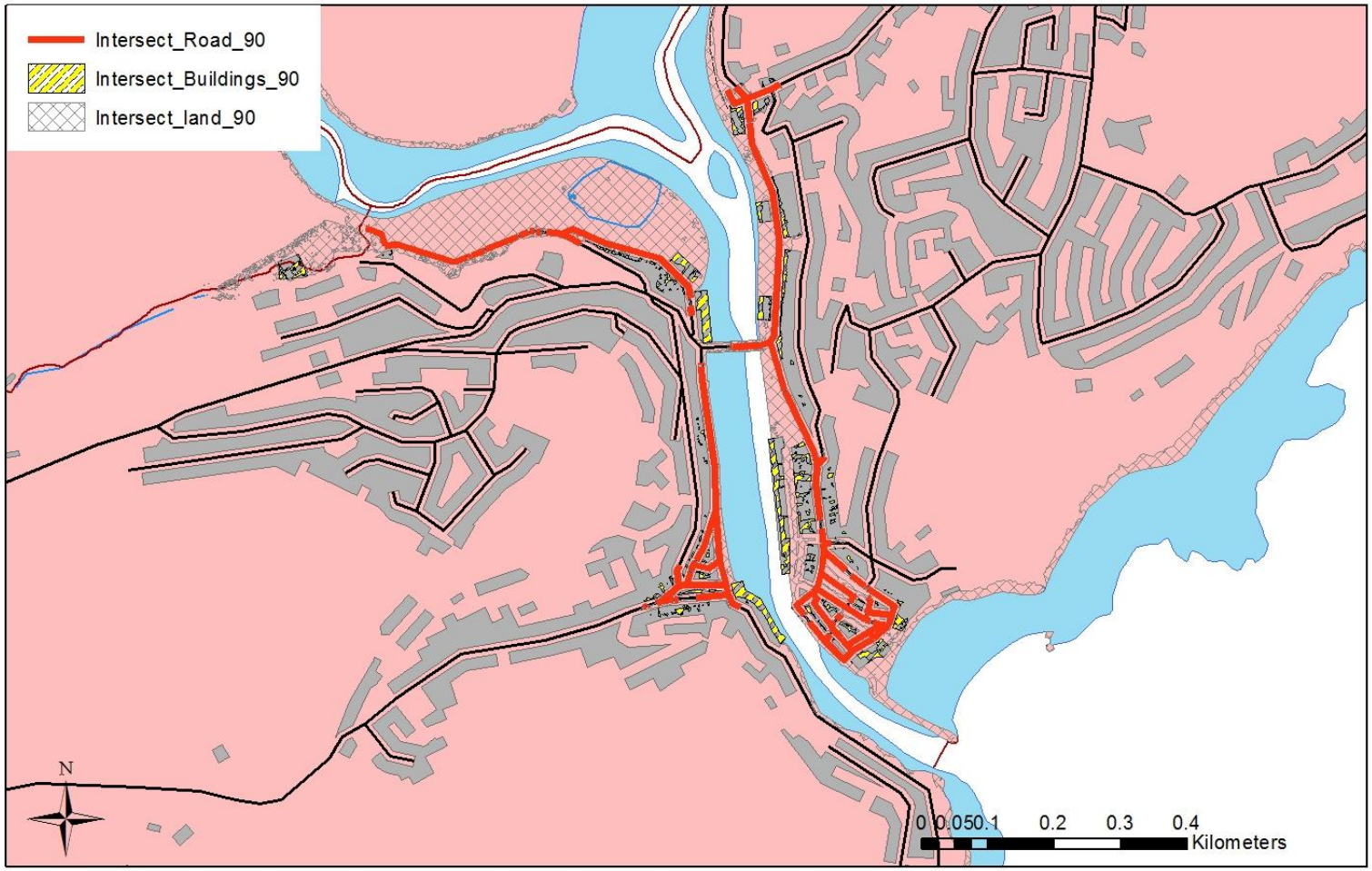

Figure 6.18 Output of the intersection of 9.0 mCD inundation level with the building, roads and land polygons within the infrastructure data for Looe Cornwall.

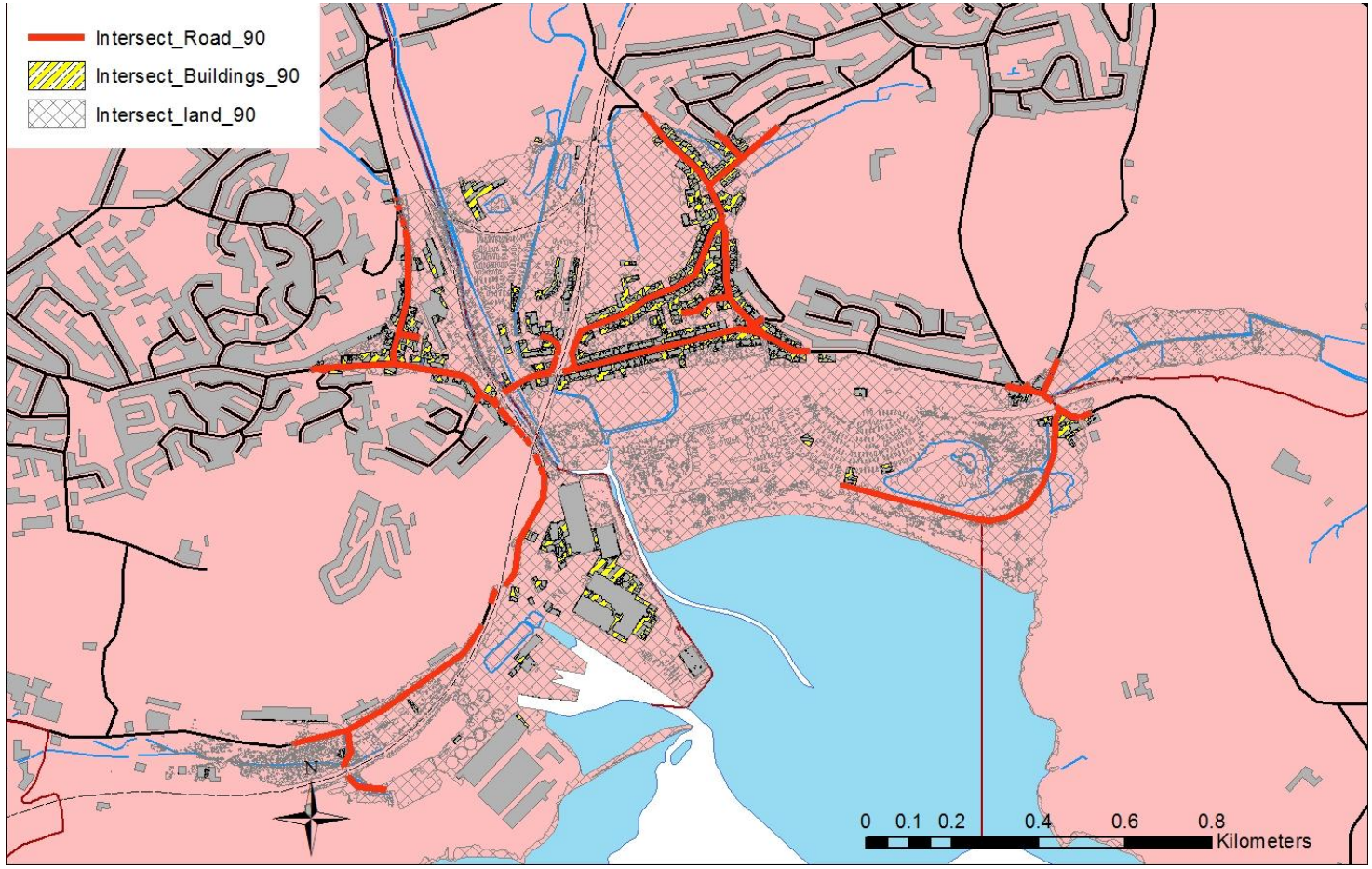

Figure 6.19 Output of the intersection of 9.0 mCD inundation level with the building, roads and land polygons within the infrastructure data for Par, Cornwall.

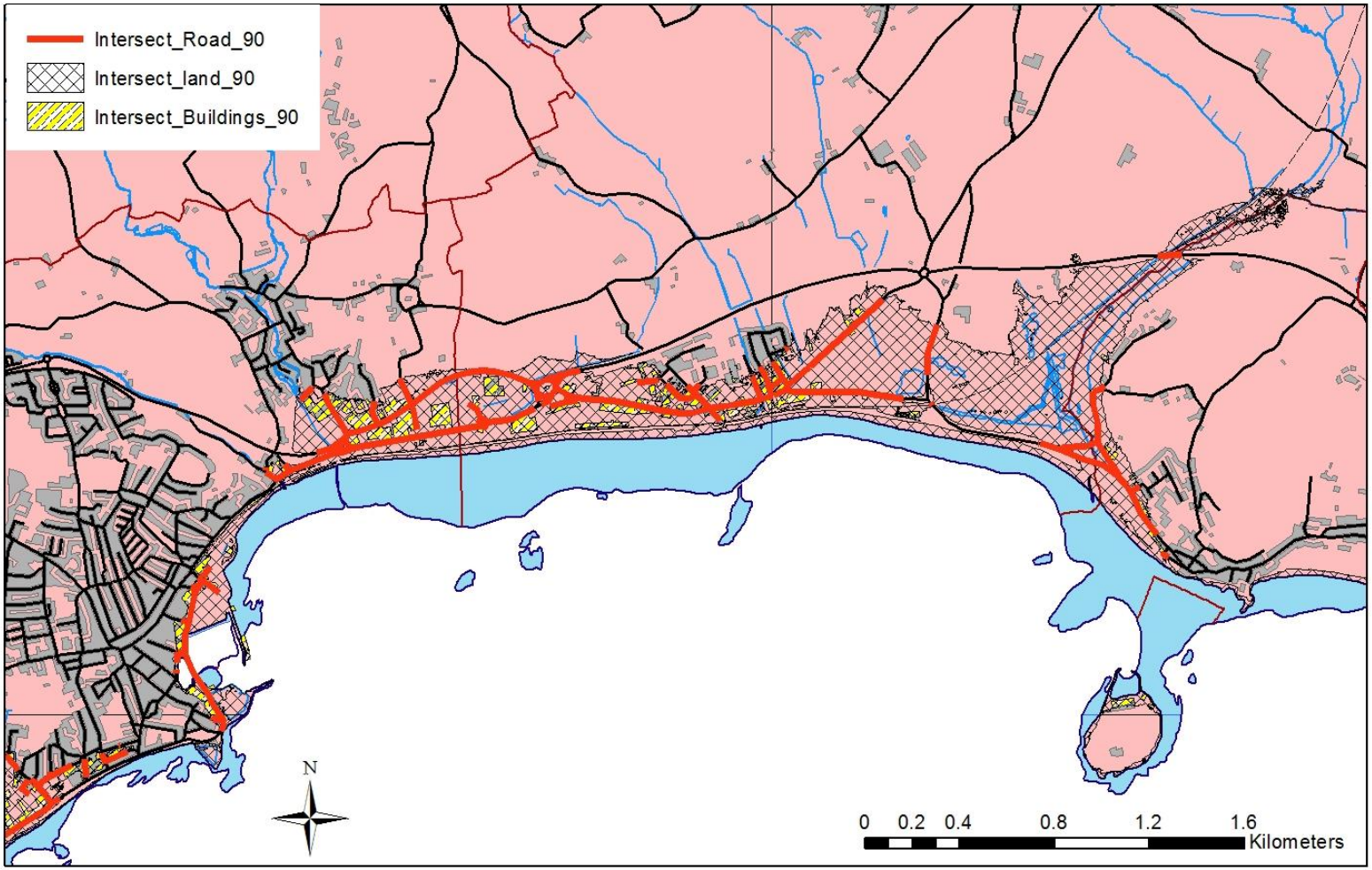

Figure 6.20 Output of the intersection of 9.0 mCD inundation level with the building, roads and land polygons within the infrastructure data for Penzance, Cornwall.

6.4 Devonport Dockyard

Devonport Dockyard is a Nuclear Licensed Site, undertaking the refit of nuclear submarines and represents critical infrastructure within the study area. It is governed by significant regulations and is required to evaluate the affect of natural phenomena such as storm surges, wind and waves (IAEA, 2008). A Nuclear Licensed Site is required to design for a natural event occurring at a frequency of 1 in 10,000 years and to consider jointly the occurrence of natural events that could lead to increased levels i.e. storm surges and waves (IAEA, 2008). To provide an indication of when Devonport Dockyard could potentially be flooded, the coincidence of waves and the inundation levels are used to evaluate the scenarios which could potentially lead to overtopping. Figure 6.21 illustrates three scenarios. The first scenario is 6.7 mCD, which represents the lowest prediction for a 1 in 250 year inundation levels (6.4 mCD) and a 1 in 250 year wave height (0.25 m). The second scenario represents a high prediction for a 1 in 1000 year inundation level (7.2 mCD) and a 1 in 1000 wave height (0.5 m). The final scenario is the same as the second scenario but includes the addition of 0.8 m sea-level rise (high prediction for 2100).

From a review of the scenarios and Figure 6.18, Devonport Dockyard would be overtopped at the present day by the combination of a 1 in 1000 inundation level and a 1 in 1000 wave. A level of 7.7 mCD would equate to an overtopping of 0.3 m. (Devonport Dockyard lies between 7.4 and 7.5 mCD), leading to inundation occurring for a short duration (<0.5hrs). However, taking in to account sea-level rise by 2100 this level could be 1.1m, meaning the duration would increase to approximately 2 hours. A H++ sea-level rise scenario would increase the overtopping level by up to 2.1 m, leading to a 4.5 hour flooding event. As a comparison without wave height, Devonport Dockyard would be overtopped in 2050 by a 1 in 1000 year event (0.4 m sea-level rise).

Devonport Dockyard also provides a method for validating the accuracy of the LiDAR DEM data and the methodology as the height of the area is known to lie between 7.4 mCD and 7.5 mCD. When overlaying an inundation level of 7.5 m which has been derived from the LiDAR DEM, Devonport Dockyard can be seen to be flooded.

6.5 Looe, Cornwall

Looe, Cornwall has been selected to evaluate the affect of wave setup, generated by near shore waves on the inundation levels, as it represents a beach environment with infrastructure situated behind. Figure 6.19 illustrated four different scenarios that have been evaluated for Looe. The first scenario is 6.9 mCD, which represents an inundation with a return frequency of 1 in 1000 years. The second scenario represents the same scenario as the first scenario but includes the addition of 0.4 m sea-level rise. Scenario 3 and scenario 4 include the addition of 1 in 250 year wave setup (0.5 m) and 1 in 1000 year wave setup (2.5 m) respectively.

From Figure 6.22, the first scenario causes extensive flooding, with the next 3 scenarios only increases the extent of the flooding to a minor degree, In terms of extent the main contributor to flooding appears to come from the inundation levels, with wave setup being only a minor contributor, despite scenario 4 including a 2.5m allowance for wave setup. However, as highlighted for Devonport, the addition contribution to flood levels by wave setup will increase the overall depth of flooding and duration of flooding. To evaluate if the fact that inundation levels is the dominant contributor, Par in Cornwall was assessed. Figure 6.23 shows that as for Looe, the dominant contributor to flood extent for Par is the inundation component, rather than wave setup or sea-level rise.

6.6 Discussion

A range of frequency magnitude relationships and sea-level rise scenarios have been modelled within a GIS to evaluate uncertainty within a coastal environment, using south-west England as a case study. The scenarios modelled include the uncertainty in frequency magnitude relationships for storm surge for a 1 in 250 and a 1 in 1000 year event and a range of sea-level rise uncertainties up to 2100. Based on the different frequency magnitude predictions for a 1 in 250 year event (0.5 m uncertainty) the area of inundation can vary by up to 40% of the total area of land affected and for buildings can vary by up to 80%. For a 1 in 1000 year event (0.7 to 0.8 m uncertainty) the total area and buildings affected can vary by up 60% and 120% respectively. This compares to the uncertainty in sea-level rise causing an uncertainty range (0.5 m) in the total area of buildings and land affected by up to 50% and 25% respectively between a low and high sea-level rise prediction (excluding H++ scenario). For the two specific areas it was identified that Devonport Dockyard could be overtopped by the combination of a 1 in 1000 year storm surge and coincident wave height at the present day, with the addition of sea-level rise this would increase the extent and duration of possible flooding. Both Looe and Par in Cornwall are inundated by a 1 in 250 year, with the addition of wave set up only marginally increases the flood extent, however due to the affect of wave set up the duration of flooding and the depth of flooding is likely to increase.

From the GIS analysis the main areas that are likely to be affected by flooding at the present day, and in to the future, include, the Plym and Tamar estuaries, including Devonport Dockyard, Looe, Seaton, Par, Penzance and Newlyn.

6.7 Appendix B Geographic Information System Database

Note to user:

The database is for viewing purposes only and must not be altered, copied, distributed, reproduced or used without permission of the author.

The viewing of the GIS database contained within Appendix B requires the user to have installed and a licence file for ARCGIS 10.3. A free viewer licence is available from www.esri.com/software/arcgis/explorer, however, some aspects of the database may not be available or be possible to visualise. The viewing of the data requires at least a basic understanding of ARCGIS.

The following steps outline the process to visualise the data:

1. Load ARCGIS and connect Western Digital External Hard drive to computer.
2. Within ARCGIS click file then open and navigate to the External hard drive location, click on “mainmodel” and open.
3. Initially only the LiDAR Digital Elevation model is shown. If this is not shown click on the layer title “all data” and repair data source under the data icon. This may require the user to map the folder connection to direct ARCGIS to the source of the data. This process should only be required once, however if other layers are not visible then the process of repairing the data source will need to be repeated.
4. Within the data base are the following layers in the order they appear on the map to allow visualisation of the flood levels on the infrastructure data (top to bottom):
    a. Flood levels (relevant levels 6.4 mCD and 9.0 mCD).
    b. Infrastructure data (Contains individual layer of roads, buildings etc).
    c. Digital Elevation Data.
5. To visualise the layer or layers click on the layer. Clicking on the main infrastructure layer will automatically show building, roads and the land polygon. N.B. to visualise the layer it will be required to zoom in and then pan along the study area.

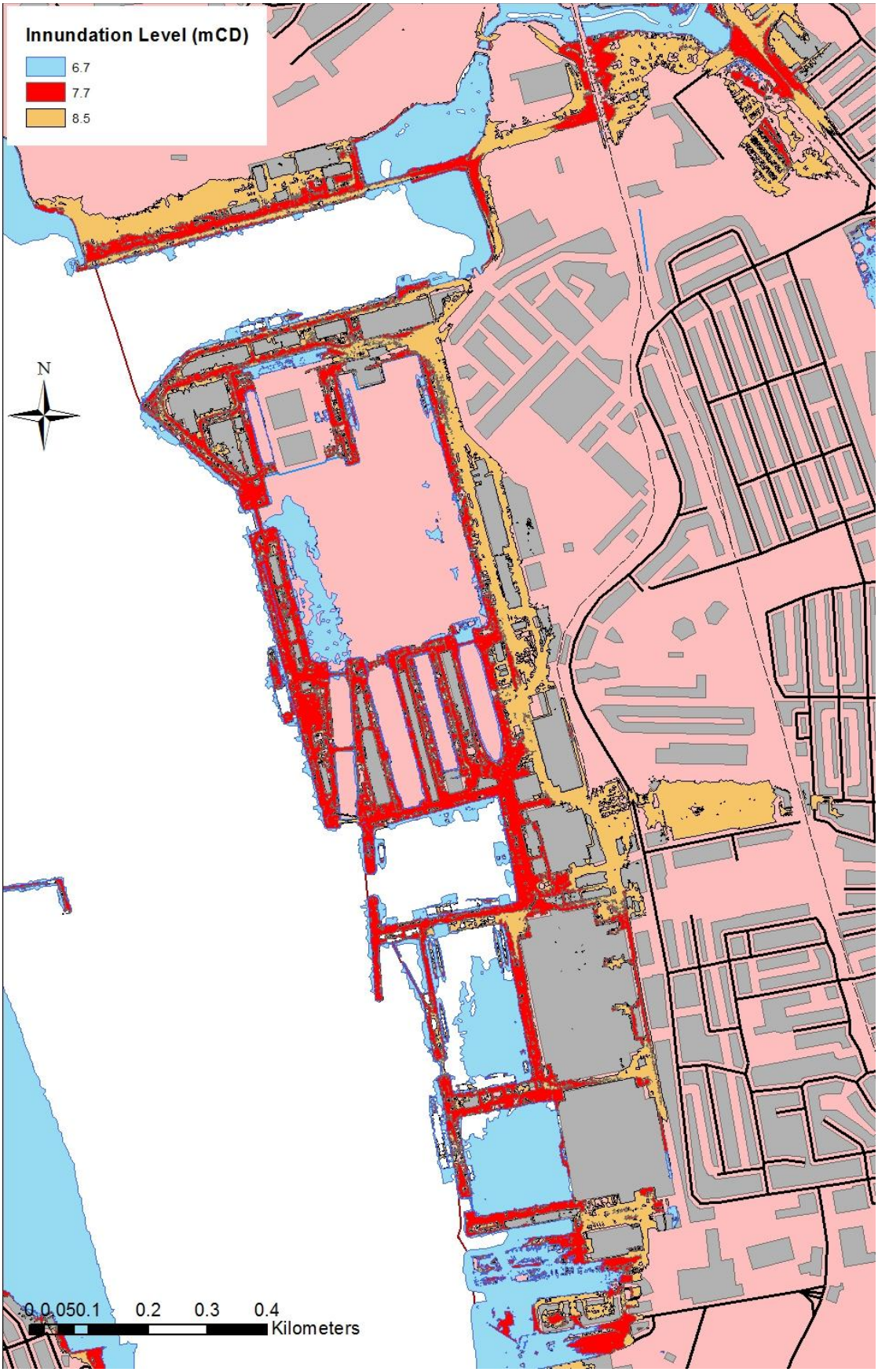

Figure 6.21 Evaluation of overtopping (inundation level and wave height) for Devonport Dockyard based on 3 different scenarios.

Figure 6.22 Evaluation of inundation and wave set up scenarios for Looe, Cornwall.

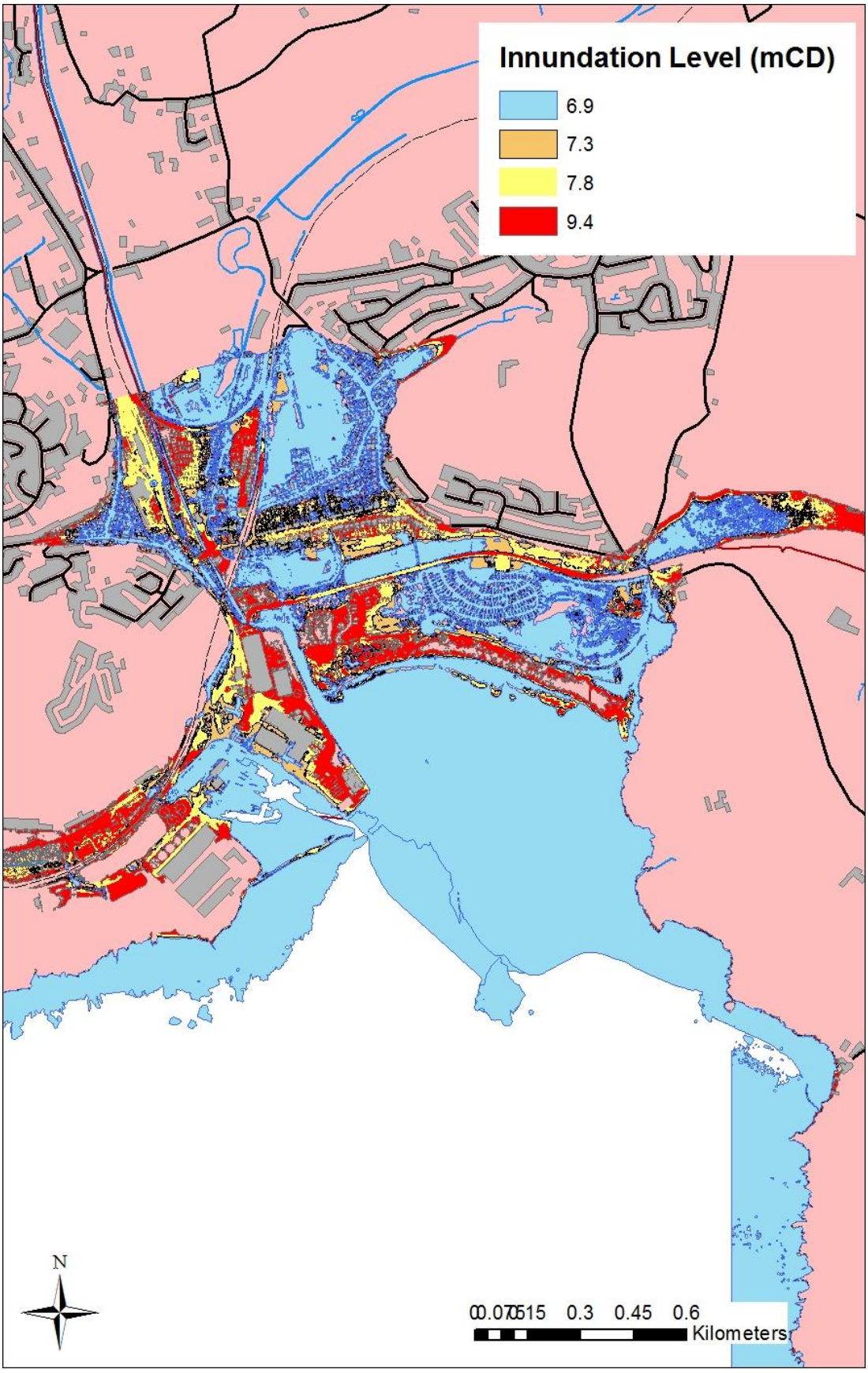

Figure 6.23 Evaluation of inundation and wave setup scenarios for Par, Cornwall.

Chapter 7 Discussion

7.1 Introduction

The study aims to evaluate the affect of statistical techniques on the inundation levels for Southwest England and to compare the outcome to the affect of increases in mean sea level over the 21st Century. The following chapter discusses the findings of this research, based on the complied data and analysis undertaken and compares the findings with the established scientific literature. Section 7.2 discusses the observed trends (Section 5.3) in the data sets identified as part of this study including, mean sea level, storm surge frequency and links these to observed trends (pressure, wind speed and wind direction) in the weather records from Mt Batten (Plymouth) (Section 5.3). The findings are linked back to the literature on discussed within Chapter 2 and the previously observed trends modelled against the North Atlantic Oscillation (NAO). Five different statistical techniques utilizing both the observed water levels and the extracted storm surge levels obtained during this research have been used to evaluate the applicability of the techniques to evaluate frequency magnitude relationships (Section 5.4). The statistical techniques have also been used to evaluate wave set up based on wave height data, and wave height within a closed basin based on wind speed frequency magnitude relationships. The ability of the statistical techniques to evaluate the frequency magnitude relationships for observed water levels, storms urge levels, wind speed and wave height undertaken as part of this study are discussed in Section 7.3, with the findings compared to the relationships and ability of the techniques to predict these relationships that have been identified within the literature review in Chapter 3. No previous studies have looked at the affect of different prediction methodologies on the magnitude of inundation levels and how these compare to the affect of sea-level rise. Within Chapter 6 a Geographical Information System (GIS) model was developed to compare the inundation levels from different statistical techniques and different sea-level rise scenarios for a case study of south-west England. The findings identified within this chapter are compared to the published research on the affects of sea-level rise for the south-west England and the United Kingdom and presented in Section 7.4.

In January and February 2014, a series of storm surges affected the U.K. coastline including several locations within the study area. Section 7.5 reviews these storms surge events based on news articles and the recorded tidal gauge readings.

Comparing the observations and recorded levels to the predictions made within this study and the areas identified within the GIS model that would be affected. As such the storms of January and February 2014 provide a method to validate the predictions made within this study and in the GIS models.

The frequency magnitude relationships and the GIS modelling undertaken within this study can help inform designers, planners and disaster response. Section 7.6 discusses how a model can be developed to inform which methodology should be adopted depending on the facility at risk and to delineate areas that are likely to be affected by both inundation levels and sea-level rise to enable an effective planning and disaster response strategy.

7.2 Observed Trends, Sea-level Rise and Storminess

Chapter 5, Section 5.3 and Figures 5.17 to 5.29 presented the results of the observed trends including sea-level rise and storminess based on the observed tidal gauge records from Devonport and Newlyn, the extracted storm surge component and the wind (speed and direction) and pressure readings from the Mt Batten weather records. Due to the short data set (7 years) no trend analysis was undertaken for the Polperro wave data.

The observed sea-level trend based on a linear relation was found to be 2.1 mm/yr +/- 0.3 (95%) and 1.8 mm/yr +/- 0.2 (95%) for Devonport and Newlyn respectively. The Newlyn rate was found to correspond to the rates of Haigh et al., (2008) and Woodworth et al., (2009); however, the Devonport rates were found to be lower, although within the confidence intervals of Haigh et al., (2008) and Woodworth et al., (2009). The higher mean sea-level rise trend for Devonport was expected to be higher than Newlyn as the data set commenced during a trough in the periodic oscillations of the data set. The discrepancies between this study and Haigh et al., (2008) and Woodworth et al., (2009) can be attributed to the longer data set developed as part of this study and extended to 2012, a detailed understanding of the data shifts of the data set (Section 4.3.1) and the inclusion of annual records with less than 11 months of data.

Figure 5.17 and Figure 5.18 showed that an exponential curve could be plotted against the sea-level rise data sets for both Devonport and Newlyn and provided a better fit to the data than a linear trend. This exponential growth equates to a rate of between 0.001 to 0.002 mm/yr^2 acceleration within the data set. The trend plotted based on the exponential curve indicates higher rates of sea-level rise for both Newlyn and Devonport, compared to the modelled linear trend. Based on the exponential modeled trend initial rates of sea-level rise for Newlyn in 1915 are 1.9 mm/yr, and for 1962 for Devonport are 2.2 mm/yr. By 2010 this rate of sea-level rise had increased to 2.05 mm/yr for Newlyn and 2.3 mm/yr for Devonport. If projected to 2100, the sea-level rise rate would be approximately 2.4 mm/yr for both Newlyn and Devonport, leading to sea levels being approximately 0.2 m higher in 2100 than 2010. This sea-level change is equivalent to the lowest prediction of sea-level rise of UKCP (2009). The rates of acceleration in sea-level rise over the 21st Century are close to the global observations of Church and White (2011) and Jevejava et al., (2008) of 0.0012 mm/yr^2 and of 0.0013 mm/yr^2 respectively.

South-west England has been undergoing subsidence due to glacial isostatic adjustment, as such the sea-level rise observed for the study area also incorporates a component of subsidence. Woodworth et al., (2009) evaluated the U.K. sea-level rise average trend, removing either the uplift or subsidence signal and identified a sea-level rise of 1.4 mm/yr +/- 0.2 mm for the U.K. Removing the average sea-level rise component of 1.4 mm/yr of Woodworth et al., (2009) from the results of the sea-level trend analysis undertaken within this study, the analysis indicates that the Newlyn is subsiding at a rate of between 0.4-0.5 mm/yr +/- 0.2 mm and Devonport between 0.7-0.8 mm/yr +/-0.3. These values are close to the assessment of Teferele et al., (2009) who evaluated the subsidence for Newlyn to be between 0.4 and 0.5 mm/yr based on Continuous GPS and Absolute Gravity data. The results for this study are lower than the predicted subsidence of 1.1 mm/yr calculated by Shennan et al., (2012) and Bradley et al., (2009). The results of Shennan et al., (2012) are calculated by radiocarbon dating Holocene samples and Bradley et al., (2009) by undertaking Glacial Isostaic Adjustment Modelling. These methods are more likely to require significant assumptions to evaluate the subsidence rates, where Teferele et al., (2009) is based on physical measurements. This study confirms that the subsidence rates calculated by Teferele et al., (2009) are more indicative of the rates for Southwest England than those of Shennan et al., (2012) and Bradley et al., (2009).

Figure 5.19 to 5.24 illustrates the change in frequency of observed levels and storm surge levels, of both independent and non-independent events. The data shows a significant change in the frequency of events over the data period for both Devonport and Newlyn, with Newlyn showing an increase in events >5.4 mCD from 40 in 1915 to 100 in 2012. Both independent events and non-independent events show an increase in both observed levels and storm surge levels. Plotted trends of the data (i.e. Figure 5.20) indicates rates close to the rates of observed sea-level rise, indicating the increase in frequency of events can be attributed to change in sea-level rise rather than an increase in storminess. These findings are comparable to the findings of Woodworth et al., (2009) and Xu et al., (2003) who found no evidence for a change in frequency of storms within Southwest England.

Several authors (i.e. Woodworth et al., 2007; Alexander and Tett, (2005); Hurrell and Deser, 2010) have identified a link between the North Atlantic Oscillation (NAO) and an increase in the frequency of storms during positive spikes in the NAO. Figure 5.29 shows a comparison between the observed trend in the NAO and the frequency of observed storm surges. From a visual comparison this research confirms that there is a correlation between a positive spike in the NAO and an

increase in frequency of storm events in south-west England. Figure 5.29 also shows the pressure readings for Mt Batten (Plymouth), from a visual comparison there is not only a link between low pressures and a positive spike in the NAO but also the periods dominated by low pressure is also dominated by an increase frequency in storm surges.

Figure 5.25 to 5.28 provides the results of the trend analysis of the weather data for Mt Batten (Plymouth). Average pressure readings (Figure 5.25) remain constant, although there appears to be a slight downward trend in the occurrence of both high and low pressure systems (Figure 5.26). This slight downward trend also occurs in the frequency of daily average wind speed (Figure 5.27). Within both the wind speed and wind direction (Figure 5.28) there a slight oscillations within the data similar, although this is not as pronounced, as observed in the pressure and storm surge observations. A clear change in the predominant wind direction occurs around the period 1995, which corresponds to a strong negative spike in the NAO. The observed changes of weather patterns, observed confirm the general finding of Hurrell and Deser (2010), who noted the NAO had strong influence on weather patterns over Northern Europe.

7.3 Statistical Techniques

7.3.1 Generalised Extreme Value Distribution

Section 5.4.1, Figures 5.30 to 5.35 and Tables 5.1 to 5.4 showed the results for the Generalised Extreme Value (GEV) analysis for Newlyn and Devonport for both observed levels and the extracted storm surge levels. These show that the GEV models the data well when compared to the actual data, with the results for both locations and the observed and storm surge levels fitting a Weibull distribution. The results compare well to previous studies; Huang et al., (2008) found that the Weibull distribution of the GEV, modelled the observed tide gauge data for the Pacific, North East and Eastern Atlantic. Xu and Huang (2011) considered the GEV and the Weibull and Gumbel distribution at evaluating observe tide gauge data separately and found that the GEV provided more accurate results than when evaluating the frequency magnitude relationships by modelling the data with either the Weibull or Gumbel distribution separately. However, the GEV model of Xu and Huang (2011) selected the Gumbel distribution rather than the Weibull. The GEV was found to be statistically the best fit when modeling observed tide gauge data in both the work undertaken by Tsimplis and Blackman (1997) and Onofrio et al., (1999). Therefore, the GEV analysis models the observed tide gauge data using either the Weibull or Gumbel. From Figure 5.34 and 5.35, a comparison between the predictions made using a Gumbel and Weibull distribution show that both fit the data for Devonport, with an r^2 value > 0.9, however the Weibull is marginally better with an r^2 0.95 vs 0.93 for the Gumbel distribution. A visual assessment of Figures 5.34 and 5.35 shows that the Weibull models the higher return levels better than compared to the Gumbel distribution. Therefore, the Devonport data lies between the boundary of the two distributions. This is confirmed when subsets of the Devonport and Newlyn data have been analysed, with some subsets (i.e. 20 years worth of data) fitting the Gumbel rather than the Weibull distributions. Furthermore the Newlyn data for the majority of the data can be modeled by either the Weibull or Gumbel distribution; only at the higher return periods does the Newlyn data start to be modeled by the Weibull distribution.

Coles and Tawn (1990) and Dupuis (1997) identified that a minimum of 20 years of observed tide gauge data are needed to fully resolve the frequency magnitude relationship and allow the extrapolation of the prediction to higher return periods, beyond the observed data. This is confirmed by this study, where 20 year subsets of the data were able to predict the relationship. However, a comparison between

Newlyn and Devonport found that to fully resolve the Probability Density Function (PDF) more than 40 years worth of data are required. This is comparable to Huang et al., (2008) and Xu and Huang (2011) who utilised 70 and 90 years worth of observed tide gauge data to model the GEV.

Compared to the utilisation of the annual maximum observed tide gauge data to evaluate frequency magnitude predictions using the GEV methodology, the evaluation of extracted storm surge maximum using the GEV has received little attention. The GEV methodology is able to effectively model the frequency magnitude relationship of the extracted storm surge component. This is comparable to the study of Olbert and Hartnet (2010) who modeled 40 years worth of data for the Irish Sea. Olbert and Hartnet (2010) showed that the storm surge component could be modeled using a GEV and Gumbel distribution, identifying that the GEV was statistically the best representation of the data.

7.3.2 r-largest Distribution

To utilise more records than the GEV the r-largest methodology was developed. Within this study the r-largest methodology has been used to evaluate the frequency-magnitude relations of observed levels and storm surge levels. In addition, the r-largest methodology has been evaluated in order to establish the optimum value of r that should be adopted and the ability of the methodology to predict for different lengths of data sets.

Section 5.4.2, Figures 5.36 to 5.39 and Tables 5.5 to 5.8 showed the results for the r-largest analysis for Newlyn and Devonport for both observed levels and the extracted storm surge levels. The r-largest methodology gives comparable results to the GEV and can be seen to fit the Weibull distribution. The findings of this study confirm the findings of Coles and Tawn (1990) and Dupuis (1997) who evaluated the effectiveness of the r-largest approach on Venice from a 50 year observed tide gauge record. Coles and Tawn (1990) and Dupuis (1997) identified that the r-largest methodology could be applied to data sets between 10 and 25 years. This study corroborates this finding, identifying that it is possible to predict with 10 years worth of data, although the optimum value when comparing the results to the complete data set was 20 years.

Previous studies have identified that the choice of the value of “r” can vary the prediction made for storm surge frequency-magnitudes (Haigh et al., 2008).

However, within this study the choice of “r” (2 to 10) had little effect on the predictions of the frequency magnitude relationship (+/- 0.1 m), yet a comparison of the diagnostic plots of the model and actual data showed that the optimum value of “r” was 2, with a value of 5 providing a significantly better fit than a value of 10. This substantiates the findings of Guares and Scotto (2004) who identified the optimum value for “r” for significant wave height was 5.

Within this study the r-largest methodology was also attempted for the Mt Batten (Plymouth) wind speed record and the Polperro (Cornwall) wave data set. Due to the limited wave data set (7 years), the r-largest methodology was not able to adequately resolve the frequency magnitude relationship (Figure 5.21). The results of the r-largest predictions provide comparable results to the assessment of storm surge frequencies. Ying and Padney (2005) undertook an analysis of wind speed statistics utilizing the r-largest. The r-largest methodology utilized by Ying and Padney (2005) provided comparable results to other prediction methodologies. However the data of Ying and Padney (2005) fitted the Gumbel distribution within the r-largest methodology, whereas within this research the data approximated a Weibull distribution. Ying and Padney (2005) found that for wind speeds a value of r between 2 and 5 provided the best fit, corroborating the findings of the analysis undertaken for Mt Batten (Plymouth) wind speed record, which identified that a value of r=2 was most appropriate and the data approximated a Weibull distribution.

7.3.3 Generalised Pareto Distribution

The Generalised Pareto Distribution (GPD), also known as the Peak Over Threshold (POT) method, utilizes values above a certain threshold. This differs from the r-largest in that the number of values per year does not need to be equal. Harris (2005) found that the GPD could be extremely sensitive to the choice of threshold, An and Padney (2005) concluded that this was due to the GPD methodology not ensuring that selected values are independent. Within this study, only independent data above a threshold was selected, so that the issues of Harris (2005), and An and Padney (2005) did not occur.

Section 5.4.3, Figures 5.40 to 5.45 and Tables 5.9 to 5.12 showed the results for the GPD analysis for Newlyn and Devonport for both observed levels and the extracted storm surge levels. The GPD was able to predict the frequency-magnitude relationship to a high degree of accuracy when comparing the model to the actual

data. The GPD return level plot fitted a Weibull distribution, similar to the GEV and r-largest, but was observed not to reach a maximum value for Devonport, unlike the Weibull and r-largest distribution which for Devonport approach a maximum value, with little change in the magnitude of the predictions for higher return periods. For the Newlyn data set the GPD methodology was not able to model the upper values. When compared to the GEV and r-largest methodology the GPD was found to under-predict.

Tsimplis and Blackman (1997) evaluated the threshold selection of the GPD with an evaluation of an average of 3 and 7 results per year with results typically found to be within +/- 0.02 m. The results of this research found that the GPD was stable for an average of 10 values per year. This shows that this method has the ability to utilise more data than the r-largest methodology which was found to be optimised with 2 values per year.

7.3.4 Joint Probability Methodology

The Joint Probability (JP) methodology utilizes all hourly readings, deconstructing the observed sea level into astronomical tide and surge, calculating the individual probabilities and recombining them to evaluate the frequency-magnitude relationship. The methodology is computationally straightforward and can be undertaken in matrix form in Excel or similar software packages.

Section 5.4.4, Figures 5.46 to 5.49 and Tables 5.13 and 5.14 showed the results for the JP analysis for Newlyn and Devonport. From these results it is observed that the JP over predicts when compared to the results for the GEV, r-largest and GPD methodologies and the raw data. This finding is confirmed by Haigh et al., (2008) who evaluated the JP methodology for several channel coast locations. This contradicts the findings of Pugh and Vassie (1980) and Tawn and Vassie (1989) who concluded that the JP agreed closely with Gumbel distribution of the r-largest methodology. The JP methodology has predominantly been used within the U.K. to evaluate storm surge relationships, although Onofrio et al., (1999) utilised the JP to evaluate storm surge frequencies for Buenos Aeries, establishing that the JP provided a good fit to the data and corresponded to the Gumbel distribution for return periods up to 1 in 1000 years. The raw data for Devonport and Newlyn has been found to be closely modelled by the Weibull distribution rather than the

Gumbel, this suggests that the JP methodology typically follows a Gumbel distribution and cannot adequately model data that fits a Weibull distribution.

7.3.5 Monte Carlo Analysis

Similar to the JP a Monte Carlo analysis utilises the hourly records, deconstructing the observed sea level in to the astronomical tidal component and storm surge component. However, instead of recombining the probabilities in the form of a matrix, the Monte Carlo analysis, fits a Probability Density Function (PDF) to the data. The fundamental difference between the JP and MC methods is that in fitting a PDF, the MC method considers data at the extremes that have not yet occurred within the observed record and assigns a probability to these extremes. The MC methodology then recombines the two components using a Monte Carlo simulation.

Section 5.4.5, Figures 5.50 to 5.59 and Tables 5.15 and 5.16 showed the results for the MC analysis for Newlyn and Devonport. The methodology over estimates the frequency magnitude relationship when compared to the other statistical methods. This is primarily due to the Monte Carlo software package being unable to model the bimodal data set of the astronomical tidal component. The adjustment of using only the positive storm surges to compensate provides comparable results to the JP. Despite the limitations of the MC method to model a bimodal distribution, it has been found that the results of the frequency-magnitude relationship are repeatable with only a year worth of data, contradicting the findings of Niedoro et al., (2002) and Tara et al., (2010) who argue that the MC method is inefficient at evaluating extremes and require a great number of storms to evaluate the relationship.

Rahmen et al., (2002) and Pinya et al., (2009) undertook a MC analysis to evaluate the probability of coastal flooding based on observed data sets, using a relatively small number of iterations (<6000), identifying that optimizing the MC methodology could predict beyond a 1 in 100 year event. Within this research the Monte Carlo simulation was conducted with 10,000 iterations, with 10 simulations and to the evaluation of confidence intervals. This yielded results to >1 in 1000 years, although only up to a 1 in 1000 year event is reported. This illustrates that although time consuming (~48 hours per run), a comprehensive MC simulation can provide a high degree of accuracy.

7.3.6 Summary

Figure 7.1 and 7.2 show the optimum results for Devonport and Newlyn, respectively for the GEV, r-largest and GPD methodology at the 95% confidence interval. Considered independently each methodology provides a good representation of the raw data. However, comparing the three methods together, there is a close agreement between the GEV and the r-largest methods, but the GPD can be seen to under-predict, especially for the upper data for Newlyn. All methods were found to predict the extracted storm surge frequency-magnitude relationship well. The findings generally confirm the literature, with the GEV requiring >40 years of data, the r-largest requiring >20 years, with an "r" of between 2 and 5, and that for the GPD the key requirement are that data is independent, with an optimum threshold equating to an average of <10 events per year. In comparison to using extracted annual maximum or a series of data sets from the observed, the JP and MC methodologies utilise the complete hourly record. The findings from this study confirm the findings of previous studies for the JP analysis. However, the MC methodology was found to be significantly more effective at evaluating frequency-magnitude relationships than previously reported, with predictions being able to be made with only a year of data. A further factor that could lead to the MC method producing higher predictions when compared to the JP method is that the MC method considers extremes that have not occurred or been recorded, whereas the JP method only considers recorded data. As the PDF probability for the MC method must always equal 1, to account for the unseen data the MC method reduces the probability of all other data.

The GEV, r-largest and GPD methodology can be considered to represent the historical record. In comparison, due to the deconstruction of the data the MC and JP methodology can be considered as being a "what if" scenario. i.e., what would be the inundation level of the highest storm surge with the highest astronomical tide, despite possibly not having occurred within the historical record. As such this approach leads to an over-estimation when compared to the other methodologies and can be considered a conservative approach.

A large component of the GEV, r-largest and GPD methodologies is the tidal component, with a range between 0-6 m, compared to the storm surge component with a range between 0 and 1 m. This large tidal component, that over the length of

the data set of almost 100 years is stable, could potentially have a dampening effect on the overall predictions.

An alternative way to evaluate the “what if“ scenario was identified by using the predictions made for the extracted storm surge frequency-magnitude predictions made using the either the GEV, r-largest or GPD and superimposing on to a mean high water spring astronomical tide level. Thus it is possible to re-create a conservative scenario using as little as two storm surge levels for 20 years. This means that locations with little or no records could utilise archives of newspapers, parish records etc. to recreate a record of historical storm surge levels and thus evaluate frequency-magnitude relationships.

Figures 7.3 and 7.4 show a comparison of the predictions made for Devonport and Newlyn, respectively, with the guidance provided by the Environment Agency (Environment Agency, 2011). The methodology adopted by the Environment Agency is the Spatial Joint Probability, a bespoke methodology developed by Dixon and Tawn, (2007), which evaluates a 7.0 mCD magnitude event for a 1 in 1000 year event for Devonport, compared to a value of 6.6 mCD based on the extrapolation of the data based on the historical data or 7.2 mCD for the Monte Carlo analysis. The Environment Agency (2011) guidance can be seen to provide close agreement with the Joint Probability and Monte Carlo results, as part of this research for both Devonport and Newlyn. The predictions of the Environment Agency (2011), in a similar manner to the JP and MC results of this research do not represent a prediction based on the historical record, rather a what if scenario.

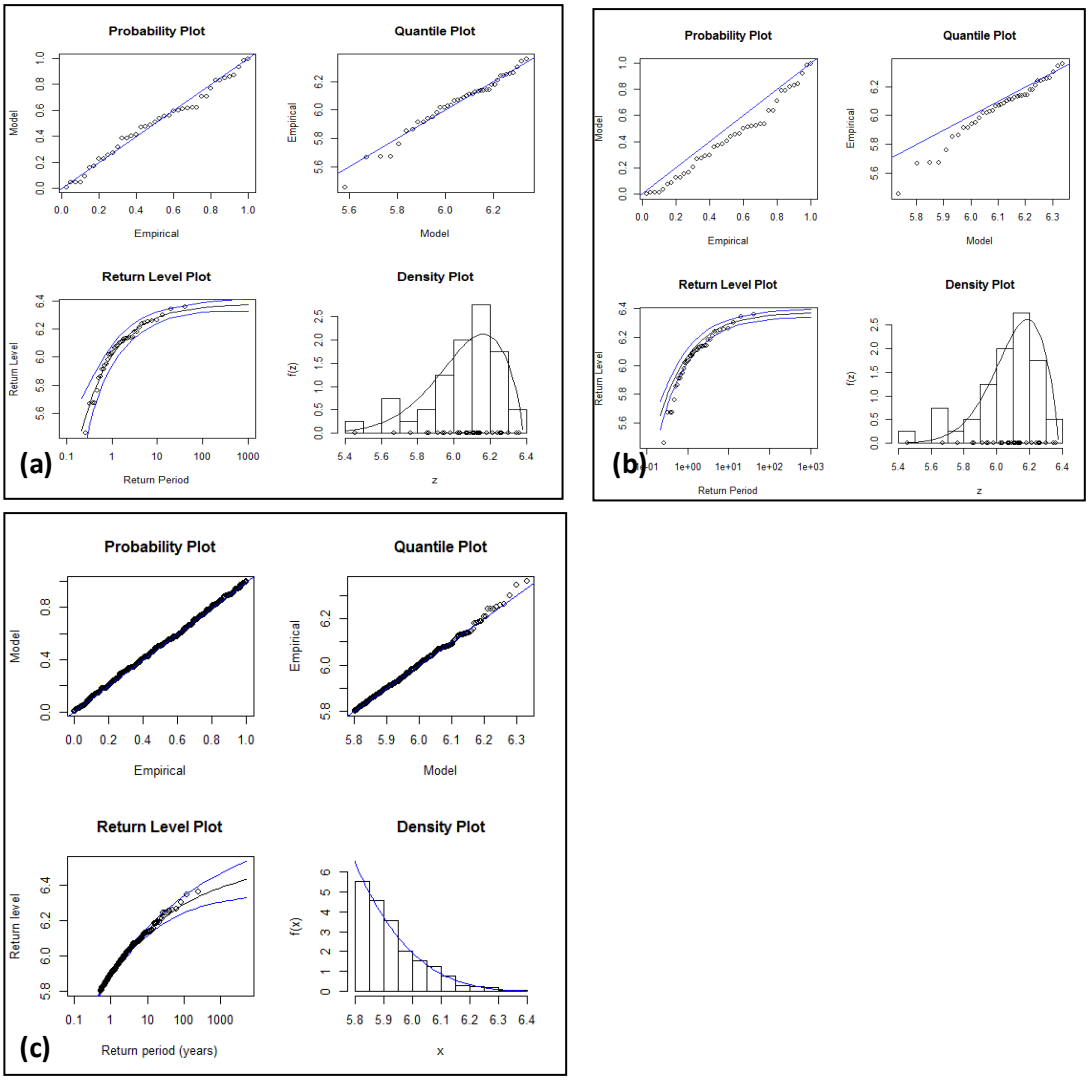

Figure 7.1 Comparison of (a) GEV, (b) r-largest and (c) GPD Diagnostic Plots for Devonport for the period 1962-2012. See Chapter 5 for more detailed graphs.

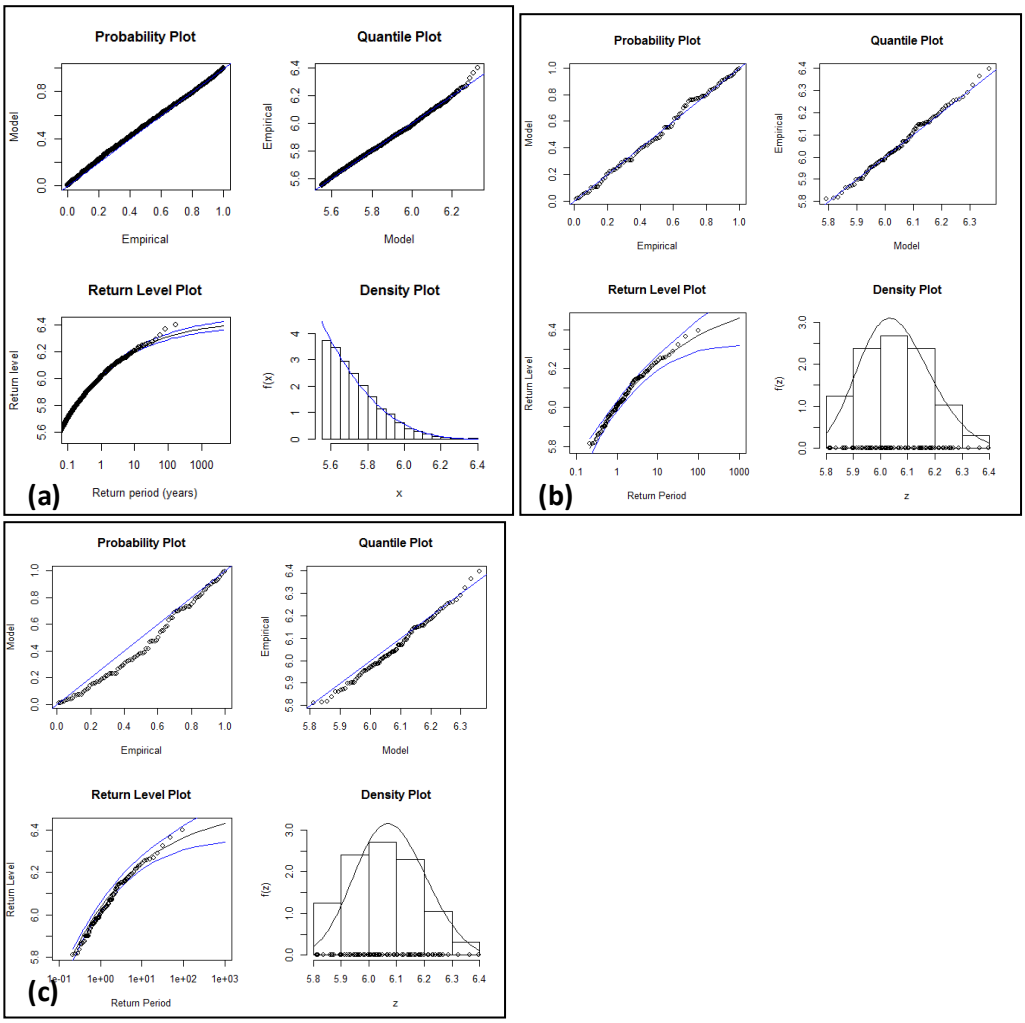

Figure 7.2 Comparison of GEV, r-largest and GPD Diagnostic Plots for Newlyn for the period 1915-2012.

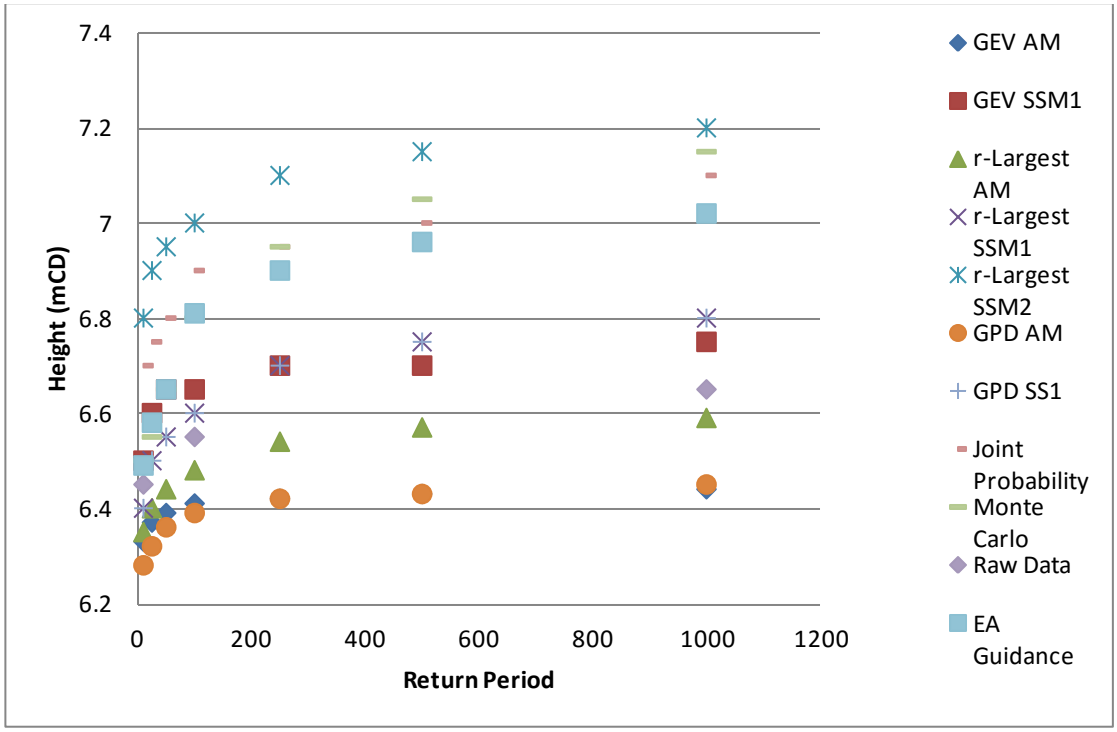

Figure 7.3 Comparison Graphs for Inundation Predictions, including Environment Agency Guidance for Devonport.

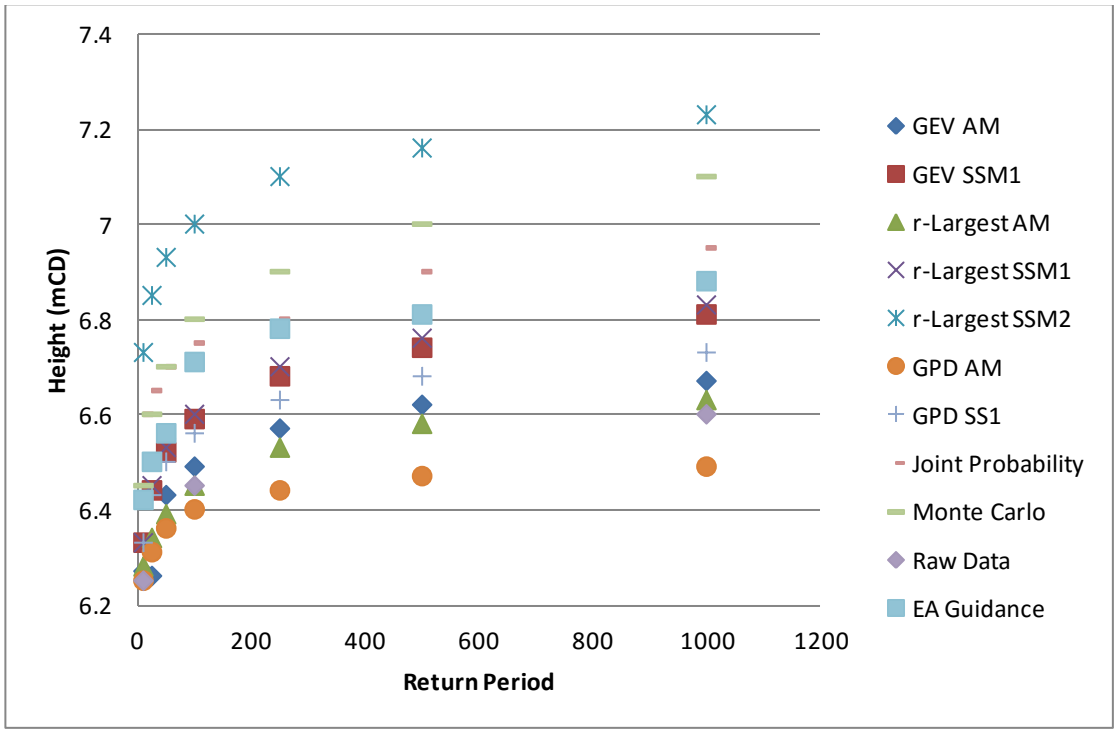

Figure 7.4 Comparison Graphs for Inundation Predictions, including Environment Agency Guidance for Newlyn.

7.4 Geographical Information System Inundation Modeling

To date no research has evaluated the effect of different scenarios and modelling the difference in inundation within a Geographical Information System (GIS). Within this research a GIS model has been developed utilising a Digital Elevation Model (DEM) and basic infrastructure data. Overlain on these data were the different inundation levels resulting from different frequency magnitude predictions and the affect of wave set and wave height. The results have been summarized in Chapter 6, with Figures 6.3 to 6.20 illustrating the different inundation levels modelled. From this analysis the total area affected and the total area of buildings affected has been calculated to provide a quantitative measure of the different scenarios. The affect of different frequency magnitude predictions have been compared to different sea-level rise predictions for south-west England (UKCP, 2009).

DEFRA (2001) estimated that the increase in flood damage (fluvial and coastal), could lead to an increase in annual cost for the U.K. from £150 million to £650 million by 2050 for a 2° to 3° temperature rise. For the south-west of England the estimated annual damages rise from £51 million to £60 million by 2075. In 2012 DEFRA produced a Climate Change Risk Assessment for the England and Wales (DEFRA, 2012). At present day levels it is estimated that 0.9 million people will be affected by flooding (fluvial and coastal), rising to 1.3 million people in 2050 and 1.7 million by 2080. The number of properties affected are estimated to increase from present day figures of 0.56 million to 0.77 million in 2050 and 0.98 million in 2080 (DEFRA, 2012). For south-west England, an area of coastline stretching from Gloucester in the north to Bournemouth in the south, it is estimated that between 0 and 50,000 people are affected by coastal flooding today, rising to between 100,000 and 200,000 people by 2050 under medium sea-level rise scenarios. The number of residential properties predicted to be affected rises from between 50,000 and 100,000 properties at present day levels to 100,000 and 200,000 by 2050 under medium emission scenarios (coastal and fluvial flooding). The figures of DEFRA (2012) appear to be low compared to the predictions of Hall et al., (2005) who undertook a U.K. wide assessment of flood risk (coastal and fluvial) and estimated a rise from 1.6-3.5 million people affected at present day levels to 4.5-6.9 million by 2080. Within the U.K. there are areas that are more vulnerable to flooding than others. Purvis et al., (2008) evaluated future coastal flood risk due to sea-level rise for the Somerset Levels and found for a 0.48 m sea-level rise that for a 1 in 100 year event the area inundated increased from 1.1 km^2 to 11.3 km^2, for a 1 in 1000

year event the area changed from 5.7 km^2 to 24.6 km^2. For the Thames estuary, in an assessment of regional scale flood risk under medium emission scenarios the annual economic impact rose from present day of £3.4 million to approximately £50 million by 2080 (Coully et al., 2010). The impact of sea-level rise in the U.K. compares with the global assessment of Nicholls (2004), who estimated that by 2080 an additional 7 to 29 million people could be affected annual, compared to 10 million people affected in 1990. The increase in the affected people and areas for the U.K. is similar to regional assessment in other countries. Haer et al., (2013) estimated that due to sea-level rise the increase in land of the eastern coast of the United States affected would increase from 30,000 km^2 to 50,000 km^2 by 2100, with the number of people affected to increase from 1.8 million to 3.2 million. A lower percentage increase of areas affected due to sea-level rise was observed by Lichter and Felenstein (2011), who found that due to an increase of 0.5 m sea-level rise the area affected within the coastal areas of Tel Aviv, Israel, changed from 19,000 m^2 to 23,000 m^2, a 20% increase compared to the study of Haer et al., (2013) who identified a 40% increase in the area affected. A "Dragon King" event has been modeled using the H++ sea=level rise scenario and indicates that 18.0 km^2/0.75 km^2 of land/buildings would be effected

Within this study four different sea-level rise scenarios were assessed based on UKCP (2009). A low value of 0.30 m, a mid-range value of 0.46 m, a high range value of 0.78 m and a H++ scenario of 1.8 m (all by 2100). At present day levels, for the study area of Southwest England based on a 1 in 250 year event 8.6 km^2 of land and 0.2 km^2 of buildings would be affected. This would increase to 9.5 km^2/0.25 km^2 (total area/buildings-Low), 10.8 km^2/0.3 km^2 (mid-range), 13.0 km^2/0.40 km^2 (high range) to 18.0 km^2/0.75 km^2 (H++). At the mid-range prediction this equates to a 25% increase in land affected and a 50% increase in buildings affected. In comparison the change in inundation for a 1 in 1000 year flood event due to different prediction methodology equates to an increase in area from 8.6 km^2 to 13.0 km^2, with an increase in buildings affected increasing from 0.2 km^2 to 0.4 km^2. This equates to >50% increase in land affected and 100% increase in buildings affected. The effect on inundation levels due to different prediction methodology is greater than the effect of mid-range sea-level rise on a 1 in 250 year event and equivalent to the affect of the high range sea-level rise predictions on the same event. Therefore there is a significant affect caused by the choice of methodology that represents the historical record (i.e. GEV, r-largest, GPD) or a methodology that represents a "what if" scenario (i.e. Joint Probability or Monte Carlo method). An alternative way to look at the results is that a level of 7.2 mCD

can be considered to provide a level of protection up to 2050 for a “what if” prediction for a 1 in 250 year event, or up to 2100 for a prediction for a 1 in 250 year event based on a methodology that represents the historical record.

The findings of the GIS modelling of the sea-level rise scenarios within this study show that the south-west of England is as susceptible to sea-level rise as other parts of the United Kingdom, with a similar change in the area affected and buildings affected when compared to DEFRA (2012). On a global scale, comparing studies of developed countries (Lichter and Felenstein, 2011 and Haer et al., 2013), the increase in area affected by sea-level rise for Southwest England is greater. Comparing globally to Nicholls (2004), the study area has similar changes. It is worth noting that within the studies of DEFRA (2012), Nicholls (2004) and other referenced work, that a population increase is incorporated within the models. Within this study population change has not been modelled and therefore the total number of buildings affected could potentially increase. However, an aim of this study is to help inform planning, which should enable the effect of sea-level rise to be mitigated. This topic will be discussed in Section 7.6.

As part of the scenario development, consideration was given to the affect of wave height at Devonport Dockyard (Plymouth) and wave set up at Looe and Par (Cornwall). It was identified that Devonport Dockyard, would be overtopped at the present day given a 1 in 1000 storm surge and coincident wave height. Although the duration would be relatively short and the height of overtopping relatively small (<0.5 m) the research identifies that under future sea-level rise overtopping and subsequent inundation could become a significant issue. For Looe and Par, the inclusion of wave setup on to the inundation levels did not significantly affect the area of inundation for the scenarios considered (1 in 250 and 1 in 1000 year inundation event). However, the inundation depth and thus the potential damage that would likely be caused would increase if wave set up is taken in to account. There is the potential that for lower magnitude events, wave setup could become more dominant and affect the point at which inundation occurs. At present modeling of flood events do not take in to account wave set up (e.g. Bates et al., 2005; Smith et al., 2012). The modeled wave height and wind setup illustrates that they play a crucial role in evaluating the potential hazard poised by inundation events and the affect they have on the probability of overtopping and the overall level of inundation. These components should be incorporated in to the evaluation of both the probability of inundation and the potential affects these levels might have on the population and infrastructure of a given area.

7.5 Model Validation-January and February 2014 Storms

During the period of January and February 2014, the south-west of England was affected by a series of storms that affected the study area (BBC, 2014). The period was classified as exceptional as there was a clustering of storms that was highly unusual (Met Office, 2014). The following documents the storms of January and February 2014, based on news and newspaper articles and tidal gauge records from Newlyn and Devonport. The findings are then analysed to evaluate how effective the statistical results and the GIS model were at representing the storms, whether or not the storms were exceptional, and whether it affects the overall predictions for the study area.

Figure 7.5 shows the locations of the areas affected by the January and February 2014 storms. Between January and February 2014, three larges storms occurred on the 4th January, 31st January and 4th February. Wind records indicate maximum gusts of >110 km/hr, with low pressure measurements <950 mb (Met Office, 2014). Minor flooding was recorded at Devonport, with wave damage to the Plymouth water front occurring on the 31st January. Due to high wind speeds the Tamar Bridge was closed on the 4th January (BBC News Feb 2014, Plymouth Herald Feb 1st, Feb 5th). Further along the coast the Kingsand (Cornwall) clock tower was damaged by waves on the 4th February, with Looe and Seaton (Cornwall) flooded on the 4th January, 31st January and 4th February and Par on the 31st January (EA correspondence, (BBC News Feb 2014, Plymouth Herald, Jan 5th, Feb 1st, Feb 5th). Damage to Penzance sea wall occurred on the 31st January and the 4th February, with flooding occurring at Newlyn.

Figure 7.6 and 7.7 show the recorded tide gauge levels and the extracted storm surge levels from Devonport and Newlyn respectively, for January and February 2014. The maximum observed tide gauge level was 6.4 mCD and 6.45 mCD for Devonport and Newlyn, with a maximum storm surge level of 0.95 m at both locations. Maximum astronomical tidal components during the storm surge were between 5.9 mCD and 6.0 mCD. Figures 7.8 to 7.11 show the 10 largest independent extracted observed and storm surge levels for January and February 2014 plotted against the data for 1962-2012 for Devonport and 1915-2012 for Newlyn. From this it can be seen that the cluster of storm events is quite exceptional, with the recorded maximum observed and storm surge levels for both Devonport and Newlyn close to the maximum recorded. The cluster of data, exceeds the records for the previous years, and this is most pronounced in the Devonport storm surge data (Figure 7.9). The data cluster for observed levels for

both Newlyn and Devonport is not quite as exceptional as the storm surge records, with the cluster of data having been repeated over previous years. The data of the observed maximum indicates a continuation in the upward trend observed since 2008 (Figure 7.8 and 7.10). From the observed record of the January and February 2014 storms it can be seen that there is a portion of missing data (Figure 7.6). From an extrapolation of the data to model the missing data, the storm surge could potentially have reached a maximum amplitude of 1.10 m (maximum value in Figure 7.6).

To evaluate the effectiveness of the predictions already made and the sensitivity to new data, the original Generalised Extreme Value (GEV) and r-largest analyses were updated with the data from the January and February 2014 storms. The results of this analysis are presented in Figures 7.12 and 7.13. From an analysis with the 2014 observations it was found that the results were within +/-0.05m at the 95% confidence interval for all results, except the Devonport storm surge data. It was found that at the 95% confidence interval the value for a 1 in 250 event was 0.1 m higher and for a 1 in 1000 year event 0.2 m higher. The mean results were within +/- 0.05 m. The main reason for this can be identified in the shape of the graph. Previously the Devonport data was observed to reach a plateau, were an increase in return period resulted in only a small increase in the magnitude. With the addition of the 2014 data a plateau in the graph has not been reached, leading to a greater increase in the magnitude of an event for the same increase in return period. This indicates that the Devonport data could be sensitive to additional data.

An attempt was undertaken to evaluate the affect of the January and February 2014 storms on the Monte Carlo Analysis. Figure 5.59 shows the prediction made utilising only the January and February storm surge values and one year of astronomical tidal observations. The prediction is approximately 0.2 m higher that the predictions made utilising the complete, and one year data set. However, the result demonstrates that potentially the Monte Carlo methodology could adequately evaluate the frequency magnitude relationship by as little as 2 months of data.

The observed locations of the inundation that occurred during the January and February 2014 storms, closely match the predicted locations within the GIS modeling. This, with the validated statistical methods provides confidence in the methodology and results of this research.

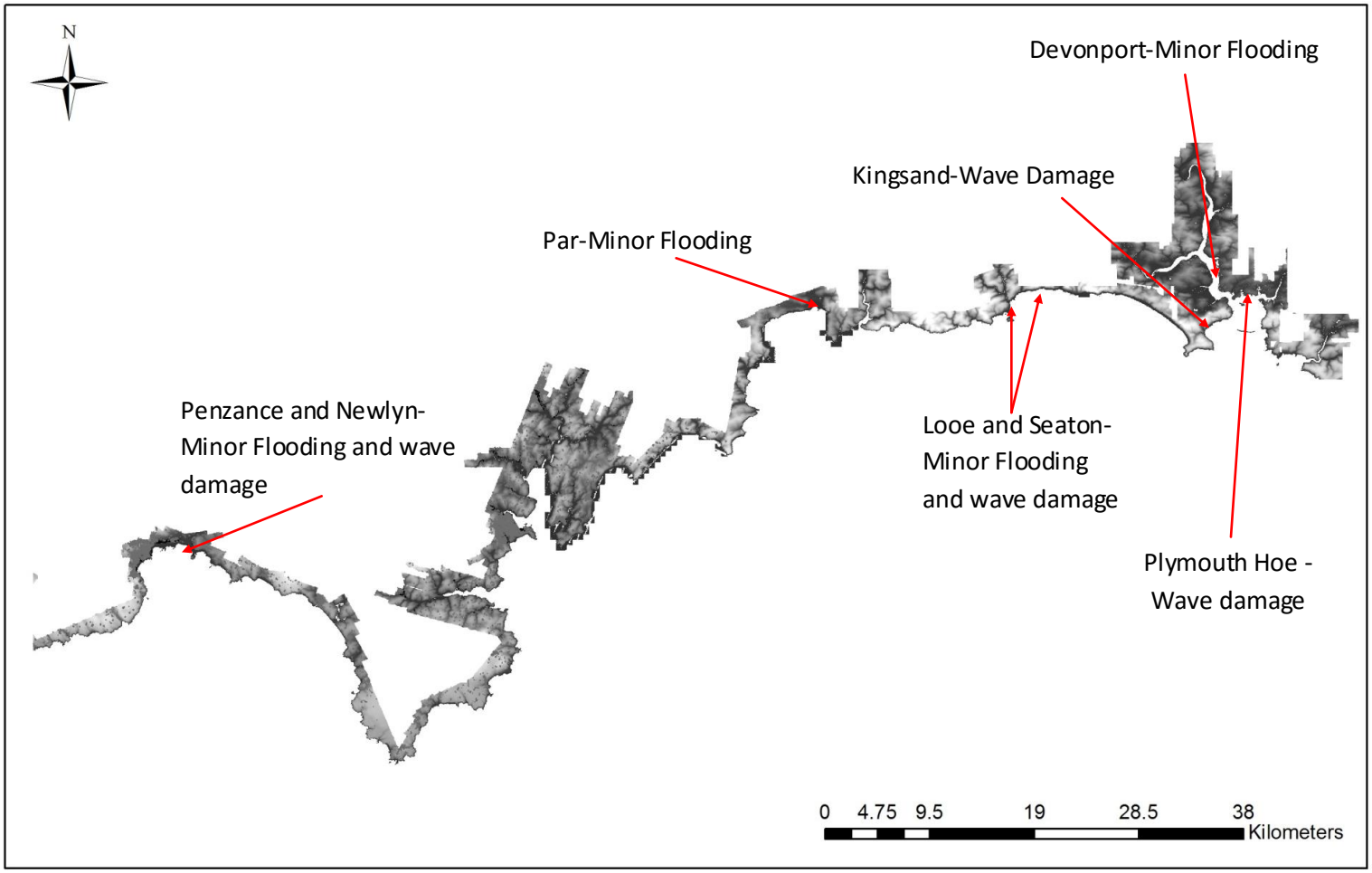

Figure 7.5 Map showing locations affected by the January and February 2014 storms.

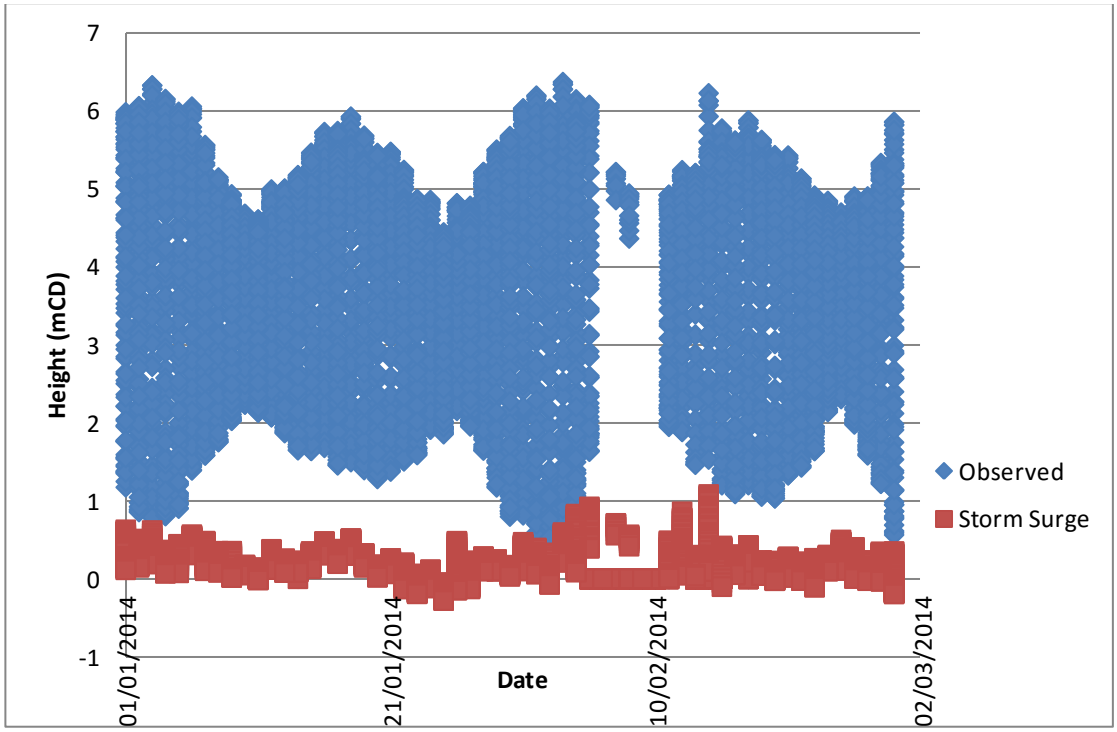

Figure 7.6 Devonport tide gauge record for January and February 2014.

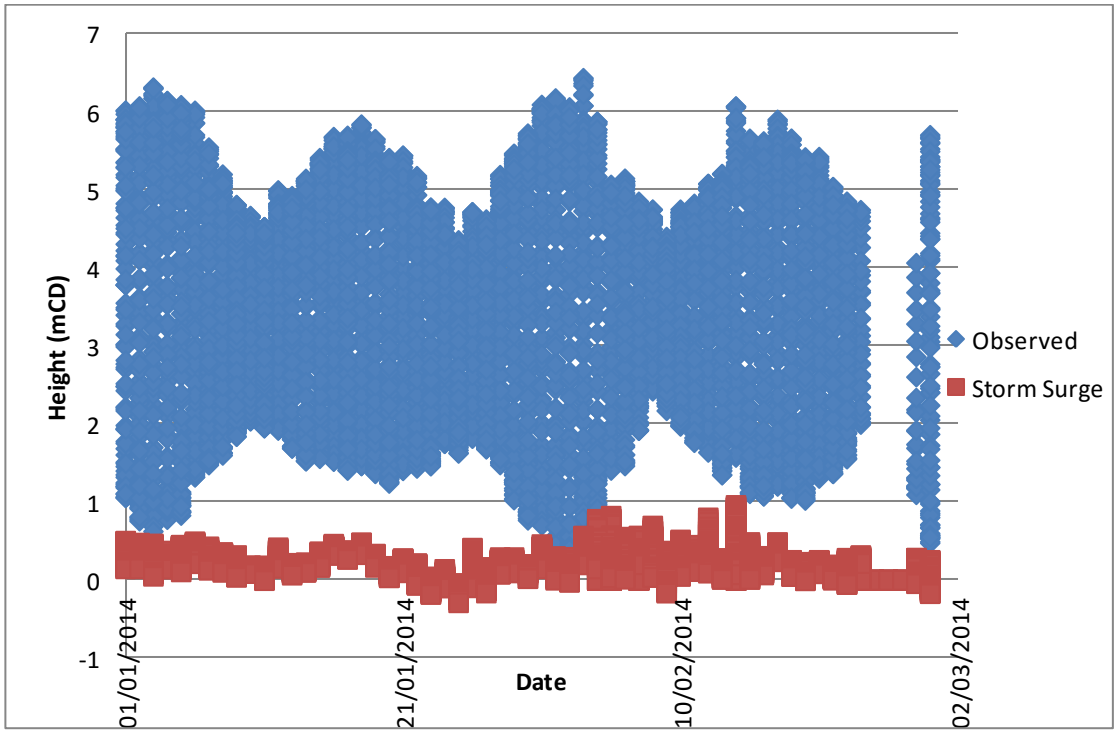

Figure 7.7 Newlyn tide gauge record for January and February 2014.

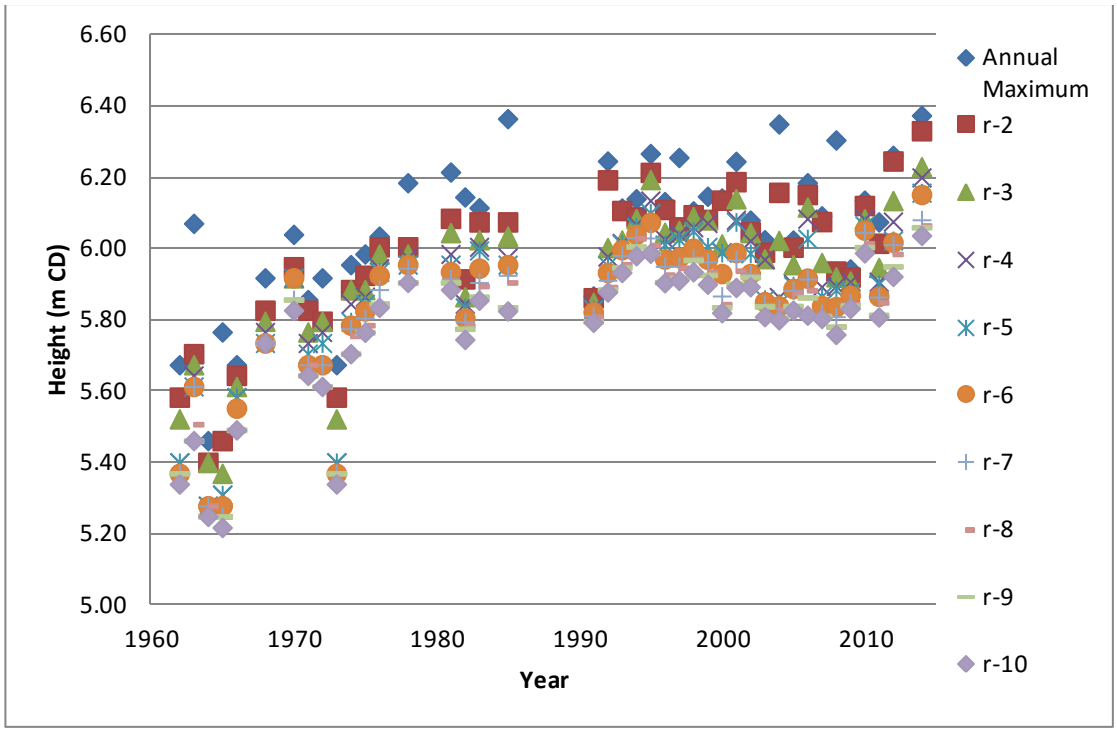

Figure 7.8 Ten largest Observed record for Devonport including the tide gauge record for January and February 2014.

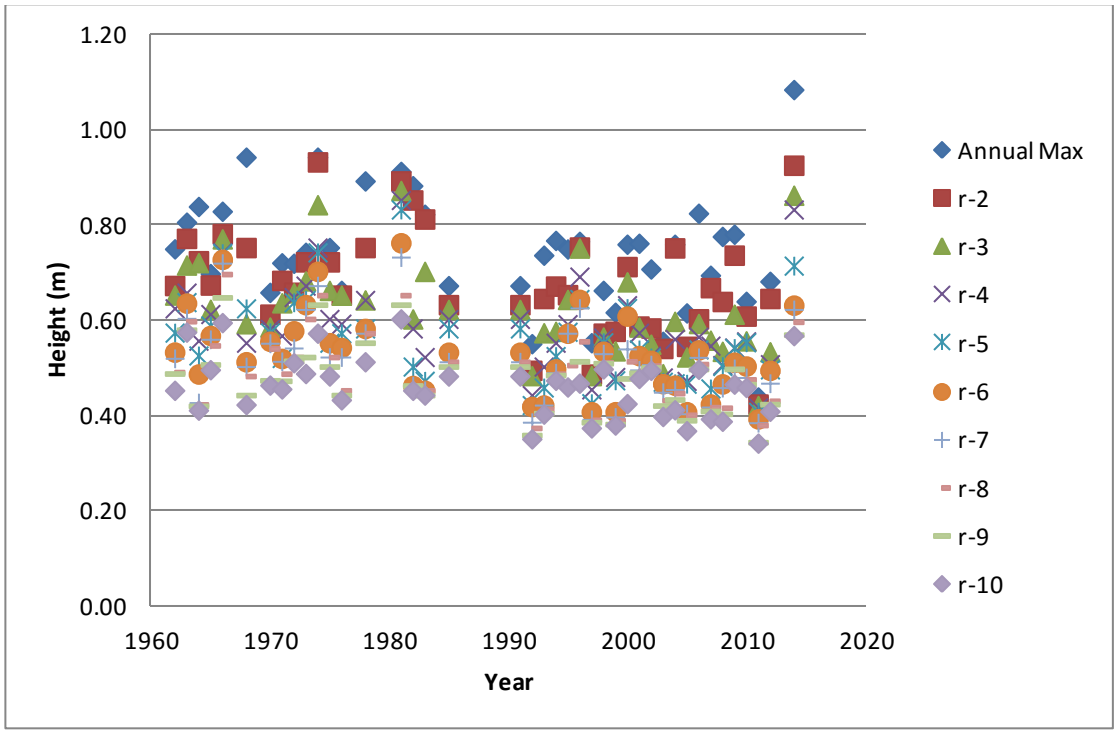

Figure 7.9 Ten largest storm surge records for Devonport including the tide gauge record for January and February 2014. The annual maximum storm surge value for 2014 is a hypothetical value based on extrapolation from missing records discussed in text.

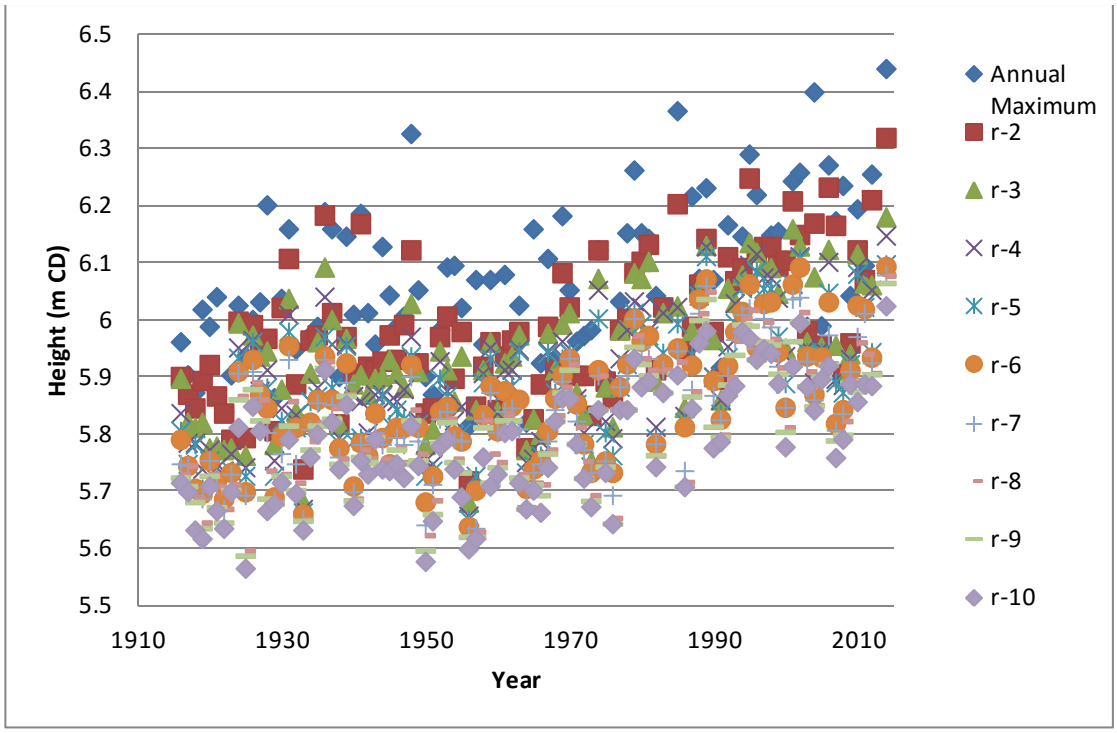

Figure 7.10 Ten largest Observed record for Newlyn including the tide gauge record for January and February 2014.

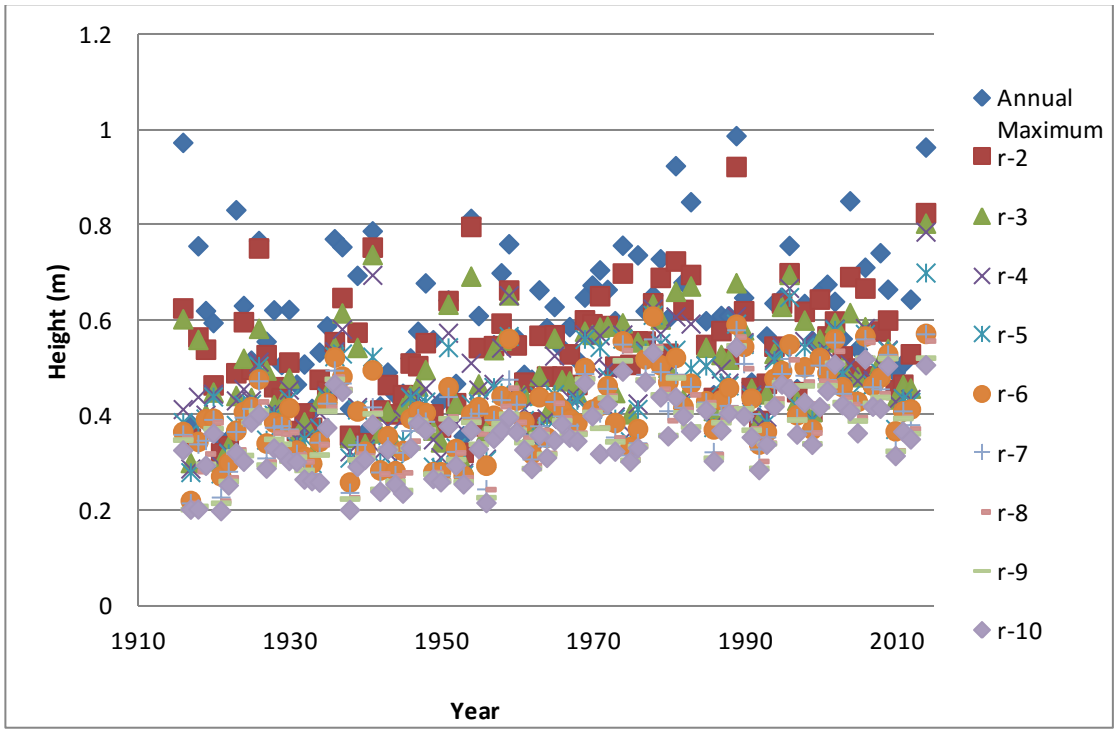

Figure 7.11 Ten largest storm surge records for Newlyn including the tide gauge record for January and February 2014.

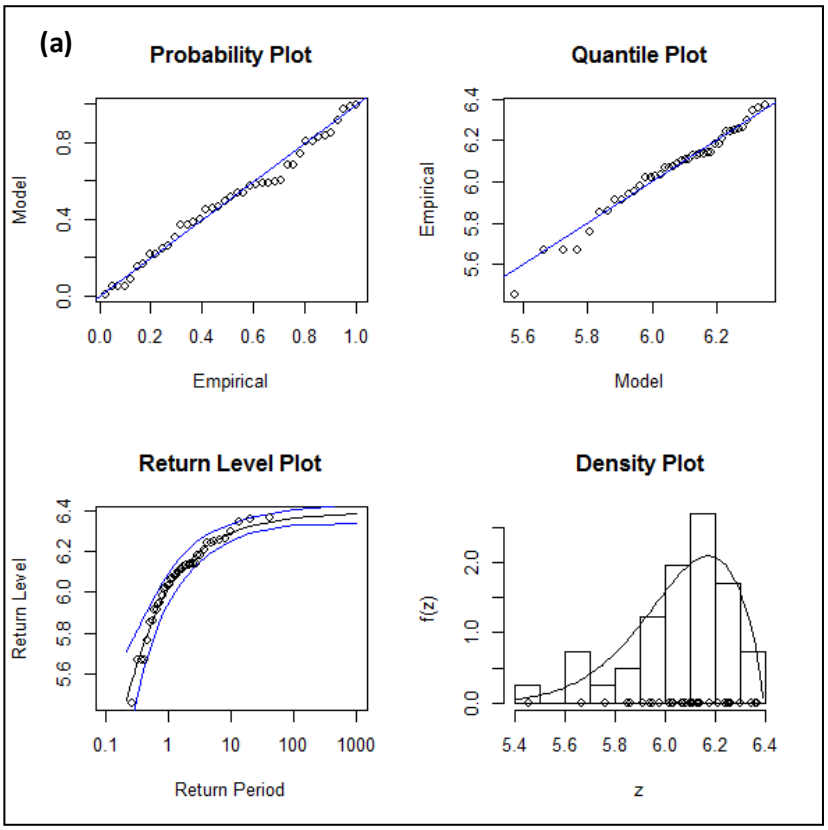

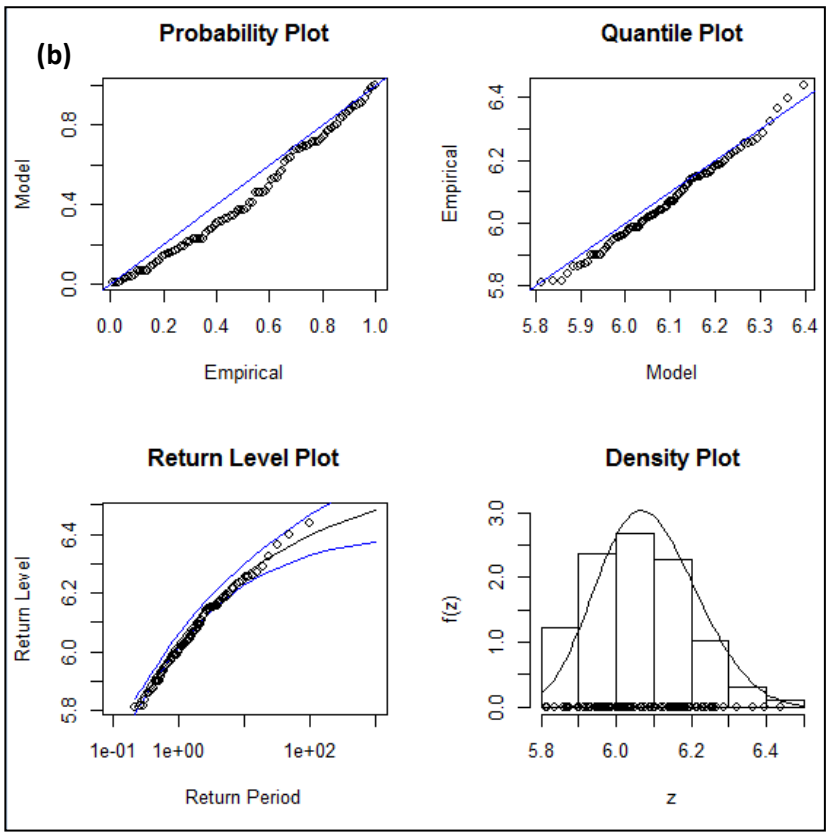

Figure 7.12. GEV (a) Annual Maximum and (b) storm surge maximum analysis for Devonport incorporating records from January and February 2012.

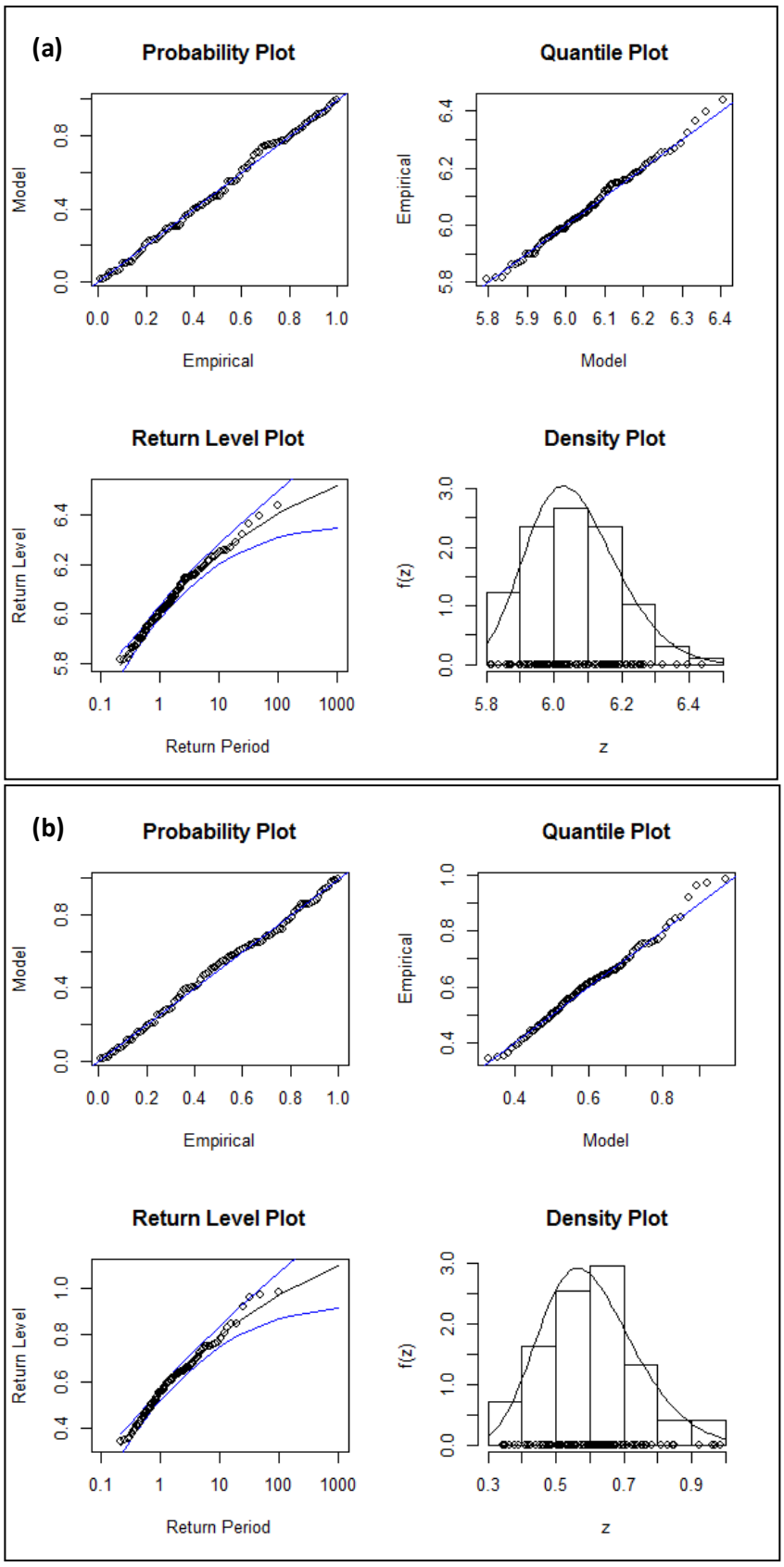

Figure 7.13 GEV (a) Annual Maximum and (b) storm surge maximum analysis for Newlyn incorporating records from January and February 2012.

7.6 Errors and Uncertainty

An important component of communicating the findings of this study is an understanding of the errors within the data and uncertainties within the study. Manning (2006) stated that that "policymakers required not only an expression of numeric ranges..., but also information on how confident scientists were of the basis of the quantitative statements. The follow Section summarises the potential errors within this study and evaluate the uncertainty of the predictions made.

7.6.1 Errors

Within this study there are several sources of error that could lead to uncertainties within the assessments made, both quantifiable and unquantifiable. The following table summarises the potential errors, how these could affect the study and the methodology adopted to reduce, limit or reduce the effect of the error.

Error Source	Implications	Methodology to identify/limit Error
Incorrect manual input of data from archival paper record for Devonport 1961-1987.	Erroneous observed tide gauge level, extracted data (i.e. annual maximum) leading to errors in Extreme Value Analysis.	1. Visual inspection of graphical data within excel to identify outliers. 2. Trend Analysis within Matlab to identify erroneous outliers. 3. Newspaper research to identify largest events in database did coincide with physically observed and recorded storm surge. 4. Trend analysis (See results) undertaken to check for unexplained trends.
Incorrect selection of extracted data.	Errors within Extreme Value Analysis leading to incorrect analysis of frequency magnitude relationships.	1. Trend analysis (See results) undertaken to check for unexplained trends. 2. Comparison between Newlyn and Devonport records to check results. 3. A random sample of years for each data set selected and checked to ensure consistent results. 4. Several Extreme Value techniques adopted within study.
Statistical Predictions.	Incorrect analysis of frequency magnitude predictions and subsequent assessment of impacts.	1. Several Extreme Value techniques adopted within study. 2. Undertaken assessment using both software and manual calculations to verify relationships. 3. All values quote to the 95% 95% confidence level.
LiDAR Digital Elevation Data.	Incorrect assessment of impacts.	1. Errors in LiDAR data quantified to +/- 0.1 m. 2. Intervals of 0.1m assessed to check that no "cliff edge effects" occur. For example no unexplained inundation occurs with addition of small flood elevation. 3. "Stitching of LiDAR data visually checked. No unexpected areas of inundation.

Table 7.1 Sources of error within the study, the potential implications and the methodology used to identify, reduce or limit the effect of the error.

7.6.2 Uncertainty

The following qualitative assessment of uncertainty is based on the guidance provided by Mannin (2006), IPCC (2007) and Risbey and Kandlikar (2007). The aim of which is to provide an indication of the confidence in the assessment. The qualitative assessment of uncertainty of each component of this study is accompanied by a series of justification to enable the end user to communicate the findings effectively. No indication of uncertainty linked to the assessment of future changes, which have been calculated based on the predictions of others has been undertaken.

There is high agreement and much evidence, giving a very high degree of confidence that indicates sea level has risen within the study area by at least 1.8mm/yr +/- 0.2 (95%) since 1915. Both Newlyn and Devonport sea-level trends indicate this as a minimum value, confirming the rates from established literature (Section 7.2).

From a review of sea-level trends, observed maximum and storm surge frequencies there is high agreement and much evidence, giving a high degree of confidence that the observed trends showing an increased frequency is due to sea-level rise rather than an increase in storminess over the study area. When subtracting the sea-level rise component from both data the Newlyn and Devonport data sets, there is no statistical significant trend. This is confirmed by established literature which indicates no increase in storminess in the study area over the 20th century.

There is a high degree of confidence that a 1 in 250 year storm surge event for the study area occurred today would be a maximum of 6.90 mCD (95%). There is medium confidence that a 1 in 1000 year storm surge event would be a maximum of 7.2 mCD. The record for Newlyn spans 100 years, with Devonport spanning 50 years. There is high agreement and much evidence for up to a 1 in 250 year event as predictions made with the two different data sets agree. In addition the methodology has been tested with an outlier from the storm surge of 2014 that found the analysis was stable with the addition of new data. The confidence in the 1 in 1000 year prediction is reduced as, caution must be adopted when extrapolating to longer return periods and the fact that the assessment cannot evaluate for the unseen outlier or “Dragon king”. The predictions made within this study for the storm surge frequency magnitude relationship lie within the bounds of the established literature (Section 7.3).

There is very high confidence that a minimum of 8.6 km^2 of land and 0.2 km^2 of buildings will be affected by a 1 in 250 year event, with this increasing to a minimum of 13 km^2 of land and 0.4 km^2 of building affected for a 1 in 1000 year event. The values correspond to the lowest and therefore, the minimum potential impact of an event, with the assessment confirmed by the established literature.

Chapter 8 Conclusions and Recommendations for Further Work

8.1. Introduction

The overall research question was:

Using a case study approach, to evaluate the utilisation of probabilistic techniques in the assessment of extreme coastal flooding frequency-magnitude relationships.

Allowing the identification of the dominant uncertainty in coastal processes, the frequency-magnitude predictions or sea-level rise predictions.

The main project objectives are:

1. To digitise data for the period 1962-1987 for Devonport, increasing the data length to 40 years. This will allow a comparison with Newlyn and an evaluation of the uncertainties in frequency magnitude relationships. In addition the increased data set will provide greater confidence in the modelled sea-level trend for the study area.
2. To critically evaluate storm surge and wave height frequency-magnitude relationships and the level of uncertainty using the following probabilistic modelling techniques:
    a. Extreme Value Analysis.
    b. Monte Carlo Simulations.
3. Using a Geographical Information System to produce visual representations of inundation levels due to storm surge, including an evaluation of the sensitivity of south-west England to inundation as a result of the uncertainty in frequency magnitude predictions and sea-level rise predictions.
4. To provide guidance on how uncertainty might be incorporated within planning and design decisions.

To achieve this, 20 years worth of hourly hard copy data for Devonport, equating to almost 200,000 data points was digitised to provide a record for the period 1962-2012 (10 years of missing data), increasing the data length by 100%, from 20 years to 40 years. This enabled a robust evaluation of sea-level rise, and evaluation of storm surge frequency magnitude relationships, allowing a comparison of the Devonport data set to Newlyn (1915-2012) to be undertaken. Five statistical techniques were utilised to evaluate the storm surge frequency magnitude relationship, each utilising the data sets in different ways. To understand the affect

the different statistical techniques had on inundation levels, a Geographical Information System (GIS) was developed to evaluate the extent of inundation levels and compare the effect of the different prediction to the effect of different sea-level rise scenarios for Southwest England. Section 8.2 summarises the findings of the research linking to the original objectives (Section 1.2) of the research, with recommendations for future work detailed in Section 8.3.

8.2 Objectives (From Section 1.2)

8.2.1 Objective 1

To digitise data for the period 1961-1987 for Devonport to provide greater confidence in the sea-level trend for Plymouth and the predictions for storm surge magnitude frequency relationships.

- A unique data set has been created, extending the Devonport data set back to 1962, allowing a comprehensive assessment of sea-level rise and storm surge frequency magnitude relationships. This is the first such study to utilise the data set for the period 1962-2012 (Devonport) and 1915-2012 (Newlyn).
- The extended data set has allowed the evaluation of storm surge frequency-magnitude relationships that would otherwise have not been possible (e.g. Generalised Extreme Value Analysis).
- Based on the new data made available in this research, the predictions for sea-level rise for Devonport (2.1 mm/yr +/- 0.3) are comparable to that made for Newlyn (1.8 mm/yr) and compare well to previous studies.
- Based on the r^2 value an exponential growth (0.0001 mm/yr^2) provides a better fit to the modelled sea-level rise indicating slightly higher rates of present day sea-level rise of 1.9 mm/yr and 2.2 mm/yr for Newlyn and Devonport, respectively. If this exponential trend continues, the increase in sea level by 2100 would equate to 0.20 m, close to the low end predictions of UKCP (2009).
- If the U.K. mean trend of sea-level rise (excluding isostatic adjustment) of Woodworth et al. (2012) is incorporated, it indicates a rate of subsidence of 0.5 mm/yr for Nelwyn and 0.7 mm/yr for Devonport, comparable to the GPS data of Teferele et al., (2009).

- The observed sea-level trends in the data sets for Devonport are comparable to the trends observed in the Newlyn data set providing confidence in the Devonport data.
- Minor differences between Devonport and Newlyn mean sea-level trend could potentially be explained by an increase in landward fluvial contribution to the Devonport tide gauge over the length of the data set.

8.2.1 Objective 2

Using a case study approach, to critically evaluate storm surge and wave height frequency-magnitude relationships using a variety of statistical techniques.

- Five statistical techniques have been utilised to evaluate both the observed levels and extracted storm surge levels. This is the first study of its kind to compare the Generalised Extreme Value (GEV), Generalised Pareto Distribution (GPD), r-largest, Joint Probability (JP) and Monte Carlo (MC) analysis to evaluate frequency magnitude relationships in relation to observed tide gauge levels and the extracted storm surge levels. To incorporate uncertainty all methods evaluated the frequency-magnitude relationship at the 95% confidence interval.
- The different statistical techniques utilise the data in different ways. The GEV utilises the extracted annual maximum; the r-largest the extracted 10 largest annual observed events; the GPD utilises the extracted events above a specified threshold. This compares to the JP and MC approaches that utilise the hourly tide gauge data, decomposing to consider separately the astronomical tide and storm surge component. It was identified that the methodology that used extracted data i.e. the annual maximum or 10 largest events gave predictions that represented the historical data well. The data that utilised the hourly observations, when compared to data to the raw data, did not represent the historical record but gave a conservative "what if" evaluation of the frequency magnitude relationships (i.e. what if the largest storm surge coincided with the highest astronomical tide).
- The results for the different analysis showed that depending on the methodology chosen at the 95% confidence the magnitude for the same frequency of storm surge event could vary by up to 0.8 m (1 in 1000 year

storm surge event). This compares to 0.5 m difference between the low and high predictions for sea-level rise by 2100 (UKCP, 2009).

- It was identified that the GEV, GPD and r-largest provided the lower bound at the 95% confidence for the storm surge frequency magnitude predictions with the JP and MC providing the upper bound.
- The identification of a significant uncertainty in the evaluation of storm surge frequency magnitude relationships has global significance in the evaluation of natural hazards. Guidance on the evaluation of external hazards including the International Atomic Energy for Nuclear sites (IAEA, 2003) and U.S. guidance on the evaluation of extreme wind speeds (Cheng and Yeung, 2002), currently does not adequately consider the effect of uncertainty, potentially leading to the failure of structures that have not been designed to cope with a specific magnitude event. An uncertainty 0.8 m identified within this study could potential affect in the region of 500 million people worldwide living close to the coast (Nicholls, 2002).
- Many areas around the world have limited data sets to allow the evaluation of storm surge magnitudes. However, this study has identified that it is possible to model a conservative "what if" scenario by combining the storm surge evaluation (rather than the observed levels) from either the GEV, GPD or r-largest with a Mean High Water Spring (MHWS) astronomical tidal component. As demonstrated in this study, this would only require 2 annual observations over approximately 20 years, which could potentially be identified from an archival historical search.
- The research has identified the following:
    - The GEV requires typically 40 years worth of data to effectively predict the frequency magnitude relationship, however, it has been found to be sensitive to additional data, which could lead to higher predictions and greater uncertainty in the evaluation of frequency magnitude relationships.
    - The r-largest methodology requires at least 20 years worth of data and has been found to be most effective when the value of r is between 2 and 5 (i.e. between 2 and 5 observations per year are utilised.
    - The GPD methodology has been found to model the data well with an average data set of 10 values per year. A key requirement of the GPD is that the selected data are independent.

- The JP methodology has been found to be effective with 10 years worth of data, although 20 years worth of data provided a better fit when compared to the predictions made for the complete data set.
- The MC methodology was found to be effective with just one year worth of data and is a key finding of this research, enabling predictions to be made with just one year of hourly storm surge and astronomical tide records.

8.2.3 Objective 3

Using a Geographical Information System to produce visual representations of inundation levels due to storm surge, including an evaluation of the sensitivity of south-west England to inundation as a result of the uncertainty in frequency magnitude predictions and sea-level rise predictions.

- The study is the first of its kind to consider the affect of different storm surge prediction methodologies on the overall area of inundation and to compare the area of inundation caused by the uncertainty in storm surge predictions with the uncertainty of future sea-level rise predictions.
- The mid-range prediction (UKCP, 2009) of sea-level rise leads to a 25% increase in land affected and a 50% increase in buildings affected. This compares to >50% increase in land affected and 100% increase in buildings affected due to different predictions for a 1 in 1000 year event.
- Due to the topography of the study area the incorporation of wave setup on to the inundation levels only slightly increases the overall area of flooding, however the depth and duration of inundation will increase, leading to an increase in damage. However, for other locations (e.g. the Somerset Levels, UK), wave setup could significantly increase the overall area of inundation.
- Taking in to account the type of facility at risk and modelling a higher degree of uncertainty relating to storm surge and wave height magnitude, Devonport Dockyard (Plymouth), would be overtopped by a 1 in 1000 year storm surge coinciding with a 1 in 1000 wave height, potentially leading to the flooding of the whole dockyard. This confirms the finding of the previous objective that failure to take in to account the uncertainty inherent in frequency magnitude predictions could have significant consequence.
- The findings of the statistical techniques and GIS modelling have been validated against the storms of Jan/Feb 2014. The areas identified to most likely to be affected by storm surge events within this study were affected

during the storms of January and February 2014. The statistical techniques were in the main able to cope with the addition of these storm surge events. The Jan/Feb 2014 storm surge events demonstrate that the techniques are stabile with the addition of new more extreme data.

8.2.4 Objective 4

To provide guidance on how uncertainty might be incorporated within planning and design decisions.

- The approach of this research has been to provide detailed methodologies to allow users to undertake not only a statistical analysis, but also to evaluate the effects of uncertainty, inundation levels and sea-level rise scenarios within a GIS environment
- The methodologies can provide an effective way of informing planning, producing design criteria and for disaster management.

8.2.4 Additional Findings

In addition to meeting the stated objectives the following has also been identified as part of the research:

- Based on the findings for south-west England the data indicates that the increase in the frequency of storm surges is linked to the increase in sea-level rise rather than a change in storminess.
- Oscillations in storm surge magnitude and sea-level rise rates are probably linked to the North Atlantic Oscillation (NAO).
- Changes in wind speed, wind direction and pressure were found to be potentially linked to the NAO.
- A “Dragon King” event was modelled utilising a sea level rise H++ scenario, this can be considered to be a “Worst case” for the study area.

8.3 Recommendations for Future Work

- Hard copy records exist for the Mt Batten (Plymouth) weather station to 1920 with data of wind speed, wind direction and pressure. These records should be transferred to digital copies and an analysis undertaken comparing the data to Newlyn tide gauge records. This will allow a more detailed trend analysis to be undertaken and provide a more definitive correlation between weather records, storm surge records and the NAO.
- There is a need to prove methodologies and presented findings for alternatives sites:
    - The closest available data set to Devonport, is the Weymouth tide gauge, which has 20 years worth of data. The techniques identified within this study should enable the evaluation of storm surge frequency magnitude relationships. The findings will enable the extent of the GIS model to be extended incorporating a greater area including the Dawlish coastline, which was significantly affected by the January and February 2014 storms and will also incorporate a range of infrastructure including the city of Exeter.
    - The south-west of England is tide dominant with a tidal range of 6 m. The findings of this study could have significant implications for coastal areas that have a larger storm surge component compared to the tidal component. Therefore, the findings of this study should be compared with locations that have a greater storm surge component.
- Acquire additional wave data to more effectively evaluate wave height, wave setup and the relationship between wave height and storm surge magnitudes with the aim of evaluating the frequency magnitude relationships for wave height and the joint probability of the coincidence of wave height and storm surge to further inform design.
- The method of overlaying flood events on to spatial data within a Geographical Information system has been criticised as being over-simplistic and frequently over estimating the flood extend (Bates et al., 2005; Mai and von Lieberman, 2001). To combat the simplicity of a GIS approach several authors have developed 2-dimensional models to simulate the flooding (for example Bates et al., 2005, Patro et al., 2009). However, a 2-dimensional approach has not been attempted on such a large extent. Therefore, there is a need to compare 2-dimensional modelling of storm surges with the GIS

approach at both the large and small scale to identify which approach is most applicable at evaluate the affect of coastal hazards.

- The landward fluvial contribution to the Devonport tide gauge should be investigated to identify if it contributes to the mean sea-level trend.
- The potential implications of a “Dragon King” event on the statistical analysis should be investigated. This should enable an understanding of the stability of the techniques to predict an outlier.

Appendix A Independent Technical Assessment Certificate

Appendix A has been removed due to Copyright restrictions

Appendix B Geographical Information System Database

Appendix B has been removed due to Copyright restrictions

Appendix C Glossary of Terms

Astronomical Tide

The periodic rise and fall of a body of water resulting from gravitational interactions between the Sun, Moon and Earth.

Consequence

An impact such as economic, social or environmental damage resulting from a natural hazard i.e. flood.

Cost Benefit Analysis

A process by which decisions are analyzed. The benefits of a given situation or action are summed and then the costs associated with taking that action are subtracted.

Density Plot

See Probability Density Function.

Deterministic

A mathematical model in which outcomes are precisely determined through known relationships, without any room for random variation.

Eustatic

Descriptive of global sea level variations due to absolute changes in the quantity of seawater, the most recent significant examples of which have been caused by the waxing and waning of continental ice sheets during glaciation cycles.

Extreme Value Analysis

Extreme value theory or extreme value analysis (EVA) is a branch of statistics dealing with the extreme deviations from the median of probability distributions. It seeks to assess, from a given ordered sample of a given random variable, the probability of events that are more extreme than any previously observed.

Extremes Software

Software package used to undertake Extreme Value Analysis.

Frequency

The rate at which an event occurs over a particular period of time

Frequency Magnitude Relationship

A quantitative correlation between the frequency of a natural hazard and the associated magnitude based on a series of historical or modelled observations. Can be defined by Extreme Value Analysis or Monte Carlo Simulation with a given level of uncertainty.

Generalised Extreme Value

The generalised extreme value (GEV) distribution is a family of continuous probability distributions developed within extreme value theory to combine the Gumbel, Fréchet and Weibull families also known as type I, II and III extreme value distributions. The GEV utilises only the annual maximum

Generalised Pareto Distribution

In statistics, the generalized Pareto distribution (GPD) is a family of continuous probability distributions. It is often used to model the tails of another distribution. It is specified by three parameters: location , scale , and shape. The GPD utilises all values above a specified threshold.

Geographical Information System

A geographic information system (GIS) is a system designed to capture, store, manipulate, analyze, manage, and present all types of spatial or geographical data**.**

Goodness of Fit

The extent to which observed data matches the values expected by theory.

Hazard

A hazard is any source of potential damage, harm to people, property or the environment.

Highest Astronomical Tide

The highest tide that can be produced under any combination of astronomical conditions.

Independent Observation

Observations that are separated by 24 hours are deemed to be independent and therefore are not either affected by the previous result or effect the outcome of the next result.

Isostacy

The equilibrium that exists between parts of the earth's crust, which behaves as if it consists of blocks floating on the underlying mantle, rising if material (such as an ice cap) is removed and sinking if material is deposited.

LiDAR (Light Detection and Ranging)

A Technology that employs a scanning laser range finder to measure surface relief

Mean Sea Level

A tidal datum. The arithmetic mean of hourly heights observed over a period of time.

Mitigation

Measures and instruments, including any process, actibity or design to avoid, reduce or compensate for adverse impacts

Monte Carlo Simulation

A problem solving technique used to approximate the probability of certain outcomes by running multiple trial runs, called simulations, using random variables

North Atlantic Oscillation

The North Atlantic Oscillation (NAO) is a climatic phenomenon in the North Atlantic Ocean of fluctuations in the difference of atmospheric pressure at sea level between the Icelandic low and the Azores high.

Observed Maximum

The maximum recorded value at a tide gauge over a given period. Includes both the astronomical ide and the storm surge component.

Observed Sea Level

The sea level as recorded by a tide gauge or other instrument

Peak Over Threshold

See Generalised Pareto Distribution

Probability

A measure of the degree of belief that an event will occur within a given time period

Probability Density Function

A probability density function (PDF), or density of a continuous random variable, is a function that describes the relative likelihood for this random variable to take on a given value.

Probability Distribution

A function of a discrete variable whose integral over any interval is the probability that the variate specified by it will lie within that interval.

Quantile Plot

A goodness of fit test that shows the results of the empirical and predicted data.

r-largest

An extreme value distribution that utilises a No. (r) of values (independent) extracted from a series of data, rather than the just the annual maximum.

r-Programming Language

Statistical software package. Background language to Extremes Software

Residual

See Storm Surge

Risk

The combination of the chance of an event with the impact that the event would cause if occurred.

Storm Surge

The local change in elevation of the ocean along the shore due to a storm. The storm surge is measured by subtracting the astronomical tidal elevation from the total elevation. Also known as Residual Level.

Still Water

Average water surface elevation at any instant, excluding local variation due to waves and wave set-up, but including the effects of tides, storm surges.

Storm Surge Maximum

The maximum storm surge value over a given period extracted from the observed tide gauge data.

Tide Gauge

A tide gauge (also known as mareograph or marigraph) is a device for measuring the change in sea level relative to a datum.

Tsunami

A shallow water wave caused by an underwater movement i.e. earthquake, volcanic eruption and submarine landslide, or movement in to a body of water i.e. landslide, volcanic collapse.

Uncertainty

Any situation or event that is not accompanied by a complete certainty of outcome whether or not described by a probability distribution

Vulnerability

A combination of the inherent susceptibility of a particular group of people, property or feature to experience damage during an event and societies preferred means of valuing the harm experienced

Wave Height

The maximum height of a wave from crest to trough caused by a variety of forces including gravitation and wind.

Wave Run Up

The surge of water up a slope from the breaking of a wave

Wave Set Up

The wave induced rise in mean sea level above the still water level due to wave action at the shoreline.

Wind Set Up

The vertical rise in the stillwater level on the leeward side of a body of water caused by wind stresses on the surface of the water.